UiT The Arctic University of Norway

Faculty of Biosciences, Fisheries and Economics

Department of Arctic and Marine Biology

Microbial community structure associated to Arctic cold seeps

Vincent Carrier

A dissertation for the degree of Philosophiae Doctor, October 2021

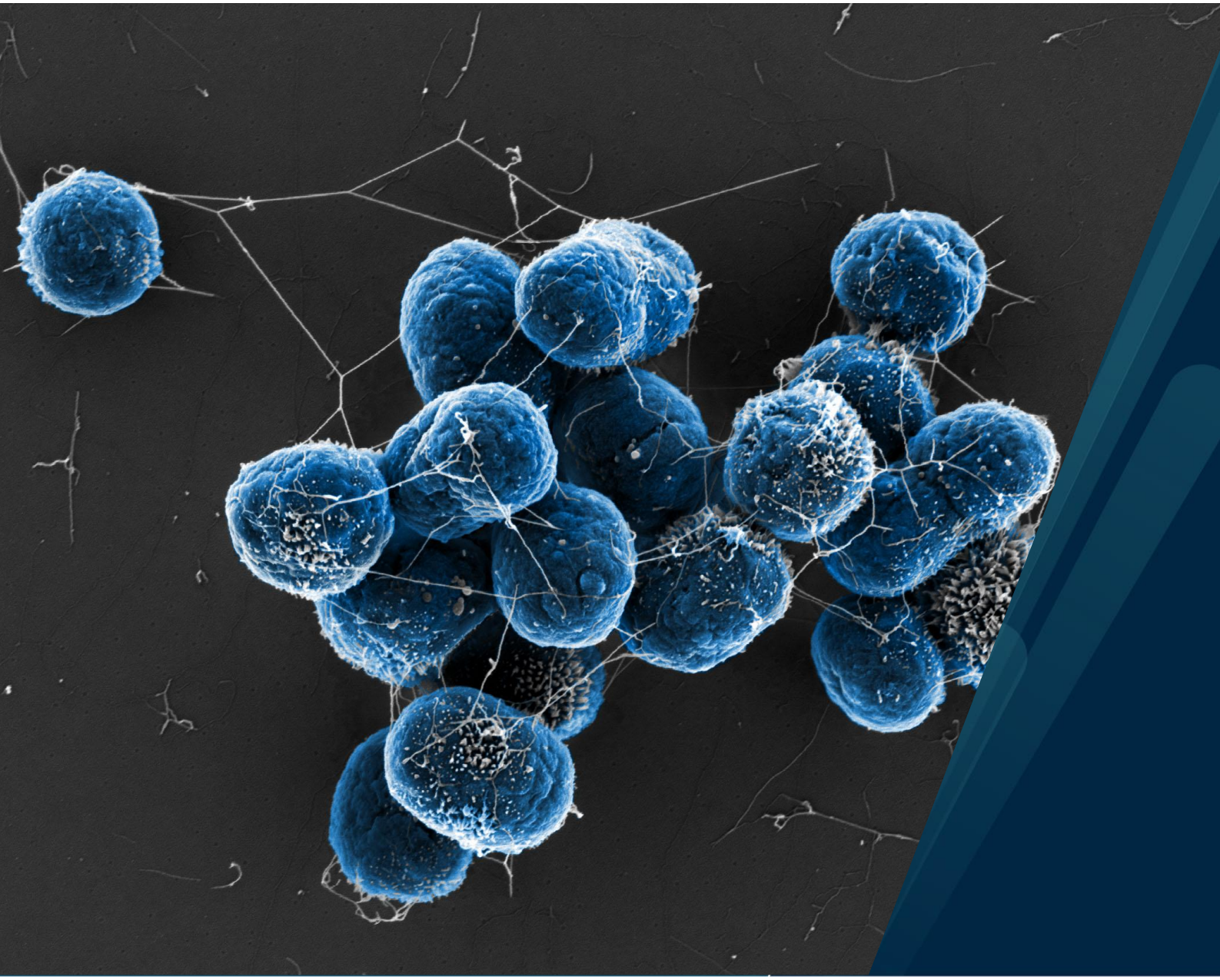

Table of Contents

List of Tables

List of Figures

Front page:

The methane oxidising bacterium *Methyloprofundus sedimenti*. It was isolated from sea water along the west coast of Svalbard.

Picture: Mette Marianne Svenning and Rudi Caeyers, UiT The Arctic University of Norway.

To my father Michel and mother Julie,
My sister Julie-Anne,
And my grandmothers Madeleine and Léa,

to those without whose support
this Thesis would not have come true.

À mon père Michel et ma mère Julie,
ma sœur Julie-Anne,
et mes grands-mères Madeleine et Léa,

Qui sans leur support,
cette thèse ne serait pas un rêve devenu réalité.

Summary

Cold seeps are locations on the seafloor where CH_4 migrates from reservoirs below sediments towards the atmosphere, sustaining thereby a high microbial and macrofaunal biomass and a diversity contrasting from the surrounding seafloor. The oxidation of methane and sulphide are typically the main sources of primary productivity of these ecosystems and have therefore gained a particular attention in the global oceans. Yet, despite the ubiquitous presence of these seeping sites and the presence of gas hydrates in the Arctic Ocean and its adjacent shelves, the impact of methane on benthic and pelagic microbial communities in this region have remained limited. Recently, five gas hydrate bearing mounds with ongoing methane seeping activity were discovered south of Svalbard, in the northern Barents Sea. In this PhD project, I studied changes in the structure of microbial communities, including both prokaryotes and eukaryotes, and geochemical profiles at these mounds to highlight key microbial groups and to provide insights on their ecological roles. Different niches were addressed, including: deep anaerobic sediments (**Paper I and II**); niches at the sediment surface at gas flare locations and within bacterial mats and siboglinid fields (**Paper III**); and above gas flares in the shallow shelf water column (**Paper IV**). The microbial biodiversity and the structure of communities were successfully identified for each of the habitats listed above. Our investigations revealed a microbial composition similar to other cold seeps: a predominance of archaeal anaerobic methanotrophs (ANME) and sulphate-reducing bacteria (SRB) in CH_4-rich sediments, a higher abundance of methane oxidizing bacteria associated to the Methylococcales in the surface sediments and water column; and a co-occurrence of other commonly found prokaryotic groups. Yet, uncommon biological traits were also uncovered at these methane seeping sites: the anaerobic oxidation of methane was merely only driven by ANME-1 without the co-occurrence of a specific SRB clade; an abundant methanotroph with little genetic similarity in databases was detected; and a strong niche differentiation of sulphide-oxidizing bacteria within the different bacterial mats. This project has thereby extended our knowledge on the microbial biodiversity at Arctic cold seeps and opened further future research perspective toward microbial activity and metabolism at these high latitudes.

Acknowledgements

At first, I would like to thank my supervisors Mette M. Svenning, Dimitri Kalenitchenko, Friederike Gründger and Helge Niemann for their support and supervision.

Mette. Thank you for your active listening, your moral support and your infinite advice from fieldwork to writing, life in Tromsø, greatest spots to enjoy nature in Northern Norway, and the best recipe to cook lutefisk. Thank you for all opportunities you let me experience during this PhD, from memorable moments at conferences to enjoying the coziness of Dividalen, and for being very comprehensive and supportive during challenging periods.

Dimitri. Our adventure started at 5h00 AM, in an airport hanger where we were about to embark on a 5 weeks journey. I would have never thought that these 5 weeks would become 6 years of continuing work together, but more important, a strong friendship. From work in the field or in the lab to data analyses and manuscript writing, you have been an important source of knowledge throughout all steps of my PhD. I look forward to our next new adventure!

Friederike. Thank you for the great and fun atmosphere on fieldwork, in the lab, at the office and during conferences; lot of great memories especially in Barentsburg! I am very grateful for the warmth welcome you gave me when I first arrive in Tromsø and your moral support. Finally, even after you moved to Denmark, thank you to have continued your precious mentoring and provided valuable feedback on my different projects, in addition of being still available to chat.

Helge. The setting of the PhD made it that we had limited face-to-face interactions, but your advice, suggestions and ideas have always been fruitful for my work and I am very grateful for that. In addition, thank you for sharing your passion for fishing, which became a central hobby during my stay in Tromsø.

For their scientific support throughout this PhD, I would like to thank Anne Grethe Hestnes, Pernille Skaset Fåne and Alena Didriksen (Arctic Marine Biology Department, UiT) in the molecular lab, and Mattteus Lindgren, Pavel Serov, Pierre-Antoine Dessandiers, Haoyi Yao, Wei-Li Hong and Guiliana Panieri (Centre for Arctic Gas Hydrates, Environment and Climate (CAGE), UiT) on fieldwork. I would like to extend my appreciation to the crew of R/V Helmer Hanssen and Kronprins Haakon for their help during fieldwork campaigns.

Thank you to my colleagues from both the Centre for Arctic Gas Hydrates, Environment and Climate (CAGE, UiT) and the Plants & Microorganisms Research Group of the Arctic Marine Biology Department. Your warm welcome and the continuous family atmosphere were meaningful for the success of this PhD. I would like to particularly thank my colleagues Kathrine M. Bender, Jørn Dietze, Lena A.-M. Lachner, Julien-Alexander Bruckmüller and Christophe Seppey for all the outdoor adventures, the social events and the moral support throughout this journey. Thank you also to the administration of the BFE Faculty for their continuous support. Thank you also to the administration of the BFE Faculty, the NT Faculty and of CAGE for their continuous support. Finally, I would like to thank my co-swimmers from TSI Plask in addition to my colleagues at National Model United Nations for their moral support.

Je voudrais remercier également mes amis au Québec, Maxfay & Patricia, Dominic & Jahelle, Louis-Philippe & Audrey-Anne, Catherine Pouliot, Samuel Lemieux, Henrik Bélanger et Philippe Bernier pour leur support moral ainsi que leur infaillible amitié à travers presque une demi-décennie de séparation et leurs encouragements.

Je voudrais aussi remercier les architectes de ce que je suis devenu, mes parents. Merci de votre dévouement, d'avoir remuer terre et ciel pour que je réalise mes rêves et d'avoir perpétuer votre support malgré que la distance a été difficile à vivre. Merci à ma mère Julie qu'on s'impose nos propres limites et qu'il n'appartient qu'à nous de les dépasser, ainsi que de m'avoir ouvert les yeux sur une multitudes d'expériences de vie que je n'aurais cru vivre il y a 10 ans. Merci à mon père Michel de m'avoir enseigné la rigueur et la débrouillardise. Ta polyvalence et ton dévouement sur la ferme et en agronomie m'a beaucoup encouragé à devenir plus indépendant et mieux contrôler les rênes de mon doctorat. Je voudrais également remercier ma sœur Julie-Anne, qui a été une source d'inspiration par sa ténacité à réaliser ses rêves, encore une fois félicitation pour être devenue vétérinaire. Merci aussi pour toutes ces aventures à travers l'Europe et j'espère qu'on découvrira de nouvelles régions du globe. Finalement, je voudrais remercier le support infini de mes deux grands-mères à travers tous mes rêves et ambitions, Léa et Madeleine, ainsi que de tout le reste de famille.

Supervisors

Prof. Dr. Mette Marianne Svenning[1,2]

Dr. Dimitri Kalenitchenko[2]

Dr. Friederike Gründger[3]

Prof. Dr. Helge Niemann[2,4,5]

[1]Department of Arctic and Marine Biology, The Arctic University of Norway, Tromsø, Norway
[2]Centre for Arctic Gas Hydrate, Environment and Climate, The Arctic University of Norway, Tromsø, Norway
[3]Department of Biology, Arctic Research Centre, Aarhus University, Aarhus, Denmark
[4]Department of Marine Microbiology and Biogeochemistry, Royal Netherlands Institute for Sea Research (NIOZ), and Utrecht University, den Burg, the Netherlands
[5]Department of Earth Sciences, Faculty of Geosciences, Utrecht University, Utrecht, the Netherlands

List of manuscripts

I) **Carrier, V**., Svenning, M. M., Gründger, F., Niemann, H., Dessandier, P. A., Panieri, G., and Kalenitchenko, D. (2020). The Impact of Methane on Microbial Communities at Marine Arctic Gas Hydrate Bearing Sediment. Front. Microbiol. 11, 1932. doi:10.3389/fmicb.2020.01932.
Link to supplementary information here.

II) Gründger, F., **Carrier, V.,** Svenning, M. M., Panieri, G., Vonnahme, T. R., Klasek, S., and Niemann, H. (2019). Methane-fuelled biofilms predominantly composed of methanotrophic ANME-1 in Arctic gas hydrate-related sediments. Sci. Rep. 9, 9725. doi:10.1038/s41598-019-46209-5.
Link to supplementary information here.

III) **Carrier V.**, Svenning, M. M., Niemann, H., Gründger, F. F., and Kalenitchenko, D. (in manuscript). Niche differentiation of prokaryotic communities and aerobic methanotrophs in surface sediments of an Arctic cold seep.

IV) Gründger, F., Probandt, D., Knittel, K., **Carrier, V.,** Kalenitchenko, D., Silyakova, A., Serov, P., Ferré, B., Svenning, M. M., and Niemann, H. (2021). Seasonal shifts of microbial methane oxidation in Arctic shelf waters above gas seeps. Limnol. Oceanogr. 9999, lno.11731. doi:10.1002/lno.11731.
Link to supplementary information here.

Author contributions

	Paper I*	Paper II*	Paper III*	Paper IV*
Concept and study design	**VC,** MMS, FG, HN	FG, **VC,** HN, MMS, DK	**VC,** DK, MMS, HN, FG	FG, HN
Data collection	**VC,** PAD	FG, MMS, HN, SK	**VC,** DK, MMS	FG, HN, **VC**, AS
Laboratory and data analyses	**VC,** PAD, DK, MS, FG, HN	**VC**, FG, TRV, SK	**VC,** DK, MMS, FG, HN	DP, **VC,** DK, KK, PS, FG, MMS, HN
Manuscript preparation	**VC**, MMS, DK, FG, HN, PAD, GP	FG, **VC**, HN, MMS, GP, TRV, SK	**VC,** DK, MMS, FG, HN	FG, HN, DP, **VC,** DK, AS, KK, BF, PS, MMS

*The list of authors was ordered from the most significant contributor to the less.

Vincent Carrier – VC
Mette M. Svenning – MMS
Friederike Gründger – FG
Helge Niemann – HN
Pierre-Antoine Dessandier – PAD
Giuliana Panieri – GP
Dimitri Kalenitchenko – DK
Tobias R. Vonnahme – TRV
Scott Klasek – SK
David Probandt – DP
Katrin Knittel – KK
Anna Silyakova – AS
Pavel Serov – PS
Bénédicte Ferré - BF

List of abbreviation

ANME-X	Anaerobic methanotrophic Archaea clades (-1, -2 or -3)
AOM	Anaerobic oxidation of methane
CAGE	Centre for Arctic Gas Hydrate, Climate and Environment
CARD-FISH	Catalyzed reporter deposition fluorescence *in situ* hybridization
cmbsf	Centimeters below seafloor
CTD	Conductivty-Temperature-Depth (instrument)
DNA	Deoxyribonucleic acid
DOPE	Double-labelling-of-oligonucleotide-probes
DSC-X	Deep-Sea Clusters (-1 to -5)
FF	Forskningsfartøyet
FISH	Fluorescence *in situ* hybridization
GHP	Gas hydrate pingo
GHSZ	Gas hydrates stability zone
HMMV	Haakon Mosby Mud Volcano
IPCC	International Panel on Climate Change
JS1	Japan Sea clade 1 (prokaryotic group)
MBG-X	Marine Benthic Group –B, -D
mbss	Meters below sea surface
MCG	Miscellaneous Crenarchaeotic Group
MOB	Methane oxidizing bacteria
MOx	Aerobic methane oxidation
OTU	Operational Taxonomic Unit
pmoA	Particulate methane monooxygenase subunit A
R/V	Research Vessel
ROV	Remotely operated vehicle
rRNA	Ribosomal ribonucleic acid
SMTZ	Sulphate-methane transition zone
SOB	Sulphide oxidizing bacteria
SR	Sulphate reduction
SRB	Sulphate-reducing bacteria
TC-MC	TowCam-Multicore system
WMO	World Meteorological Organization

1. Introduction chapter

1.1 Cold seeps

Cold seeps are locations on the seabed found at various depths where hydrocarbon-rich fluids, primarily composed of methane (CH_4), are emitted from the seafloor to the hydrosphere. They were first discovered in early 80's in the Gulf of Mexico by CK et al. (1984). On a seafloor generally deprived of marine life, they observed a high biomass and diversity at what resembled biological communities typically found near venting systems but without hydrothermal activity measured. The area was particularly characterized by large bacterial mats and fields of vestimentiferans worms, in addition to a high abundance of mussels, starfishes and shrimps. Such biodiversity hotspots were later observed to be sustained by chemoautotrophy through the assimilation of carbon from the available CH_4, both in aerobic (Distel and Cavanaugh, 1994; Valentine et al., 2001; Tavormina et al., 2008) and anaerobic environment (Hoehler et al., 1994; Hinrichs et al., 1999; Boetius et al., 2000). In addition to their roles in the local food webs, later studies also showed that the CH_4 oxidizing microorganisms, also named methanotrophs, prevent 20 to 80% of the CH_4 emitted through the sediments to reach the atmosphere and accelerate the ongoing global warming (Boetius and Wenzhöfer, 2013). These ecological roles stressed thereby over the past decades the need to understand the diversity and function of microbes at cold seeps.

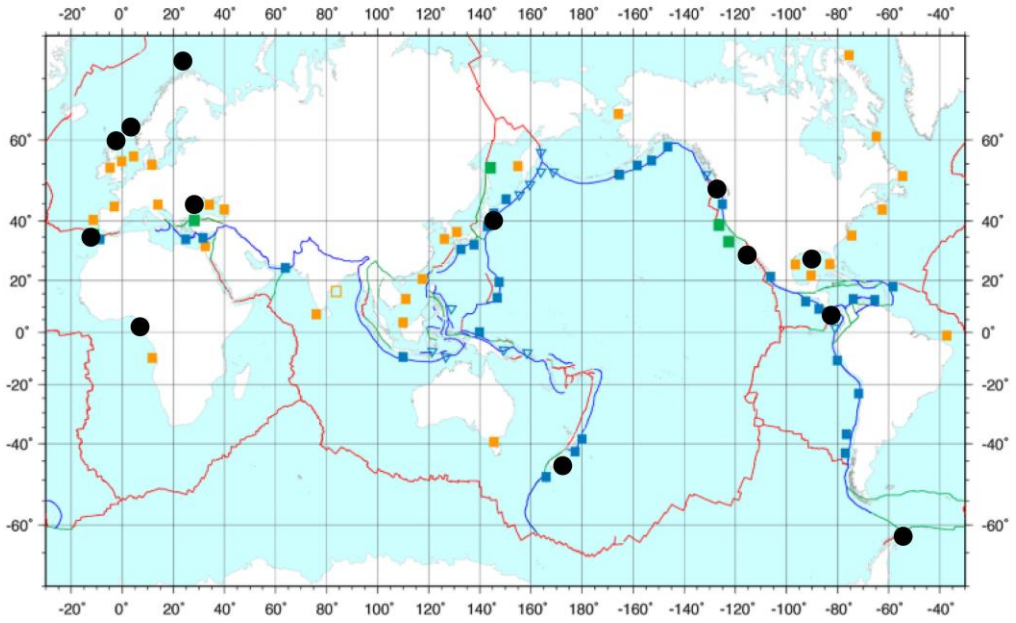

Figure 1: Global distribution of cold seeps along active (blue), passive (orange) and transformative (green) margins. Black dots represents cold seeps where microbial communities were investigated in Ruff et al. (2015). The figure was modified from Suess (2014).

Following the publication of the observations from the cold seeps system in the Gulf of Mexico in 1984, similar CH_4-fuelled environments have been found throughout the global oceans (Figure 1). Cold seeps are primarily found along active margins where oceanic and continental plate convergences cause splay faults through which fluids are expelled (Kulm et al., 1986; Le Pichon et al., 1987; Torres et al., 2002). In addition, cold seeps can also be found along passive margins, but then their geological settings are more diverse as various geological events leading

to differences of permeability in the sediments can open ways for CH_4 to migrate upward (Suess, 2014).

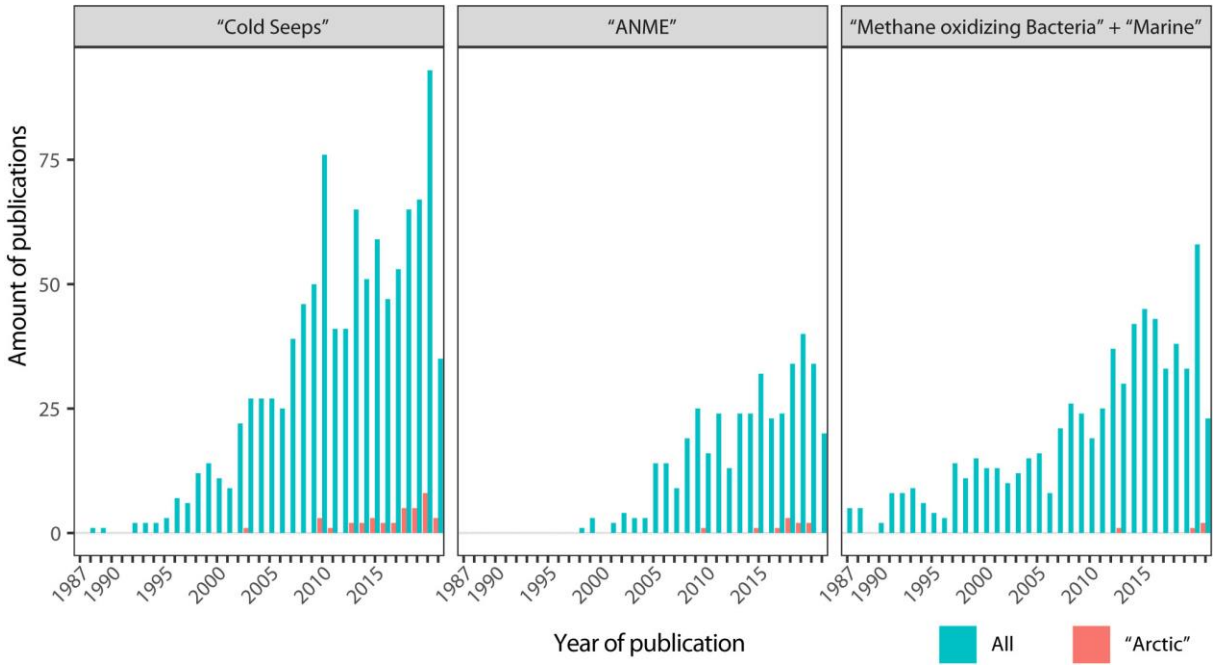

Figure 2: Results count of publications on *Web of Knowledge* where the words "Cold Seeps" (left), "ANME" (middle) and "Methane oxidizing Bacteria"+"Marine"(right) were used either within the title, keywords or abstract of a publication. In the figure, addition of the word "Arctic" (red bars) is compared to the overall available publications (blue bars). The timescale span from the first discovery of cold seeps in 1987 until July 2021.

Trends in the number of publications related to cold seeps per year have been rapidly increasing (Figure 2). Similar pattern can also be found for archaeal anaerobic methanotrophs (ANME) and aerobic methane oxidizing bacteria (MOB), two key microbial groups involved in CH_4 consumption at cold seep ecosystems (Distel and Cavanaugh, 1994; Boetius et al., 2000). Today, some of the most investigated cold seeps microbial communities include the areas of the Guaymas Basin (Teske et al., 2002; Dhillon et al., 2003; Vigneron et al., 2013, 2019; Portail et al., 2016), the Gulf of Mexico (Aharon, 1994; Joye et al., 2004; Cordes et al., 2007; Lessard-Pilon et al., 2010), the Hydrate Ridge (Boetius et al., 2000; Boetius and Suess, 2004; Knittel et al., 2005; Marlow et al., 2014) and the Haakon Mosby Mud Volcano (HMMV; Milkov et al., 2004; Beer et al., 2006; Niemann et al., 2006a; Lösekann et al., 2007a, 2008). Microbial communities at other cold seeps have also been studied, but at a lesser extend. Nevertheless, the recent work of Ruff et al. (2015) illustrates well the geographical distribution of microbial investigated CH_4 seep systems (Figure 1). In addition to the known areas listed above, Ruff et al. also integrated additional microbial communities retrieved from the Black Sea, Antarctica, along the eastern Asian continent and near Africa. The investigated CH_4 seeping sites are

obviously not limited to this study, as microbial communities from cold seeps have also been investigated near South America and in the Mediterranean Sea (Omoregie et al., 2009; Giongo et al., 2016). However, the study of Ruff et al. (2015) reflects well the latitudinal distribution of research efforts conducted in microbial biodiversity at cold seeps, where our knowledge rapidly diminishes at high latitudes.

Above the Arctic Circle, investigations at cold seeps remain scarce and the HMMV in the Barents Sea (~72°N) is the only relatively well described cold seep ecological system (see list of references above). Furthermore, it presents geomorphological settings (mud volcano) that differ to other cold seeps systems observed in other parts of the Arctic Ocean, such as the Beaufort (Paull et al., 2007), Kara (Serov et al., 2015) and Laptev (Savvichev et al., 2018) Seas. In the Barents Sea, several thousands of CH_4 gas flares have been detected around Svalbard and some sites have gained recent attention from geophysicists and macrobiologists, such as the Vestnessa Ridge, the shelf near Prins Karl Forland and at the mouth of Storfjordrenna (Sahling et al., 2014; Åström et al., 2016; Serov et al., 2017; Sen et al., 2018a), all demonstrating different geochemical and biological settings compared to the HMMV.

1.1.1 Origin of methane in the global oceans

Methane is the second most abundant greenhouse gas in the atmosphere after carbon dioxide (CO_2). Despite having an atmospheric concentration that is more than 200 times lower than CO_2, it still contributes for approximately 20 to 23% of the radiative forcing in the atmosphere (Myhre et al., 2013; Etminan et al., 2016). This is because of its global warming potential being 28 times stronger than CO_2. While CH_4 emissions from anthropogenic activities contribute to a significant fraction (approximately 60%) of the atmospheric CH_4 pool, CH_4 also originate from natural sources, such as wetlands, termites and from freshwater/marine environments (Reeburgh, 2007; WMO, 2019). Ecosystems releasing CH_4 can also uptake it through physical, chemical, or biological processes. Globally, 5-25 Tg CH_4 yr^{-1} are estimated to be emitted from the oceans to the atmosphere, representing 2.7 to 10% of the CH_4 emitted from natural sources (Saunois et al., 2016, 2020; Weber et al., 2019).

In the oceans, CH_4 is mainly formed through biogenic or thermogenic processes (Schoell, 1983, 1988; Joye et al., 2010). Biogenic CH_4 is formed by some archaeal groups through methanogenesis, a step in the remineralization process of organic matter that can be performed in marine sediments primarily through CO_2 reduction and at a lesser extent by acetate fermentation (Whiticar et al., 1986; Ferry and Lessner, 2008). Methanogenesis primarily occurs

in anoxic sediments, although it can also be observed within anoxic micro-environments in pelagic particles (van der Maarel et al., 1999). Methane of thermogenic origin is formed by the break down of buried organic molecules through thermocatalytic reaction in sedimentary basins (Floodgate and Judd, 1992). The CH_4 produced in marine sediments can either migrate toward the hydrosphere or be trapped in reservoirs of impermeable geological layers, such as submerged permafrost (Yakushev and Chuvilin, 2000; Shakhova et al., 2010) or layers of gas hydrates (Dickens et al., 1997; Archer, 2015), that prevents its upward movement.

1.1.1.1 Methane and gas hydrates in marine environments

Methane in marine sediments, either locally produced or transiting through, can be trapped in ice-like crystalline cages of water molecules. These latter are referred as gas hydrates and are formed under certain thermobaric conditions, at high pressure and low temperature (Sloan and Koh, 2008). This range of environmental conditions is referred to as the gas hydrate stability zone (GHSZ) and the depth and thickness of this GHSZ vary in the different sections of the globe (Kvenvolden, 1988; Wallmann et al., 2011). In the Arctic Ocean, the upper limit of the GHSZ may be as shallow as 300 meters below sea surface (Ruppel, 2007) and usually deepen with warmer bottom waters, as in the Barents Sea (Ferré et al., 2012) where it reaches nearly 500m depth in the southern section. Gas hydrates are globally distributed (Ruppel, 2007) and are also widely found in the Arctic Ocean (Collett et al., 2011). An estimated 100-9000 Gt of CH_4 is stored as gas hydrate in Arctic marine sediments (Kvenvolden, 1988; Biastoch et al., 2011; Hunter et al., 2013; Kretschmer et al., 2015), and an additional ~2-1400Gt could be trapped as either hydrate or free gas under submerged permafrost.

A shallower GHSZ in the Arctic Ocean has raised concerns over the ongoing increase in bottom seawater temperature that is particularly stronger in the Arctic Ocean that could further deepen the upper boundary of the GHSZ (Westbrook et al., 2009). This process could expose gas hydrates to dissociation, and explain the observation of CH_4 gas flare slightly above the GHSZ (Westbrook et al., 2009; Sahling et al., 2014). However, whether the warming ocean will subsequently lead to the dissociation of large reservoirs of gas hydrates in the Arctic Ocean remains unknown. Several factors, such as depth of gas hydrates in the sediments, could mitigate the influence of increasing bottom water temperature on gas hydrates dissociation (Hong et al., 2017; Ruppel and Kessler, 2017). While changes in bottom water temperature may not lead to the previously suggested catastrophic scenarios of vast quantities of CH_4 reaching the atmosphere , investigations revealed seasonality on CH_4 seeping activity in the Barents Sea, where colder bottom water in May correlated with reduced CH_4 fluxes from the seafloor (Ferré

et al., 2020). Thereby, changes in bottom water temperatures may still have an effect on the biogeochemistry of cold seeps, and eventually also on the microbial communities hosted in the sediments.

In addition of gas hydrate formation, other physical events can also contribute to prevent the CH4 to reach the atmosphere. As the CH_4 escapes the seafloor, it reaches the hydrosphere and migrate toward the sea surface. Yet, low or negligible concentrations of CH_4 were measured at sea surface level above cold seeps (Myhre et al., 2016; Mau et al., 2017; Silyakova et al., 2020). This rather low fraction is caused by a combination of physical, chemical, and biological processes that dissipate the CH_4 before it reaches the atmosphere, acting as important CH_4 sinks in the oceans. Examples of physical and chemical processes include bubble-stripping (i.e. the replacement of CH_4 with O_2 or N_2 in the gas bubbles from gas flares; McGinnis et al., 2006), in addition to lateral water mass movements that disperse the CH_4 horizontally away from the cold seeps (Silyakova et al., 2020). Furthermore, changes in water masses through vertical mixing, stratification and advection, was shown to influence CH_4 fluxes (Steinle et al., 2015). A large fraction of CH_4 is also removed in its ascent through biologically mediated oxidation (Beer et al., 2006; Niemann et al., 2006; Roalkvam et al., 2012; Hong et al., 2016). The aerobic and anaerobic biological oxidation of CH_4 acts thereby as a biological filter and can uptake generally 20 to 80% of the CH_4 emitted (Boetius and Wenzhöfer, 2013). These biological processes will be further described in subsection 1.2.1.

1.1.1.2 Geomorphology of cold seeps

Cold seeps are a broad concept of geological features referring to an area at the seafloor where hydrocarbon-rich fluid seepage occurs. In addition of hydrocarbons, these fluids can also contain sulfur compounds, silica, phosphate, and ammonia (Suess, 2014). Regimes of CH_4 transiting through the sediments and the environmental conditions can further shape the topography of the seeping sites. For instance, the pressure created by CH_4 flow and the formation or dissociation of gas hydrates has been suggested to generate various seafloor features such as pockmarks, craters and gas domes (Vogt et al., 1994; Hovland and Svensen, 2006; Suess, 2014; Koch et al., 2015; Portnov et al., 2016; Serov et al., 2017; Riboulot, 2018). In the Barents Sea five gas hydrates bearing mounds, referred as gas hydrates pingos (GHPs), have been located and were suggested to be formed by the formation of gas hydrates (Serov et al., 2017). Similar features in the Arctic have been observed in the Beaufort (Paull et al., 2007) and South Kara (Serov et al., 2015) Seas.

Finally, the biological communities thriving at cold seeps influence the biogeochemistry of the environment. For instance, the oxidation of CH_4 can enhance the pore water sulphide (H_2S) concentrations, beneficial for chemosynthetic organisms but toxic for most background species (biological implications of H_2S toxicity are reviewed in Wang and Chapman (1999). It can also lead to the formation of authigenic carbonates, adding hard substrates for sessile organisms to attach to (Cordes et al., 2007, 2009; Vaughn Barrie et al., 2011; Levin et al., 2015). In or near H_2S-rich sediments, fields of siboglinid worms proliferating near H_2S-rich sediments retroactively irrigate the seabed surface (Berner, 1980), allowing a deeper penetration of oxygen, a major environmental factor in the distribution of microbes in the sediments (Hughes and Gage, 2004; Fischer et al., 2012; Guillon et al., 2017). Thereby, cold seeps represent a complex mosaic of micro-habitats. These should be considered when investigating the microbial communities thriving at those cold seeps, their roles and metabolism and their impact on the biogeochemistry.

1.1.1.3 Geochemical and hydrological settings of cold seeps in the northern Barents Sea

In the Barents Sea, sources of hydrocarbons are widely distributed and include organic-rich Triassic-Jurassic formations (Mørk and Bjorøy, 1984; Grogan et al., 1999). During the last glaciation maximum that was initiated approx. 35,000 years ago, an ice sheet covered the Barents Sea and its carbon-rich sediment layers, creating subglacial high pressure and low temperature across the continental shelf, which in turn extended the GHSZ up to 500m thickness (Portnov et al., 2016). Both the thick GHSZ and the formation of subsea permafrost acted as geological sinks and seals. This limited the vertical flux of CH_4 or organic matter to be decomposed, causing accumulation of CH_4. Since the ice sheet started to retreat approx. 20,000 years ago, changes in temperature and pressure linked to the latest glacial period and last glacial maximum have been influencing CH_4 seeping activity that is suggested to have been ongoing in the northern Barents Sea for several millennia (Portnov et al., 2016). In Storfjordrenna, the observation of CH_4 seeping activity above gas chimneys suggest that faults built a connection between the deeper hydrocarbon reservoirs and the seafloor surface (Waage et al., 2019). Today, the GHSZ is estimated to have been reduced to few tens of meters (Serov et al., 2017). Several cold seep features have been observed in the northern Barents Sea, including pockmarks (Goswami et al., 2015; Portnov et al., 2016), craters (Andreassen et al., 2017) and GHPs (Serov et al., 2017). Along the western coast of Svalbard, gas flares are observed at a depth higher than the upper boundary of the GHSZ without showing signs of gas hydrate

storage or faults below the CH_4 seeping sites. Instead, it was proposed that fractions of the CH_4 could originate from lateral migration paths from a deeper shelf reservoir (Sarkar et al., 2012). Isotopic signature of CH_4 (Whiticar, 2000) revealed that seeps along the western coast of Svalbard was formed by biogenic processes (Graves et al., 2017; Mau et al., 2017), while CH_4 from seeps in Storfjordrenna, south of Svalbard, is of thermogenic origin (Serov et al., 2017).

The hydrodynamics around Svalbard are complex and known to influence CH_4 fluxes along the shallow shelf (Silyakova et al., 2020). The location of Svalbard near the Polar Front lead to the influence of two major water masses: the warm, saline and nutrients-rich Atlantic Water (salinity >34.65, >3.0°C) travelling along the western coast of Svalbard (Western Spitsbergen Current) and to the colder and fresher Arctic Water (salinity 34.30-34.80,-1.5 to 1.0°C) that circulates downward from the Arctic Ocean northeast of Svalbard resulting in the Eastern Spitsbergen Current to deviate around Sørkapp to finally move northward along the shallow shelf west of Svalbard (Figure 7; Aagaard et al., 1987; Nilsen et al., 2008). Both water masses can further mix and, with the influence of local environmental conditions and seasons, lead to the formation of additional water masses, including the Transformed Atlantic Water and Intermediate Water (Cottier et al., 2005).

1.2 Microbial diversity and functions at cold seeps

Cold seeps are commonly regarded as biodiversity hotspots on the seafloor because they often visually contrast from the surrounding environment with a higher biomass and a larger macrofauna diversity (Sibuet and Olu, 1998; Vanreusel et al., 2009; Cordes et al., 2010; Åström et al., 2016). Because the macrofauna cannot directly benefit from the CH_4-rich fluids, macrofaunal species rely on microbial activity to connect the geochemical settings at cold seeps to its occupants (Duperron et al., 2007; Van Gaever et al., 2009; Niemann et al., 2013; Portail et al., 2016; Toone and Washburn, 2020). Methane acts as carbon sources for the ecosystem and is uptaken by methanotrophs (Kohzu et al., 2004; Fernández-Carrera et al., 2016; Portail et al., 2016; Demopoulos et al., 2018), which in turn provide energy in form of their for the upper food webs. Subsequently, H_2S, a product of the oxidation of CH_4 with sulphate (SO_4^2), is reduced, which then can become a source of energy for chemosynthetic organisms through endosymbionts or for mat-forming bacteria, supporting colonies of clams, siboglinid worms

and crustaceans (Figure 3; Fisher, 1990; Fisher et al., 1993; Duperron et al., 2007b, 2008; Bernardino et al., 2012).

Authigenic carbonates, to which various sessile macrofaunal species can attach to, are product derived from the microbial anaerobic oxidation of CH_4 (Levin et al., 2003, 2015; Quéric and Soltwedel, 2007; Gaudron et al., 2010). Furthermore, microbes are involved in several biogeochemical cycles within the cold seep ecosystems and are therefore unequivocally the foundation supporting this observed oasis of life.

Figure 3: Lithotid crabs grazing on bacterial mats at the Haakon Mosby Mud Volcano. Picture modified from Niemann et al. (2013).

Microbial communities at cold seeps compose with contrasting environmental conditions to the surrounding environment, such as highly sulfidic porewater toxic for several common benthic taxa, shaping the biota composition and structure (Powell and Somero, 1986; Bagarinao, 1992; Sears et al., 2004; Bouillaud and Blachier, 2011). These communities are commonly composed of several taxa that have yet not been cultivated, limiting further our understanding of their roles and impacts on the local habitat (Ruff et al., 2015). The environment of the Arctic Ocean poses conditions that are known to affect the composition and structure of pelagic (Lovejoy et al., 2007; Falk-Petersen et al., 2009) and benthic (Balmonte et al., 2018) microbial communities. Some of these conditions include: i) the exposure to sub-zero temperature in bottom waters (Carmack and Wassmann, 2006) and ii) the dynamical movements along the Polar Front and the properties exchanges between the warm and saline Atlantic Water and the colder and fresher Arctic Water (Vernet et al., 2019). Another characteristic is iii) the strong sedimentation of organic matter following spring blooms combined with long starvation periods of allochthonous carbon deposited to the seabed (Piepenburg et al., 1997; Carmack and Wassmann, 2006; Renaud et al., 2008). Thereby, in addition of cold seeps hosting distinct microbial communities from CH_4-absent arctic sediments, these could also potentially contrast from other cold seeps found at lower latitudes.

Microbes are involved in several metabolic cycles, including carbon, sulphur and nitrogen among others. Covering actors involved in all of these cycles would thereby be too voluminous for the scope of this Thesis. Therefore, this introduction will primarily focus only on microbial processes relevant for this Thesis, i.e. on the carbon, more precisely on the CH_4 oxidation pathways, and on sulphur biogeochemical cycles, both SO_4^{2-} reduction and H_2S oxidation.

1.2.1 Methane oxidation

As CH_4 migrates from hydrocarbon source layers to the hydrosphere, its fate through the biological filter depends primarily on the availability or absence of oxygen (Figure 4). Therefore, CH_4 is initially oxidized in anaerobic sediments relying on electron acceptors other than oxygen. This mode of CH_4 oxidation has been termed the anaerobic oxidation of CH_4 (AOM). At the sediment surface and within the water column, the availability of oxygen favors the aerobic oxidation of methane (MOx).

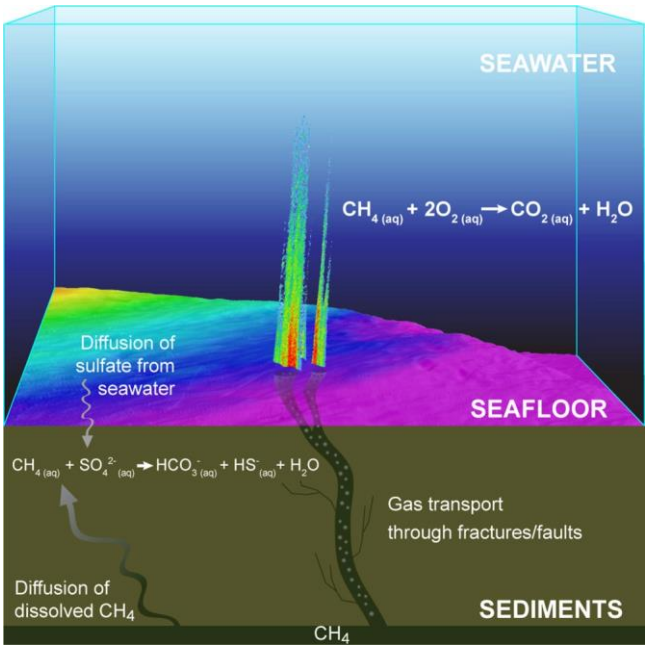

Figure 4: Anaerobic oxidation of methane (AOM) in combination with sulphate reduction to form HCO_3^- and H_2S, before reaching the seafloor surface and the seawater column where it is aerobically oxidized to form CO_2. Figure from James et al. (2016).

1.2.1.1 Anaerobic oxidation of methane (AOM) and sulphate reduction (SR)

AOM is the major biological sink of CH_4 in marine environments (Reeburgh, 2007; Knittel and Boetius, 2009) because it is estimated that AOM could filter 20 to 80% of the CH_4 released (Boetius and Wenzhöfer, 2013), and even higher amounts at some locations (Wegener et al., 2008).. The anaerobic oxidation of CH_4 in marine sediments is primarily mediated by the transfer of electrons from the CH_4 to SO_4^{2-} through the combination of CH_4 oxidation and SO_4^{2-} reduction, leading to the formation of HCO_3^-, HS^- and H_2O (Hoehler et al., 1994), according to the net reaction:

$$CH_4 + SO_4^{2-} \rightarrow HCO_3^- + HS^- + H_2O$$

The SO_4^{2-} concentration in seawater is generally around 28 mM (Canfield, 2004). The occurrence of methyl-coenzyme M reductase, a key enzyme for methanogenesis and AOM, extracted from various CH_4 oxidation zones in the environment suggest CH_4 uptake by microbes to be a reverse methanogenesis process resulting from a coevolution of the processes (Hallam et al., 2003; Krüger et al., 2003; Holler et al., 2009; Wegener et al., 2021). Zones of high activity of AOM can be inferred from steep variations of CH_4 and SO_4^{2-} concentrations, referred to the sulphate-methane transition zone (SMTZ). The depth of the SMTZ depends on various environmental settings such as the CH_4 production and the penetration depth of the SO_4^{2-}. The shallower the SMTZ is, the higher the CH_4 flux is suggested to be (Valentine and Reeburgh, 2000; Knab et al., 2009; Meister et al., 2013). AOM has also been observed to be coupled with the reduction of oxidized iron, manganese and nitrate/nitrite (Beal et al., 2009; Ettwig et al., 2010, 2016; Hu et al., 2014). However, the contribution of these electron acceptors in the AOM budget remains less constrained, especially in the Arctic Ocean (Boetius and Wenzhöfer, 2013).

AOM is driven by anaerobic methanotrophic archaea (ANME) and three main ANME clades of phylogenetically distinct groups have been detected: ANME-1 forms a distinct group within the Halobacterota while ANME-2 and ANME-3 are placed within the Methanosarcinales, in accordance to the latest classification made within the SILVA Database v138.1 (Knittel et al., 2005; Quast et al., 2012; Yilmaz et al., 2014). However, assigning ecotypes or specific metabolism particularities to the different clades has remained unresolved. Several hypotheses were proposed, but they are accompanied with contradicting observations at other cold seeps. Results from previous studies suggested that ANME-2, the most widely distributed ANME clade in global oceans, might be more sensitive to high concentrations of H_2S and/or low concentrations of SO_4^{2-} than ANME-1 (Timmers et al., 2015; Bhattarai et al., 2018). The ANME-2 group would then often be limited to the layers above the SMTZ and ANME-1 would dominate in more sulfidic sediments, at deeper layers (Ruff et al., 2015). This distribution pattern has been observed in the southern Barents Sea, at the Nyegga Ridge (Roalkvam et al., 2011). However, in other studies, ANME-2 groups were also retrieved in H_2S-rich sediments (Knittel et al., 2003), indicating that other factors than levels of H_2S or SO_4^{2-} might affect stratification of ANME groups. Additional environmental conditions that were suggested to select for differential ANME groups include temperature (Nauhaus et al., 2005; Rossel et al.,

2011), salinity (Maignien et al., 2013) or CH_4 flux rates (Girguis et al., 2005; Yanagawa et al., 2011; Vigneron et al., 2013, 2019; Marlow et al., 2014).

AOM generally relies on sulphate reducing bacteria (SRB; Boetius et al., 2000; Knittel et al., 2003) and therefore syntrophic consortia between ANME and SRB are commonly observed (Boetius et al., 2000; Wegener et al., 2015). SRB are ubiquitous in marine sediments where they play a role in degrading organic matter. However, distinctive clades, referred as SEEP-SRB 1 to 4, have been exclusively found at cold seeps. Typically, ANME-1 and -2 would be found associated with the clades SEEP-SRB1 or SEEP-SRB2 (Orphan et al., 2001; Michaelis et al., 2002; Knittel et al., 2003; Pernthaler et al., 2008), and epifluorescence micrographs visualized by Fluorescence in situ hybridization (FISH) or CARD-FISH have demonstrated aggregates of ANME and SRB (Knittel and Boetius, 2009). However, in the last decade, community studies of methanotrophs have shown evidence of free-living cells particularly assigned to the ANME-1 group, but also to the ANME-2 group (Orphan et al., 2002; Knittel et al., 2005; Roalkvam et al., 2011; Milucka et al., 2012; Stokke et al., 2012). One suggested idea is that they could be able to perform SO_4^{2-} reduction alone. The detection of F430-dependent sulfite reductase in ANME-1 could support this hypothesis (Vigneron et al., 2019), although the presence of other key genes to reduce H_2S to sulfite, such as the adenosine-59-phosphosulphate and the sulfite reductase, has not been detected (Hallam et al., 2003; Pernthaler et al., 2008).

1.2.1.2 Aerobic oxidation of methane

In aerobic environments, which are generally limited to the water column and the first few mm to cm below seabed sediment surface (Boetius and Wenzhöfer, 2013; Niemann et al., 2013), the oxidation of CH_4 is driven by methane oxidizing bacteria that utilize oxygen as the electron acceptor (Hanson and Hanson, 1996; Trotsenko and Murrell, 2008). These methanotrophs oxidize CH_4 with the available oxygen to form formaldehyde for living and cell mass production, and subsequently metabolize it in CO_2 according to the net formula:

$$CH_4 + 2\,O_2 \rightarrow CO_2 + 2\,H_2O$$

Aerobic microbial methane oxidation (MOx) is generally filtering less CH_4 than AOM in marine systems (Knittel and Boetius, 2009), but is the final biological sink for CH_4 before it is liberated to the atmosphere (Reeburgh, 2007; Tavormina et al., 2008; Valentine, 2011). The impact of MOx can be significant: for instance, high amounts of CH_4 were rapidly consumed

by MOB following the deep-water horizon accident and MOB were found to effectively consume CH_4 from the water column if hydrographic conditions and nutrients would provide continuity for MOB (Dubinsky et al., 2013; Kleindienst et al., 2015; Rogener et al., 2018). However, MOx can also be low despite high CH_4 concentrations in marine waters for reasons that are still unclear. Absence of benthic biomass and strong gas emissions are factors that can further reduce the efficiency down to 10% (Niemann et al., 2006).

MOB have been described primarily within the Gammaproteobacteria and Alphaproteobacteria, commonly referred to Type I and II methanotrophs, respectively, in addition to Verrucomicrobia and Crenotrix (Stoecker et al., 2006; Dunfield et al., 2007; Dedysh and Knief, 2018; Kalyuzhnaya et al., 2019). Yet, clustering particulate methane monooxygenase (*pmoA)* gene sequences of cultivated and uncultivated methanotrophs at the genus level showed that only half of the formed operational taxonomic units (OTUs) contained cultivated representatives (Knief, 2015). This suggests a large diversity remains yet undiscovered, especially within the Gammaproteobacteria, further supported through phylogenetic analyses using both 16S rRNA and *pmoA* genes with the formation of several ecotypes of uncultivated sequences. Some clades, such as the Deep-Sea Clusters (DSC) 1-5 (Lüke and Frenzel, 2011; Knief, 2015), are almost exclusively found in the oceans. Environmental factors driving the nature of the dominating MOB include CH_4, H_2S and O_2 concentration (Graham et al., 1993), pH (Rahman et al., 2011; Danilova and Dedysh, 2014) and temperature (Trotsenko and Khmelenina, 2002).

1.2.1.3 Sulphide oxidation

Sulphide oxidizers are another major microbial functional group in cold seeps ecosystems, being in addition to methanotrophs an alternative source of primary/secondary production of biomass for higher trophic levels (Taylor et al., 2001; Lichtschlag et al., 2010; Niemann et al., 2013). They are diverse and are found within the Archaea and Bacteria (SOB), common H_2S oxidizers taxa in H_2S-rich sediments include the Campylobacterota, previously known as the Epsilonproteobacterota, particularly the Sulfurimonadaceae and Sulfurimonadaceae families, and the gammaproteobacterial Beggiatoales (Friedrich et al., 2005; O'Brien et al., 2015).

SOB are ubiquitous in marine sediments, but they present shifts in dominating SOB taxa depending on environmental conditions (Friedrich et al., 2005; and see Figure 5). They also present different life strategies as some chemoautotrophs can be present as intracellular or extracellular symbionts within larger fauna (Fisher et al., 1993; Cary et al., 1997; Dubilier et al., 2001; Nakagawa and Takai, 2008; Thurber et al., 2011), such as siboglinid worms (Figure 6) or crabs, but also in eukaryotic euglenozoans and ciliates (Ott et al., 1998; Buck et al., 2000; Rosati, 2001; Dziallas et al., 2012).

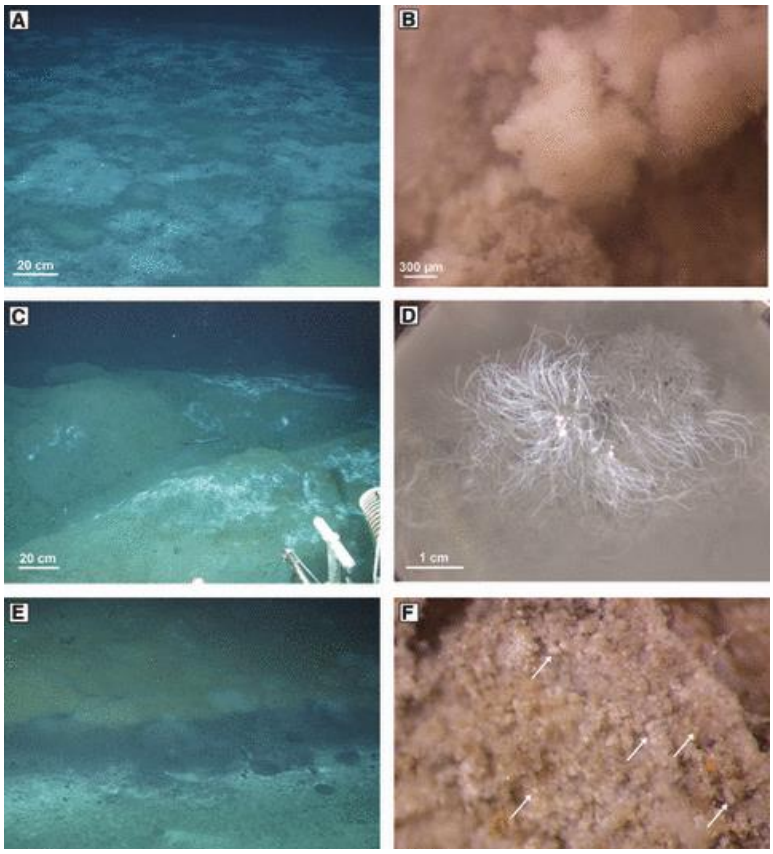

Figure 5: Bacterial mats composed of different sulphide-oxidizing bacteria and retrieved at different locations of a cold seeps (A-C-E). Bacterial mats particularly showed distinctive characteristics at higher magnification (B-D-F). Pictures are from Grünke et al. (2011).

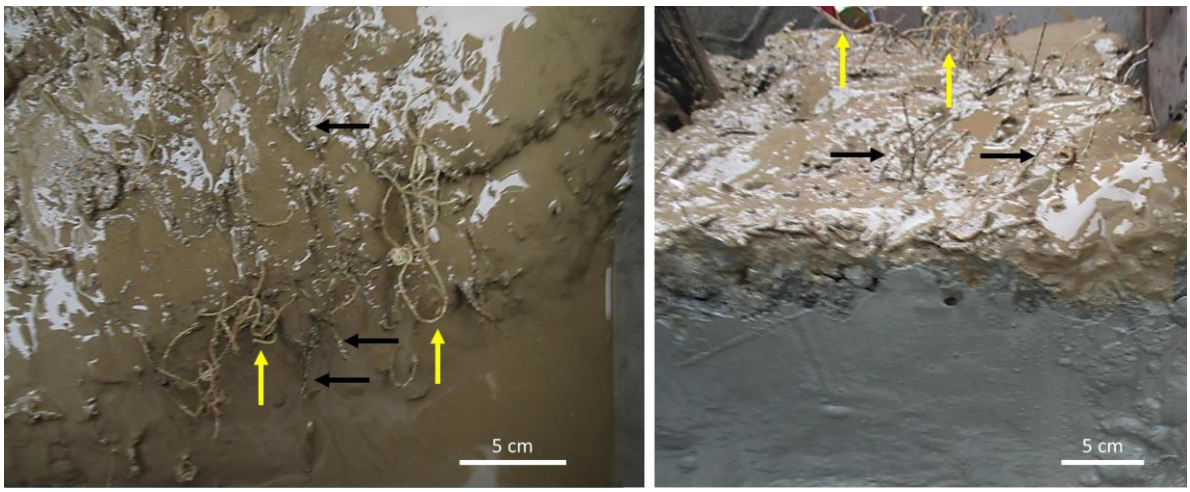

Figure 6: Sediment surface at cold seeps in the northern Barents Sea showing two different species (yellow and black arrows) of frenulates tubeworms hosting H_2S oxidizing endosymbionts. Picture from Sen et al. (2020).

Siboglinids are frenulates known to host SOB as endosymbionts. Recent studies in the northern Barents Sea confirmed the presence of gammaproteobacterial SOB in fields of *Oligobrachia* species (Sen et al., 2018b, 2020). Investigations on niche differentiation by SOB, although they remain limited at cold seeps, highlighted that availability and flux rates of O_2 and nitrate, electron acceptors and H_2S, the electron donor, were key environmental factors driving changes in the SOB communities (Grünke et al., 2011; Anderson et al., 2013; Meier et al., 2017). Campylobacterota were found to dominate environments with both availability of H_2S and electron acceptors at the oxic-anoxic interfaces (Madrid et al., 2001; Macalady et al., 2008; Grünke et al., 2011). In contrast, the Beggiatoales create suitable conditions and dominate sediments where H_2S and O_2 do not overlap. Because Beggiatoales are motile and can store nitrate in vacuoles (McHatton et al., 1996), they are able to migrate vertically in the sediments to reach H_2S-richer sediments (Preisler et al., 2007).

1.2.1.4 Grazers, organic compounds degraders and other functional roles

Other "signature" groups of cold seeps (Ruff et al., 2015) include the *Chloroflexi* spp. (Zhang et al., 2012; Cruaud et al., 2017) and the uncultivated groups of Thermoplasmata Marine Benthic Groups (MBG) B and D (Vigneron et al., 2014; Cruaud et al., 2017; Ramírez et al., 2020), Bathyarchaeota (Bathyarcheia) and the candidate division Japan Sea 1 (JS1; Webster et al., 2004, 2007; Zhang et al., 2012). The Bathyarcheia, previously known as the Miscellaneous Crenarchaeotal Group (MCG), and the thermoplasmatales MBGs B-D are globally abundant in marine sediments and therefore not necessarily unique to CH_4-rich sediments. The detection of protein-degrading enzymes in some representatives of these groups suggests a role in anaerobic organic matter degradation (Webster et al., 2010; Kubo et al., 2012; Lloyd et al., 2013). However, they may contain ecotypes adapted to cold seep habitats that are not detectable at the genetic resolution of available databases due to the lack of cultivated species or metagenomes (Zhou et al., 2018). The Wosearchaeales is another abundant group found in marine sediments potentially pursuing a fermentation-based lifestyle (Castelle et al., 2015), but large gaps of knowledge on their distribution and metabolism exist (Liu et al., 2018). Beyond the degradation of organic compounds, additional roles played by these groups in CH_4-rich sediments have been investigated. For instance, correlations suggested links between CH_4 cycle and Bathyarchaeia (Evans et al., 2015; Harris et al., 2018; Zhou et al., 2018; Qi et al., 2021), in addition to between JS1 and AOM (Phelps et al., 1998; Cambon-Bonavita et al., 2009; Harrison et al., 2009; Vigneron et al., 2014). Finally, some members of these groups may also be more resilient toward H_2S-rich sediments than others, favoring their selection in CH_4-rich sediments where

AOM is ongoing (Suominen et al., 2021). Our knowledge of these groups in global oceans is limited; the genetic diversity within some of these groups demonstrated different metabolisms and the assignation of habitats to ecotypes has remain generally unresolved (Liu et al., 2018; Zhou et al., 2018).

In addition to prokaryotes, eukaryotes are a microbial group that is often neglected in microbial investigations at cold seeps, despite the observed changes at cold seeps on their community composition and structure (Edgcomb et al., 2007; Takishita et al., 2007, 2010; Olsen et al., 2014; Wang et al., 2014; Takishita, 2015; Kouduka et al., 2017). RNA-based studies have suggested particularly strong activity of ciliates at cold seeps (Takishita et al., 2010). These eukaryotes are generally bacterivorous, suggesting that they can play a role as grazers. However, they are found in a wide range of habitats, including aerobic and anaerobic sediments, and have been observed to adopt to a wide diversity of life strategies (Embley et al., 2003; Rinke et al., 2006; Searcy, 2006; Lynn, 2008). The higher densities of prokaryotes involved directly or indirectly in AOM can therefore be a food source for these potential heterotrophic eukaryotes. However the toxicity of sulfidic may also have an selective effect that impacts eukaryotic growth negatively (Massana et al., 1994; Coyne et al., 2013). Eukaryotic groups thriving in CH_4-rich sediments may also included parasitic species, such as Apicomplexa, that could be benefiting from a higher biomass of larger fauna at cold seeps (Moreira and López-García, 2003; Takishita et al., 2007; Guillou et al., 2008).

A significant number of metabolic processes related to other taxonomic groups at cold seeps, are not presented in this introduction. For instance, while functions related to the nitrogen cycle have not been addressed, nitrogen compounds remain important elements for the distribution of MOB (Lees et al., 1991; Lee and Childress, 1994; Tavormina et al., 2015) and SOB (Han and Perner, 2015). Therefore, the role of microbes involved in the consumption/production of ammonium/nitrate/nitrite likely have a significant impact on the distribution of the functional groups mentioned above. Just as for the groups listed above, distinct nitrogen cycling microbes have also been observed at other cold seeps, but the degree of influence of CH_4-rich fluids on these groups remain poorly understood.

1.3 Objectives

The overall aim with the PhD Thesis was to study the microbial community structure and activity at cold seeps in the northern Barents Sea, with a particular focus on microbes responsible for the oxidation of CH_4. We particularly focused on three gas hydrates bearing pingos retrieved south of Svalbard in Storfjordrenna and along the western coast of Svalbard to present microbial diversity along the migration path of CH_4 from few meters below the seafloor to the water column. The specific objectives were:

1. To assess the prokaryotic and eukaryotic diversity that form the Arctic cold seeps microbial community impacted by CH_4;
2. To study the composition, distribution and activity of methane oxidizing bacteria in cold seep sediments and the Arctic water column;
3. To summarize the interaction between environmental factors and habitats based on the microbial community structure and activity.

2 Materials and Methods

2.1 Sampling area

In the current Thesis, different study sites along the southern and western coast of Svalbard, an Arctic archipelago in the northern Barents Sea, have been investigated. The Barents Sea is located on a continental shelf, with an averaged depth of 230m. The archipelago of Svalbard is placed along the edge of the continental shelf, and water depth vary from few tens of meters along the coastline to 2,000-3,000m depth behind the shelf break toward the Fram Strait.

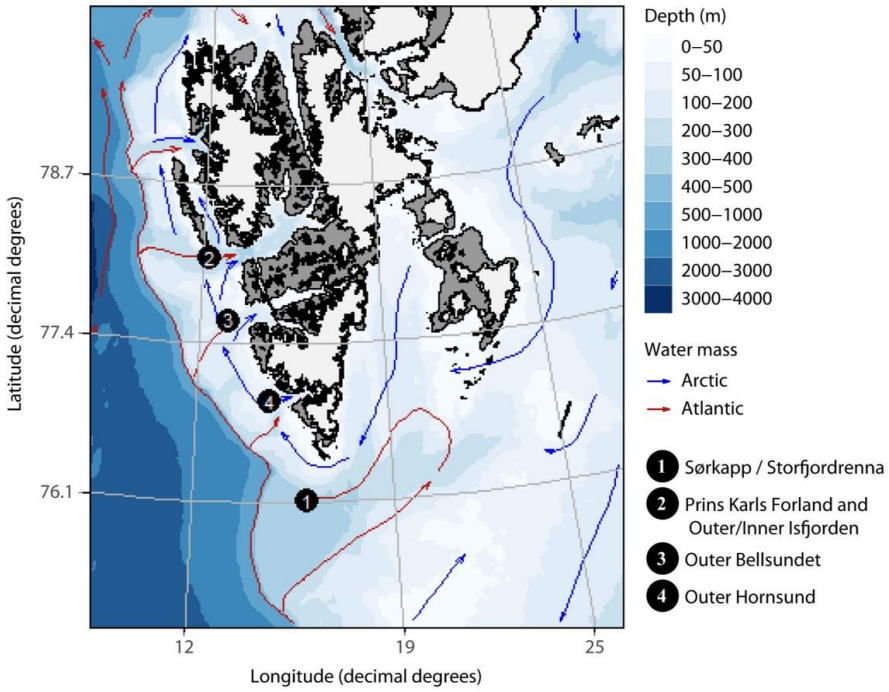

Figure 7: Bathymtric map of the study areas west and south of Svalbard, in the northern Barents Sea, with the illustrated paths of the main Atlantic Water (red arrows) and Arctic Water (blue arrows) masses. Investigations in **Papers I, II and III** were conducted in Storfjordrenna (1) while seawater samples were taken for **Paper IV** nearby Prins Karls Forland and Isfjodren (2), Outer Bellsundet (3) and Hornsund (4), in addition to around Sørkapp.

Storfjordrenna

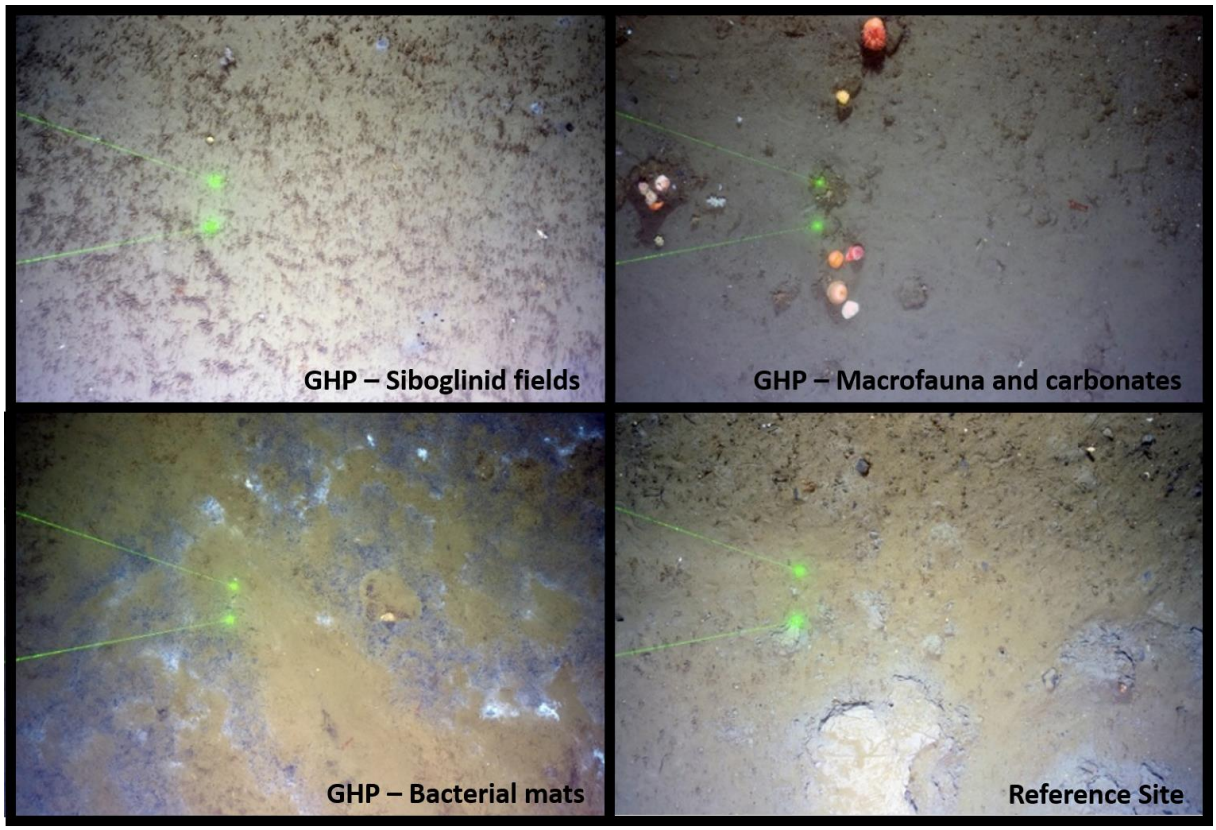

Figure 8: Seafloor characteristics of GHP 1 including fields of siboglinid worms (top left), a diversity of macrofauna attached to carbonates (top right) and large areas covered by bacterial mats (lower left). The distance between the two green lasers is 20 cm. The lower right picture was taken at a reference site outside of the GHPs area and showed a muddier seafloor with little biomass and biodiversity.

Study area in **papers I, II and III** is located at gas hydrate bearing domes that were discovered in Storfjordrenna, at ~390 m below sea level (Figure 7; Serov et al., 2017), south of Svalbard. They are referred to as pingos, after similar terrestrial features observed in glacial valleys (Mackay, 1998), although they differ by their formation (i.e. CH_4 flow pressure and gas hydrates instead of regular water ice; Serov et al., 2017). Hydroacoustic observations have revealed acoustic flares originating from CH_4 gas bubbles in the water column. These were primarily located at the summit on four of the five Storfjordrenna pingos. At the water depth of the gas hydrate pingos (GHP; ~390 m, ~0.5–2.5°C bottom water temperature), the gas hydrates remain within the gas hydrate stability zone (GHSZ), but are close to its upper limit and are sensitive to even small changes of temperature and pressure (Hong et al., 2018). The dating of CH_4 derived authigenic carbonates suggested that CH_4 seepage has been active for several thousand years (Serov et al., 2017) across a chaotic distribution of channels on the GHPs (Waage et al., 2019). Visual observations have revealed a higher biomass in sediments of the

pingos compared to the surrounding seafloor (Figure 8; Åström et al., 2018; Sen et al., 2018a), including the chaotic distribution of large white bacterial mats and fields of siboglinid worms.

Western shelf of Svalbard

In **paper IV**, we focused on the pelagic methanotrophic communities and therefore our study area stretched along the continental margin off western Svalbard. Study sites include the shallow shelf west of Prins Karls Forland towards the southern tip of Svalbard including Isfjorden, Isfjorden Trough, Outer Bellsundet, Outer Hornsund, and Sørkappøya (Figure 7). Water depth in these areas ranges from 50 to 160 m. The shallow shelf west of Prins Karls Forland is characterized by an irregular bathymetry showing numerous large depressions encompassed by a series of moraine ridges termed the Forlandet moraine complex (Landvik et al., 2005). Here, along the Forlandet moraine complex in 80–90 m water depth, a vast number of gas flares (~200 flares, identified by acoustic signatures of gas bubbles in the water) were previously mapped (Sahling et al., 2014; Silyakova et al., 2020).

2.2 Sampling procedure

Samples analyzed within the different publications and manuscript were taken during several CAGE research campaigns (Table 1) onboard research vessels R/V Helmer Hanssen and R/V Kronprins Haakon. Sediments samples were taken using various platforms and tools. Those sampling platforms included a TowCam-Multicore System (TC-MC), a Remotely Operated Vehicle (ROV) and a gravity corer (Figure 9). The ROV is a submersible vehicle that is controlled from the ship. It has its own propelling system, allowing operations requiring manoeuvers on the seafloor and can be equipped with different sampling tools. The TC-MC is also lowered from the boat, but it is dragged by the movement of the ship. On both ROVs and TC-MC a live camera system was mounted that allowed the visual observation of the seafloor (Daniel et al., 2003). On research campaigns CAGE 16-5 and 18-5, the use of ROV allowed to precisely target features of the cold seep ecosystem, such as CH_4 gas flares, bacterial mats and worm fields. The arms of the ROVs were used to deploy either push cores or blade cores to sample sediments.

Table 1: Research campaigns where samples analyzed in the different papers of this Thesis. Information regarding the dates, the location, the sample type (sediment or water samples) in addition to the publications in which samples from this campaign were used is listed. In superscript is indicated the vessel (R/V Helmer Hanssen or R/V Kronprins Haakon) on which the research campaign was performed. The * indicated campaigns where VC participated.

Research campaign (date)	Location	Sample type	Publication
CAGE 15-3[1] (1-3/07/2015)	Western shelf of Svalbard	Water	Paper III
CAGE 16-4[1] (2-4/05/2016)	Western shelf of Svalbard	Water	Paper III
CAGE 16-5[1] (16/06-04/07/2016)	Storfjordrenna, Western shelf of Svalbard	Sediments, Water	Papers I, II, III
CAGE 17-1[1] (16-20/05/2017)	Western shelf of Svalbard	Water	Paper III
CAGE 17-2[1*] (21/06-03/07/2017)	Storfjordrenna	Sediments	Paper I
CAGE 18-5[2*] (22/10-02/11/2018)	Storfjordrenna	Sediments	Paper III

[1]Research campaign done onboard R/V Helmer Hanssen

[2]Research campaign done onboard R/V Kronprins Haakon

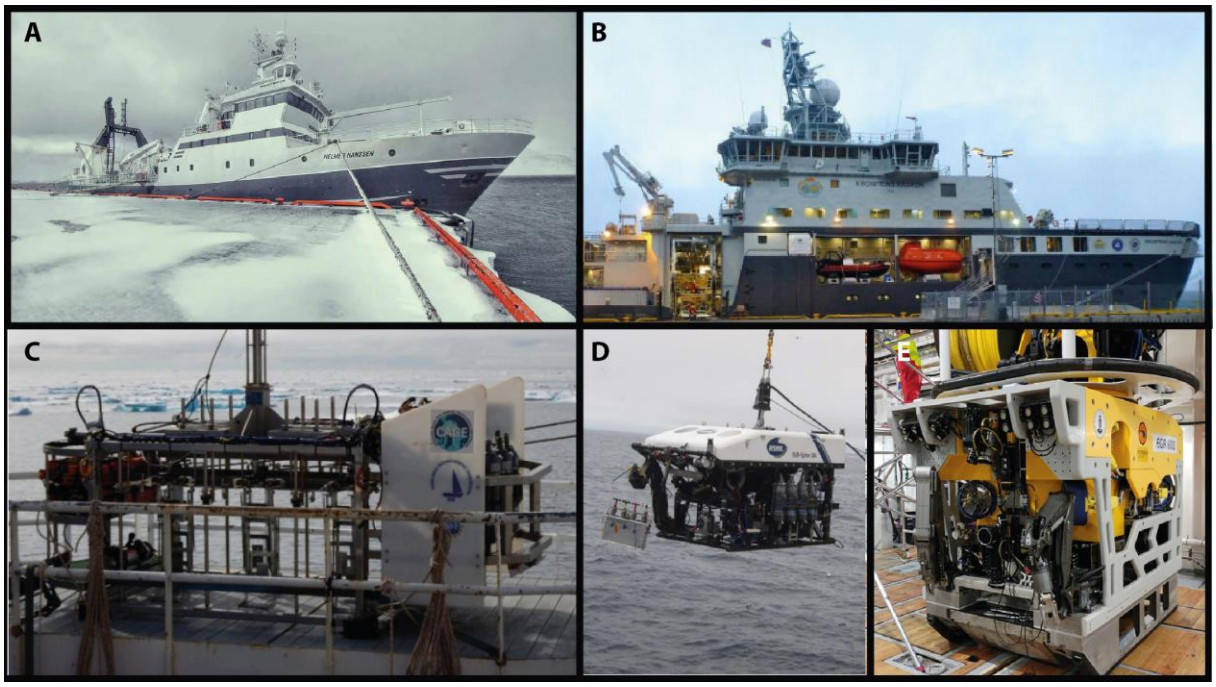

Figure 9: Fieldwork campaigns were performed onboard the vessels (A) R/V Helmer Hanssen and (B) R/V Kronprins Haakon. To sample sediments, a (C) TowCam-Multicore System and two (D-E) remotely operated vehicles were used to deploy push and blades cores.

The TC-MC performs less precise sampling compared to the ROV: the platform cannot move itself and relies on the movements of the ship to target sites and it is not possible to visualize the seafloor characteristic specifically sampled by each core of the multicore system. However, the platform is cost efficient and easier to implement. In addition, the platform allowed us to collect several cores in a short period of time. Finally, the sediment depth sampled with the coring systems of both ROVs and TC-MC was generally limited to 30 to 40 cmbsf, at some locations even down to 15 cmbsf. The use of a gravity corer allows sediment sampling up to approximately 3 meters below seafloor (mbsf). However, it is a time-consuming sediment coring system and is generally preferred for a limited number of cores. Hereby, combining the different sediment sampling platforms allowed to investigate the microbial ecosystem at the Storfjordrenna GHPs at various scale. Further processing for the retrieved sediment cores was immediately performed either on deck or in cold rooms.

2.3 Environmental geo- and physico-chemistry

Within sediments (**Papers I, II, III**), CH_4 was measured with a head space technique and gas chromatography equipped with a flame ionization detector (Hoehler et al., 2000; Panieri et al., 2017). For this, 3 mL of bulk sediments at selected 2 cm intervals in a core were immediately transferred to a 20 mL headspace vial with 7mL of NaOH solution (1M) and two glass beads,

before being instantly capped. After an equilibration period of 24h, samples were analyzed and porosity was determined from weight and volume measurements (Boyce, 1973). In **Paper I**, alkalinity and dissolved iron was measured onboard by titration and by spectrophotometry. Sulphate and H_2S were measured onshore using ion chromatography and a spectrophotometer, respectively(Cline, 1969; Hong et al., 2017). In **Paper III**, probes were used to measure *in situ* concentrations of oxygen and sulfur. Microsensor profiling of the oxygen in the upper sediments was performed using a miniaturized 100 µm width Clarks type electrode (OX-100, Unisense, Aarhus, Denmark) and a microsensor multimeter (Unisense, Aarhus, Denmark). Oxygen concentrations were profiled vertically, perpendicular to the surface of the sediment, with a resolution of 100 to 250 µm using a motorized micromanipulator. Sulfur was measured using a micro sensor that converts H_2S into HS^- ions in the electrode tip, which contained alkaline electrolyte. It is then immediately oxidized by ferricyanide, producing sulfur and ferrocyanide. The sensor signal is generated by the re-oxidation of ferrocyanide at the anode within the tip of the sensor (Jeroschewski et al., 1996).

For the physicochemical profiles of the water column in **Paper IV**, hydrographic parameters (salinity, temperature, pressure) were recorded at 24 Hz with a Conductivity-temperature-depth profilers (SBE 911 plus CTD; Sea-Bird Electronics, Inc., USA). With the CTD-mounted Niskin bottles, we collected discrete water samples from selected depths to measure CH_4 concentrations.

2.4 Microbial communities

Amplification of environmental total nucleotides, sequencing and sequences analyses

For **Papers I, II and III**, sediment cores were extruded, and 2 cm thick layers were transferred in Whirl-Pak® sterile sampling bags (Nasco, United States) and stored at -80°C. For **Papers I and II**, following the measurements of the different environmental parameters in the laboratory, 55 samples were selected for amplicon libraries sequencing. These samples were selected at regular depths (surface, ~5, ~10, and ~15 cm) and at clear geochemical interfaces as detected by porewater geochemical gradients (e.g., SMTZ). Sediments were manually ground and homogenized in liquid nitrogen using a sterilized mortar. The DNA was extracted using the DNeasy PowerSoil Kit (Qiagen, Germany). For **Paper III**, the top 2 cm sediment layer were similarly transferred in sterile sampling bags. However, samples were homogenized using a TissueLyzer II (Qiagen, Germany) and the total nucleotides were extracted following a phenol/chloroform extraction protocol (Griffiths et al., 2000; Urich et al., 2008). Seawater

samples for molecular analysis (**Paper IV)** were collected in sterile, high-density polyethylene bottles and usually processed immediately after subsampling. We filtered a volume of 1 liter of sample on membrane filters (Whatman Nuclepore Track-Etched PC, 0.22 μm, Merck Millipore. Total DNA from membrane filters was extracted following the method of Pilloni et al. (2012).

All samples for molecular community analyses were sent to the IMGM Laboratories GmbH for library preparation and amplicon sequencing. Prokaryotic communities for each sample in our studies were investigated by the amplification of the V3-V4 region of 16S rRNA gene using the same pair of degenerate primers (Alm et al., 1996; Jorgensen et al., 2012; Klindworth et al., 2013), while eukaryotic communities in **Paper I** were amplified using 18S rRNA gene degenerate primers to target the V4 region (Hugerth et al., 2014). For **Papers III and IV**, the bacterial methanotrophic communities were investigated using a modified pair of degenerated primers targeting the particulate monooxygenase gene (*pmoA*) adapted for the marine environment (Tavormina et al., 2008). Library generation was conducted in accordance with the company's protocols before being sequenced using a Miseq System (Illumina inc., United States). Paired-end nucleotide reads were deposited at Sequence Read Archive Genebank as BioProjects, with the exception of sequences from Paper IV which will be available upon the submission of the manuscript to a journal. Subsequently, obtained sequences were quality filtered (generally following the suggested USEARCH protocol[1] with USEARCH v.10.0.240; Edgar, 2010) before being clustered in OTUs at 97% similarity for 16S and 18S rRNA gene libraries, and at 86% similarity for *pmoA* libraries (Wen et al., 2016), estimated to represent diversity at the genus level. Representative sequences from the OTUs were thereafter assigned to taxonomy using the SILVA database v132 (**Papers II and IV)** and the SILVA database v138 (**Papers I and III)** (Quast et al., 2012; Yilmaz et al., 2014). Libraries built from *pmoA* gene were assigned using the database published by Yang et al. (2016). Subsequent statistical analyses varied between the different manuscripts. Therefore, please find the details within the respective publications or manuscript.

[1] http://drive5.com/usearch/manual/uparse_pipeline.html

Complementary microbial community and activity analyses

Additional to the amplification and sequencing of environmental nucleotides, we used complementary methods throughout the different studies. In **Paper II**, we used fluorescence-in-situ-hybridization (FISH) to visually observe the densities of ANME and SRB cells. We performed FISH using double-labelling-of-oligonucleotide-probes (DOPE; Stoecker et al., 2010) for Archaea (ARCH915; Stahl, 1991) and Desulfobacteraceae (DSS658; Mußmann et al., 2005). Imaging was done with a confocal laser scanning microscope.

In **Paper IV**, we combined microbial community analyses based on libraries of the 16S rRNA and *pmoA* genes with measurements of oxidation rates to monitor microbial activity in the water column. We used ex situ incubations with trace amounts of tritium-labelled CH_4 (C^3H_4), allowing tracing of ^3H-label transfer from the substrate to the MOx product pool, to measure MOx rates by measurement of the activities of the produced ^3H_2O.

3 Summary of Papers

3.1 Paper I: The Impact of Methane on Microbial Communities at Marine Arctic Gas Hydrate Bearing Sediment

Cold seeps are characterized by high biomass, which is supported by the microbial oxidation of the available CH_4 by capable microorganisms. The carbon is subsequently transferred to higher trophic levels. South of Svalbard, five geological mounds shaped by the formation of CH_4 gas hydrates, have been recently located. Methane gas seeping activity has been observed on four of them, and flares were primarily concentrated at their summits. At three of these mounds, and along a distance gradient from their summit to their outskirt, we investigated the eukaryotic and prokaryotic biodiversity linked to 16S and 18S rRNA gene. Here we show that local CH_4 seepage and other environmental conditions, particularly the availability of O_2 and CH_4, did affect the microbial community structure and composition. We could not demonstrate a community gradient from the summit to the edge of the mounds, in contrast to what is found at mud volcanos. Instead, a similar community structure in any CH_4-rich sediments could be retrieved at any location on these mounds. Both prokaryotic and eukaryotic communities were similarly influenced by the porewater geochemistry, as dissimilatory analyses revealed that formed clusters for each Domain usually included the same sediment samples. The oxidation of CH_4 was largely driven by ANME-1 and the communities also hosted high relative abundances of SO_4^{2-} reducing bacterial groups although none demonstrated a clear co-occurrence with the predominance of ANME-1. This ANME was represented by a single OTU that was distributed over a 2.5 km^2 area, highlighting its importance for the local ecosystem. In contrast to ANME, MOB were only detected at the gas flare. The absence or low detection of CH_4 detected near sediment surface could be a factor in MOB distribution. Additional common taxa were observed, and their abundances were likely benefiting from the end products of CH_4 oxidation. Sulphide-oxidizing Campilobacterota *Sulfurimonas* and *Sulfurovum* were particularly abundant at the gas flare and could be detected in communities above ANME-1 dominated sediment layers, although at a lower fraction. Other bacteria able to use the H_2S generated by AOM, such as *Beggiatoa*, could not be detected. The higher microbial biomass also likely explained the higher observed abundance of organic matter degraders, such as Bathyarchaeota, Woesearchaeota, or thermoplasmatales marine benthic group D, and heterotrophic ciliates and Cercozoa.

3.2 Paper II: Methane-fuelled biofilms predominantly composed of methanotrophic ANME-1 in Arctic gas hydrate-related sediments

Sedimentary biofilms comprising microbial communities mediating the anaerobic oxidation of CH_4 are rare. Here, we describe two biofilm communities discovered in sediment cores recovered from Arctic cold seep sites (gas hydrate pingos) in the north-western Barents Sea, characterized by steady CH_4 fluxes. We found macroscopically visible biofilms in pockets in the sediment matrix at the depth of the SMTZ, at ~70 and ~300 cm below seafloor. 16S rRNA gene surveys revealed that the microbial community in one of the two biofilms comprised exclusively of putative anaerobic methanotrophic archaea of which ANME-1 was the sole archaeal taxon. However, two genetically different ANME-1 OTUs dominated each biofilm and were also distinct from the ubiquitous ANME-1 OTU from Paper I. The bacterial community consisted of relatives of SRB belonging to uncultured Desulfobacteraceae clustering into SEEP-SRB1 (i.e. the typical SRB associated to ANME-1), and members of the atribacterial JS1 clade. The biofilm retrieved at a shallower depth showed nevertheless a higher biodiversity, where the archaeal groups Bathyarchaeia, Thermoplasmata and Woesearchaeia, in addition to the bacterial groups Aceothermiia and Chloroflexi, were also detected. The co-existence of ANME-1 and SEEP-SRB1 could support the hypothesis of a consortium to perform anaerobic oxidation of CH_4. However, the confocal laser scanning microscopy demonstrates that this biofilm is composed of multicellular strands and patches of ANME-1 that are loosely associated with SRB cells and were not tightly connected in aggregates. This observation differs from previously observed wall-to-wall clusters of ANME and SRB observed, suggesting different mechanisms on how AOM is mediated. This discovery of methanotrophic biofilms in sediment pockets closely associated with CH_4 seeps constitutes a hitherto overlooked and potentially widespread sink for CH_4 and SO_4^{2-} in marine sediments.

3.3 Paper III (manuscript): Niche differentiation of prokaryotic communities and aerobic methanotrophs in surface sediments of an Arctic cold seep

At cold seeps in the Storfjordrenna, south of Svalbard, distinctive features characterized the sediment seafloors: white bacterial mats, dense fields of siboglinids and zones where CH_4 gas flares were emitted from the seafloor. These different features are suggested to present different geochemical characteristics of the pore water, thereby influencing the microbial biodiversity. However, our knowledge on this biodiversity at sediment surface of Arctic cold seeps, and how particularly the functional group of MOB is influenced within these different microhabitats, is limited. In this study, we collected two clusters of nearby sediment cores covering those different features. Geochemistry analyses of the porewater revealed steep changes where CH_4 and HS^- concentrations were higher and shallower at gas flare and below bacterial mats. In contrast, penetration of O_2 was deeper in fields of siboglinids. We investigated thereafter for each sediment cores surface layers the prokaryotic biodiversity linked to 16S rRNA gene and attempted at identifying key aerobic methanotrophs based on the 16S rRNA and the *pmoA* genes. Dissimilatory analyses demonstrated distinct community composition for both Archaea and Bacteria. At CH_4 gas flares, the Archaea were characterized by the detection of ANME-1, the same OTU retrieved in Paper I, near the surface. Archaeal within siboglinid fields were instead distinct from the composition of Woesaerchaeota. Bacterial communities at CH_4 gas flares were largely dominated by the SOB Campylobaterota. The relative abundance of SOB is reduced at other features and *Beggiatoa* became only detected at the edges of bacterial mats. SOB in fields of siboglinids were barely detected, despite that SOB endosymbionts were detected in these worms. Another key bacterial functional group investigated was the MOB. Relative abundances of Methylococcales were higher at CH_4 gas flares and within bacterial mats, and both 16S rRNA and pmoA gene analyses suggest CH_4 oxidation to be mediated by three bacteria: one methanotroph appeared to growth preference at CH_4 gas flare, while another one was more predominant within bacterial mats. The latter showed limited genetic similarity to available sequences on sequence databases. Finally, the third one showed an approximately homogenized distribution. Bacterial groups also demonstrate different community structure where siboglinid fields contained a higher diversity of abundant groups. These included representatives of Chloroflexi, Desulfobacterota, Steroidobacterales and Verrucomicrobiota. Overall, our study demonstrates distinct microbial communities, suggesting key activity rates, including CH_4 and HS^- oxidation, to vary between these habitats.

3.4 Paper IV: Seasonal shifts of microbial methane oxidation in Arctic shelf waters above gas seeps

The Arctic Ocean subseabed holds vast reservoirs of the potent greenhouse gas CH_4, often seeping into the ocean water column. Today, CH_4 is largely retained in the water column due to physical processes, but also by the activity of MOB that thrive there. Predicted future oceanographic changes, bottom water warming and increasing CH_4 release may alter efficacy of this microbially mediated CH_4 sink. Here we investigate the composition and principle controls on abundance and activity of the MOB communities at the shallow continental shelf west of Svalbard, which is subject to strong seasonal changes in oceanographic conditions. Covering a large area (364 km^2), we measured vertical distribution of MOx rates, MOB community composition, dissolved CH_4 concentrations, temperature and salinity four times throughout spring and summer during three consecutive years. Temperature and salinity were used to identify the water masses. We found highest MOx rates (7 $nM\,d^{-1}$) in summer in bathymetric depressions filled with stagnant Atlantic Water containing moderate concentrations of dissolved CH_4 (< 100 nM). MOx rates in these depressions during spring were much lower (< 0.5 $nM\,d^{-1}$) due to lower temperatures and mixing of Transformed Atlantic Water flushing MOB with the Atlantic Water out of the depressions. Sequencing analyses of the *pmoA* gene revealed a small, relatively uniform community mainly composed of type-Ia methanotrophs (deep-sea 3 clade). Our results show that MOB and MOx in CH_4-rich bottom waters are highly affected by geomorphology and seasonal conditions.

4 Results and Discussion

The primary goal of this Thesis was to provide new insights on the microbial community structure and activity at cold seeps in the Arctic Ocean, presenting cold seeps under different dimensions (Figure 10).

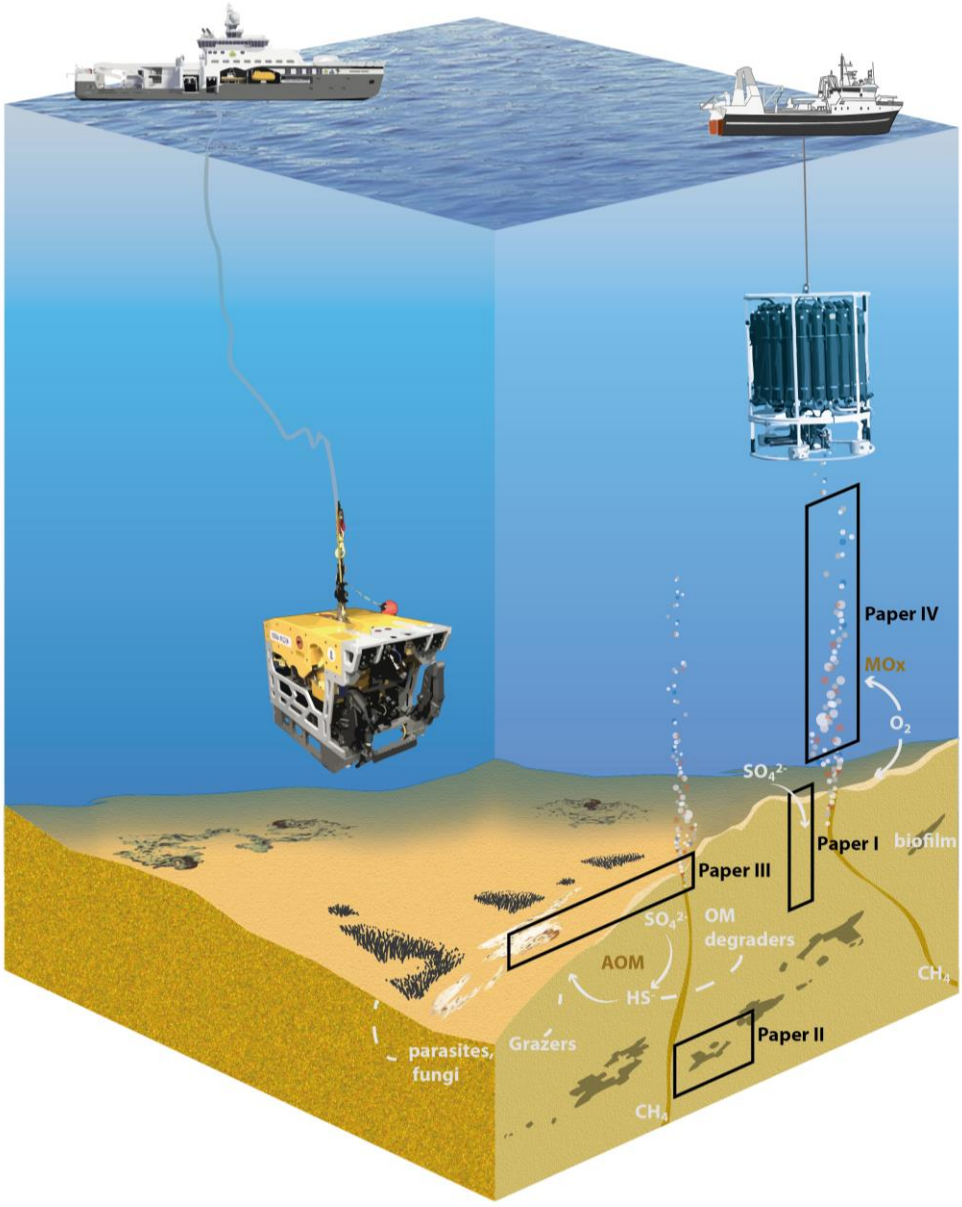

Figure 10: Illustrational overview of studies included in this Thesis and some of the devices used for sampling (ROV on the left, and CTD-rosette on the right, section 2.2). Major microbial interactions and environmental influences at gas hydrate bearing pingos in Storfjordrenna, including AOM in anaerobic sediments and MOx in the oxygenated water column and surface sediments are shown. The illustration also depicts the areas of interest in which the different publications are focusing on, i.e. microbial communities along depth gradients (**Paper I**), in a biofilm in deeper sediments (**Paper II**), along different niches in surface sediments (**Paper III**) and in the water column (**Paper IV**). Figure was made by Rudi Caeyers, UiT The Arctic University of Norway.

Throughout this Thesis, we have been able to describe the whole microbial communities at cold seeps along the migration path of CH_4 along vertical and horizontal gradients, in addition to above, on and below the seafloor (Figure 10). The combination of **all papers** shows the microbial community shifts in CH_4-rich environments from deeper anoxic sediments toward aerobic surface sediments and seawater. This Thesis illustrates the structure of microbial communities of various sections of an arctic cold seep along the upward flow of CH_4 (Figure 10), including: (1) rarely observed ANME-1 biofilms in deep sediments (**Paper II**), (2) the shallow anaerobic sediments (<40 cm depth) (**Paper I & III**), (3) the surface sediments (**Paper III**), and (4) the oxygenated overlaying water column (**Paper IV**). We integrated horizontal gradients in community composition, both at large scale (>20m distance between sediment cores) and smaller scale (<1 m distance between cores) across various microhabitats.

Such combination of studies combined in this Thesis presents one of the most thorough microbial investigations at a cold seeps site. Its importance is further strengthened as most of the well studied CH_4-fuelled microbial systems are located at low and mid latitudes. Furthermore, multiple observations of similar GHPs in other Arctic Seas (Paull et al., 2007; Serov et al., 2015; Savvichev et al., 2018). My work presents thereby a strong background for further studies on microbial community structures and functions at marine cold seeps in the Arctic. I will further discuss below the novelty of our findings, and I will address especially (i) how the cold seeps in Storfjordrenna do compare to other CH_4 seeping sites, (2) how the local geochemical/geohydrological settings within the sediments and the overlaying seawater at studied cold seeps affect the composition of the microbial communities in the Arctic, and (3) what the key drivers for microbial methane oxidizing along the southern and western coastline of Svalbard are. Through each section I will place the main findings in perspective to the current knowledge of cold seep ecosystems and I will open the discussion for further questions needed to be answered.

4.1 Biogeochemistry of cold seeps in the Arctic

Two of the GHPs (GHPs 1 & 3) showed gas flare activity visible on echo sounder, while none was found on GHP 5 (**Papers I & III**). These gas flares have been mainly observed at the apex of the mounds, suggesting thereby higher CH_4 fluxes and concentrations. Nevertheless, our visual surveys using ROVs also revealed flares several tens of meters away from the apex of GHP 3 (**Paper III**). Through the measurements of geochemical parameters at the GHPs (**Papers I, II & III**), we identified SMTZs at various depths ranging from 15 cmbsf at GHP 1

(**Paper I**) and 8-10 cmbsf at GHP 3 (**Paper III**) to >300 cmbsf (**Paper II**). Similarly to the distribution of CH_4 gas flares, sediment cores characterized by shallow SMTZ (< 30 cmbsf) were found at various distances from the apex of GHPs 1 or 3, presenting a heterogeneous distribution of CH_4 fluxes in the investigated area, causing subsequently the observed patterns of microhabitats dispersed on the GHPs. This suggests a more chaotic distribution of CH_4 in the sediments at these mounds than at other CH_4-derived geological structures, such as the HMMV, which is characterized by a stronger CH_4 flux in the center with a specific microbial assemblage (Beer et al., 2006; Niemann et al., 2006; Lösekann et al., 2007). The active center of HMMV is surrounded by transition zones of few hundreds' meters length with shifts in both environmental conditions and microbial communities.

Our analyses of the porewater geochemistry in **Paper III** showed microhabitats separated only by less than a meter resulting in steep gradients in O_2, CH_4 and HS^-. Such heterogeneity is important to consider for future investigation. Despite the particularities of the GHPs mentioned above, similar range of SMTZ depths, in addition to comparable profiles of H_2S and O_2, have also been observed at other cold seeps, such as along the Nyegga Ridge further south in the Barents Sea (Roalkvam et al., 2012). This makes the GHPs a suitable location to compare the microbial communities found at the GHPs with more southern cold seeps.

4.2 Microbial community changes in CH_4-rich Arctic environments

In **Paper I**, distant sediment cores shared higher community similarity under the presence of CH_4 than two nearby cores with contrasting porewater characteristics. Similar observations were made in surface sediments in **Paper III** where communities retrieved from similar microhabitats (CH_4 gas flares, bacterial mats, siboglinid fields) shared higher similarity than two proximate cores. Our results are therefore aligned with a stronger role of environmental selection rather than geographical barriers in determining the microbial community composition in these environments, supporting the Baas Becking hypothesis where "everything is everywhere, but the environment selects" (Becking, 1931; Wit and Bouvier, 2006). Nevertheless, pelagic communities in **Paper IV** showed strong dissimilarity between different water masses, suggesting that the relative weight of geographical barriers in the establishment of local microbial communities could be more predominant in the water column. The dominating ANME-1 OTU retrieved from the GHPs in **Papers I, II & III** shared highest similarity with environmental sequences retrieved from along the eastern Asian coast, supporting the widespread distribution of few identical OTUs at global cold seeps (Ruff et al.,

2015). It is possible therefore that our findings in the composition of microbial communities is reflective of communities at other cold seeps in the northern Barents Sea and Fram Strait. Determining the biogeography of the different taxonomic groups is an important aspect for future studies to anticipate the colonization of new CH_4-rich locations on the seafloor that could emerge from new sources of CH_4 releases originating from the dissociation of shallow gas hydrates as a consequence of the increase of bottom water temperature.

Another particular aspect of this Thesis is that it contains a thorough analysis of the biodiversity of Archaea, Bacteria and Eukarya Domains within the same study, where the latter has often been ignored in microbial investigations on marine cold seeps. In **Paper I**, our results further supported the importance of eukaryotes inCH_4-rich sediments at cold seeps presenting a high relative abundance of sequences assigned particularly to ciliates, Cercozoa and parasites-related genera. These may hold potential roles as sources of top-down pressure on other microbes and megafauna via parasitology or predation, or through hosting SOB or MOB as symbionts. Their contribution to the uptake of CH_4-originated carbon in the food web remains still poorly understood but could represent missing links in the cold seep ecosystems. Our findings strongly emphasize the need for additional studies on the role of eukaryotes at cold seeps.

4.2.1 Anaerobic sediments

Overall, prokaryotic groups retrieved from GHP sediments were not unique in comparison to the reference community (i.e. communities thriving in the surrounding CH_4-poor environment) or to other cold seeps. The predominant taxonomic groups found in the GHP sediments (**Papers I, II & III**; Figure 11) were the archaeal ANME-1 clade, the thermoplasmatales MBG-D and the Nanoarchaiea Woesearchaeota. They were also regularly found in CH_4-poor sediments, although at lower relative abundances, outside of the GHP area, similarly to the bacterial SO_4^{2-} reducers Desulfobacterota, including seeps-related clades SEEP-SRB1 and SEEP-SRB2, the atribacteria JS1 group and Chloroflexi. The diversity and role of ANME-1 in AOM at the GHPs is further discussed in subsection 4.3.1.

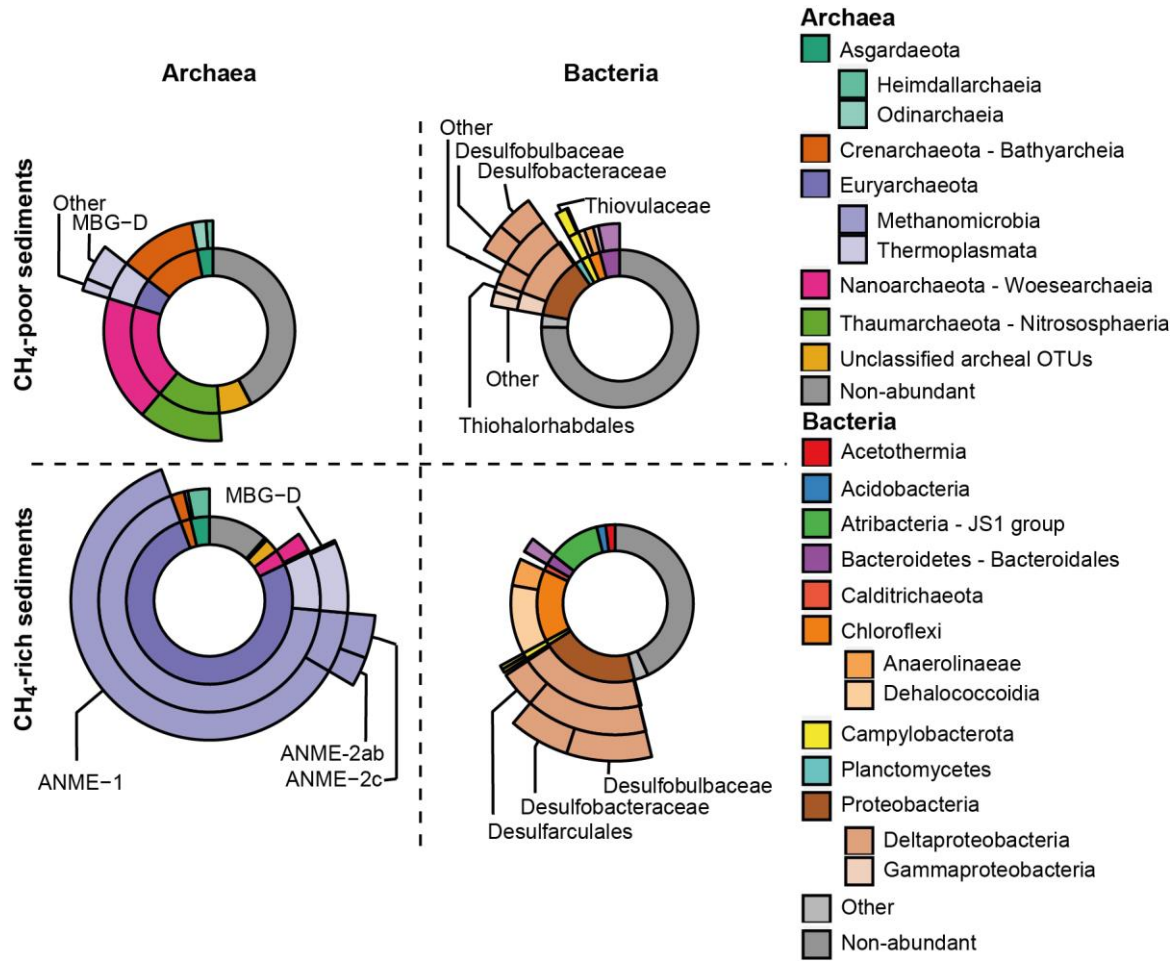

Figure 11: Archaeal (left diagrams) and bacterial (right diagrams) typical communities of abundant OTUs retrieved in anaerobic CH_4-poor and –rich sediments. The group non-abundant includes all sequences assigned to OTUs that did not represent at least 1% of the sequence in one sample.

Yet, preliminary analyses at the OTUs level for the Woesearchaeota presented in **Papers I & III** demonstrated that CH_4- and H_2S-rich sediments favor the growth of few abundant OTUs that are not present (or only in low abundance) in sediments, which are less influenced by CH_4 seeping activity. Woesearchaeota, similarly to the thermoplasmatales MBG-D or the Bathyarchaiea, are vast genetically diverse clades of uncultivated representatives that can also possess a wide variety of metabolisms - a hypothesis supported by preliminary metagenomic analyses (Liu et al., 2018; Zhou et al., 2018). Filling gaps of knowledge related to these groups could potentially demonstrate additional traits in the vertical succession of other groups than ANME-1, highlighting additional particularities of cold seeps at high latitudes.

4.2.2 Aerobic sediments and water column

The seafloor at the GHPs primarily featured four distinct microhabitats: CH_4 gas flares, large white bacterial mats, dense siboglinid fields and areas of regular surface sediments showing no

particular features. These different habitats also enhanced niche differentiation in the prokaryotic communities, especially within the H_2S oxidizers. H_2S-rich sediments, at the CH_4 gas flares and bacterial mats were mainly composed of the Campylobacterota Sulfurovaceae and Sulfurimonadaceae. At the GHPs, the gammaproteobacterial *Beggiatoa*, typically found in bacterial mats at other cold seeps (Barry et al., 1996; Mills et al., 2004; Zhang et al., 2005; Grünke et al., 2011) were instead found in high relative abundance toward the edges of bacterial mats and siboglinid fields. This shift of SOB is potentially caused by the availability of H_2S, where the free-living Campylobacterota are not able to store nitrate and/or oxygen and migrate toward H_2S-rich sediment layers, in contrast to the *Beggiatoa* (McHatton et al., 1996). Finally, the fraction of H_2S oxidizers was smaller within the siboglinid fields, but the known chemosynthetic endosymbionts SOB were also not detected (Sen et al., 2018b). The absence of SOB in siboglinid fields could be due to their presence in the lower section of tubeworms, below the sampled depth.

While we were speculating about the suitable adaptation of each SOB to its respective habitat, questions arose on how this succession was established. Environmental characteristics could cause the spatial distribution of SOB, but it was also suggested that the SOB could follow a temporal succession (Patwardhan et al., 2018). Furthermore, at the HMMV, it was reported that bacterial mats and tubeworm fields did not overlap (Beer et al., 2006; Niemann et al., 2006), but at the GHPs we observed overlaps of siboglinid fields and bacterial mats. Expanding our knowledge on SOB at arctic cold seeps could further fill the gaps of knowledge in understanding the establishment of these oasis of life within those special habitats.

Another key process in aerobic environments we identified is the aerobic oxidation of CH_4. We observed a higher relative abundance of MOB within the 16S rRNA gene libraries at gas flares and within bacterial mats in contrast to fields of tubeworms or without noticeable features. Similar preliminary observations could be made at a gas flare at the GHPs described in **Paper I**, being the only site characterized by more than 1% of the sequences assigned to the Methylococcales in the surface sediment. While CH_4 gas flares are sporadically distributed on the GHPs, bacterial mats occupy large areas on the GHPs and MOx could therefore play an important role in filtering CH_4. Biodiversity of MOB will be further discussed in section 4.3.

4.3 Methane oxidation at arctic cold seeps

4.3.1 Anaerobic methane oxidizing ANME-1

In **Papers I and II**, we noted the predominance of ANME-1 throughout all samples; a community profile distinctive from most global cold seeps that are typically dominated by ANME-2 (Ruff et al., 2015). We showed that a single ANME-1 OTU dominated regardless of CH_4 and H_2S concentrations or depth. In contrast, representatives from ANME-2 were never found to predominate in any sediment layers, including the layers above the SMTZ. Yao et al. (2021) demonstrated a strong influence of ANME-1 at Vestnessa Ridge, in the Fram Strait along the northeastern coast of Svalbard. Thereby, the ANME-1 OTU ubiquitous in my studies, or closely genetically related representatives, could potentially be responsible of most of the AOM in the northern Barents Sea and the Arctic Ocean basin.

Another particular finding about this ANME-1 is the absence of correlation with any particular sulphate-reducing bacteria groups. At global cold seeps, representatives of ANME-1 have been known to form these consortium with representatives of the SEEP-SRB1 or -2 groups (Knittel et al., 2003, 2005; Knittel and Boetius, 2009). In **Paper II**, we show that we have found a high representation for both ANME-1 and SEEP-SRB1, and these observations would support the assumption that ANME-1 would be mediating AOM in synthrophy with SEEP-SRB1. However, the abundance of the different ANME and SRB groups change along the SMTZ within two sediment cores taken at GHP 1 (**Paper I**) demonstrated different patterns of distribution of SEEP-SRB groups. Furthermore, the detection of ANME-1 at CH_4 gas flares at the GHPs described in **Paper III** could not correlate with the detection of any SEEP-SRB groups. Overall, our findings have revealed particular traits of an ANME-1, demonstrating potentially different metabolism to the generally assumed traits of this clade. Further approaches are needed to better understand this ubiquitous ANME-1 OTU in Storfjordrenna. Extending the use of microscopic platforms, such as FISH, particularly along the SMTZ, would allow to confirm or infirm the agglomeration of ANME-1 and SRB cells. Using metagenomics analyses could further describe pathways for both taxa.

4.3.2 Aerobic methane oxidizers

We used both *pmoA* and 16S rRNA genes to investigate the MOB communities in the water column (**Paper IV**) and in surface sediments (**Paper I & III**). Both the water column and the surface sediments presented a different composition of methanotrophic communities, whereas most dominating OTUs in the *pmoA* libraries belonged to the uncultivated clades Deep-Sea

Clusters (DSC) 1 and 3 within the Methylococcales. One particularly abundant OTU in the surface sediment also belonged to the Methylomonas-like group. Overall, OTUs belonging to the DSC1 dominated surface sediments while DSC3 was more predominant in the seawater (**Paper IV**). Such distinction between the pelagic and benthic systems has been observed at multiple cold seeps (Tavormina et al., 2008), although both DSC groups were alternatively found in both environments (Knief, 2015), preventing further assumption on their ecological preferences. In **Paper III**, we present the occurrence of two possibly different MOB presenting contrasting distribution patterns both assigned to the DSC1, but in two different subclades. Those patterns were visible concomitantly within the *pmoA* and 16S rRNA gene libraries, further strengthening the interpretation of our results. Various environmental factors were found to influence the composition of aerobic methanotrophic communities, including levels of CH_4, O_2 and H_2S (Hernandez et al., 2015; Mayr et al., 2020; Delgado Vela et al., 2021). In **Paper III**, we could not clearly explain why the MOB community shifted between dominance of different aerobic methanotrophs based on these environmental parameters. Further studies on cultivation experiments would be required to identify these MOB and the growing factors that caused these distribution patterns. In addition, these differences could also be represented in their CH_4 oxidation ability, impacting future estimates on the CH_4 oxidation activity at the GHPs.

5 Conclusion

In this project, microbial communities at CH_4 seeping sites in the northern Barents Sea demonstrated a contrasting composition compared to the surrounding environment, both within the sediments and the water column. In the following, I like to summarize the biological fate of CH_4 following its migration upward through the sediments and to the sea surface and I will highlight key microbial groups, which are influencing this process:

1- <u>Anoxic sediments:</u> The CH_4 is first anaerobically oxidized primarily by **ANME-1**. These were found ubiquitous at the seeping sites and while **SRB** were also abundant, both groups did not show significant correlation. Both ANME and SRB were shown at the GHPs to dominate the composition of biofilms, an uncommon feature observed at other cold seeps. Within the same anoxic sediments, other key prokaryotic groups demonstrating high relative abundances and that were suggested to be involved in different organic compounds degraders included the archaeal **thermoplasmatales MBG-D**, the **Asgardarchaeota** and the **Woesearchaeota**. Within the Bacteria, **Chloroflexi** was particularly abundant in deeper sediments whereas

Campylobacterota was primarily abundant in deeper sediments only at a gas flare. At the GHPs, the chaotic distribution of faults through which the CH_4 escapes create a similar distribution of the microbial communities. Two communities further distant but with similar environmental conditions were more similar at the OTUs level than two sediment cores taken nearby.

2- Aerobic sediments: The chaotic dispersal of CH_4 seeping through the sediments at the GHPs and the consequential distribution of H_2S generated from AOM contributed to the observed tumultuous dissemination of bacterial mats, siboglinid fields and gas fares visible at the oxic sediment surface. These created different microhabitats that were hosting different microbial communities. Gas flares and bacterial mats were hotspots for the detection of aerobic methanotrophs, where the Paper III showed MOx to be mediated by three distinct **Methylococcales**: two affiliated to the DSC1 and one genetically similar to *Methylomonas* sp. The different habitats also harbor different SOB diversity: gas flares and bacterial mats are more densely populated by **Campylobacterota**, while ***Beggiatoa*** are more abundant at boundaries between mats and siboglinid fields. In siboglinid fields SOB represented a small fraction, but its density could be higher in deeper sediments in the trophosome of the worms. Finally, the different habitats shaped the rest of the microbial communities, including a higher proportion of **ANME-1** at gas flares, and a more diverse composition of different organic compounds degraders toward the H_2S-poor sediments in siboglinid fields.

3- Water column: High level of CH_4 was only detected in the bottom water where geological depressions limited the dissipation of CH_4 through hydrodynamic process. Within these water layers, MOx were also higher and methanotrophic communities were primarily represented by **Methyloccales** associated within the pmoA database to the Type Ia Deep-Sea Cluster 3. This contrasted with the MOB community retrieved at sediment surface of cold seeps in Paper III, adding a fourth potential key player in MOx in the northern Barents Sea.

This PhD project has therefore been able to identify how CH_4 impact the microbial biodiversity in the northern Barents Sea, in addition of providing insights within the Arctic Ocean, and identified key microbial players. Our scope included various gradients, including depth related (anoxic sediments, oxic sediments, water column), distance related (both at few meters scale (Paper III), few tens and hundred meters scale (Paper I & II) and tens of kilometer scale (Paper IV), and geochemistry related (such as changes in CH_4, O_2, H_2S). Results demonstrate on one side similar microbial characteristics observed also at other cold seeps, such as the

predominance of a known ANME clade near SMTZ. But on another side, our results also highlighted uncommon observations, such as AOM being mainly mediated by ANME-1, raising further questions for future research.

6 Outlook

When considering the broad distribution of CH_4 sources and their importance in the Arctic Ocean, there is emphasis on extending microbial investigations to the other uninvestigated Arctic regions. Geomorphological and biogeochemical properties of the different Arctic shelves strongly vary, leading potentially to a different selection of microbes thriving. Furthermore, this Thesis provided particularly an in-depth analysis of the methane and sulphur related microbial diversity, but microbes associated to other biogeochemical cycles were only superficially covered. Consequently, gaps of knowledge on the biodiversity of several other functional groups, such as groups associated to nitrogen cycle and degradation of organic matter, remain to be addressed. Yet, microbial ecosystems investigated in this Thesis presented particular traits, extending our original question of *Who is there?* into a myriad of new questions.

Our research efforts set foundations to extend further knowledge on metabolism and distribution of key taxa identified in these studies, in addition to improving our comprehension of the CH_4 budget (sinks and sources) in the Arctic Ocean. In addition, conditions in the Arctic Ocean are predicted to experience amplified impacts from climate changes compared to other oceans (Carton et al., 2015; James et al., 2016; Lewis et al., 2020; Timmermans and Marshall, 2020), underlining the importance of knowledge to investigate potential impacts on the local microbial communities at cold seeps. The impact of other anthropogenic activities on benthic microbial communities, such as bottom trawling where traces where clearly visible near our sampling sites, remain unknown. With the growing interest in the Arctic Ocean to extend economic activities such as fisheries, oil & gas, and mining industries, there are legitimately some concerns for the environmental stability of these microbes, where some require several months for doubling generation time.

Bibliography

1. Aagaard, K., Foldvik, A., and Hillman, S. R. (1987). The West Spitsbergen Current: Disposition and water mass transformation. *J. Geophys. Res. Ocean.* 92, 3778–3784. doi:10.1029/jc092ic04p03778.
2. Aharon, P. (1994). Geology and biology of modern and ancient submarine hydrocarbon seeps and vents: An introduction. *Geo-Marine Lett. 1994 142* 14, 69–73. doi:10.1007/bf01203716.
3. Alm, E. W., Oerther, D. B., Larsen, N., Stahl, D. A., and Raskin, L. (1996). The oligonucleotide probe database. *Appl. Environ. Microbiol.* 62, 3557–9. Available at: http://www.ncbi.nlm.nih.gov/pubmed/8837410 [Accessed December 5, 2018].
4. Anderson, R. E., Beltrán, M. T., Hallam, S. J., and Baross, J. A. (2013). Microbial community structure across fluid gradients in the Juan de Fuca Ridge hydrothermal system. *FEMS Microbiol. Ecol.* 83, 324–339. doi:10.1111/j.1574-6941.2012.01478.x.
5. Andreassen, K., Hubbard, A., Winsborrow, M., Patton, H., Vadakkepuliyambatta, S., Plaza-Faverola, A., et al. (2017). Massive blow-out craters formed by hydrate-controlled methane expulsion from the Arctic seafloor. *Science (80-.).* 356, 948–953. doi:10.1126/science.aal4500.
6. Archer, D. (2015). A model of the methane cycle, permafrost, and hydrology of the Siberian continental margin. *Biogeosciences* 12, 2953–2974. doi:10.5194/bg-12-2953-2015.
7. Åström, E., Carroll, M., Ambrose, W., and Carroll, J. (2016). Arctic cold seeps in marine methane hydrate environments: impacts on shelf macrobenthic community structure offshore Svalbard. *Mar. Ecol. Prog. Ser.* 552, 1–18. doi:10.3354/meps11773.
8. Åström, E. K. L., Carroll, M. L., Ambrose, W. G., Sen, A., Silyakova, A., and Carroll, J. (2018). Methane cold seeps as biological oases in the high-Arctic deep sea. *Limnol. Oceanogr.* 63, S209–S231. doi:10.1002/lno.10732.
9. Bagarinao, T. (1992). Sulfide as an environmental factor and toxicant: tolerance and adaptations in aquatic organisms. *Aquat. Toxicol.* 24, 21–62. doi:10.1016/0166-445x(92)90015-f.
10. Balmonte, J. P., Teske, A., and Arnosti, C. (2018). Structure and function of high Arctic pelagic, particle-associated and benthic bacterial communities. *Environ. Microbiol.* 20, 2941–2954. doi:10.1111/1462-2920.14304.
11. Barry, J. P., Gary Greene, H., Orange, D. L., Baxter, C. H., Robison, B. H., Kochevar, R. E., et al. (1996). Biologic and geologic characteristics of cold seeps in Monterey Bay, California. *Deep Sea Res. Part I Oceanogr. Res. Pap.* 43, 1739–1762. doi:10.1016/s0967-0637(96)00075-1.
12. Beal, E. J., House, C. H., and Orphan, V. J. (2009). Manganese- and iron-dependent marine methane oxidation. *Science* 325, 184–7. doi:10.1126/science.1169984.
13. Becking, L. G. M. B. (1931). *Gaia of Leven en aarde.* Martinus Nijhoff.
14. Beer, D. de, Sauter, E., Niemann, H., Kaul, N., Foucher, J.-P., Witte, U., et al. (2006). In situ fluxes and zonation of microbial activity in surface sediments of the Håkon Mosby Mud Volcano. *Limnol. Oceanogr.* 51, 1315–1331. doi:10.4319/lo.2006.51.3.1315.
15. Bernardino, A. F., Levin, L. A., Thurber, A. R., and Smith, C. R. (2012). Comparative composition, diversity and trophic ecology of sediment macrofauna at vents, seeps and organic falls. *PLoS One* 7. doi:10.1371/journal.pone.0033515.
16. Berner, R. A. (1980). Early Diagenesis. *Early Diagenes.* doi:10.1515/9780691209401/html.
17. Bhattarai, S., Cassarini, C., Rene, E. R., Zhang, Y., Esposito, G., and Lens, P. N. L. (2018). Enrichment of sulfate reducing anaerobic methane oxidizing community dominated by ANME-1 from Ginsburg Mud Volcano (Gulf of Cadiz) sediment in a biotrickling filter. *Bioresour. Technol.* 259, 433–441. doi:10.1016/j.biortech.2018.03.018.
18. Biastoch, A., Treude, T., Rpke, L. H., Riebesell, U., Roth, C., Burwicz, E. B., et al. (2011). Rising Arctic Ocean temperatures cause gas hydrate destabilization and ocean acidification. *Geophys. Res. Lett.* 38. doi:10.1029/2011gl047222.
19. Boetius, A., Ravenschlag, K., Schubert, C. J., Rickert, D., Widdel, F., Gieseke, A., et al. (2000). A marine microbial consortium apparently mediating anaerobic oxidation of methane. *Nature* 407, 623–626. doi:10.1038/35036572.
20. Boetius, A., and Suess, E. (2004). Hydrate Ridge: a natural laboratory for the study of microbial life fueled by methane from near-surface gas hydrates. *Chem. Geol.* 205, 291–310. doi:10.1016/j.chemgeo.2003.12.034.
21. Boetius, A., and Wenzhöfer, F. (2013). Seafloor oxygen consumption fuelled by methane from cold seeps. *Nat. Geosci.* 6, 725–734. doi:10.1038/ngeo1926.
22. Bouillaud, F., and Blachier, F. (2011). Mitochondria and Sulfide: A Very Old Story of Poisoning, Feeding, and Signaling? *Antioxidants & Redox Signaling* 15, 379–391. doi:10.1089/ars.2010.3678.
23. Boyce, R. E. (1973). "Appendix I. Physical Properties - Methods," in *Initial Reports of the Deep Sea Drilling Project, Volume 15*, ed. J. B. et al. Edgar, N.T., Saunders (U.S. Government Printing Office),

1115–1128.
24. Buck, K. R., Barry, J. P., and Simpson, A. G. B. (2000). Monterey Bay cold seep biota: Euglenozoa with chemoautotrophic bacterial epibionts. *Eur. J. Protistol.* 36, 117–126. doi:10.1016/s0932-4739(00)80029-2.
25. Cambon-Bonavita, M. A., Nadalig, T., Roussel, E., Delage, E., Duperron, S., Caprais, J. C., et al. (2009). Diversity and distribution of methane-oxidizing microbial communities associated with different faunal assemblages in a giant pockmark of the Gabon continental margin. *Deep Sea Res. Part II Top. Stud. Oceanogr.* 56, 2248–2258. doi:10.1016/j.dsr2.2009.04.007.
26. Canfield, D. E. (2004). The evolution of the Earth surface sulfur reservoir. *Am. J. Sci.* 304, 839–861. doi:10.2475/ajs.304.10.839.
27. Carmack, E., and Wassmann, P. (2006). Food webs and physical-biological coupling on pan-Arctic shelves: Unifying concepts and comprehensive perspectives. *Prog. Oceanogr.* 71, 446–477. doi:10.1016/j.pocean.2006.10.004.
28. Carton, J. A., Ding, Y., and Arrigo, K. R. (2015). The seasonal cycle of the Arctic Ocean under climate change. *Geophys. Res. Lett.* 42, 7681–7686. doi:10.1002/2015gl064514.
29. Cary, S. C., Cottrell, M. T., Stein, J. L., Camacho, F., and Desbruyères, D. (1997). Molecular identification and localization of filamentous symbiotic bacteria associated with the hydrothermal vent annelid Alvinella pompejana. *Appl. Environ. Microbiol.* 63, 1124–1130. doi:10.1128/aem.63.3.1124-1130.1997.
30. Castelle, C. J., Wrighton, K. C., Thomas, B. C., Hug, L. A., Brown, C. T., Wilkins, M. J., et al. (2015). Genomic expansion of domain archaea highlights roles for organisms from new phyla in anaerobic carbon cycling. *Curr. Biol.* 25, 690–701. DOI:10.1016/j.cub.2015.01.014.
31. Cline, J. D. (1969). Spectrophotometric determination of hydrogen sulfide in natural waters. *Limnol. Oceanogr.* 14, 454–458. doi:10.4319/lo.1969.14.3.0454.
32. Collett, T. S., Lee, M. W., Agena, W. F., Miller, J. J., Lewis, K. A., Zyrianova, M. V., et al. (2011). Permafrost-associated natural gas hydrate occurrences on the Alaska North Slope. *Mar. Pet. Geol.* 28, 279–294. doi:10.1016/j.marpetgeo.2009.12.001.
33. Cordes, E. E., Bergquist, D. C., and Fisher, C. R. (2009). Macro-Ecology of Gulf of Mexico Cold Seeps. *http://dx.doi.org/10.1146/annurev.marine.010908.163912* 1, 143–168. doi:10.1146/annurev.marine.010908.163912.
34. Cordes, E. E., Carney, S. L., Hourdez, S., Carney, R. S., Brooks, J. M., and Fisher, C. R. (2007). Cold seeps of the deep Gulf of Mexico: Community structure and biogeographic comparisons to Atlantic equatorial belt seep communities. *Deep Sea Res. Part I Oceanogr. Res. Pap.* 54, 637–653. doi:10.1016/j.dsr.2007.01.001.
35. Cordes, E. E., Cunha, M. R., Galéron, J., Mora, C., Olu-Le Roy, K., Sibuet, M., et al. (2010). The influence of geological, geochemical, and biogenic habitat heterogeneity on seep biodiversity. *Mar. Ecol.* 31, 51–65. doi:10.1111/j.1439-0485.2009.00334.x.
36. Cottier, F., Tverberg, V., Inall, M., Svendsen, H., Nilsen, F., and Griffiths, C. (2005). Water mass modification in an Arctic fjord through cross-shelf exchange: The seasonal hydrography of Kongsfjorden, Svalbard. *J. Geophys. Res. Ocean.* 110, 1–18. doi:10.1029/2004jc002757.
37. Coyne, K. J., Countway, P. D., Pilditch, C. A., Lee, C. K., Caron, D. A., and Cary, S. C. (2013). Diversity and Distributional Patterns of Ciliates in Guaymas Basin Hydrothermal Vent Sediments. *J. Eukaryot. Microbiol.* 60, 433–447. doi:10.1111/jeu.12051.
38. Cruaud, P., Vigneron, A., Pignet, P., Caprais, J.-C., Lesongeur, F., Toffin, L., et al. (2017). Comparative Study of Guaymas Basin Microbiomes: Cold Seeps vs. Hydrothermal Vents Sediments. *Front. Mar. Sci.* 4, 417. doi:10.3389/fmars.2017.00417.
39. Daniel, J., Fornari, D. J., and Group, W. T. (2003). A new deep-sea towed digital camera and multi-rock coring system. *Eos, Trans. Am. Geophys. Union* 84, 69–73. doi:10.1029/2003eo080001.
40. Danilova, O. V., and Dedysh, S. N. (2014). Abundance and diversity of methanotrophic Gammaproteobacteria in northern wetlands. *Microbiol. (Russian Fed.* 83, 67–76. doi:10.1134/s0026261714020040.
41. Dedysh, S. N., and Knief, C. (2018). "Diversity and phylogeny of described aerobic methanotrophs," in *Methane Biocatalysis: Paving the Way to Sustainability* (Springer International Publishing), 17–42. doi:10.1007/978-3-319-74866-5_2.
42. Delgado Vela, J., Bristow, L. A., Marchant, H. K., Love, N. G., and Dick, G. J. (2021). Sulfide alters microbial functional potential in a methane and nitrogen cycling biofilm reactor. *Environ. Microbiol.* 23, 1481–1495. doi:10.1111/1462-2920.15352.
43. Demopoulos, A. W. J., Bourque, J. R., Durkin, A., and Cordes, E. E. (2018). The influence of seep habitats on sediment macrofaunal biodiversity and functional traits. *Deep. Res. Part I Oceanogr. Res. Pap.* 142, 77–93. doi:10.1016/j.dsr.2018.10.004.

44. Dhillon, A., Teske, A., Dillon, J., Stahl, D. A., and Sogin, M. L. (2003). Molecular characterization of sulfate-reducing bacteria in the Guaymas basin. *Appl. Environ. Microbiol.* 69, 2765–2772. doi:10.1128/aem.69.5.2765-2772.2003.
45. Dickens, G. R., Paull, C. K., and Wallace, P. (1997). Direct measurement of in situ methane quantities in a large gas-hydrate reservoir. *Nat. 1997 3856615* 385, 426–428. doi:10.1038/385426a0.
46. Distel, D. L., and Cavanaugh, C. M. (1994). Independent phylogenetic origins of methanotrophic and chemoautotrophic bacterial endosymbioses in marine bivalves. *J. Bacteriol.* 176, 1932–1938. doi:10.1128/jb.176.7.1932-1938.1994.
47. Dubilier, N., Mülders, C., Ferdelman, T., de Beer, D., Pernthaler, A., Klein, M., et al. (2001). Endosymbiotic sulphate-reducing and sulphide-oxidizing bacteria in an oligochaete worm. *Nat. 2001 4116835* 411, 298–302. doi:10.1038/35077067.
48. Dubinsky, E. A., Conrad, M. E., Chakraborty, R., Bill, M., Borglin, S. E., Hollibaugh, J. T., et al. (2013). Succession of Hydrocarbon-Degrading Bacteria in the Aftermath of the Deepwater Horizon Oil Spill in the Gulf of Mexico. *Environ. Sci. Technol.* 47, 10860–10867. doi:10.1021/es401676y.
49. Dunfield, P. F., Yuryev, A., Senin, P., Smirnova, A. V., Stott, M. B., Hou, S., et al. (2007). Methane oxidation by an extremely acidophilic bacterium of the phylum Verrucomicrobia. *Nat. 2007 4507171* 450, 879–882. doi:10.1038/nature06411.
50. Duperron, S., Halary, S., Lorion, J., Sibuet, M., and Gaill, F. (2008). Unexpected co-occurrence of six bacterial symbionts in the gills of the cold seep mussel Idas sp. (Bivalvia: Mytilidae). *Environ. Microbiol.* 10, 433–445. doi:10.1111/j.1462-2920.2007.01465.x.
51. Duperron, S., Sibuet, M., MacGregor, B. J., Kuypers, M. M. M., Fisher, C. R., and Dubilier, N. (2007). Diversity, relative abundance and metabolic potential of bacterial endosymbionts in three Bathymodiolus mussel species from cold seeps in the Gulf of Mexico. *Environ. Microbiol.* 9, 1423–1438. doi:10.1111/j.1462-2920.2007.01259.x.
52. Dziallas, C., Allgaier, M., Monaghan, M. T., and Grossart, H.-P. (2012). Act together—implications of symbioses in aquatic ciliates. *Front. Microbiol.* 0, 288. doi:10.3389/fmicb.2012.00288.
53. Edgar, R. C. (2010). Search and clustering orders of magnitude faster than BLAST. *Bioinformatics* 26, 2460–2461. doi:10.1093/bioinformatics/btq461.
54. Edgcomb, V. P., Bernhard, J. M., and Jeon, S. (2007). Deep-Sea Microbial Eukaryotes in Anoxic, Microoxic, and Sulfidic Environments. 711–734. doi:10.1007/978-1-4020-6112-7_39.
55. Embley, T. M., Giezen, M. van der, Horner, D., Dyal, P., Bell, S., and Foster, P. (2003). Hydrogenosomes, Mitochondria and Early Eukaryotic Evolution. *IUBMB Life* 55, 387–395. doi:10.1080/15216540310001592834.
56. Etminan, M., Myhre, G., Highwood, E. J., and Shine, K. P. (2016). Radiative forcing of carbon dioxide, methane, and nitrous oxide: A significant revision of the methane radiative forcing. *Geophys. Res. Lett.* 43, 12,614-12,623. doi:10.1002/2016gl071930.
57. Ettwig, K. F., Butler, M. K., Le Paslier, D., Pelletier, E., Mangenot, S., Kuypers, M. M. M., et al. (2010). Nitrite-driven anaerobic methane oxidation by oxygenic bacteria. *Nature* 464, 543–548. doi: 10.1038/nature08883.
58. Ettwig, K. F., Zhu, B., Speth, D., Keltjens, J. T., Jetten, M. S. M., and Kartal, B. (2016). Archaea catalyze iron-dependent anaerobic oxidation of methane. *Proc. Natl. Acad. Sci.* 113, 12792–12796. doi:10.1073/pnas.1609534113.
59. Evans, P. N., Parks, D. H., Chadwick, G. L., Robbins, S. J., Orphan, V. J., Golding, S. D., et al. (2015). Methane metabolism in the archaeal phylum Bathyarchaeota revealed by genome-centric metagenomics. *Science (80-.).* 350, 434–438. doi:10.1126/science.aac7745.
60. Falk-Petersen, S., Mayzaud, P., Kattner, G., and Sargent, J. R. (2009). Lipids and life strategy of Arctic *Calanus*. *Mar. Biol. Res.* 5, 18–39. doi:10.1080/17451000802512267.
61. Fernández-Carrera, A., Rogers, K. L., Weber, S. C., Chanton, J. P., and Montoya, J. P. (2016). Deep Water Horizon oil and methane carbon entered the food web in the Gulf of Mexico. *Limnol. Oceanogr.* 61, S387–S400. doi:10.1002/lno.10440.
62. Ferré, B., Jansson, P. G., Moser, M., Serov, P., Portnov, A., Graves, C. A., et al. (2020). Reduced methane seepage from Arctic sediments during cold bottom-water conditions. *Nat. Geosci.* 13, 144–148. doi:10.1038/s41561-019-0515-3.
63. Ferré, B., Mienert, J., and Feseker, T. (2012). Ocean temperature variability for the past 60 years on the Norwegian-Svalbard margin influences gas hydrate stability on human time scales. *J. Geophys. Res. Ocean.* 117. doi:10.1029/2012jc008300.
64. Ferry, J. G., and Lessner, D. J. (2008). Methanogenesis in marine sediments. in *Annals of the New York Academy of Sciences* (Blackwell Publishing Inc.), 147–157. doi:10.1196/annals.1419.007.
65. Fischer, D., Sahling, H., Nöthen, K., Bohrmann, G., Zabel, M., and Kasten, S. (2012). Interaction between hydrocarbon seepage, chemosynthetic communities, and bottom water redox at cold seeps of the Makran

accretionary prism: Insights from habitat-specific pore water sampling and modeling. *Biogeosciences* 9, 2013–2031. doi:10.5194/bg-9-2013-2012.
66. Fisher, C. R., Brooks, J. M., Vodenichar, J. S., Zande, J. M., Childress, J. J., and Jr., R. A. B. (1993). The Co-occurrence of Methanotrophic and Chemoautotrophic Sulfur-Oxidizing Bacterial Symbionts in a Deep-sea Mussel. *Mar. Ecol.* 14, 277–289. doi:10.1111/j.1439-0485.1993.tb00001.x.
67. Fisher, R. C. (1990). Chemoautotrophic and methanotrophic symbioses in marine invertebrates. *Rev. Aquat. Sci.* 2, 399–436. Available at: https://ci.nii.ac.jp/naid/10012481670 [Accessed August 1, 2021].
68. Floodgate, G. D., and Judd, A. G. (1992). The origins of shallow gas. *Cont. Shelf Res.* 12, 1145–1156. doi:10.1016/0278-4343(92)90075-u.
69. Friedrich, C. G., Bardischewsky, F., Rother, D., Quentmeier, A., and Fischer, J. (2005). Prokaryotic sulfur oxidation. *Curr. Opin. Microbiol.* 8, 253–259. doi:10.1016/j.mib.2005.04.005.
70. Gaudron, S. M., Pradillon, F., Pailleret, M., Duperron, S., Le Bris, N., and Gaill, F. (2010). Colonization of organic substrates deployed in deep-sea reducing habitats by symbiotic species and associated fauna. *Mar. Environ. Res.* 70, 1–12. doi:10.1016/j.marenvres.2010.02.002.
71. Giongo, A., Haag, T., Simão, T. L. L., Medina-Silva, R., Utz, L. R. P., Bogo, M. R., et al. (2016). Discovery of a chemosynthesis-based community in the western South Atlantic Ocean. *Deep Sea Res. Part I Oceanogr. Res. Pap.* 112, 45–56. doi:10.1016/j.dsr.2015.10.010.
72. Girguis, P. R., Cozen, A. E., and DeLong, E. F. (2005). Growth and population dynamics of anaerobic methane-oxidizing archaea and sulfate-reducing bacteria in a continuous-flow bioreactor. *Appl. Environ. Microbiol.* 71, 3725–33. doi:10.1128/aem.71.7.3725-3733.2005.
73. Goswami, B. K., Weitemeyer, K. A., Minshull, T. A., Sinha, M. C., Westbrook, G. K., Chabert, A., et al. (2015). A joint electromagnetic and seismic study of an active pockmark within the hydrate stability field at the Vestnesa Ridge, West Svalbard margin. *J. Geophys. Res. Solid Earth* 120, 6797–6822. doi:10.1002/2015jb012344.
74. Graham, D. W., Chaudhary, J. A., Hanson, R. S., and Arnold, R. G. (1993). Factors Affecting Competition Between Type I and Type II Methanotrophs in Two-organism, Continuous-flow Reactors. *Microb Ecol* 25, 1-17. doi: 10.1007/bf00182126.
75. Graves, C. A., James, R. H., Sapart, C. J., Stott, A. W., Wright, I. C., Berndt, C., et al. (2017). Methane in shallow subsurface sediments at the landward limit of the gas hydrate stability zone offshore western Svalbard. *Geochim. Cosmochim. Acta* 198, 419–438. doi:10.1016/j.gca.2016.11.015.
76. Griffiths, R. I., Whiteley, A. S., O'Donnell, A. G., and Bailey, M. J. (2000). Rapid method for coextraction of DNA and RNA from natural environments for analysis of ribosomal DNA- and rRNA-based microbial community composition. *Appl. Environ. Microbiol.* 66, 5488–5491. doi:10.1128/aem.66.12.5488-5491.2000.
77. Grogan, P., Østvedt-GhaziI, A.-M., Larseen, G. B., Fotland, B., Nyberg, K., Dahlgren, S., et al. (1999). Structural elements and petroleum geology of the Norwegian sector of the northern Barents Sea. *Geol. Soc. London, Pet. Geol. Conf. Ser.* 5, 247–259. doi:10.1144/0050247.
78. Grünke, S., Felden, J., Lichtschlag, A., Girnth, A. C., De Beer, D., Wenzhöfer, F., et al. (2011). Niche differentiation among mat-forming, sulfide-oxidizing bacteria at cold seeps of the Nile Deep Sea Fan (Eastern Mediterranean Sea). *Geobiology* 9, 330–348. doi:10.1111/j.1472-4669.2011.00281.x.
79. Guillon, E., Menot, L., Decker, C., Krylova, E., and Olu, K. (2017). The vesicomyid bivalve habitat at cold seeps supports heterogeneous and dynamic macrofaunal assemblages. *Deep Sea Res. Part I Oceanogr. Res. Pap.* 120, 1–13. doi:10.1016/j.dsr.2016.12.008.
80. Guillou, L., Viprey, M., Chambouvet, A., Welsh, R. M., Kirkham, A. R., Massana, R., et al. (2008). Widespread occurrence and genetic diversity of marine parasitoids belonging to Syndiniales (Alveolata). *Environ. Microbiol.* 10, 3349–3365. doi:10.1111/j.1462-2920.2008.01731.x.
81. Hallam, S. J., Girguis, P. R., Preston, C. M., Richardson, P. M., and DeLong, E. F. (2003). Identification of methyl coenzyme M reductase A (mcrA) genes associated with methane-oxidizing archaea. *Appl. Environ. Microbiol.* 69, 5483–5491. doi:10.1128/aem.69.9.5483-5491.2003.
82. Han, Y., and Perner, M. (2015). The globally widespread genus Sulfurimonas: Versatile energy metabolisms and adaptations to redox clines. *Front. Microbiol.* 6. doi:10.3389/Fmicb.2015.00989.
83. Hanson, R. S., and Hanson, T. E. (1996). Methanotrophic Bacteria. *Microbiol. Rev.* 60, 439–471. Available at: http://mmbr.asm.org/ [Accessed February 14, 2020]. doi: 10.1128/Mr.60.2.439-471.1996.
84. Harris, R. L., Lau, M., Onstott, T. C., Harris, R. L., Lau, M., and Onstott, T. C. (2018). A Putatively Denitrifying Anaerobic Methanotroph from South Africa's Deep Biosphere Belonging to Candidate Phylum Bathyarchaeota. *AGUFM* 2018, B43F-14. Available at: https://ui.adsabs.harvard.edu/abs/2018AGUFM.B43F..14H/abstract [Accessed August 3, 2021].
85. Harrison, B. K., Zhang, H., Berelson, W., and Orphan, V. J. (2009). Variations in archaeal and bacterial diversity associated with the sulfate-methane transition zone in continental margin sediments (Santa Barbara Basin, California). *Appl. Environ. Microbiol.* 75, 1487–1499. doi:10.1128/aem.01812-08.

86. Hernandez, M. E., Beck, D. A. C., Lidstrom, M. E., and Chistoserdova, L. (2015). Oxygen availability is a major factor in determining the composition of microbial communities involved in methane oxidation. *PeerJ* 2015, e801. doi:10.7717/Peerj.801.
87. Hinrichs, K.-U., Hayes, J. M., Sylva, S. P., Brewer, P. G., and DeLong, E. F. (1999). Methane-consuming archaebacteria in marine sediments. *Nat. 1999 3986730* 398, 802–805. doi:10.1038/19751.
88. Hoehler, T. M., Alperin, M. J., Albert, D. B., and Martens, C. S. (1994). Field and laboratory studies of methane oxidation in an anoxic marine sediment: Evidence for a methanogen-sulfate reducer consortium. *Global Biogeochem. Cycles* 8, 451–463. doi:10.1029/94gb01800.
89. Hoehler, T. M., Borowski, W. S., Alperin, M. J., Rodriguez, N. M., and Paull, C. K. (2000). Model, stable isotope, and radiotracer characterization of anaerobic methane oxidation in gas hydrate-bearing sediments of the Blake Ridge. in *Proceedings of the Ocean Drilling Program: Scientific Results*, 79–85. doi:10.2973/odp.proc.sr.164.242.2000.
90. Holler, T., Wegener, G., Knittel, K., Boetius, A., Brunner, B., Kuypers, M. M. M., et al. (2009). Substantial 13C/12C and D/H fractionation during anaerobic oxidation of methane by marine consortia enriched in vitro. *Environ. Microbiol. Rep.* 1, 370–376. doi:10.1111/j.1758-2229.2009.00074.x.
91. Hong, W.-L., Sauer, S., Panieri, G., Ambrose, W. G., James, R. H., Plaza-Faverola, A., et al. (2016). Removal of methane through hydrological, microbial, and geochemical processes in the shallow sediments of pockmarks along eastern Vestnesa Ridge (Svalbard). *Limnol. Oceanogr.* 61, S324–S343. doi:10.1002/lno.10299.
92. Hong, W.-L. W. -L., Torres, M. E., Portnov, A., Waage, M., Haley, B., and Lepland, A. (2018). Variations in Gas and Water Pulses at an Arctic Seep: Fluid Sources and Methane Transport. *Geophys. Res. Lett.* 45, 4153–4162. doi:10.1029/2018gl077309.
93. Hong, W. L., Torres, M. E., Carroll, J., Crémière, A., Panieri, G., Yao, H., et al. (2017). Seepage from an arctic shallow marine gas hydrate reservoir is insensitive to momentary ocean warming. *Nat. Commun.* 8, 1–14. doi:10.1038/ncomms15745.
94. Hovland, M., and Svensen, H. (2006). Submarine pingoes: Indicators of shallow gas hydrates in a pockmark at Nyegga, Norwegian Sea. *Mar. Geol.* 228, 15–23. doi:10.1016/j.margeo.2005.12.005.
95. Hu, B., Shen, L., Lian, X., Zhu, Q., Liu, S., Huang, Q., et al. (2014). Evidence for nitrite-dependent anaerobic methane oxidation as a previously overlooked microbial methane sink in wetlands. *Proc. Natl. Acad. Sci. U. S. A.* 111, 4495–500. doi:10.1073/pnas.1318393111.
96. Hugerth, L. W., Muller, E. E. L., Hu, Y. O. O., Lebrun, L. A. M., Roume, H., Lundin, D., et al. (2014). Systematic Design of 18S rRNA Gene Primers for Determining Eukaryotic Diversity in Microbial Consortia. *PLoS One* 9, e95567. doi:10.1371/journal.pone.0095567.
97. Hughes, D. J., and Gage, J. D. (2004). Benthic metazoan biomass, community structure and bioturbation at three contrasting deep-water sites on the northwest European continental margin. *Prog. Oceanogr.* 63, 29–55. doi:10.1016/j.pocean.2004.09.002.
98. Hunter, S. J., Goldobin, D. S., Haywood, A. M., Ridgwell, A., and Rees, J. G. (2013). Sensitivity of the global submarine hydrate inventory to scenarios of future climate change. *Earth Planet. Sci. Lett.* 367, 105–115. doi:10.1016/j.epsl.2013.02.017.
99. James, R. H., Bousquet, P., Bussmann, I., Haeckel, M., Kipfer, R., Leifer, I., et al. (2016). Effects of climate change on methane emissions from seafloor sediments in the Arctic Ocean: A review. *Limnol. Oceanogr.* 61, S283–S299. doi:10.1002/lno.10307.
100. Jorgensen, S. L., Hannisdal, B., Lanzén, A., Baumberger, T., Flesland, K., Fonseca, R., et al. (2012). Correlating microbial community profiles with geochemical data in highly stratified sediments from the Arctic Mid-Ocean Ridge. *Proc. Natl. Acad. Sci. U. S. A.* 109, E2846-55. doi:10.1073/pnas.1207574109.
101. Joye, S. B., Boetius, A., Orcutt, B. N., Montoya, J. P., Schulz, H. N., Erickson, M. J., et al. (2004). The anaerobic oxidation of methane and sulfate reduction in sediments from Gulf of Mexico cold seeps. *Chem. Geol.* 205, 219–238. doi:10.1016/j.chemgeo.2003.12.019.
102. Joye, S. B., Bowles, M. W., Samarkin, V. A., Hunter, K. S., and Niemann, H. (2010). Biogeochemical signatures and microbial activity of different cold-seep habitats along the Gulf of Mexico deep slope. *Deep. Res. Part II Top. Stud. Oceanogr.* 57, 1990–2001. doi:10.1016/j.dsr2.2010.06.001.
103. Kalyuzhnaya, M. G., Gomez, O. A., and Murrell, J. C. (2019). The Methane-Oxidizing Bacteria (Methanotrophs) 14. doi:10.1007/978-3-030-14796-9_10.
104. Kleindienst, S., Grim, S., Sogin, M., Bracco, A., Crespo-Medina, M., and Joye, S. B. (2015). Diverse, rare microbial taxa responded to the Deepwater Horizon deep-sea hydrocarbon plume. *ISME J. 2016 102* 10, 400–415. doi:10.1038/ismej.2015.121.
105. Klindworth, A., Pruesse, E., Schweer, T., Peplies, J., Quast, C., Horn, M., et al. (2013). Evaluation of general 16S ribosomal RNA gene PCR primers for classical and next-generation sequencing-based diversity studies. *Nucleic Acids Res.* 41, e1–e1. doi:10.1093/nar/gks808.
106. Knab, N. J., Cragg, B. A., Hornibrook, E. R. C., Holmkvist, L., Pancost, R. D., Borowski, C., et al. (2009).

Regulation of anaerobic methane oxidation in sediments of the black sea. *Biogeosciences* 6, 1505–1518. doi:10.5194/bg-6-1505-2009.
107. Knief, C. (2015). Diversity and habitat preferences of cultivated and uncultivated aerobic methanotrophic bacteria evaluated based on pmoA as molecular marker. *Front. Microbiol.* 6. doi:10.3389/fmicb.2015.01346.
108. Knittel, K., and Boetius, A. (2009). Anaerobic Oxidation of Methane : Progress with an Unknown Process. *Annu. Rev. Microbiol.* 63, 311–334. doi:10.1146/Annurev.Micro.61.080706.093130.
109. Knittel, K., Boetius, A., Lemke, A., Eilers, H., Lochte, K., Pfannkuche, O., et al. (2003). Activity, distribution, and diversity of sulfate reducers and other bacteria in sediments above gas hydrate (Cascadia margin, Oregon). *Geomicrobiol. J.* 20, 269–294. doi:10.1080/01490450303896.
110. Knittel, K., Lösekann, T., Boetius, A., Kort, R., and Amann, R. (2005). Diversity and distribution of methanotrophic archaea at cold seeps. *Appl. Environ. Microbiol.* 71, 467–79. doi:10.1128/aem.71.1.467-479.2005.
111. Koch, S., Berndt, C., Bialas, J., Haeckel, M., Crutchley, G., Papenberg, C., et al. (2015). Gas-controlled seafloor doming. *Geology* 43, 571–574. doi:10.1130/g36596.1.
112. Kohzu, A., Kato, C., Iwata, T., Kishi, D., Murakami, M., Nakano, S., et al. (2004). Stream food web fueled by methane-derived carbon. *Aquat. Microb. Ecol.* 36, 189–194. doi:10.3354/ame036189.
113. Kouduka, M., Tanabe, A. S., Yamamoto, S., Yanagawa, K., Nakamura, Y., Akiba, F., et al. (2017). Eukaryotic diversity in late Pleistocene marine sediments around a shallow methane hydrate deposit in the Japan Sea. *Geobiology* 15, 715–727. doi:10.1111/gbi.12233.
114. Kretschmer, K., Biastoch, A., Rüpke, L., and Burwicz, E. (2015). Modeling the fate of methane hydrates under global warming. *Global Biogeochem. Cycles* 29, 610–625. doi:10.1002/2014gb005011.
115. Krüger, M., Meyerdierks, A., Glöckner, F. O., Amann, R., Widdel, F., Kube, M., et al. (2003). A conspicuous nickel protein in microbial mats that oxidize methane anaerobically. *Nat. 2004 4266968* 426, 878–881. doi:10.1038/nature02207.
116. Kubo, K., Lloyd, K. G., Biddle, J. F., Amann, R., Teske, A., and Knittel, K. (2012). Archaea of the Miscellaneous Crenarchaeotal Group are abundant, diverse and widespread in marine sediments. *ISME J.* 6, 1949–1965. doi:10.1038/ismej.2012.37.
117. Kulm, L. D., Suess, E., Moore, J. C., Carson, B., Lewis, B. T., Ritger, S. D., et al. (1986). Oregon Subduction Zone: Venting, Fauna, and Carbonates. *Science (80-.).* 231, 561–566. doi:10.1126/SCIENCE.231.4738.561.
118. Kvenvolden, K. A. (1988). Methane hydrate - A major reservoir of carbon in the shallow geosphere? *Chem. Geol.* 71, 41–51. doi:10.1016/0009-2541(88)90104-0.
119. Landvik, J. Y., Ingolfsson, Ó., Mieniert, J., Lehman, S. J., Solheim, A., Elverhøi, A., et al. (2005). Rethinking Late Weichselian ice-sheet dynamics in coastal NW Svalbard. *Boreas* 34, 7–24. doi:10.1111/J.1502-3885.2005.TB01001.X.
120. Le Pichon, X., Iiyama, T., Boulègue, J., Charvet, J., Faure, M., Kano, K., et al. (1987). Nankai Trough and Zenisu Ridge: a deep-sea submersible survey. *Earth Planet. Sci. Lett.* 83, 285–299. doi:10.1016/0012-821X(87)90072-0.
121. Lee, R. W., and Childress, J. J. (1994). Assimilation of inorganic nitrogen by marine invertebrates and their chemoautotrophic and methanotrophic symbionts. *Appl. Environ. Microbiol.* 60, 1852–1858. doi:10.1128/AEM.60.6.1852-1858.1994.
122. Lees, V., Owens, N. J. P., and Murrell, J. C. (1991). Nitrogen metabolism in marine methanotrophs. *Arch. Microbiol. 1991 1571* 157, 60–65. doi:10.1007/BF00245336.
123. Lessard-Pilon, S., Porter, M. D., Cordes, E. E., MacDonald, I., and Fisher, C. R. (2010). Community composition and temporal change at deep Gulf of Mexico cold seeps. *Deep Sea Res. Part II Top. Stud. Oceanogr.* 57, 1891–1903. doi:10.1016/J.DSR2.2010.05.012.
124. Levin, L. A., Etter, R. J., Rex, M. A., Gooday, A. J., Smith, C. R., Pineda, J., et al. (2003). Environmental Influences on Regional Deep-Sea Species Diversity1. *http://dx.doi.org/10.1146/annurev.ecolsys.32.081501.114002* 32, 51–93. doi:10.1146/ANNUREV.ECOLSYS.32.081501.114002.
125. Levin, L. A., Mendoza, G. F., Grupe, B. M., Gonzalez, J. P., Jellison, B., Rouse, G., et al. (2015). Biodiversity on the Rocks: Macrofauna Inhabiting Authigenic Carbonate at Costa Rica Methane Seeps. *PLoS One* 10, e0131080. doi:10.1371/JOURNAL.PONE.0131080.
126. Lewis, K. M., Van Dijken, G. L., and Arrigo, K. R. (2020). Changes in phytoplankton concentration now drive increased Arctic Ocean primary production. *Science (80-.).* 369, 198–202. doi:10.1126/science.aay8380.
127. Lichtschlag, A., Felden, J., Brüchert, V., Boetius, A., and de Beer, D. (2010). Geochemical processes and chemosynthetic primary production in different thiotrophic mats of the Håkon Mosby Mud Volcano (Barents Sea). *Limnol. Oceanogr.* 55, 931–949. doi:10.4319/lo.2010.55.2.0931.

128. Liu, X., Li, M., Castelle, C. J., Probst, A. J., Zhou, Z., Pan, J., et al. (2018). Insights into the ecology, evolution, and metabolism of the widespread Woesearchaeotal lineages. *Microbiome* 6, 1–16. doi:10.1186/s40168-018-0488-2.
129. Lloyd, K. G., Schreiber, L., Petersen, D. G., Kjeldsen, K. U., Lever, M. A., Steen, A. D., et al. (2013). Predominant archaea in marine sediments degrade detrital proteins. *Nature* 496, 215–218. doi:10.1038/nature12033.
130. Lösekann, T., Knittel, K., Nadalig, T., Fuchs, B., Niemann, H., Boetius, A., et al. (2007). Diversity and abundance of aerobic and anaerobic methane oxidizers at the Haakon Mosby Mud Volcano, Barents Sea. *Appl. Environ. Microbiol.* 73, 3348–3362. doi:10.1128/aem.00016-07.
131. Lösekann, T., Robador, A., Niemann, H., Knittel, K., Boetius, A., and Dubilier, N. (2008). Endosymbioses between bacteria and deep-sea siboglinid tubeworms from an Arctic Cold Seep (Haakon Mosby Mud Volcano, Barents Sea). *Environ. Microbiol.* 10, 3237–3254. doi:10.1111/j.1462-2920.2008.01712.x.
132. Lovejoy, C., Vincent, W. F., Bonilla, S., Roy, S., Martineau, M.-J., Terrado, R., et al. (2007). Distribution, phylogeny, and growth of cold-adapted picoprasinophytes in Arctic Seas. *J. Phycol.* 43, 78–89. doi:10.1111/j.1529-8817.2006.00310.x.
133. Lüke, C., and Frenzel, P. (2011). Potential of pmoA amplicon pyrosequencing for methanotroph diversity studies. *Appl. Environ. Microbiol.* 77, 6305–6309. doi:10.1128/aem.05355-11.
134. Lynn, D. H. (2008). *The ciliated protozoa : characterization, classification, and guide to the literature*. Springer Available at: https://books.google.no/books?hl=en&lr=&id=Hd3jKGDBR48C&oi=fnd&pg=PA1&ots=EsCUAqTtdD&sig=94kRNuFqaIQz2NxnJh4tPbILPWo&redir_esc=y#v=onepage&q&f=false [Accessed August 31, 2019].
135. Macalady, J. L., Dattagupta, S., Schaperdoth, I., Jones, D. S., Druschel, G. K., and Eastman, D. (2008). Niche differentiation among sulfur-oxidizing bacterial populations in cave waters. *ISME J.* 2, 590–601. doi:10.1038/ismej.2008.25.
136. Mackay, J. R. (1998). Pingo growth and collapse, Tuktoyaktuk Peninsula area, western arctic coast, Canada: A long-term field study. *Geogr. Phys. Quat.* 52, 271–323. doi:10.7202/004847ar.
137. Madrid, V. M., Taylor, G. T., Scranton, M. I., and Chistoserdov, A. Y. (2001). Phylogenetic Diversity of Bacterial and Archaeal Communities in the Anoxic Zone of the Cariaco Basin. *Appl. Environ. Microbiol.* 67, 1663–1674. doi:10.1128/aem.67.4.1663-1674.2001.
138. Maignien, L., Parkes, R. J., Cragg, B., Niemann, H., Knittel, K., Coulon, S., et al. (2013). Anaerobic oxidation of methane in hypersaline cold seep sediments. *FEMS Microbiol. Ecol.* 83, 214–231. doi:10.1111/j.1574-6941.2012.01466.x.
139. Marlow, J. J., Steele, J. A., Case, D. H., Connon, S. A., Levin, L. A., and Orphan, V. J. (2014). Microbial abundance and diversity patterns associated with sediments and carbonates from the methane seep environments of Hydrate Ridge, OR. *Front. Mar. Sci.* 0, 44. doi:10.3389/fmars.2014.00044.
140. Massana, R., Stumm, C. K., and Pedros-Alio, C. (1994). Effects of temperature, sulfide, and food abundance on growth and feeding of anaerobic ciliates. *Appl. Environ. Microbiol.* 60, 1317–1324. doi: 10.1128/aem.60.4.1317-1324.1994.
141. Mau, S., Römer, M., Torres, M. E., Bussmann, I., Pape, T., Damm, E., et al. (2017). Widespread methane seepage along the continental margin off Svalbard - from Bjørnøya to Kongsfjorden. *Sci. Rep.* 7, 42997. doi:10.1038/srep42997.
142. Mayr, M. J., Zimmermann, M., Guggenheim, C., Brand, A., and Bürgmann, H. (2020). Niche partitioning of methane-oxidizing bacteria along the oxygen–methane counter gradient of stratified lakes. *ISME J.* 14, 274–287. doi:10.1038/s41396-019-0515-8.
143. McGinnis, D. F., Greinert, J., Artemov, Y., Beaubien, S. E., and Wüest, A. (2006). Fate of rising methane bubbles in stratified waters: How much methane reaches the atmosphere? *J. Geophys. Res. Ocean.* 111. doi:10.1029/2005JC003183.
144. McHatton, S. C., Barry, J. P., Jannasch, H. W., and Nelson, D. C. (1996). High Nitrate Concentrations in Vacuolate, Autotrophic Marine Beggiatoa spp. *Appl. Environ. Microbiol.* 62. doi: 10.1128/aem.62.3.954-958.1996.
145. Meier, D. V., Pjevac, P., Bach, W., Hourdez, S., Girguis, P. R., Vidoudez, C., et al. (2017). Niche partitioning of diverse sulfur-oxidizing bacteria at hydrothermal vents. *ISME J.* 11, 1545–1558. doi:10.1038/ismej.2017.37.
146. Meister, P., Liu, B., Ferdelman, T. G., Jørgensen, B. B., and Khalili, A. (2013). Control of sulphate and methane distributions in marine sediments by organic matter reactivity. *Geochim. Cosmochim. Acta* 104, 183–193. doi:10.1016/j.gca.2012.11.011.
147. Michaelis, W., Seifert, R., Nauhaus, K., Treude, T., Thiel, V., Blumenberg, M., et al. (2002). Microbial Reefs in the Black Sea Fueled by Anaerobic Oxidation of Methane. *Science (80-.).* 297, 1013–1015.

doi:10.1126/science.1072502.
148. Milkov, A. V., Vogt, P. R., Crane, K., Lein, A. Y., Sassen, R., and Cherkashev, G. A. (2004). Geological, geochemical, and microbial processes at the hydrate-bearing Håkon Mosby mud volcano: a review. *Chem. Geol.* 205, 347–366. doi:10.1016/j.chemgeo.2003.12.030.
149. Mills, H. J., Martinez, R. J., Story, S., and Sobecky, P. A. (2004). Identification of members of the metabolically active microbial populations associated with Beggiatoa species mat communities from Gulf of Mexico cold-seep sediments. *Appl. Environ. Microbiol.* 70, 5447–5458. doi:10.1128/aem.70.9.5447-5458.2004.
150. Milucka, J., Ferdelman, T. G., Polerecky, L., Franzke, D., Wegener, G., Schmid, M., et al. (2012). Zero-valent sulphur is a key intermediate in marine methane oxidation. *Nature* 491, 541–546. doi:10.1038/nature11656.
151. Moreira, D., and López-García, P. (2003). Are hydrothermal vents oases for parasitic protists? *Trends Parasitol.* 19, 556–558. doi:10.1016/j.pt.2003.09.013.
152. Mørk, A., and Bjorøy, M. (1984). Mesozoic source rocks on Svalbard. *Pet. Geol. north Eur. margin. Proc. NEMS '83, Trondheim, 1983*, 371–382. doi:10.1007/978-94-009-5626-1_28.
153. Mußmann, M., Ishii, K., … R. R.-E., and 2005, undefined (2005). Diversity and vertical distribution of cultured and uncultured Deltaproteobacteria in an intertidal mud flat of the Wadden Sea. *Wiley Online Libr.* 7, 405–418. doi:10.1111/j.1462-2920.2005.00708.x.
154. Myhre, C. L., Ferré, B., Platt, S. M., Silyakova, A., Hermansen, O., Allen, G., et al. (2016). Extensive release of methane from Arctic seabed west of Svalbard during summer 2014 does not influence the atmosphere. *Geophys. Res. Lett.* 43, 4624–4631. doi:10.1002/2016gl068999.
155. Myhre, G., Shindell, D., Bréon, F., … W. C.-, J., U., Nauels, U., et al. (2013). Climate change 2013: the physical science basis. Contribution of Working Group I to the Fifth Assessment Report of the Intergovernmental Panel on Climate Change. *K., Tignor, M., Allen, SK, Boschung, J., Nauels, A., Xia, Y., Bex, V., and Midgley, PM, Cambridge University Press Cambridge, United Kingdom and New York, NY, USA.*
156. Nakagawa, S., and Takai, K. (2008). Deep-sea vent chemoautotrophs: Diversity, biochemistry and ecological significance. *FEMS Microbiol. Ecol.* 65, 1–14. doi:10.1111/j.1574-6941.2008.00502.x.
157. Nauhaus, K., Treude, T., Boetius, A., and Kruger, M. (2005). Environmental regulation of the anaerobic oxidation of methane: a comparison of ANME-I and ANME-II communities. *Environ. Microbiol.* 7, 98–106. doi:10.1111/j.1462-2920.2004.00669.x.
158. Niemann, H., Linke, P., Knittel, K., Macpherson, E., Boetius, A., Brü Ckmann, W., et al. (2013). Methane-Carbon Flow into the Benthic Food Web at Cold Seeps-A Case Study from the Costa Rica Subduction Zone. *PLoS One* 8. doi:10.1371/journal.pone.0074894.
159. Niemann, H., Lösekann, T., de Beer, D., Elvert, M., Nadalig, T., Knittel, K., et al. (2006). Novel microbial communities of the Haakon Mosby mud volcano and their role as a methane sink. *Nat. 2006 4437113* 443, 854–858. doi:10.1038/nature05227.
160. Nilsen, F., Cottier, F., Skogseth, R., and Mattsson, S. (2008). Fjord–shelf exchanges controlled by ice and brine production: The interannual variation of Atlantic Water in Isfjorden, Svalbard. *Cont. Shelf Res.* 28, 1838–1853. doi:10.1016/j.csr.2008.04.015.
161. O'Brien, C. E., Giovannelli, D., Govenar, B., Luther, G. W., Lutz, R. A., Shank, T. M., et al. (2015). Microbial biofilms associated with fluid chemistry and megafaunal colonization at post-eruptive deep-sea hydrothermal vents. *Deep. Res. Part II Top. Stud. Oceanogr.* 121, 31–40. doi:10.1016/j.dsr2.2015.07.020.
162. Olsen, B. R., Troedsson, C., Hadziavdic, K., Pedersen, R.-B., and Rapp, H. T. (2014). The influence of vent systems on pelagic eukaryotic micro-organism composition in the Nordic Seas. *Polar Biol. 2014 384* 38, 547–558. doi:10.1007/s00300-014-1621-8.
163. Omoregie, E. O., Niemann, H., Mastalerz, V., de Lange, G. J., Stadnitskaia, A., Mascle, J., et al. (2009). Microbial methane oxidation and sulfate reduction at cold seeps of the deep Eastern Mediterranean Sea. *Mar. Geol.* 261, 114–127. doi:10.1016/j.margeo.2009.02.001.
164. Orphan, V. J., Hinrichs, K. U., Ussler, W., Paull, C. K., Taylor, L. T., Sylva, S. P., et al. (2001). Comparative Analysis of Methane-Oxidizing Archaea and Sulfate-Reducing Bacteria in Anoxic Marine Sediments. *Appl. Environ. Microbiol.* 67, 1922–1934. doi:10.1128/aem.67.4.1922-1934.2001.
165. Orphan, V. J., House, C. H., Hinrichs, K.-U., McKeegan, K. D., and DeLong, E. F. (2002). Multiple archaeal groups mediate methane oxidation in anoxic cold seep sediments. *Proc. Natl. Acad. Sci. U. S. A.* 99, 7663–8. doi:10.1073/pnas.072210299.
166. Ott, J. A., Bright, M., and Schiemer, F. (1998). The Ecology of a Novel Symbiosis Between a Marine Peritrich Ciliate and Chemoautotrophic Bacteria. *Mar. Ecol.* 19, 229–243. doi:10.1111/j.1439-0485.1998.tb00464.x.
167. P. Jeroschewski, *,†, C. Steuckart, † and, and Kühl‡, M. (1996). An Amperometric Microsensor for the

Determination of H2S in Aquatic Environments. *Anal. Chem.* 68, 4351–4357. doi:10.1021/ac960091b.
168. Panieri, G., Bünz, S., Fornari, D. J., Escartin, J., Serov, P., Jansson, P., et al. (2017). An integrated view of the methane system in the pockmarks at Vestnesa Ridge, 79°N. *Mar. Geol.* 390, 282–300. doi:10.1016/j.margeo.2017.06.006.
169. Patwardhan, S., Foustoukos, D. I., Giovannelli, D., Yücel, M., and Vetriani, C. (2018). Ecological succession of sulfur-oxidizing epsilon- And gammaproteobacteria during colonization of a shallow-water gas vent. *Front. Microbiol.* 9, 2970. doi:10.3389/fmicb.2018.02970.
170. Paull, C., Hecker, B., Commeau, R., Freeman-Lynde, R., Neumann, C., Corso, W., et al. (1984). Biological communities at the Florida escarpment resemble hydrothermal vent taxa. *Science* 226, 965–967. doi:10.1126/science.226.4677.965.
171. Paull, C. K., Ussler, W., Dallimore, S. R., Blasco, S. M., Lorenson, T. D., Melling, H., et al. (2007). Origin of pingo-like features on the Beaufort Sea shelf and their possible relationship to decomposing methane gas hydrates. *Geophys. Res. Lett.* 34, L01603. doi:10.1029/2006gl027977.
172. Pernthaler, A., Dekas, A. E., Brown, C. T., Goffredi, S. K., Embaye, T., and Orphan, V. J. (2008). Diverse syntrophic partnerships from deep-sea methane vents revealed by direct cell capture and metagenomics. *Proc. Natl. Acad. Sci.* 105, 7052–7057. doi:10.1073/pnas.0711303105.
173. Phelps, C. D., Kerkhof, L. J., and Young, L. Y. (1998). Molecular characterization of a sulfate-reducing consortium which mineralizes benzene. *FEMS Microbiol. Ecol.* 27, 269–279. doi:10.1111/j.1574-6941.1998.tb00543.x.
174. Piepenburg, D., Ambrose, W. G., Brandt, A., Renaud, P. E., Ahrens, M. J., and Jensen, P. (1997). Benthic community patterns reflect water column processes in the Northeast Water Polynya (Greenland). *J. Mar. Syst.* 10, 467–482. doi:10.1016/s0924-7963(96)00050-4.
175. Pilloni, G., Granitsiotis, M. S., Engel, M., and Lueders, T. (2012). Testing the Limits of 454 Pyrotag Sequencing: Reproducibility, Quantitative Assessment and Comparison to T-RFLP Fingerprinting of Aquifer Microbes. *PLoS One* 7, e40467. doi:10.1371/journal.pone.0040467.
176. Portail, M., Olu, K., Dubois, S. F., Escobar-Briones, E., Gelinas, Y., Menot, L., et al. (2016). Food-web complexity in Guaymas Basin hydrothermal vents and cold seeps. *PLoS One* 11. doi:10.1371/journal.pone.0162263.
177. Portnov, A., Vadakkepuliyambatta, S., Mienert, J., and Hubbard, A. (2016). Ice-sheet-driven methane storage and release in the Arctic. *Nat. Commun.* 7, 1–7. doi:10.1038/ncomms10314.
178. Powell, M. A., and Somero, G. N. (1986). Adaptations to sulfide by hydrothermal vent animals: sites and mechanisms of detoxification and metabolism. *Biol. Bull.* 171, 274–290. doi:10.2307/1541923.
179. Preisler, A., De Beer, D., Lichtschlag, A., Lavik, G., Boetius, A., and Joørgensen, B. B. (2007). Biological and chemical sulfide oxidation in a Beggiatoa inhabited marine sediment. *ISME J.* 1, 341–353. doi:10.1038/ismej.2007.50.
180. Qi, Y.-L., Evans, P. N., Li, Y.-X., Rao, Y.-Z., Qu, Y.-N., Tan, S., et al. (2021). Comparative Genomics Reveals Thermal Adaptation and a High Metabolic Diversity in " *Candidatus* Bathyarchaeia." *mSystems*. doi:10.1128/msystems.00252-21.
181. Quast, C., Pruesse, E., Yilmaz, P., Gerken, J., Schweer, T., Yarza, P., et al. (2012). The SILVA ribosomal RNA gene database project: improved data processing and web-based tools. *Nucleic Acids Res.* 41, D590–D596. doi:10.1093/nar/gks1219.
182. Quéric, N. V., and Soltwedel, T. (2007). Impact of small-scale biogenic sediment structures on bacterial distribution and activity in Arctic deep-sea sediments. *Mar. Ecol.* 28, 66–74. doi:10.1111/j.1439-0485.2007.00177.x.
183. Rahman, M. T., Crombie, A., Chen, Y., Stralis-Pavese, N., Bodrossy, L., Meir, P., et al. (2011). Environmental distribution and abundance of the facultative methanotroph Methylocella. *ISME J.* 5, 1061–1066. doi:10.1038/ismej.2010.190.
184. Ramírez, G. A., McKay, L. J., Fields, M. W., Buckley, A., Mortera, C., Hensen, C., et al. (2020). The Guaymas Basin Subseafloor Sedimentary Archaeome Reflects Complex Environmental Histories. *iScience* 23, 101459. doi:10.1016/j.isci.2020.101459.
185. Reeburgh, W. S. (2007). Oceanic methane biogeochemistry. *Chem. Rev.* 107, 486–513. doi:10.1021/cr050362v.
186. Renaud, P. E., Morata, N., Carroll, M. L., Denisenko, S. G., and Reigstad, M. (2008). Pelagic-benthic coupling in the western Barents Sea: Processes and time scales. *Deep. Res. Part II Top. Stud. Oceanogr.* 55, 2372–2380. doi:10.1016/j.dsr2.2008.05.017.
187. Riboulot, V. (2018). Geomorphology of Gas Hydrate-Bearing Pockmark. *Gas Hydrates 2 Geosci. Issues Potential Ind. Appl.*, 37–48. doi:10.1002/9781119451174.ch4.
188. Rinke, C., Schmitz-Esser, S., Stoecker, K., Nussbaumer, A. D., Molnár, D. A., Vanura, K., et al. (2006). "Candidatus Thiobios zoothamnicoli," an ectosymbiotic bacterium covering the giant marine ciliate Zoothamnium niveum. *Appl. Environ. Microbiol.* 72, 2014–21. doi:10.1128/aem.72.3.2014-

2021.2006.
189. Roalkvam, I., Dahle, H., Chen, Y., Jørgensen, S. L., Haflidason, H., and Steen, I. H. (2012). Fine-Scale Community Structure Analysis of ANME in Nyegga Sediments with High and Low Methane Flux. *Front. Microbiol.* 3, 216. doi:10.3389/fmicb.2012.00216.
190. Roalkvam, I., Jørgensen, S. L., Chen, Y., Stokke, R., Dahle, H., Hocking, W. P., et al. (2011). New insight into stratification of anaerobic methanotrophs in cold seep sediments. *FEMS Microbiol. Ecol.* 78, 233–243. doi:10.1111/j.1574-6941.2011.01153.x.
191. Rogener, M. K., Bracco, A., Hunter, K. S., Saxton, M. A., and Joye, S. B. (2018). Long-term impact of the Deepwater Horizon oil well blowout on methane oxidation dynamics in the northern Gulf of Mexico. *Elem. Sci. Anthr.* 6. doi:10.1525/elementa.332.
192. Rosati, G. (2001). Ectosymbiosis in Ciliated Protozoa. *Symbiosis*, 475–488. doi:10.1007/0-306-48173-1_30.
193. Rossel, P. E., Elvert, M., Ramette, A., Boetius, A., and Hinrichs, K. U. (2011). Factors controlling the distribution of anaerobic methanotrophic communities in marine environments: Evidence from intact polar membrane lipids. *Geochim. Cosmochim. Acta* 75, 164–184. doi:10.1016/j.gca.2010.09.031.
194. Ruff, S. E., Biddle, J. F., Teske, A. P., Knittel, K., Boetius, A., and Ramette, A. (2015). Global dispersion and local diversification of the methane seep microbiome. *Proc. Natl. Acad. Sci. U. S. A.* 112, 4015–20. doi:10.1073/pnas.1421865112.
195. Ruppel, C. (2007). Tapping Methane Hydrates for Unconventional Natural Gas. *Elements* 3, 193–199. doi:10.2113/gselements.3.3.193.
196. Ruppel, C. D., and Kessler, J. D. (2017). The interaction of climate change and methane hydrates. *Rev. Geophys.* 55, 126–168. doi:10.1002/2016rg000534.
197. Sahling, H., Römer, M., Pape, T., Bergès, B., Dos Santos Fereirra, C., Boelmann, J., et al. (2014). Gas emissions at the continental margin west of Svalbard: Mapping, sampling, and quantification. *Biogeosciences* 11, 6029–6046. doi:10.5194/bg-11-6029-2014.
198. Sarkar, S., Berndt, C., Minshull, T. A., Westbrook, G. K., Klaeschen, D., Masson, D. G., et al. (2012). Seismic evidence for shallow gas-escape features associated with a retreating gas hydrate zone offshore west Svalbard. *J. Geophys. Res. Solid Earth* 117, 9102. doi:10.1029/2011jb009126.
199. Saunois, M., Bousquet, P., Poulter, B., Peregon, A., Ciais, P., Canadell, J. G., et al. (2016). The global methane budget 2000-2012. *Earth Syst. Sci. Data* 8, 697–751. doi:10.5194/essd-8-697-2016.
200. Saunois, M., Stavert, A. R., Poulter, B., Bousquet, P., Canadell, J. G., Jackson, R. B., et al. (2020). The Global Methane Budget 2000–2017. *Greet Janssens-Maenhout* 12, 45. doi:10.5194/essd-12-1561-2020.
201. Savvichev, A. S., Kadnikov, V. V., Kravchishina, M. D., Galkin, S. V., Novigatskii, A. N., Sigalevich, P. A., et al. (2018). Methane as an Organic Matter Source and the Trophic Basis of a Laptev Sea Cold Seep Microbial Community. *https://doi.org/10.1080/01490451.2017.1382612* 35, 411–423. doi:10.1080/01490451.2017.1382612.
202. Schoell, M. (1983). Genetic characterization of natural gases. *Am. Assoc. Pet. Geol. Bull.* 67, 2225–2238. doi:10.1306/ad46094a-16f7-11d7-8645000102c1865d.
203. Schoell, M. (1988). Multiple origins of methane in the Earth. *Chem. Geol.* 71, 1–10. doi:10.1016/0009-2541(88)90101-5.
204. Searcy, D. G. (2006). Rapid hydrogen sulfide consumption by Tetrahymena pyriformis and its implications for the origin of mitochondria. *Eur. J. Protistol.* 42, 221–231. doi:10.1016/j.ejop.2006.06.001.
205. Sears, K., Alleman, J. E., Barnard, J. L., and Oleszkiewicz, J. A. (2004). Impacts of reduced sulfur components on active and resting ammonia oxidizers. *J. Ind. Microbiol. Biotechnol.* 31, 369–378. doi:10.1007/s10295-004-0157-2.
206. Sen, A., Aström, E. K. L., Hong, W. L., Portnov, A., Waage, M., Serov, P., et al. (2018a). Geophysical and geochemical controls on the megafaunal community of a high Arctic cold seep. *Biogeosciences* 15, 4533–4559. doi:10.5194/bg-15-4533-2018.
207. Sen, A., Didriksen, A., Hourdez, S., Svenning, M. M., and Rasmussen, T. L. (2020). Frenulate siboglinids at high Arctic methane seeps and insight into high latitude frenulate distribution. *Ecol. Evol.* 10, 1339–1351. doi:10.1002/ece3.5988.
208. Sen, A., Duperron, S., Hourdez, S., Piquet, B., Léger, N., Gebruk, A., et al. (2018b). Cryptic frenulates are the dominant chemosymbiotrophic fauna at Arctic and high latitude Atlantic cold seeps. *PLoS One* 13, e0209273. doi:10.1371/journal.pone.0209273.
209. Serov, P., Portnov, A., Mienert, J., Semenov, P., and Ilatovskaya, P. (2015). Methane release from pingo-like features across the South Kara Sea shelf, an area of thawing offshore permafrost. *J. Geophys. Res. Earth Surf.* 120, 1515–1529. doi:10.1002/2015jf003467.
210. Serov, P., Vadakkepuliyambatta, S., Mienert, J., Patton, H., Portnov, A., Silyakova, A., et al. (2017). Postglacial response of Arctic Ocean gas hydrates to climatic amelioration. *Proc. Natl. Acad. Sci.* 114,

6215–6220. doi:10.1073/pnas.1619288114.
211. Shakhova, N., Semiletov, I., Salyuk, A., Yusupov, V., Kosmach, D., and Gustafsson, Ö. (2010). Extensive methane venting to the atmosphere from sediments of the East Siberian Arctic Shelf. *Science (80-.).* 327, 1246–1250. doi:10.1126/science.1182221.
212. Sibuet, M., and Olu, K. (1998). Biogeography, biodiversity and fluid dependence of deep-sea cold-seep communities at active and passive margins. *Deep Sea Res. Part II Top. Stud. Oceanogr.* 45, 517–567. doi:10.1016/s0967-0645(97)00074-x.
213. Silyakova, A., Jansson, P., Serov, P., Ferré, B., Pavlov, A. K., Hattermann, T., et al. (2020). Physical controls of dynamics of methane venting from a shallow seep area west of Svalbard. *Cont. Shelf Res.* 194, 104030. doi:10.1016/j.csr.2019.104030.
214. Sloan, E. J., and Koh, C. (2008). *Clathrate hydrates of natural gases, Third Edition*. CRC Press, Boca Raton, FL Available at: https://www.google.com/books?hl=en&lr=&id=T7LC8ldaVR4C&oi=fnd&pg=PP1&dq=Clathrate+Hydrates+of+Natural+Gases,&ots=HzdyakP_Us&sig=ZmqlVJ_MopBJJu4-36N5Cm_MymM [Accessed July 30, 2021].
215. Stahl, A. D. (1991). Development and application of nucleic acid probes. *Nucleic Acid Tech. Bact. Syst.* 96, 205–248. doi:10.1016/s1389-1723(04)70148-6.
216. Steinle, L., Graves, C. A., Treude, T., Ferré, B., Biastoch, A., Bussmann, I., et al. (2015). Water column methanotrophy controlled by a rapid oceanographic switch. *Nat. Geosci.* 8, 378–382. doi:10.1038/ngeo2420.
217. Stoecker, K., Bendinger, B., … B. S.-P. of the, and 2006, U. (2006). Cohn's Crenothrix is a filamentous methane oxidizer with an unusual methane monooxygenase. *Natl. Acad. Sci.* 103, 2363–2367. Available at: https://www.pnas.org/content/103/7/2363.short [Accessed August 2, 2021].
218. Stoecker, K., Dorninger, C., Daims, H., and Wagner, M. (2010). Double labeling of oligonucleotide probes for fluorescence in situ hybridization (DOPE-FISH) improves signal intensity and increases rRNA accessibility. *Appl. Environ. Microbiol.* 76, 922–926. doi:10.1128/aem.02456-09.
219. Stokke, R., Roalkvam, I., Lanzen, A., Haflidason, H., and Steen, I. H. (2012). Integrated metagenomic and metaproteomic analyses of an ANME-1-dominated community in marine cold seep sediments. *Environ. Microbiol.* 14, 1333–1346. doi:10.1111/j.1462-2920.2012.02716.x.
220. Suess, E. (2014). Marine cold seeps and their manifestations: geological control, biogeochemical criteria and environmental conditions. *Int. J. Earth Sci.* 103, 1889–1916. doi:10.1007/s00531-014-1010-0.
221. Suominen, S., Dombrowski, N., Damsté, J. S. S., and Villanueva, L. (2021). A diverse uncultivated microbial community is responsible for organic matter degradation in the Black Sea sulphidic zone. *Environ. Microbiol.* 23, 2709–2728. doi:10.1111/1462-2920.14902.
222. Takishita, K. (2015). Diversity of Microbial Eukaryotes in Deep Sea Chemosynthetic Ecosystems Illuminated by Molecular Techniques. *Mar. Protists Divers. Dyn.*, 47–61. doi:10.1007/978-4-431-55130-0_3.
223. Takishita, K., Kakizoe, N., Yoshida, T., and Maruyama, T. (2010). Molecular Evidence that Phylogenetically Diverged Ciliates Are Active in Microbial Mats of Deep-Sea Cold-Seep Sediment. *J. Eukaryot. Microbiol.* 57, 76–86. doi:10.1111/j.1550-7408.2009.00457.x.
224. Takishita, K., Yubuki, N., Kakizoe, N., Inagaki, Y., and Maruyama, T. (2007). Diversity of microbial eukaryotes in sediment at a deep-sea methane cold seep: surveys of ribosomal DNA libraries from raw sediment samples and two enrichment cultures. *Extremophiles* 11, 563–576. doi:10.1007/s00792-007-0068-z.
225. Tavormina, P. L., Hatzenpichler, R., McGlynn, S., Chadwick, G., Dawson, K. S., Connon, S. A., et al. (2015). Methyloprofundus sedimenti gen. nov., sp. nov., an obligate methanotroph from ocean sediment belonging to the 'deep sea-1' clade of marine methanotrophs. *Int. J. Syst. Evol. Microbiol.* 65, 251–259. doi:10.1099/ijs.0.062927-0.
226. Tavormina, P. L., Ussier, W., and Orphan, V. J. (2008). Planktonic and sediment-associated aerobic methanotrophs in two seep systems along the North American margin. *Appl. Environ. Microbiol.* 74, 3985–3995. doi:10.1128/aem.00069-08.
227. Taylor, G. T., Iabichella, M., Ho, T. Y., Scranton, M. I., Thunell, R. C., Muller-Karger, F., et al. (2001). Chemoautotrophy in the redox transition zone of the Cariaco Basin: A significant midwater source of organic carbon production. *Limnol. Oceanogr.* 46, 148–163. doi:10.4319/lo.2001.46.1.0148.
228. Teske, A., Hinrichs, K. U., Edgcomb, V., De Vera Gomez, A., Kysela, D., Sylva, S. P., et al. (2002). Microbial diversity of hydrothermal sediments in the Guaymas Basin: Evidence for anaerobic methanotrophic communities. *Appl. Environ. Microbiol.* 68, 1994–2007. doi:10.1128/aem.68.4.1994-2007.2002.
229. Thurber, A. R., Jones, W. J., and Schnabel, K. (2011). Dancing for Food in the Deep Sea: Bacterial Farming by a New Species of Yeti Crab. *PLoS One* 6, e26243. doi:10.1371/journal.pone.0026243.

230. Timmermans, M. L., and Marshall, J. (2020). Understanding Arctic Ocean Circulation: A Review of Ocean Dynamics in a Changing Climate. *J. Geophys. Res. Ocean.* 125. doi:10.1029/2018jc014378.
231. Timmers, P. H. A., Widjaja-Greefkes, H. C. A., Ramiro-Garcia, J., Plugge, C. M., and Stams, A. J. M. (2015). Growth and activity of ANME clades with different sulfate and sulfide concentrations in the presence of methane. *Front. Microbiol.* 6, 988. doi:10.3389/fmicb.2015.00988.
232. Toone, T. A., and Washburn, T. W. (2020). Phytodetritus, chemosynthesis, and the dark biosphere: Does depth influence trophic relationships at deep-sea Barbados seeps. *Deep Sea Res. Part I Oceanogr. Res. Pap.* 165, 103367. doi:10.1016/j.dsr.2020.103367.
233. Torres, M. E., McManus, J., and Huh, C. A. (2002). Fluid seepage along the San Clemente Fault scarp: basin-wide impact on barium cycling. *Earth Planet. Sci. Lett.* 203, 181–194. doi:10.1016/s0012-821x(02)00800-2.
234. Trotsenko, Y. A., and Khmelenina, V. N. (2002). Biology of extremophilic and extremotolerant methanotrophs. *Arch. Microbiol.* 177, 123–131. doi:10.1007/s00203-001-0368-0.
235. Trotsenko, Y. A., and Murrell, J. C. (2008). Metabolic aspects of aerobic obligate methanotrophy. *Adv. Appl. Microbiol.* 63, 183–229. Available at: https://www.sciencedirect.com/science/article/pii/S0065216407000056 [Accessed August 2, 2021].
236. Urich, T., Lanzén, A., Qi, J., Huson, D. H., Schleper, C., and Schuster, S. C. (2008). Simultaneous Assessment of Soil Microbial Community Structure and Function through Analysis of the Meta-Transcriptome. *PLoS One* 3, e2527. doi:10.1371/journal.pone.0002527.
237. Valentine, D. L. (2011). Emerging topics in marine methane biogeochemistry. *Ann. Rev. Mar. Sci.* 3, 147–171. doi:10.1146/annurev-marine-120709-142734.
238. Valentine, D. L., Blanton, D. C., Reeburgh, W. S., and Kastner, M. (2001). Water column methane oxidation adjacent to an area of active hydrate dissociation, Eel river Basin. *Geochim. Cosmochim. Acta* 65, 2633–2640. doi:10.1016/S0016-7037(01)00625-1.
239. Valentine, D. L., and Reeburgh, W. S. (2000). New perspectives on anaerobic methane oxidation. *Environ. Microbiol.* 2, 477–484. doi:10.1046/j.1462-2920.2000.00135.x.
240. van der Maarel, M. J. E. C., Sprenger, W., Haanstra, R., and Forney, L. J. (1999). Detection of methanogenic archaea in seawater particles and the digestive tract of a marine fish species. *FEMS Microbiol. Lett.* 173, 189–194. doi:10.1111/j.1574-6968.1999.tb13501.x.
241. Van Gaever, S., Moodley, L., Pasotti, F., Houtekamer, M., Middelburg, J. J., Danovaro, R., et al. (2009). Trophic specialisation of metazoan meiofauna at the Håkon Mosby Mud Volcano: fatty acid biomarker isotope evidence. *Mar. Biol. 2009 1566* 156, 1289–1296. doi:10.1007/s00227-009-1170-9.
242. Vanreusel, A. N. N., Andersen, A. N. N. C., Boetius, A., Connelly, D., Cunha, M. R., Decker, C., et al. (2009). Biodiversity of Cold Seep Ecosystems Along the European Margins. *Oceanography* 22, 110–127. Available at: http://www.jstor.org/stable/24860929.
243. Vaughn Barrie, J., Cook, S., and Conway, K. W. (2011). Cold seeps and benthic habitat on the Pacific margin of Canada. *Cont. Shelf Res.* 31, S85–S92. doi:10.1016/j.csr.2010.02.013.
244. Vernet, M., Ellingsen, I. H., Seuthe, L., Slagstad, D., Cape, M. R., and Matrai, P. A. (2019). Influence of Phytoplankton Advection on the Productivity Along the Atlantic Water Inflow to the Arctic Ocean. *Front. Mar. Sci.* 6, 1–18. doi:10.3389/fmars.2019.00583.
245. Vigneron, A., Alsop, E. B., Cruaud, P., Philibert, G., King, B., Baksmaty, L., et al. (2019). Contrasting Pathways for Anaerobic Methane Oxidation in Gulf of Mexico Cold Seep Sediments. *mSystems* 4. doi:10.1128/msystems.00091-18.
246. Vigneron, A., Cruaud, P., Pignet, P., Caprais, J.-C., Cambon-Bonavita, M.-A., Godfroy, A., et al. (2013). Archaeal and anaerobic methane oxidizer communities in the Sonora Margin cold seeps, Guaymas Basin (Gulf of California). *ISME J. 2013 78* 7, 1595–1608. doi:10.1038/ismej.2013.18.
247. Vigneron, A., Cruaud, P., Pignet, P., Caprais, J.-C., Gayet, N., Cambon-Bonavita, M.-A., et al. (2014). Bacterial communities and syntrophic associations involved in anaerobic oxidation of methane process of the Sonora Margin cold seeps, Guaymas Basin. *Environ. Microbiol.* 16, 2777–2790. doi:10.1111/1462-2920.12324.
248. Vogt, P. R., Crane, K., Sundvor, E., Max, M. D., and Pfirman, S. L. (1994). Methane-generated(?) pockmarks on young, thickly sedimented oceanic crust in the Arctic: Vestnesa Ridge, Fram Strait. *Geology* 22, 255–258. doi:10.1130/0091-7613(1994)022<0255:mgpoyt>2.3.co;2.
249. Waage, M., Portnov, A., Serov, P., Bünz, S., Waghorn, K. A., Vadakkepuliyambatta, S., et al. (2019). Geological Controls on Fluid Flow and Gas Hydrate Pingo Development on the Barents Sea Margin. *Geochemistry, Geophys. Geosystems* 20, 630–650. doi:10.1029/2018gc007930.
250. Wallmann, K., Burwicz, E., Ruepke, L. H., Marquardt, M., Pinero, E., Haeckel, M., et al. (2011). Constraining the global inventory of methane hydrate in marine sediments. *Proc. 7th Int. Conf. Gas Hydrates (ICGH2011). HWU, Edinburgh, UK, 129/1-13.* .
251. Wang, F., and Chapman, P. M. (1999). Biological implications of sulfide in sediment—a review focusing

on sediment toxicity. *Environ. Toxicol. Chem.* 18, 2526–2532. doi:10.1002/etc.5620181120.
252. Wang, Y., Zhang, W. P., Cao, H. L., Shek, C. S., Tian, R. M., Wong, Y. H., et al. (2014). Diversity and distribution of eukaryotic microbes in and around a brine pool adjacent to the Thuwal cold seeps in the Red Sea. *Front. Microbiol.* 0, 37. doi:10.3389/fmicb.2014.00037.
253. Weber, T., Wiseman, N. A., and Kock, A. (2019). Global ocean methane emissions dominated by shallow coastal waters. *Nat. Commun.* 10, 1–10. doi:10.1038/s41467-019-12541-7.
254. Webster, G., Parkes, R. J., Fry, J. C., and Weightman, A. J. (2004). Widespread occurrence of a novel division of bacteria identified by 16S rRNA gene sequences originally found in deep marine sediments. *Appl. Environ. Microbiol.* 70, 5708–5713. doi:10.1128/aem.70.9.5708-5713.2004.
255. Webster, G., Rinna, J., Roussel, E. G., Fry, J. C., Weightman, A. J., and Parkes, R. J. (2010). Prokaryotic functional diversity in different biogeochemical depth zones in tidal sediments of the Severn Estuary, UK, revealed by stable-isotope probing. *FEMS Microbiol. Ecol.* 72, 179–197. doi:10.1111/j.1574-6941.2010.00848.x.
256. Webster, G., Yarram, L., Freese, E., Köster, J., Sass, H., Parkes, R. J., et al. (2007). Distribution of candidate division JS1 and other Bacteria in tidal sediments of the German Wadden Sea using targeted 16S rRNA gene PCR-DGGE. *FEMS Microbiol. Ecol.* 62, 78–89. doi:10.1111/j.1574-6941.2007.00372.x.
257. Wegener, G., Gropp, J., Taubner, H., Halevy, I., and Elvert, M. (2021). Sulfate-dependent reversibility of intracellular reactions explains the opposing isotope effects in the anaerobic oxidation of methane. *Sci. Adv.* 7, eabe4939. doi:10.1126/sciadv.abe4939.
258. Wegener, G., Krukenberg, V., Riedel, D., Tegetmeyer, H. E., and Boetius, A. (2015). Intercellular wiring enables electron transfer between methanotrophic archaea and bacteria. *Nature* 526, 587–590. doi:10.1038/nature15733.
259. Wegener, G., Shovitri, M., Knittel, K., Niemann, H., Hovland, M., and Boetius, A. (2008). Biogeochemical processes and microbial diversity of the Gullfaks and Tommeliten methane seeps (Northern North Sea). *Biogeosciences* 5, 1127–1144. doi:10.5194/bg-5-1127-2008.
260. Wen, X., Yang, S., and Liebner, S. (2016). Evaluation and update of cutoff values for methanotrophic pmoA gene sequences. *Arch. Microbiol.* 198, 629–636. doi:10.1007/s00203-016-1222-8.
261. Westbrook, G. K., Thatcher, K. E., Rohling, E. J., Piotrowski, A. M., Pälike, H., Osborne, A. H., et al. (2009). Escape of methane gas from the seabed along the West Spitsbergen continental margin. *Geophys. Res. Lett.* 36. doi:10.1029/2009gl039191.
262. Whiticar, M. J. (2000). Can Stable Isotopes and Global Budgets Be Used to Constrain Atmospheric Methane Budgets? *Atmos. Methane*, 63–85. doi:10.1007/978-3-662-04145-1_5.
263. Whiticar, M. J., Faber, E., and Schoell, M. (1986). Biogenic methane formation in marine and freshwater environments: CO2 reduction vs. acetate fermentation-Isotope evidence. *Geochim. Cosmochim. Acta* 50, 693–709. doi:10.1016/0016-7037(86)90346-7.
264. Wit, R. De, and Bouvier, T. (2006). 'Everything is everywhere, but, the environment selects'; what did Baas Becking and Beijerinck really say? *Environ. Microbiol.* 8, 755–758. doi:10.1111/j.1462-2920.2006.01017.x.
265. WMO, W. M. O. (2019). /. Geneva: WMO.
266. Yakushev, V. S., and Chuvilin, E. M. (2000). Natural gas and gas hydrate accumulations within permafrost in Russia. *Cold Reg. Sci. Technol.* 31, 189–197. doi:10.1016/s0165-232x(00)00012-4.
267. Yanagawa, K., Sunamura, M., Lever, M. A., Morono, Y., Hiruta, A., Ishizaki, O., et al. (2011). Niche Separation of Methanotrophic Archaea (ANME-1 and-2) in Methane-Seep Sediments of the Eastern Japan Sea Offshore Joetsu. *Tetsuro Urabe Fumio Ina.* 28, 118–129. doi:10.1080/01490451003709334.
268. Yang, S., Wen, X., and Liebner, S. (2016). pmoA gene reference database (fasta-formatted sequences and taxonomy). Available at: https://doi.org/10.5880/gfz.5.3.2016.001.
269. Yao, H., Panieri, G., Lehmann, M. F., Himmler, T., and Niemann, H. (2021). Biomarker and Isotopic Composition of Seep Carbonates Record Environmental Conditions in Two Arctic Methane Seeps. *Front. Earth Sci.* 0, 755. doi:10.3389/feart.2020.570742.
270. Yilmaz, P., Parfrey, L. W., Yarza, P., Gerken, J., Pruesse, E., Quast, C., et al. (2014). The SILVA and "'All-species Living Tree Project (LTP)'" taxonomic frameworks. *Nucleic Acids Res.* 42, D643–D648. doi:10.1093/nar/gkt1209.
271. Zhang, C. L., Huang, Z., Cantu, J., Pancost, R. D., Brigmon, R. L., Lyons, T. W., et al. (2005). Lipid biomarkers and carbon isotope signatures of a microbial (Beggiatoa) mat associated with gas hydrates in the Gulf of Mexico. *Appl. Environ. Microbiol.* 71, 2106–2112. doi:10.1128/aem.71.4.2106-2112.2005.
272. Zhang, Y., Su, X., Chen, F., Jiao, L., Jiang, H., Dong, H., et al. (2012). Abundance and diversity of candidate division JS1- and Chloroflexi-related bacteria in cold seep sediments of the northern South China Sea. *Front. Earth Sci. 2012 64* 6, 373–382. doi:10.1007/s11707-012-0324-0.
273. Zhou, Z., Pan, J., Wang, F., Gu, J.-D. D., and Li, M. (2018). Bathyarchaeota: Globally distributed metabolic generalists in anoxic environments. *FEMS Microbiol. Rev.* 42, 639–655. doi:10.1093/femsre/fuy023.

Paper I

frontiers in Microbiology

ORIGINAL RESEARCH
published: 24 September 2020
doi: 10.3389/fmicb.2020.01932

The Impact of Methane on Microbial Communities at Marine Arctic Gas Hydrate Bearing Sediment

Vincent Carrier[1,2], Mette M. Svenning[1,2]*, Friederike Gründger[3], Helge Niemann[2,4,5], Pierre-Antoine Dessandier[2], Giuliana Panieri[2] and Dimitri Kalenitchenko[2]*

[1] Department of Arctic and Marine Biology, The Arctic University of Norway, Tromsø, Norway, [2] Centre for Arctic Gas Hydrate, Environment and Climate, The Arctic University of Norway, Tromsø, Norway, [3] Department of Bioscience, Arctic Research Centre, Aarhus University, Aarhus, Denmark, [4] Department of Marine Microbiology and Biogeochemistry, Royal Netherlands Institute for Sea Research, and Utrecht University, Den Burg, Netherlands, [5] Department of Earth Sciences, Faculty of Geosciences, Utrecht University, Utrecht, Netherlands

OPEN ACCESS

Edited by:
Levente Bodrossy, Oceans and Atmosphere (CSIRO), Australia

Reviewed by:
Marshall Wayne Bowles, Louisiana Universities Marine Consortium, United States
Cassandre Sara Lazar, Université du Québec à Montréal, Canada

***Correspondence:**
Vincent Carrier
vincent.carrier@uit.no;
vincent.carrier.90@gmail.com
Mette M. Svenning
mette.svenning@uit.no

Specialty section:
This article was submitted to Aquatic Microbiology, a section of the journal Frontiers in Microbiology

Received: *21 February 2020*
Accepted: *22 July 2020*
Published: *24 September 2020*

Citation:
Carrier V, Svenning MM, Gründger F, Niemann H, Dessandier P-A, Panieri G and Kalenitchenko D (2020) The Impact of Methane on Microbial Communities at Marine Arctic Gas Hydrate Bearing Sediment. Front. Microbiol. 11:1932. doi: 10.3389/fmicb.2020.01932

Cold seeps are characterized by high biomass, which is supported by the microbial oxidation of the available methane by capable microorganisms. The carbon is subsequently transferred to higher trophic levels. South of Svalbard, five geological mounds shaped by the formation of methane gas hydrates, have been recently located. Methane gas seeping activity has been observed on four of them, and flares were primarily concentrated at their summits. At three of these mounds, and along a distance gradient from their summit to their outskirt, we investigated the eukaryotic and prokaryotic biodiversity linked to 16S and 18S rDNA. Here we show that local methane seepage and other environmental conditions did affect the microbial community structure and composition. We could not demonstrate a community gradient from the summit to the edge of the mounds. Instead, a similar community structure in any methane-rich sediments could be retrieved at any location on these mounds. The oxidation of methane was largely driven by anaerobic methanotrophic Archaea-1 (ANME-1) and the communities also hosted high relative abundances of sulfate reducing bacterial groups although none demonstrated a clear co-occurrence with the predominance of ANME-1. Additional common taxa were observed and their abundances were likely benefiting from the end products of methane oxidation. Among these were sulfide-oxidizing Campilobacterota, organic matter degraders, such as Bathyarchaeota, Woesearchaeota, or thermoplasmatales marine benthic group D, and heterotrophic ciliates and Cercozoa.

Keywords: Arctic, methane seeps, prokaryotes, methanotrophs, ANME, Sulfate-reducing bacteria, eukaryotes, foraminifera

INTRODUCTION

Cold seep microbial communities thrive where geofluids, characterized by high concentrations of hydrocarbons, in particular methane (CH_4), provide a primary energy source for these organisms (Boetius et al., 2000; Orphan et al., 2002; Niemann et al., 2013). These geofluids and/or free gas migrate upward through faults, cracks, and sediment pores that provide a transport vector from

sub-seafloor reservoirs to the seafloor. The origin of methane can be either from the geological cracking of organic matter at high temperature or from biologically mediated decomposition of organic matter (Schoell, 1988; Joye et al., 2010). Under certain thermobaric conditions, CH_4 forms gas hydrates, i.e., an ice-like lattice comprising molecules of CH_4 trapped in crystalline cages of water molecules. The formation or the dissociation of gas hydrates can modify the seafloor morphology, and subsequently can lead to the genesis of pockmarks, craters, and gas domes (Vogt et al., 1994; Hovland and Svensen, 2006; Koch et al., 2015; Portnov et al., 2016; Serov et al., 2017; Waage et al., 2019).

The CH_4 present in the fluid can be oxidized aerobically or anaerobically (Krüger et al., 2005; James et al., 2016). In aerobic environments, the oxidation of CH_4 is driven by methane oxidizing bacteria that utilize oxygen as an electron acceptor. Most of them are associated with the alpha and gamma proteobacteria, but also with Verrucomicrobia or *Crenothrix* (Hanson and Hanson, 1996; Knief, 2015). Nevertheless, microbial activity at the cold seep seafloor rapidly depletes the available oxygen in marine sediments and limits its penetration depth to a small surface layer, usually of a few millimeters thickness at most (Niemann et al., 2006, 2009; Reeburgh, 2007; Boetius and Wenzhöfer, 2013). In the absence of oxygen, methane is oxidized anaerobically through a process that has been termed the anaerobic oxidation of methane (AOM; Reeburgh, 2007). Anaerobic oxidation of methane is driven by anaerobic methanotrophic Archaea (ANME) and so far, three main ANME clades of phylogenetically distinct groups were detected: ANME-2 and ANME-3 are placed within the methanosarcinales, while ANME-1 forms a distinct group within the Halobacterota (Knittel and Boetius, 2009; Quast et al., 2012; Yilmaz et al., 2014). The phylogenetic dissimilarity of these ANME groups suggests different levels of tolerance to various environmental parameters. Previous study results suggested that ANME-2 might be more sensitive than ANME-1 to high concentrations of sulfide and low concentrations of sulfate (Timmers et al., 2015; Bhattarai et al., 2018). The ANME-2 group would then often be limited to the layers at the sulfate-methane transition zone (SMTZ) and ANME-1 would dominate in more sulfidic sediments, at deeper layers (Knittel et al., 2005; Roalkvam et al., 2012). Nevertheless, ANME-2 groups were also retrieved in sulfide-rich sediments (for example at the Hydrate Ridge; Knittel et al., 2003), insinuating the impact of other factors on the observed stratification of ANME groups. Additional environmental conditions that were suggested to select for differential ANME groups include temperature (Nauhaus et al., 2005; Rossel et al., 2011), salinity (Maignien et al., 2013), or CH_4 flux rates (Girguis et al., 2005; Yanagawa et al., 2011; Marlow et al., 2014).

Most ANME use sulfate, but some were also found to use iron, manganese, and nitrite/nitrate as electron acceptors (Beal et al., 2009; Ettwig et al., 2010, 2016; Hu et al., 2014). Reduction of sulfate at the SMTZ generally requires sulfate reducing bacteria (SRB) and a syntrophic consortium with ANME that are commonly found as AOM drivers (Boetius et al., 2000; Wegener et al., 2015). However, in the last decade, community studies of methanotrophs have shown evidence of free-living ANME cells particularly assigned to the ANME-1 group, but also to the ANME-2 group, that might perform sulfate reduction alone (Orphan et al., 2002; Knittel et al., 2005; Roalkvam et al., 2011; Milucka et al., 2012; Stokke et al., 2012; Gründger et al., 2019).

The AOM coupled with sulfate reduction generates HS^- which can subsequently be oxidized by sulfide-oxidizing bacteria, such as the bacterial mat forming *Beggiatoa* or Campilobacterota species. Some chemoautotrophs can also be present as intracellular and extracellular symbionts within larger fauna, but also in the eukaryotic euglenozoans and ciliates (Buck et al., 2000; Rinke et al., 2006). Additionally, a higher bacterial and archaeal biomass becomes a trophic basis for grazing megafauna or microbial eukaryotes, including diverse bacterivore ciliates, Cercozoa, and stramenopiles (Werne et al., 2002; Takishita et al., 2007, 2010; Niemann et al., 2013). Potentially parasitic or pathogenic eukaryotes, such as Apicomplexa, Ichthyosporea, and fungi, are also likely to benefit from the denser faunal community (Atkins et al., 2002; Takishita et al., 2006).

In the Arctic, gas hydrate bearing domes were observed 50 km south of Svalbard in Storfjordrenna, at ∼390 m below sea level (Serov et al., 2017). They are referred to as pingos, after similar terrestrial features observed in glacial valleys (Mackay, 1998), although they differ by their formation (i.e., gas hydrates instead of regular water ice; Serov et al., 2017). At the water depth of the gas hydrate pingos (GHP; ∼390 m, ∼0.5–2.5°C bottom water T°C), the gas hydrates remain within the gas hydrate stability zone (GHSZ), but are close to its upper limit and are sensitive to even small changes of temperature and pressure (Hong et al., 2018). Hydroacoustic observations have revealed acoustic flares originating from methane gas bubbles in the water column. These were primarily located at the summit on four of the five Storfjordrenna pingos. The dating of methane derived authigenic carbonates suggested that CH_4 seepage has been active for several thousand years (Serov et al., 2017). Visual observations have revealed a higher biomass in sediments of the pingos compared to the surrounding seafloor (Åström et al., 2018). This can be explained by the presence of a carbonate crust induced by AOM, which offers a hard substrate for the attachment of benthic organisms, such as sponges and anemones (Niemann et al., 2005; Cordes et al., 2010; Vaughn Barrie et al., 2011).

Past investigations at the Storfjordrenna pingos have primarily addressed the geochemical conditions (Serov et al., 2017; Hong et al., 2018) or the biodiversity of larger fauna (Sen et al., 2018; Åström et al., 2018), but the microbial community structure remains mostly unknown [with the exception of a biofilm retrieved within deeper sediments at the pingos (Gründger et al., 2019)]. At a circular seep further south, the Haakon Mosby Mud Volcano (HMMV), the composition of the bacterial and archaeal communities varied between concentric zones around the apex of the edifice, i.e., along a methane flux/concentration gradient (Niemann et al., 2006; Lösekann et al., 2007). In Storfjordrenna, the gas flares at the summit of the structures could suggest a similar concentric arrangement of microbial habitats. However, these pingos contrast with HMMV by presenting a multitude of small geological fractures and gas hydrates chaotically distributed around the structures through

which methane migrates to the seafloor surface (Hong et al., 2018; Waage et al., 2019).

Our study aimed at determining spatial variations in the microbial community structure along a gradient from the apex to the edge of three pingos. We addressed key environmental factors that are influencing the prokaryotic and eukaryotic community structures and their spatial distribution. Finally, we identified key taxa characteristics for these Arctic CH_4-rich environments, demonstrating the uniqueness of this ecosystem.

MATERIALS AND METHODS

Study Site

The sampling site was located in the Arctic Ocean at the mouth of Storfjordrenna, 50 km south of Svalbard at approximatively 390 m water depth (Serov et al., 2017). A group of 5 GHPs (∼10 m high, 500 m in width) distributed on the seabed over a 2.5 km^2 area were recently found[1]. Hydroacoustic surveys and real time visually guided observations with a TowCam-Multicore (see footnote 1) System (TC-MC) and Remotely Operated Vehicle (ROV) dives[2] have revealed acoustic flares of gas bubbles consisting predominantly of CH_4 and being emitted from 4 of the 5 GHPs. One structure (GHP 5) did not show any visible flares or gas hydrate in sediments (Serov et al., 2017). During the sampling campaigns for this study, seep activity at the different sampling sites was assessed by tracking flares through hydro acoustic surveys with a multibeam echosounder (Kongsberg Simrad EM 302) or by visual observations using a TC-MC system configuration (Panieri et al., 2017).

Sampling Procedure

Field campaigns were conducted with RV Helmer Hanssen and sediment cores at the GHP 3 and at GHPs 1 and 5 were taken in June 2016(see footnote 2) and June 2017[3], respectively. Cores were taken along a spatial gradient from the apex of the geological feature to its edge. Core IDs MC_900 (apex), MC_902, MC_918, and MC_919 (edge) were taken at GHP 1. Core IDs MC_1061 (apex), MC_1062, MC_1063, and MC_1065 (edge) were collected at GHP 3 while core IDs MC_920 (apex), MC_922, and MC_923 (edge) were collected at GHP 5 (**Figure 1**). A reference core (core ID 898) was retrieved at one kilometer away from the closest GHP. The use of the multicore system KC Denmark DK8000 integrated with a TC-MC with a real time transmission of images (Daniel et al., 2003) allowed for the collection of six 60 cm long real time visually guided cores. The combined TC-MC was used to visually survey and sample sediments from the study site and the sediment recovery varied between 15 and 40 cm. Exceptionally, core ID BC_1029 was taken using a blade core mounted on a Sperre Subfighter 30k ROV to target directly sediments in close vicinity to a CH_4 gas flare at GHP 3 in June 2016.

[1]https://cage.uit.no/wp-content/uploads/2019/02/15-2.cage-cruise-report-public-1.pdf

[2]https://cage.uit.no/wp-content/uploads/2019/02/16-5.cage-cruise-report-public.pdf

[3]https://cage.uit.no/wp-content/uploads/2019/02/17-2.cage-cruise-report-public.pdf

Porewater Geochemistry

Porewater geochemistry was measured for all cores, and data for BC_1029 and MC_1063 were collected from Hong et al. (2020). CH_4 concentrations were measured with a head space technique and gas chromatography (Thermoscientific Trace 1310) equipped with a flame ionization detector (Hoehler et al., 2000; Panieri et al., 2017). For this, we extruded 3 mL of bulk sediments per 2 cm intervals in all cores which were immediately transferred to a 20 mL headspace vial with 7 mL of NaOH solution (1 M) and two glass beads, and instantly capped. Samples were analyzed subsequently to an equilibration period of 24 h and are represented as concentration per sediment volume. Sediment porosity was determined from weight and volume measurements as presented in Boyce et al. (1973).

Dissolved iron (Fe^{2+}), alkalinity, total sulfide (ΣHS), sulfate (SO_4^{2-}), and dissolved inorganic carbon (DIC) were measured from a neighboring core of the multicore system, recovered during the same sampling round. Using rhizon samplers (Seeberg-Elverfeldt et al., 2005), up to 18 mL of porewater was collected at each cm in the upper 10 cm and at intervals of 4–10 cm in the lower part of the core. Alkalinity and Fe^{2+} were measured onboard by titration and by spectrophotometry, respectively (Hong et al., 2017). SO_4^{2-} was measured onshore using ion chromatography (Hong et al., 2017), while ΣHS was measured using a spectrophotometer at a wavelength of 670 nm (Cline, 1969). A detailed protocol on the measurement of ΣHS can be found in the **Supplementary Material** of Hong et al. (2020). Due to equipment availability on the two field cruises, ΣHS and DIC concentrations were not measured for all sediment cores while alkalinity and Fe^{2+} concentrations were only measured for a selection of sediment layers (**Supplementary Tables 1–5**).

DNA Extraction, Sequencing, and Sequences Analyses

Sediment cores were extruded and 2 cm thick layers were transferred in Whirl-Pak® sterile sampling bags (Nasco, United States) and stored at -80°C. Following the measurements of the different environmental parameters in the laboratory, 55 of these samples were selected for amplicon libraries sequencing. These samples were selected at regular depths (surface, ∼5, ∼10, and ∼15 cm) and at clear geochemical interfaces as detected by porewater geochemical gradients (e.g., SMTZ). In a cold room (4°C), sediments were manually ground in liquid nitrogen using a sterilized mortar. The DNA was extracted using the DNeasy PowerSoil Kit (Qiagen, Germany). The manufacturer protocol was followed, except that the samples were placed in G2 DNA/RNA Enhancer beads tubes (Ampliqon, Denmark) for physical lysis (Jacobsen et al., 2018) instead of the kit lysis tubes. Once the DNA samples were quality checked using electrophoresis gels, the DNA concentrations were measured using a NanoDrop™ 2000 spectrophotometer (Thermo Fisher Scientific, United States)

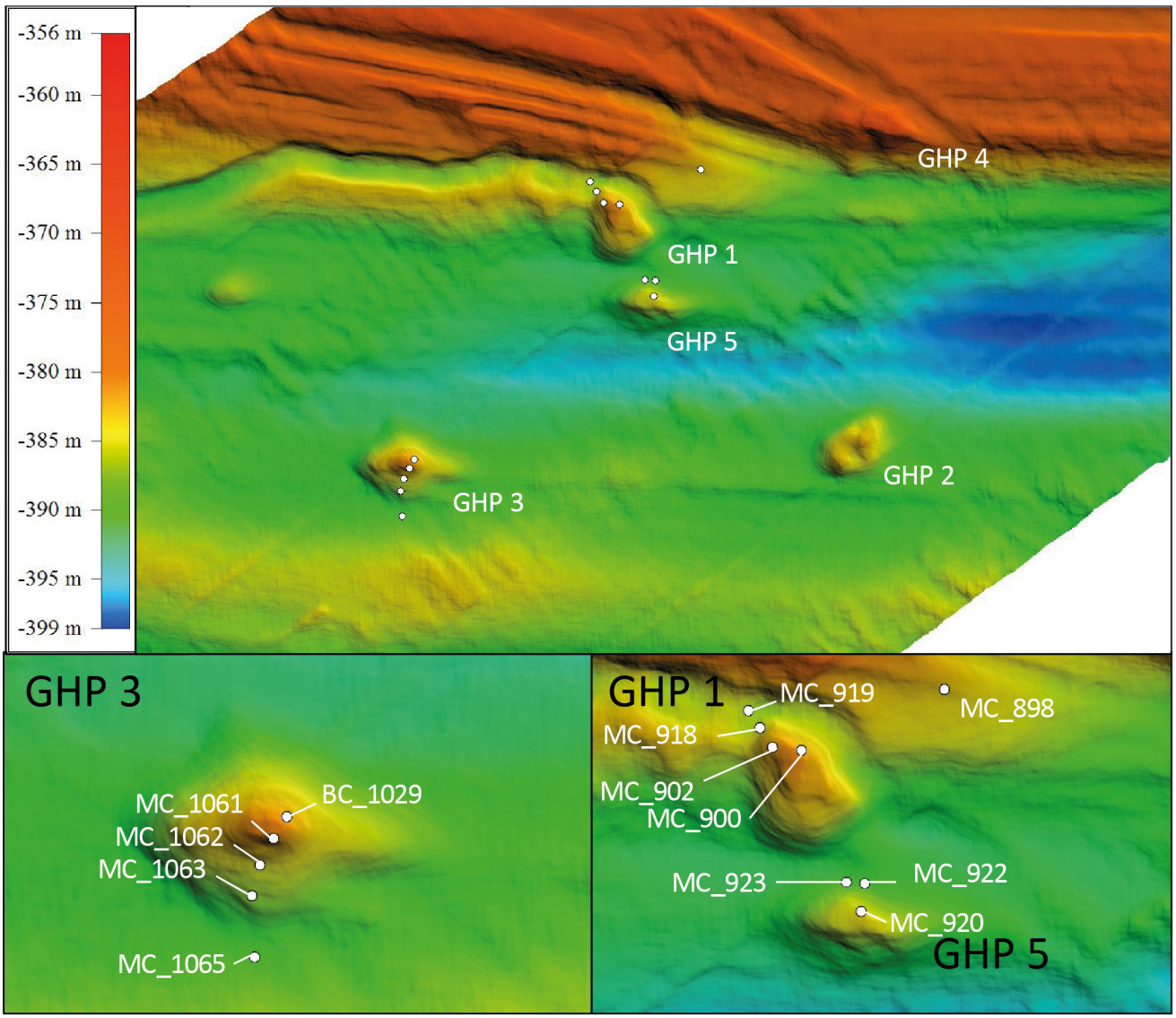

FIGURE 1 | Geological dome structures referred to as Gas Hydrate Pingo (GHP) located at the mouth of Storfjordrenna, 50 km south of Svalbard. The upper panel gives an overview of this area. The lower panels show the three selected GHPs for this study. White dots represent locations of the different sediment cores at GHPs 1, 3, and 5 using a multicore system. Core MC_898 was sampled as reference site and core BC_1029. GHP 3 was taken using a blade core mounted on a ROV to sample in the vicinity of a methane gas flare.

and normalized before being sent to the IMGM Laboratories GmbH for library preparation and amplicon sequencing. For each sample, eukarya were amplified using 18S rDNA degenerate primers to target the V4 region, and bacteria and archaea were amplified using 16S rDNA degenerate primers to target the V3-V4 region (**Supplementary Table 6**). Library generation was conducted in accordance with the company's protocols before being sequenced using a Miseq System (Illumina inc., United States). Paired-end nucleotide reads were deposited at Sequence Read Archive Genebank[4] as BioProject accession number PRJNA593930.

Paired-end reads were meticulously processed and the workflow was derived from the USEARCH suggested protocol[5]. Pairs were merged before being length trimmed and quality filtered with USEARCH v10.0.240. Thereafter, operational taxonomic units (OTUs) were constructed using the UPARSE-OTU greedy algorithm at 97% pairwise sequence identity. Singleton OTUs were removed and taxonomy was assigned using the method Wang implemented in Mothur to the SILVA database release 138 (Edgar, 2010; Quast et al., 2012; Yilmaz et al., 2014). Sequences that were not classified to their domain were discarded prior to further statistical analyses. Finally, sequences from

[4]http://www.ncbi.nlm.nih.gov/sra

[5]http://drive5.com/usearch/manual/uparse_pipeline.html

multicellular organisms are likely detected within the 18S rDNA libraries and therefore OTUs that were assigned to Metazoan groups and unclassified eukaryotes were discarded to focus only on the microbial community.

Statistical Analyses

Archaeal, bacterial, and eukaryotic libraries were rarefied at 8900, 4700, and 1300 sequences, respectively, corresponding to the lowest number of sequences in one sample. Preliminary analyses of the libraries demonstrated a large fraction of OTUs that contained just a few sequences in a sample, especially for the bacterial communities (**Figure 6**). In this study, we aimed to determine the distribution patterns of key microbes. The inclusion of a large fraction of rarer taxa in the diversity analyses, despite sharp gradients in the dominating OTUs, prevented the visualization of these gradients of community changes. Therefore, only OTUs containing at least 1% of the overall sequences of one sample were kept for further statistical analyses.

For the bacterial and archaeal communities, beta diversity, measuring changes in the composition of communities between different samples, was calculated on the relative abundance of the selected abundant OTUs using the Bray–Curtis dissimilarity index implemented in the Vegan v2.5-5 package on R (Oksanen et al., 2019). Clusters of sediment samples sharing similar OTUs abundance and composition for both domains of life were formed at a dissimilarity index of ca. 0.5–0.6. For each cluster, the relative abundance of each OTU was averaged and used to build a doughnut diagram with the R package ggplot2 v3.2.1. Thereafter, distance-based redundancy analyses (dbRDA) were performed to reveal whether the environmental parameters measured had an impact on the observed community dissimilarity between the different sediment cores. A dissimilarity matrix was built using the Bray–Curtis dissimilarity index. As the environmental parameters differed between the GHPs, and the fact that missing values can affect the outcome of the analyses, the dbRDA were performed and presented for each GHP separately. Environmental parameters were logarithmically transformed and standardized through Z scoring (Legendre and Legendre, 1998). The significance of the resulting axis from the dbRDA was evaluated through permutation tests (n = 999). Both functions for dbRDA and permutations tests are implemented in the Vegan v2.5-5 package on R (Oksanen et al., 2019).

For the eukaryotic libraries, biodiversity analyses were likely affected by the removal of sequences assigned to Metazoa, as in some samples they could represent on average 40% of the sequences. Furthermore, a large fraction of the community structure at the GHPs site was dominated by reads assigned to photosynthetic eukaryotes that might have originated from the sedimentation of phytoplankton cells, undermining any subsequent attempts at describing the structure of the eukaryotic communities thriving at the GHPs and evaluating the impact of environmental factors on the biodiversity (Rey and Rune Skjoldal, 1987). Therefore, a different approach was used for the eukaryotic libraries and we emphasized instead on the contrast of the abundant OTUs composition between the reference site and CH_4-rich sediments. To do so, once sequences assigned to Metazoa or unclassified eukaryotes were removed and eukaryotic libraries were rarefied, OTUs that were abundant at the reference site were subtracted and presented separately. We hypothesized that the remaining abundant OTUs would be indicators of taxonomic groups influenced by local conditions at the GHPs. Analyses on the relative abundances of these taxonomic groups were calculated using the Bray-Curtis dissimilarity index (Oksanen et al., 2019) and clusters of sediment samples were formed at a dissimilarity index of 0.5–0.6.

Benthic Foraminiferal Analyses

We observed that the relative abundances of certain prokaryotic taxonomic groups, including the genus *Sulfurimonas*, increased in CH_4-rich sediments. To ensure that the changes in relative abundances of these taxonomic groups were caused by the presence of CH_4, we compared results from DNA sequences with an independent proxy for surface CH_4-rich sediments. Agglutinated foraminifera are often observed in Arctic seas (Wollenburg and Mackensen, 1998; Jernas et al., 2018) and are particularly sensitive to cold seeps where they are very rare or even absent (Panieri and Sen Gupta, 2008; Martin et al., 2010; Dessandier et al., 2019). Accordingly, changes in their abundances can be used to assess the impact of CH_4 seepage disturbance on the local biological communities. Foraminiferal samples (0–1 cm sediment depth) from GHP 1 were stored for 14 days at 4°C in a 2 g L^{-1} Rose Bengal solution in ethanol 96%, in order to identify the living (Schönfeld et al., 2012), or recently alive individuals (Rose Bengal stained foraminifera; Corliss, 1991). All samples were wet sieved using 63 and 125 μm mesh sieves and dried at 40°C (48 h). We considered "living" individuals as the ones characterized by a pink stain of all chambers in their test, with the exception of the last one. In case of doubt, the test was broken to investigate the staining of the endoplasm (Schönfeld et al., 2012). All benthic foraminiferal specimens from >125 μm size fraction were handpicked, identified, and counted. The density was calculated by dividing the number of agglutinated foraminiferal individuals (**Supplementary Table 10**) in each core by the surface of the core (5.02×10^3 m^2). The relationship between the density of agglutinated foraminiferal cells and the logarithm of the number of resampled *Sulfurimonas* sequences was tested using a linear model.

RESULTS

Environmental Characterization and Geochemistry

At the reference site, CH_4 was nearly absent, gas flares were not detected on the echosounder, and CH_4 sediment concentrations did not exceed 4 μM (**Figure 2**). ΣHS remained undetectable throughout the reference core, while measured concentrations of SO_4^{2-} slightly decreased from 28 mM at the sediment surface to 26 mM at 11 cm below seafloor (bsf), correlating

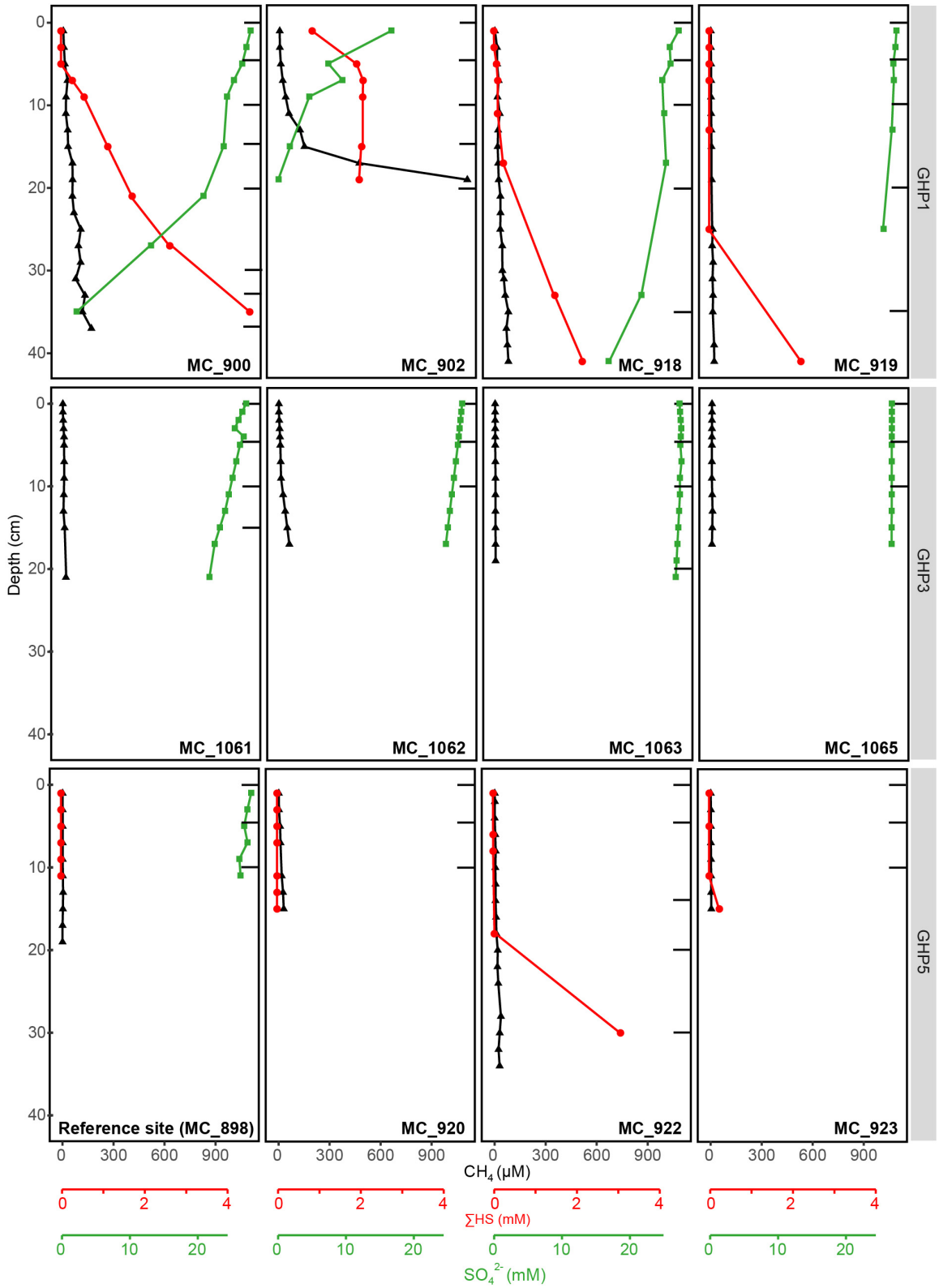

FIGURE 2 | Geochemical profiles of the different sediment cores collected at the reference site (MC_898) and GHPs 1, 3, and 5, with the exception of BC_1029 that is presented in **Figure 3**. Profiles for CH_4, SO_4^{2-}, and ΣHS at these sediment depths are given. Black bars correspond to the sediment layers from which the DNA was extracted and sequenced.

to seawater concentration of the Barents Sea. The seafloor was muddy and authigenic carbonates were not observed (**Supplementary Table 4**).

At GHP 1, gas flares and high CH_4 sediment concentrations were suggestive of high CH_4 seepage activity (**Figures 1**, **2**). Dense patches of chemosynthetic organisms, such as siboglinids, as well as carbonate crusts colonized by anemones and sponges, were scattered across GHP 1 (**Supplementary Table 4**). Concentrations of CH_4 were low in the sediment surface layer, ranging from 0.61 to 6.73 μM, and increased with depth in cores taken at the GHP 1 apex, reaching a maximum of 169 μM at 37 cmbsf in core MC_900 and 1109 μM at 19 cmbsf in core MC_902 (**Figure 2**). MC_902 was also characterized by a stronger depletion of SO_4^{2-} with depth than at the reference site as concentration dropped below 5 mM at 15 cmbsf. With the decrease in SO_4^{2-}, ΣHS concentrations increased, peaking at 4558 and 2078 μM in MC_900 and MC_902, respectively. MC_918 was collected close to the rim of the GHP, where concentrations of CH_4 and ΣHS increased with depth, but at lower concentrations than at cores taken near the apex of GHP 1. The SO_4^{2-} concentrations values at MC_918 ranged from 27.8 mM at the surface to 25.9 mM at 19 cmbsf. MC_919 was taken outside the GHP, but close to its edge. Here, environmental parameters became more similar to the reference site. Low concentrations of CH_4 (yet still slightly higher than at the reference site) were detectable and SO_4^{2-} concentrations were only slightly lower than at the reference site and remained above 26 mM within this core.

At GHP 3, BC_1029 had the highest CH_4 concentrations of all sites, reaching up to 12.8 mM at 12 cmbsf (**Figure 3**). This core was taken in the vicinity of a CH_4 gas flare (**Figure 1**). The four other cores from GHP 3 had lower CH_4 concentrations than BC_1029 (<15 μM). Still, the cores MC_1061 and MC_1062, located close to the GHP 3 apex, had higher CH_4 concentrations than cores MC_1063 and MC_1065, collected near the edge and outside GHP 3, respectively. SO_4^{2-} maximum concentrations in the surface sediment layers were in the range of 27-28 mM for all cores, but the SO_4^{2-} level decreased to 12.21 mM at 12 cmbsf and at 23.83 mM at 14 cmbsf for BC_1029 and MC_1061, respectively. Within other cores taken at GHP 3, the decreasing concentrations of SO_4^{2-} showed a similar pattern to the reference site. Fe^{2+} concentrations were only measured in two cores (BC_1029 and MC_1063) and showed a sharp decrease at the sediment surface in core BC_1029, but remained high in core MC_1063, where it was depleted only at 20 cmbsf (**Supplementary Table 2**).

At GHP 5, similar CH_4 concentrations in the upper sediment layer were measured in core MC_920 and at the apex of GHP 3 (**Figure 2**). However, gas flares were not visible on the echosounder at the apex of GHP 5. In addition, a CH_4 concentration of ∼18 μM was measured at 19 cmbsf in core MC_922, occurring concomitantly with an increasing concentration of ΣHS. The seafloor was covered with hard surfaces, mostly ice raft debris, and colonized by anemones and sponges (**Supplementary Table 5**). Complementary information on visual observations at the sampling sites and on concentrations of Fe^{2+}, alkalinity, and DIC are available as **Supplementary Information** (**Supplementary Tables 4, 5**).

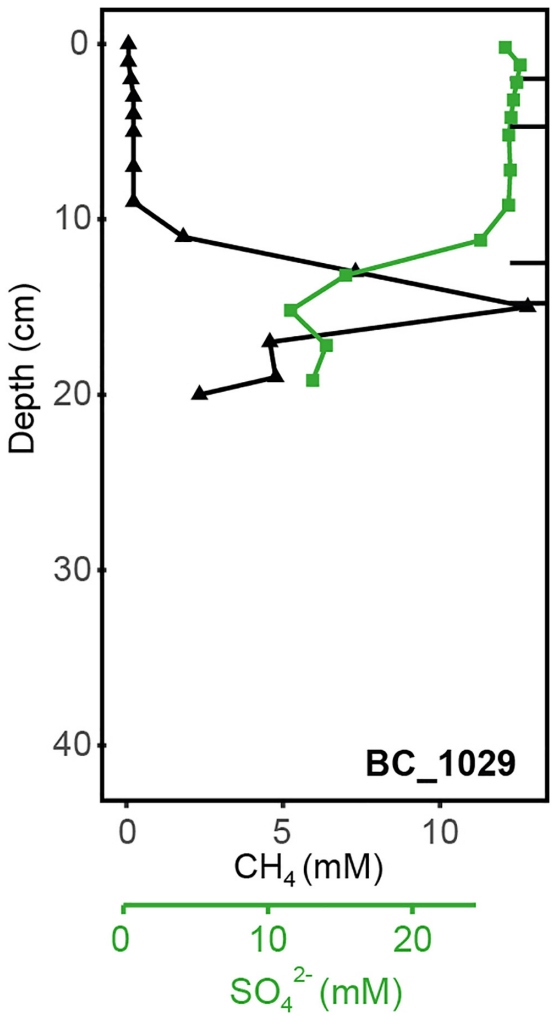

FIGURE 3 | Geochemical profiles of the sediment core BC_1029 collected at GHP 3 near a CH_4 gas flare. Profiles for CH_4 and SO_4^{2-} at these sediment depths are shown. Black bars correspond to the sediment layers from which the DNA was extracted and sequenced.

Taxonomy and Abundant OTUs

Once pair-ends reads were quality filtered, 8 129, 36 301, and 8184 OTUs were successfully assigned to the archaeal, bacterial, and eukaryotic domains, respectively (**Supplementary Table 7**). After rarefaction, within the archaeal OTUs, 87 were found to be abundant in at least one of the sediment layers collected from the reference site or the GHPs. Among the bacteria and eukaryotes, 107 and 140 abundant OTUs were identified, respectively.

Composition Similarities of the Microbial Communities

Based on the beta-diversity dissimilarity analyses in the GHP sediments (**Figure 4**), six different community clusters designated A1, A2, A3, A4, A5, and A6 were identified for the archaeal domain. Cluster A1 included nearly all surface sediment samples and was dominated by the Crenarchaeota Nitrososphaera and

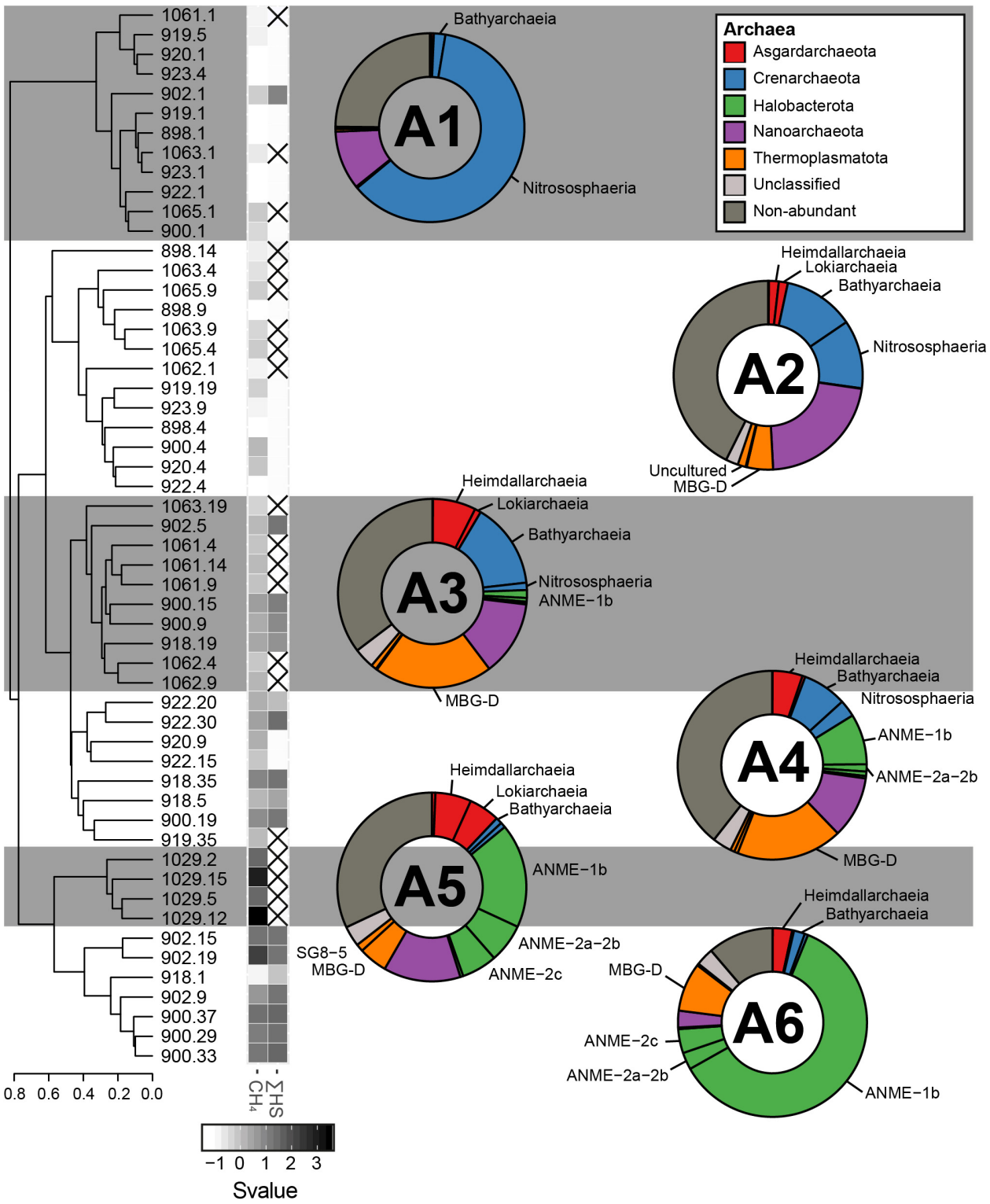

FIGURE 4 | The sediment archaeal communities clustered in six different groups, calculated based on the Bray–Curtis dissimilatory index from the composition of abundant archaeal OTUs (A1, A2, A3, A4, A5, and A6). The averaged taxonomic composition of each cluster is illustrated in a doughnut chart with colors indicating taxa listed in the box. "Non-abundant" includes sequences assigned to archaeal OTUs that were not retrieved in abundance in this study. Finally, the heatmap gives standardized values (Svalue) of depth and of the logarithmic concentrations of CH_4 and HS. Non-available data are represented by striped squares.

the Nanoarchaeota Woeserchaeales, with 61.4 and 10.0% of the total archaeal community, respectively. Sediment layers associated to the cluster A2 were from different depths, although most were collected between 4 and 10 cmbsf. The cluster A2 was characterized by a stronger dominance of Woeserchaeales (21.86%), Bathyarchaeia (12.14%), Nitrososphaera (11.73%), the marine benthic group D (MBG-D) within the Thermoplasmatota (4.49%), and Asgardarchaeota (3.35%). In addition, 2.1% of the sequences were associated to an unclassified archaeal OTU. The community of the cluster A3 was driven by the MBG-D (20.1%), the Bathyarchaiea (14.5%), and the Woesearchaeales (12.7%). The Asgardaeota groups of Heimdallarchaeia (7.3%) and Lokiarchaeia (1.1%), and the Halobacterota ANME-1 group (1.3%) were also predominant. The cluster A4 had a similar community composition to the cluster A3 and was dominated by the MBG-D (18.5%), the Wosearchaeales (10.8%), and ANME-1 (8.8%). Bathyarchaeia (7.7%) and Asgardarchaeota (5.8%) were also major components of the A4. The clusters A5 and A6 differed from the other groups particularly by a higher relative abundance of sequences associated to ANME groups. The cluster A5, representing sediment layers at the gas flare (core BC_1029) was mainly composed of ANME-1 (17.9 %), ANME-2a/-2b (6.6 %), and ANME-2c (6.1%). Other abundant taxonomic groups included Wosearchaeales (13.2 %) and the MBG-D (4.9%), in addition to the Asgardarchaeota Heimdallarchaeia (6.1%) and Lokiarchaeia (5.3%). The ANME communities of A6 was in contrast to A5 by a stronger dominance of ANME-1 (60.7%; **Figure 7**), in comparison to the ANME-2a-2b (2.9%) and ANME-2c (4.1%; **Figure 5**), were also abundant in the cluster A6 representatives from the MBG-D (8.3%).

For the bacterial domain, five community clusters, designated B1, B2, B3, B4, and B5, were identified for the GHP sediments (**Figure 6**). The rare biosphere represented by the non-abundant OTUs composed of a large fraction of all the bacterial communities and particularly for the clusters B1 and B2. Within these two clusters, the rare biosphere composed of an average of 76.7% of the bacterial sequences. Among the abundant OTUs, sequences within the cluster B1 were mostly assigned to the Gammaproteobacteria (5.2%), the Verrucomicrobiota (3.2%), and the Campilobacterota Sulfurimonadaceae (1.6%). The cluster B2 had stronger presence of Desulfobacterota Desulfobacterales (4.5%), including sequences associated to the cold seeps clade SEEP-SRB1 and Desulfobulbales (3.1%), in addition of Bacteroidota (4.7%). Cluster B3 represented sediment communities retrieved at the gas flare (core BC_1029) and was dominated by the Campilobacterota Sulfurovaceae (20.2%) and Sulfurimonadaceae (13.5%). Throughout all cores, the Sulfurovaceae and Sulfurimonadaceae were strictly represented by the genera *Sulfurovum* and *Sulfurimonas*, respectively. Additionally, B3 was characterized by the occurrence of Dissulfuribacterales (1.5%), mainly due to an OTU of the SEEP-SRB2 group, Desulfatiglandales (1.6%) and Desulfobacterales (2.9%). Remaining abundant taxa of the cluster B3 were assigned to the Bacteroidota (7.8%) and the Chloroflexi Anaerolinaeae (3.2%). It is also to be noted the presence of the Gammaproteobacteria Methylococcales in cluster B3 (1.2%). Communities within the cluster B4 primarily hosted sequences assigned to the Desulfobacterota (9.0%), largely included within the Desulfobacterales (5.2%), and the Chloroflexi Anaerolinaeae (6.1%) and Dehalococcoidia (3.6%). Additionally, abundant OTUs characterizing the cluster B4 were assigned to the Bacteroidota (4.3%), the Caldatribacteriota Japan Sea 1 (JS1) clade (4.8%), the Campilobacterota Sulfurimonadaceae (2.2%), and Sulfurovaceae (1.6%). The cluster B5 was dominated by the Desulfobacterota (19.6%), including representatives of Desulfobacterales (6.0%), Desulfatiglandales (4.4%), and Dissulfuribacterales (9.1%). One OTU assigned to SEEP-SRB2 and two OTUs assigned to SEEP-SRB1 composed 9.1 and 4.7% of the overall sequences, respectively (**Figure 5**). In comparison to other bacterial clusters, the cluster B5 was also characterized by a higher relative abundance of the Caldatribacteriota JS1 (10.7%) in addition to the Chloroflexi Dehalococcoidia (11.7%) and Anaerolinaeae (4.4%). Sediment samples clustering within the groups B3–B5 were mostly dominated by abundant OTUs, as the rare biosphere composed ca. 43% of the overall sequences.

With the eukaryotic primers, 39 abundant OTUs were retrieved at the reference core MC_898 and they composed from 20 to 100% of the sequences in all sediment communities. In **Figure 7**, these 39 OTUs are presented separately from the 101 eukaryotic OTUs retrieved exclusively at the GHPs. Beta diversity in the relative abundances of the taxonomic groups of these 101 OTUs retrieved in sediment communities at the GHPs site resulted in four clusters, designated as E1, E2, E3, and E4 (**Figure 7**). The proportions of sequences assigned to these OTUs varied between clusters, where an average of 8.5, 19.8, 29.8, and 24.1% of the sequences for the clusters E1, E2, E3, and E4 were assigned to them, respectively. In cluster E1, Cercozoa and ciliates corresponded respectively to 2.7 and 1.5% of the overall sequences. Within the cluster E2, these groups were more abundant, and their relative abundances increased to 8.2% for the Cercozoa and to 5.4% for the ciliates. For clusters B1 and B2, sequences were primarily assigned to an unclassified group of Cercozoa, while the class Spirotrichea primarily dominated the ciliates. Within the cluster E3, the taxonomic diversity was higher than for E1 or E2. Other cercozoan groups, such as Granofilosea, Phytomyxea, and Thecofilosea, in addition to the ciliates classes Armophorea and Conthreep, are frequently seen in higher abundances. In addition to Cercozoa and ciliates, abundant taxa exclusive to these sediment layers included representatives of the Holozoa, uncultivated marine stramenopiles (MAST) groups 6 and 12, in addition to the fungi (Ascomycota, Basidiomycota, and Chrytridiomycota). Sediment samples clustering within the cluster E4 were characterized by a higher proportion of Apicomplexa among the OTUs.

Similarly to the distribution of the 101 eukaryotic OTUs presented above, the community structure of the 39 OTUs also thriving at the reference site varied between the clusters. The relative abundances of Ochrophyta were lower in clusters E2, E3, and E4, which are more predominantly composed by Cercozoa and ciliates. Finally, alpha diversity metrics that were used to assess biodiversity richness and evenness and the taxonomic composition for all domains within each sediment community

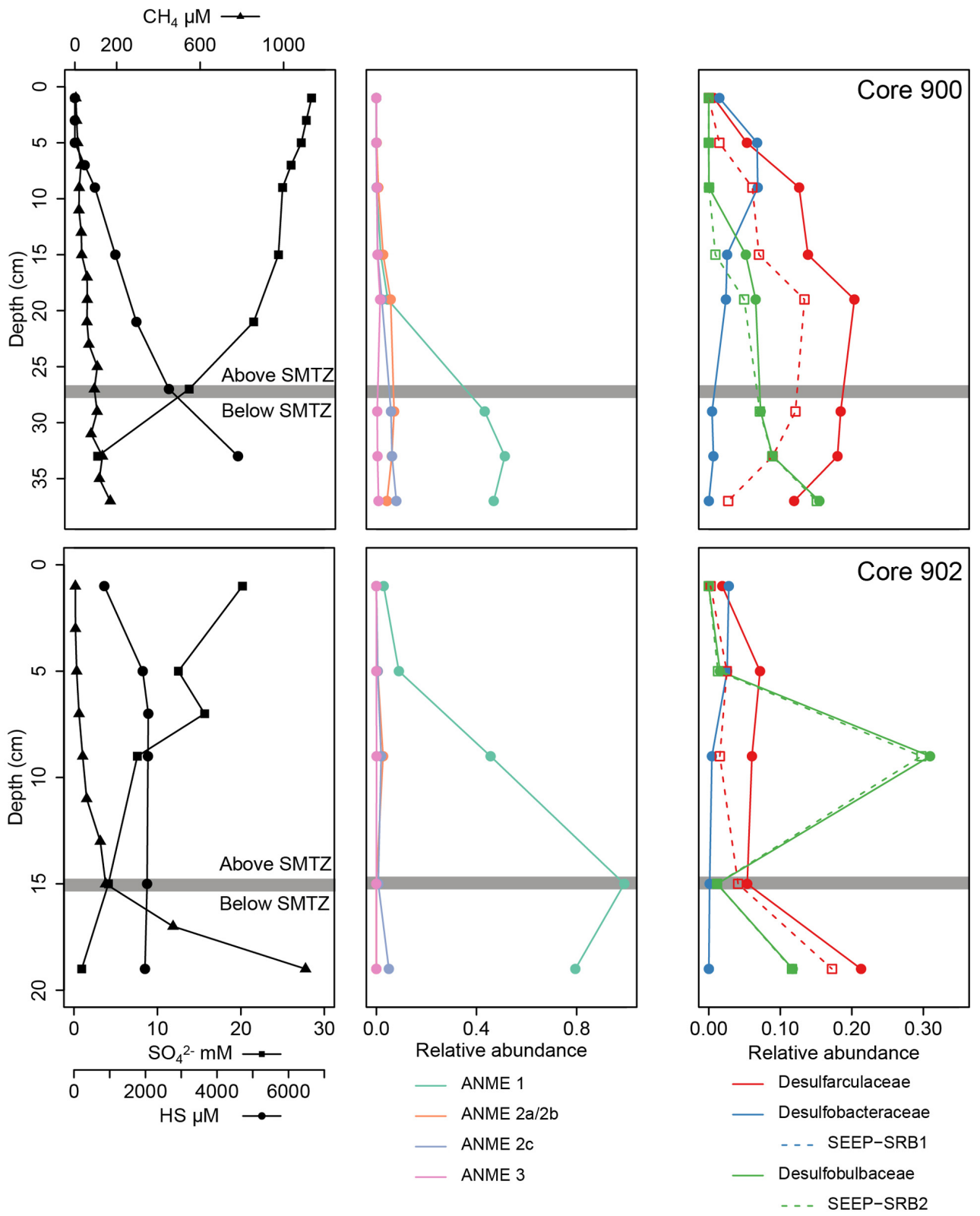

FIGURE 5 | Physico-chemical and biological vertical profiles of the cores MC_900 and MC_902 (GHP 1) where a SMTZ was identified. For each core, the left figure presents the CH_4, SO_4^{2-}, and HS concentration profiles. The centered and right figures present the relative abundances of archaeal methane oxidizers (ANME groups) and sulfate-reducing bacteria groups, respectively.

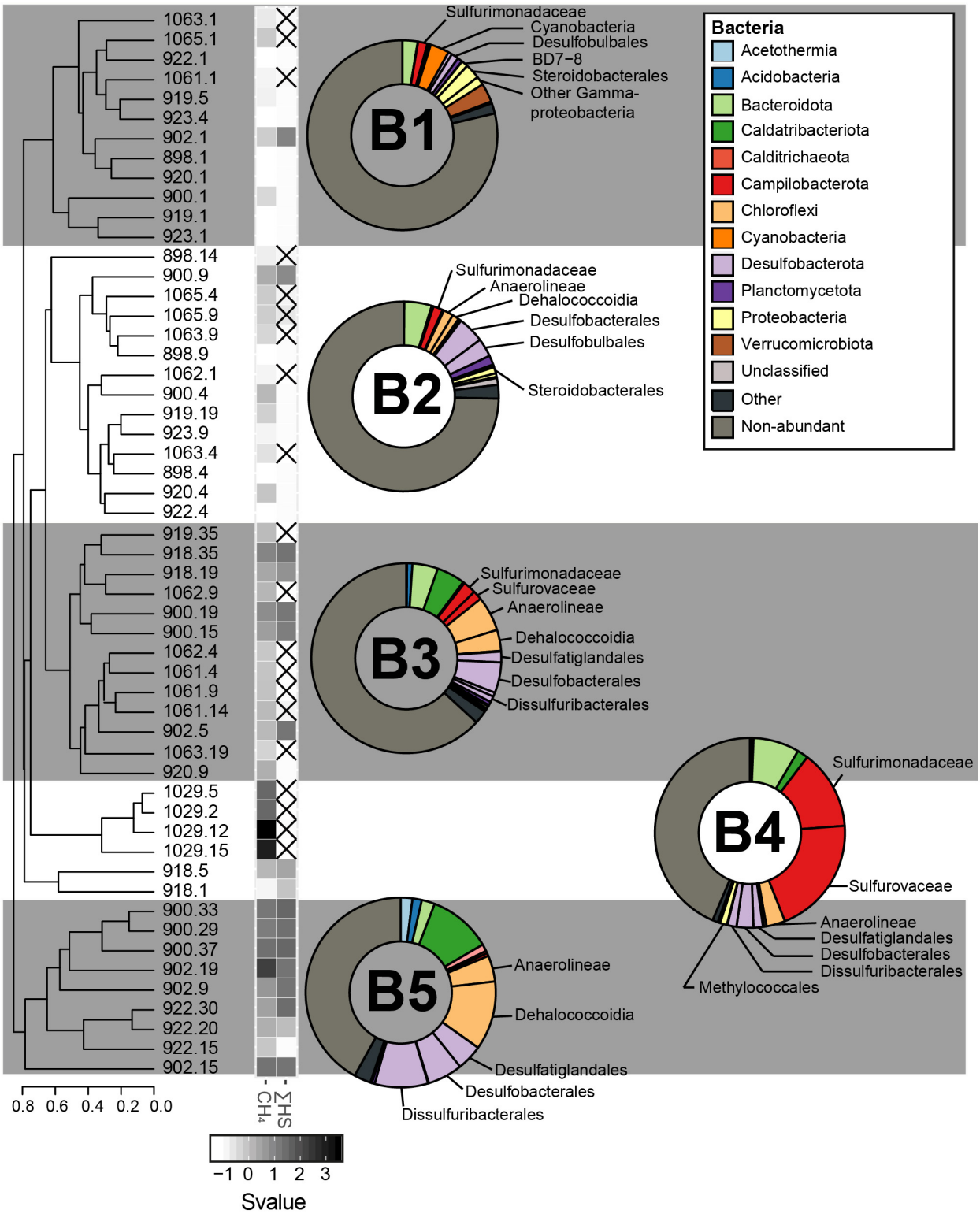

FIGURE 6 | The sediment bacterial communities clustered in five different groups, calculated based on the Bray–Curtis dissimilatory index from the composition of abundant bacterial OTUs (B1, B2, B3, B4, and B5). The averaged taxonomic composition of each cluster is illustrated in a doughnut chart with colors indicating taxa listed in the box. "Other" relates to sequences that are assigned to OTUs abundant throughout the whole communities, but not within the illustrated cluster. As for the group "non-abundant", it includes sequences assigned to bacterial OTUs that were not retrieved in abundance in this study. Finally, the heatmap gives standardized values (Svalue) of depth and of the logarithmic concentrations of CH_4 and HS. Non-available data are represented by striped squares.

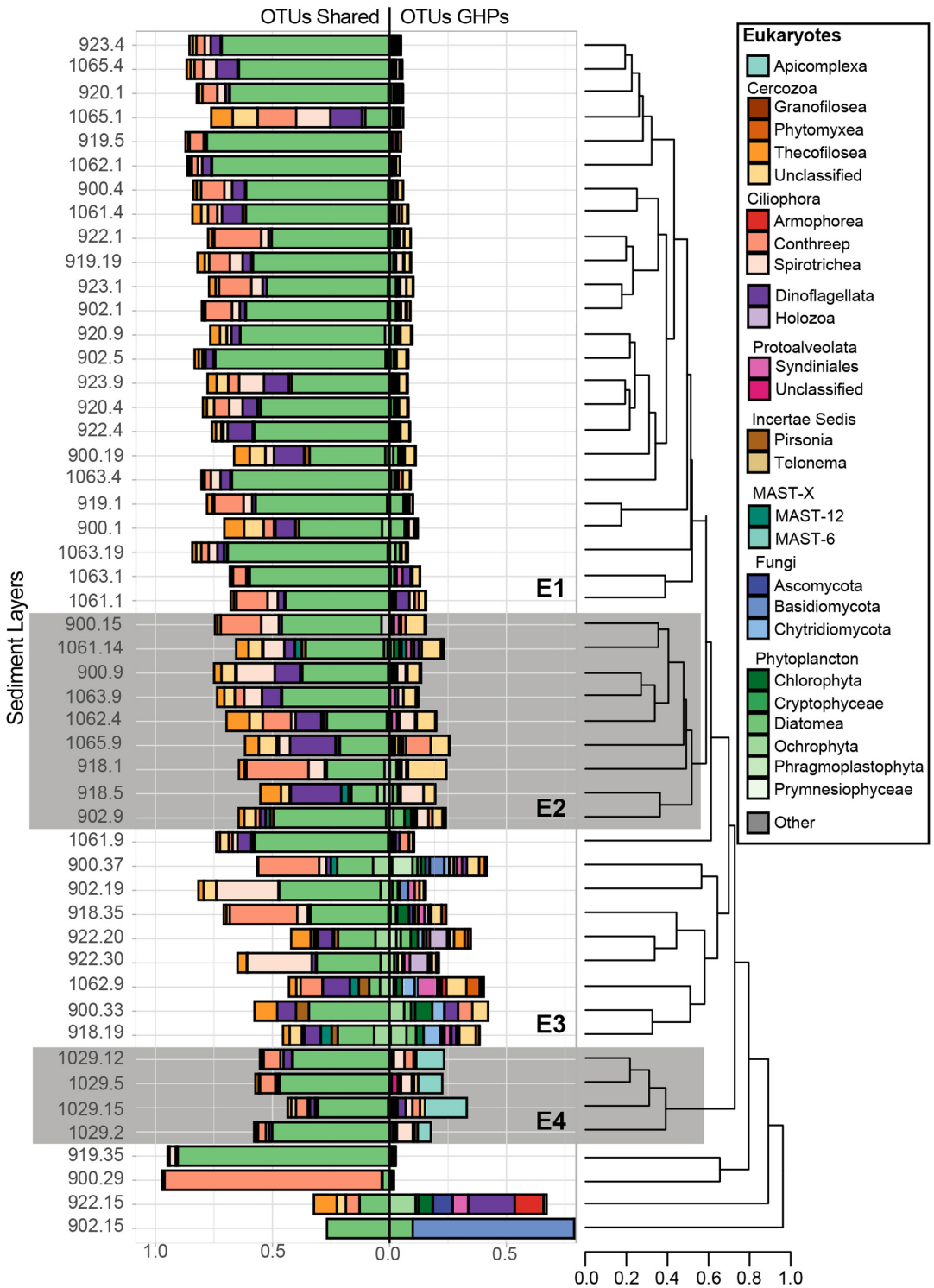

FIGURE 7 | Relative abundance of the taxonomic groups that contain sequences associated to abundant eukaryotic OTUs. Overall, 140 abundant OTUs were retrieved, but 39 of them, abundant at the reference site, were mostly associated to taxa that are suggested to be allochthones and have fallen from surface waters. Therefore, for each sediment community library, these 39 OTUs were separated and are shown in the left bar charts (OTUs shared), while the remaining GHP OTUs are shown to the right (OTUs GHP). Bray-Curtis dissimilarity hierarchical clustering of the microbial communities at selected sediment depths was based on the GHP OTUs and separated these in four different clusters (E1, E2, E3, and E4). The eukaryotic communities from MC_902 at 15 cmbsf, from MC_900 at 29 cmbsf, from MC_919 at 35 cmbsf, and from MC_922 at 15 cmbsf strongly diverged and were therefore not included in these clusters. Leaves correspond to the core ID of the sediment layer and its depth [CoreID – depth (cm)]. "Other" corresponds to the relative abundance of sequences that were associated to taxonomic groups that are not illustrated in the figure.

are available as **Supplementary Information** (**Supplementary Tables 8, 9** and **Figures 1–3**).

Distribution and Co-occurrence of the Domain Clusters

The community clusters showed particular patterns of co-occurrence between each domain, especially for the prokaryotes (**Supplementary Figure 4**). For instance, 12 of the 13 sediments communities within cluster A1 were associated with the bacterial cluster B1. The pairs A2/B2, A3-A4/B4, and A6/B5 were also commonly co-occurring. However, concomitance patterns between prokaryotic and eukaryotic clusters were less supported. Still, the eukaryotic cluster E1 usually fell together with the pairs A1/B1 or A2/B2. The clusters E2 and E3, instead, coincided with the pairs A3-A4/B4 and A6/B5, respectively. The paired clusters A1/B1 were retrieved at the surface of nearly all sediment cores while the clusters A2/B2 generally corresponded to the subsurface communities at the reference site and at cores taken toward the edge of a GHP. Pairs of A3/B4 or A4/B4 occurred below the sediment surface at the apex of GHP 1 (cores MC_900 and MC_902) and of GHP 3 (MC_1061 and MC_1062). The pair A6/B5 occurred in subsurface sediments at the apex of GHP 1, but also toward the outskirt of the GHPs at the surface of MC_918 (GHP 1) and in subsurface sediments of GHP 5 (core MC_922). Finally, the microbial communities retrieved at the gas flare (core BC_1029) of the GHP 3 could not be related to other communities at the GHPs site for all domains of life and clustered separately. Communities from all sediment depths at BC_1029 clustered within A5, B3, and E4.

Impact of Environmental Conditions on the Microbial Community Structure

The community clusters for the two prokaryotic domains demonstrated a profile primarily related to sediment depth and methane availability (**Figure 8**). The impact of measured environmental parameters on the dissimilarity between the different prokaryotic communities, observed through the formation of six archaeal and five bacterial community types, was assessed through dbRDA. Overall, the unconstrained proportions of the two principal axes (RDA 1 and 2) explained 43.71–62.52% of the dissimilarity between the different prokaryotic communities and were all significant (**Figure 8**). Depth correlated negatively with the prokaryotic community types A1 and B1 while CH_4 concentrations drove the dissimilarity between the other community types. At all GHPs, A2 and B2 correlated negatively with CH_4 concentrations, while A3-4-5-6 and B3-4-5 correlated positively. At GHP 1, these community types were also impacted by higher concentrations of ΣHS, while types A2 and B2 thrived in sediments richer in Fe^{2+} and $SO_4{}^{2-}$.

Sulfurimonas and Agglutinated Foraminifera Relationship

In general, we found lower numbers of agglutinated foraminifera at habitats characterized by higher densities of the sulfide-oxidizing Suflurimonas. The relationship between the logarithm of the number of resampled *Sulfurimonas* sequences at the sediment surface and the density of agglutinated foraminiferal species showed a significant (F = 43.122, p-value = 0.007183), negative, and linear correlation (**Supplementary Figure 5**).

DISCUSSION

Community Types Distribution Across the Pingos

Our first objective was to test the hypothesis that variations in the community structure occur along a radial gradient from the apex of the GHPs, which was expected to concentrate most of the gas seeping activity (Serov et al., 2017). Investigating the microbial communities thriving along spatial and depth pingos gradients led to the distinction of different community clusters for each domain of life (**Figures 4**, **6**, **7**). CH_4-rich sediments hold distinct community clusters (A3–A6, B3–B5, E2–E4) while communities retrieved in CH_4-poor sediments were more similar to the reference site (**Figure 8**). According to our hypothesis, CH_4-rich sediments were recovered from coring locations close to the apex of GHP 1 (MC_900 and MC_902) or GHP 3 (BC_1029) where active gas flares were visible. However, we did also find high dissolved methane concentrations sediments hosting the CH_4-rich community clusters we have described at the edge of GHPs 1 (MC_918) and 5 (MC_922; **Supplementary Figure 4**). This unpredicted spatial distribution of the different microbial community types at the GHPs was further supported through the observed significant negative correlation between the relative abundance of *Sulfurimonas* and the density of agglutinated foraminifera on the seafloor (**Supplementary Figure 5**). While *Sulfurimonas* is a genus that is often retrieved in higher relative abundances in CH_4-rich sediments (**Figure 6**; Niemann et al., 2013; Bomberg et al., 2015), agglutinated foraminifera are known to be sensitive to CH_4-rich environments (Panieri and Sen Gupta, 2008; Martin et al., 2010; Dessandier et al., 2019).

The use of these two independent methods further confirmed that there was no radial gradient at the GHPs. This contrasted thereby with earlier studies on active mud volcanoes where the community composition and the nature of the dominating methane oxidizers varied along concentric zones around the apex of the structure (Niemann et al., 2006; Lösekann et al., 2007; Lee et al., 2019). Instead, across the GHPs, community types were scarcely distributed and mainly depth and the availability of CH_4 appeared to drive the transition between them (**Figure 8**). Furthermore, changes in community composition at the GHPs occurred on a smaller scale than at the HMMV, where the identified concentric zones extended over tenth to hundreds meters. In our study, nearby sediments cores MC_918 and MC_919, or BC_1029 and MC_1061, were less than 40 m apart, but the first hosted a community type dominated by ANME-1 while the latter was more similar to the reference site. This suggests that the microbial community spatial succession at these pingos is still not yet fully grasped. Thereby, further investigations on the variability of the microbial community composition should be addressed at a higher site resolution.

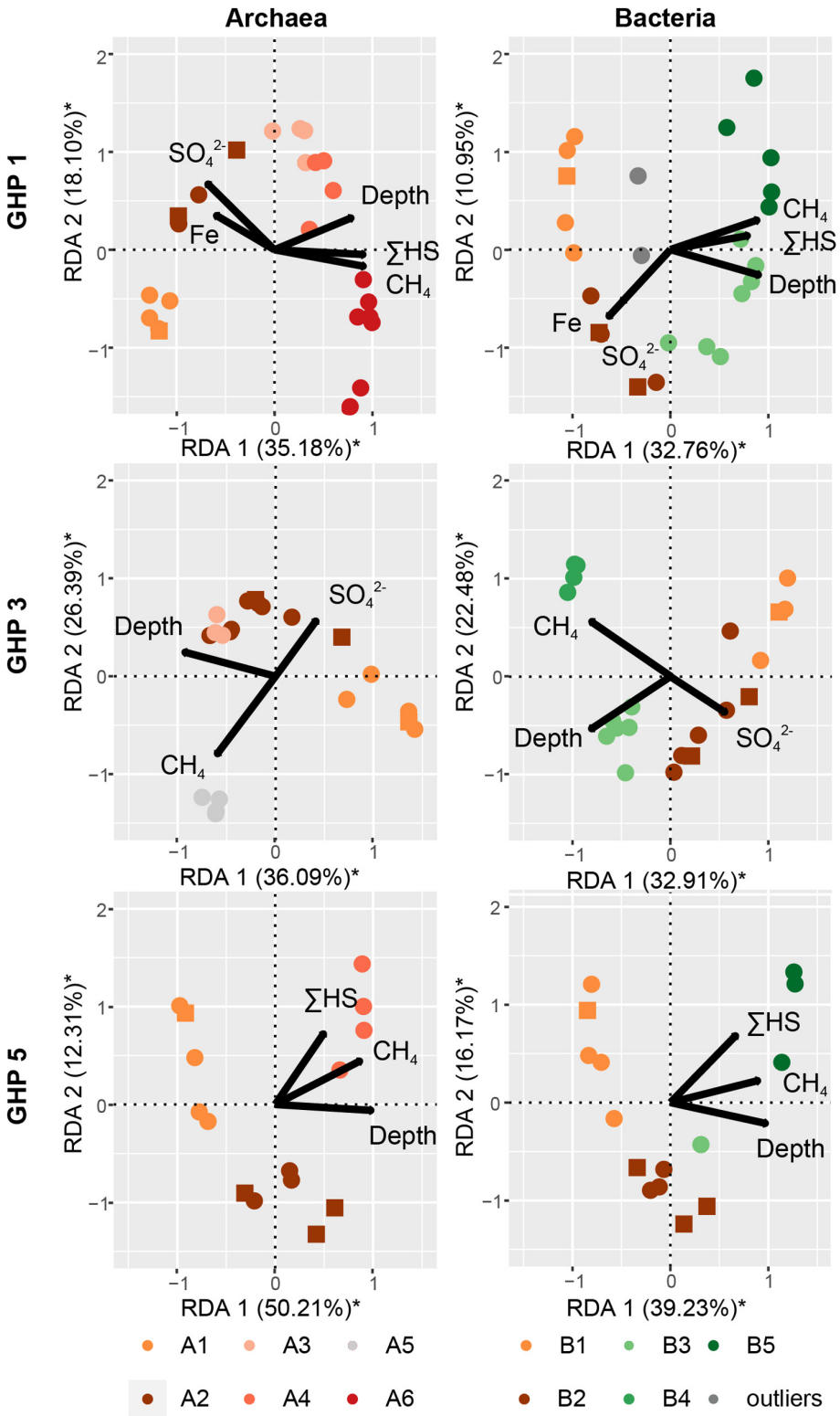

FIGURE 8 | The impact of different environmental parameters on the archaeal and bacterial community structure within the sediments of the different GHPs assessed through dbRDA. A distance matrix was calculated based on the Bray-Curtis dissimilarity index from the composition of abundant archaeal and bacterial OTUs for each GHP. The correlation between the environmental variables and the built distance matrices are presented by biplots. The unconstrained proportion for each axis explaining the variability in a distance matrix is presented in percentage along the axis. Permutation tests were used to assess the solidity of the analyses and axes with a * were found significant.

Microbial Biodiversity Across the Study Area

Our second objective was to describe the microbial biodiversity at the GHPs and to identify key taxa influenced by this CH_4-rich environment. Overall, the communities presented different assemblages, depending on their vertical positioning in the sediment matrix; i.e., surface, a few cm below the seafloor, in CH_4-rich sediments, or at the gas flare (BC_1029). The variability in the structure of eukaryotic communities and the nature and quantities of Foraminifera at the GHPs were analyzed differently than for prokaryotes. We therefore discuss the composition of the prokaryotic and eukaryotic communities within the different sediment habitats separately.

Prokaryotes

Sediment characterized by a CH_4 depletion and ΣHS increase hosted a microbial community dominated by ANME and SRBs, strongly suggesting ongoing AOM. The archaeal community was primarily dominated across all GHPs by the anaerobic CH_4 oxidizing group ANME-1 (**Figures 4**, **5**). Interestingly, methanotrophic communities primarily driven by ANME-1 have been less frequently observed than by ANME-2, or were found only in deeper sediments (Girguis et al., 2005; Ruff et al., 2015; Gründger et al., 2019). Our understanding of the factors favoring the growth of the different ANME groups is still limited. Their tolerance levels to various environmental factors and the impact of CH_4 flux rates on their growth rate have been two common orientations used by studies to investigate their biogeography. Within the first orientation, it is suggested that the ANME-1 would be more tolerant to broader ranges of environmental conditions, and could predominate over ANME-2 in low SO_4^{2-} and high HS^- environments (Timmers et al., 2015). These different tolerances to the presence of SO_4^{2-} and HS^- has been suggested to explain vertical successions in dominance of these groups along different SMTZ (Roalkvam et al., 2011; Biddle et al., 2012; Ruff et al., 2015). However, at the GHPs, although ANME-2 and ANME-3 were also detected, their relative abundances remained low, and there was no clear vertical transition in the nature of the dominant ANME group along the SMTZ in cores MC_900 and MC_902. This could suggest that other factors at the GHPs favor the growth of ANME-1 and/or inhibit the proliferation of ANME-2. Within the second orientation, observations were made at the Hydrate Ridge or the Gulf of Mexico that ANME-2 groups were more commonly retrieved in areas with highly active CH_4 seepage (Vigneron et al., 2013, 2019). In our study, although ANME-1 still predominated the methanotrophic community near the gas flare (BC_1029), the relative abundances of ANME-2 groups were in contrast higher than in other clusters. However, this hypothesis would contradict previous observations where ANME-2 demonstrated higher growth rates than ANME-1 at low CH_4 flux rates (Girguis et al., 2005). Beyond these two hypotheses presented above, the hydrographic conditions above the GHPs could also induce an additional set of environmental constraints, as the bottom-water temperature seasonally varies (Ferré et al., 2020). This creates fluctuations in both CH_4 seeping activity from the sediments and subsequently CH_4 oxidation rates in the water column. This seasonality in CH_4 seepage activity could potentially also impact the selection of the ANME groups. The biogeography of ANME groups remains therefore still unclear. With its five GHPs presenting different CH_4 flux history and its multiple ecological niches, the GHPs, combined with the usage of appropriate tools for sampling sediments at a higher precision, present thereby an ideal site to provide further insights into the distribution of ANME groups.

Furthermore, to mediate AOM, ANME groups require an electron acceptor, such as sulfate, and have therefore been frequently observed in consortia with microorganisms capable of reducing these compounds. The ANME-1 group have regularly been assigned to the uncultured groups of SEEP-SRB1 and SEEP-SRB2, where both are detected in CH_4-rich sediments at the GHPs. In our study, the relative abundance of Desulfobacterota was higher in microbial communities dominated by ANME groups (**Figure 6**). Furthermore, the decreasing concentration of SO_4^{2-} with depth in CH_4-rich sediments, combined with an increasing availability of ΣHS, strongly suggested the use of sulfate as the electron acceptor for AOM. However, across all the GHPs, there was no positive correlation between the relative abundance of ANME-1 and a particular SRB group, either SEEP-SRB 1 or 2, further supporting the hypothesis that ANME-1 could metabolize CH_4 alone (**Figures 4–6**). Indeed, it was observed that ANME-1 could perform both AOM and sulfate reduction within the same cell (Milucka et al., 2012) and the detection of F420-dependent sulfite reductase in ANME-1 communities may be part of this novel pathway (Vigneron et al., 2019). Nevertheless, a previous study could not find a correlation of ANME-1 and the abundance of dissimilatory sulfite reductase, an essential enzyme for active SRB (Vigneron et al., 2019), demonstrating that ANME-1 may not be able to perform SR. Finally, a different explanation of the absent correlation between ANME-1 and SRB groups could be due to the usage of intercellular wires forming cell-to-cell connections for electron transfers, a hypothesis supported by the detection of genes expressing for extracellular cytochrome production, between distanced ANME-1 and SRB cells (Wegener et al., 2015). Our results, based on the sulfate and sulfide profiles, advocate an anaerobic oxidation of CH_4 supported by the reduction of sulfate, but the role of Desulfobacterota and its relation with the ANME groups remain unclear.

While AOM is mediated by ANME in anaerobic environment, methanotrophy in an aerobic environment is primarily performed by distinct bacterial groups (Hanson and Hanson, 1996; Knief, 2015). In our study, higher concentrations of CH_4 than at the reference site were detected at the surface of some sediment cores collected at the GHPs. However, despite the availability of oxygen suggested by the presence of aerobic taxonomic groups, aerobic bacterial methanotrophs were barely detected. We retrieved abundant Verrucomicrobiales OTUs at the surface of most sediment cores, but their assigned family Rubritaleaceae is not known to include aerobic methanotrophs. Aerobic methanotrophs (Methyloccocales) could only be detected at the surface of BC_1029, collected near the gas flare, but this OTU was composed of only 1.2% of all bacterial

sequences. Surprisingly, the apparent rarity of aerobic CH_4 oxidizers is contrasting to most seep sites where they were found when both CH_4 and O_2 are present (Lösekann et al., 2007; Roalkvam et al., 2011; Ruff et al., 2015). Nevertheless, we cannot disregard that the near absence of aerobic methanotrophs in our amplicon libraries could be caused by the choice of primers used (McDonald et al., 2008). Different approaches, including the use of primers targeting functional genes such as *pmoA*, would be required to improve the study of the biodiversity of aerobic methane oxidizers. Finally, CH_4-rich sediments also harbored higher relative abundances of other groups, but which are likely not directly involved in the AOM. Chloroflexi, the Caldatribacteriota JS1, and Campilobacterota groups were also in higher abundance in CH_4-rich sediments than at other sediment layers. Similarly to the distribution of ANME groups, these bacterial groups showed different relative abundances between CH_4-rich sediments collected at the gas flare to the other samples. While most communities in CH_4-rich sediments demonstrated high proportions of Chloroflexi and JS1, the bacterial communities at the gas flare was primarily dominated by sulfide oxidizing bacteria (**Figure 6**). More precisely, two Campilobacterota genera mediating the oxidation of sulfur, sulfide or thiosulfate, *Sulfurimonas* and *Sulfuvorum*, were found in abundance. These genera are commonly found in abundance near hydrothermal plumes and in diffusive flow sediments, as well as at cold seeps (Yamamoto and Takai, 2011; Adams et al., 2013), while sulfide oxidization in marine sediments tends to be driven primarily by Alphaproteobacteria or Gamma proteobacteria (Lenk et al., 2011). In our study, similar observations suggest that these bacteria play an important role in sulfur cycling and largely dominated the bacterial communities at the gas flare, in comparison to the other sites.

In the absence of CH_4, the sediment microbial composition at the GHPs was highly similar to the reference site and was primarily driven by depth (**Figure 8**). Depth is likely influencing the shape of microbial communities at the GHPs through the presence or absence of oxygen, a parameter well-known to shape the structure of microbial communities in sediments (Fenchel and Finlay, 2008). Surface sediments were primarily dominated by the aerobic ammonia-oxidizing archaea (AOA) Nitrosopumilaceae that plays, along with ammonia-oxidizing bacteria, an important role in the transformation of nitrogen compounds in marine systems, including cold seeps or at hydrothermal vents (Könneke et al., 2005; Dang et al., 2009; Miyazaki et al., 2009; Stahl and de la Torre, 2012). In deeper sediments, the archaeal community (A2) was dominated by Woesearchaeales and Bathyarchaeia (**Figure 4**). The most abundant OTU of the 38 associated to the Woeserchaeia across all clusters was found predominantly at nearly all sediment layers below the seafloor, including in the CH_4-rich sediments. As oxygen availability is suggested to be the main factor determining the nature of the thriving Wosearchaeales (Liu et al., 2018), its detection in deeper sediments likely suggest an anoxic ecotype that may be involved in a fermentation-based lifestyle (Castelle et al., 2015). Bathyarcheia, previously known as the Miscellaneous Crenarchaeotal Group (MCG), and the thermoplasmatales MBG-D are globally abundant in marine sediments. The detection of protein-degrading enzymes suggest a role in organic matter anaerobic degradation (Webster et al., 2010; Kubo et al., 2012; Lloyd et al., 2013). The relative abundance of OTUs assigned to the Desulfobacterota within the bacterial community increased with depth, but remained lower than in CH_4-rich sediments (cluster B5). The presence of these Desulfobacterota groups are common in marine sediments as they play a major role in mineralizing organic matter through sulfate reduction (Jørgensen, 1982; Abu Laban et al., 2015; Robador et al., 2016).

Eukaryotes

Microbial eukaryotic communities at cold seeps have received less attention than the prokaryotes, despite their active role as part of bacterial mat type habitats for instance, or the capacity of some to harbor sulfur oxidizing bacteria (Buck and Barry, 1998; Buck et al., 2000). In this study, we investigated protists and fungi based on the V4 region of the 18S rDNA and have identified key taxonomic groups thriving at the GHP sites. Across all sediments layers, large fractions of sequences that clustered into OTUs were assigned to Metazoa and to sedimenting allochthonous cells. The removal of these sequences likely affected the following analyses of the GHPs eukaryotic communities. Therefore, we assessed separately the 39 OTUs proliferating at the reference site from the 101 OTUs found in abundance only at the GHPs to highlight eukaryotic taxa thriving in CH_4-rich sediments. Communities clustering in E1 demonstrated high similarity to the reference site and could be retrieved at different distances from the apex of all GHPs, but were limited to sediments characterized by low CH_4 concentrations. We thereby demonstrated that in the absence of CH_4, eukaryotic communities across the GHPs have similar composition than to the reference site. In contrast, clusters E2–E4 were retrieved in or near CH_4-rich sediments and demonstrated higher relative abundances of OTUs that are absent or barely found at the reference site.

Within the cluster E2, these OTUs were primarily assigned to ciliates and Cercozoa. We also noted that within the 39 subtracted OTUs, the fraction of alveolates and Cercozoa increased and even surpassed their relative abundances in E3 and E4. Higher densities of prokaryotes involved directly or indirectly in AOM can be a food source for these potential heterotrophic eukaryotes, but their growth in communities clustering in E3 and E4 may be limited by the toxicity of sulfidic conditions (Massana et al., 1994; Coyne et al., 2013). Communities clustering in E3 occurred primarily in CH_4-rich sediments with the prokaryotic communities of clusters A4-A6/B5, composed of taxa involved in AOM and sulfate reduction (**Supplementary Figure 4**). Nearly all communities within the cluster E3 hosted the highest relative abundances of sequences associated to the 101 OTUs that are exclusively found in abundance at the GHPs (**Figure 7**). The contrast in these relative abundances, in comparison to the cluster E1, demonstrates the impact of CH_4 on the eukaryotic diversity. The assignment of these OTUs was strongly heterogeneous as several taxonomic groups, such as the Protoalveolata Syndiniales, were present only in few communities (**Figure 7**). The eukaryotic communities within this cluster were also characterized by the emergence of fungal taxonomic groups. Communities within the cluster E3 were especially affected by the proportion of sequences

associated to Metazoa, as on average 40% of the sequences were assigned to this taxon and had to be removed. Thereby, while the heterogeneity in the structure of the communities clustering in E3 could be caused by local conditions, we cannot rule out that it may be due to limitations in the coverage of the eukaryotic biodiversity. Communities at the gas flare (BC_1029), similarly as for the prokaryotes, hosted a distinctive eukaryotic biodiversity clustering exclusively in E4. Among the sequences assigned to the OTUs exclusively abundant at the GHPs within E4, most were primarily assigned to Apicomplexa (up to 15%). Apicomplexa are parasitic alveolates, but the nature of potential hosts at the gas flare remains unknown. Overall, our results demonstrated that changes in the eukaryotic biodiversity occur in CH_4-rich sediments. Using different approaches, such as targeting specific genes or using blocking primers, may provide a more accurate profile of eukaryotic biodiversity at the GHPs. These investigations would further improve our understanding on the role of these protists and fungi at the GHPs site on the microbial community, the biogeochemical cycles, and on food web structures.

Overall, our approach suggests that CH_4 and oxygen are two key factors influencing the microbial community structure. Nevertheless, communities within a cluster had up to approximately 60% similarity and the dendrograms (**Figures 4**, **6**, **7**) present additional sub-clusters at higher thresholds. It advocates therefore for additional factors influencing the distribution patterns of the microbial taxonomic groups at the GHPs site. Thereby, our study revealed that the GHP ecosystem has to be considered in further investigations as a myriad of ecological niches. In this perspective, the distance between the cores (approx. 20 m) at a GHP is likely too long to investigate gradual changes in microbial communities in relation to fluxes of CH_4. Designing an approach at a small scale may better fill these gaps of knowledge.

SUMMARY AND CONCLUDING REMARKS

This study shows that both prokaryotic and eukaryotic communities at the GHPs formed a unique structure influenced by the complex distribution of CH_4 seepage. The distribution of the community types presented similar chaotic patterns and methane oxidizing communities could be retrieved at different locations over a GHP. In CH_4-rich sediments, AOM seemed to be primarily driven by a single OTU associated to ANME-1 and had no correlation with a group of SRB. This further supports the hypotheses that ANME-1 can mediate AOM alone or use different sources of electron receptors. Our approach also illustrated that at the GHPs site, metabolites of AOM, such as sulfide and organic compounds, likely explain the predominance of additional taxa, including the Campilobacterota, the thermoplasmatales MBG-D, and the Bathyarchaeia. Eukaryotic communities in the CH_4-rich sediments had a dominance of heterotrophic ciliates and Cercozoa, likely benefiting from the higher abundances of prokaryotes as a food source. The retrieval of these taxa, distributed specifically among the GHPs, suggests a complex functional microbial system supported by, or contributing to, the local oxidation of CH_4.

DATA AVAILABILITY STATEMENT

The datasets generated for this study can be found in the Sequence Read Archive Genebank as BioProject accession number PRJNA593930.

AUTHOR CONTRIBUTIONS

VC, MS, FG, and HN initially designed the project. VC, FG, MS, HN, and P-AD contributed to the sampling. VC and P-AD performed the laboratory manipulations, sequences analyses, and statistics with advice from DK, MS, FG, and HN. VC wrote the manuscript with input from DK, MS, HN, FG, P-AD, and GP. All authors contributed to the article and approved the submitted version.

FUNDING

The study was funded by the Research Council of Norway through the Centre of Excellence for Arctic Gas Hydrate, Environment, and Climate (grant number: 223259).

ACKNOWLEDGMENTS

The authors are grateful for the help from the crew of the R/V *Helmer Hanssen* and would like to acknowledge the contribution of the chief scientists during the CAGE 16-5 and 17-2 campaigns. The authors would also like to acknowledge the technical assistance of Wei-Li Hong, Haoyi Yao, Simone Sauer, Matteus Lindgren, and Pavel Serov in the analyses of the physico-chemical parameters. Finally, the authors would like to recognize members of the Centre for Arctic Gas Hydrate and Environment (The Arctic University of Norway, Tromsø) for their expertise. Antje Boetius and Frank Wenzhöfer (AWI, Bremeherhaven and MPI, Bremen, Germany) are thanked for their support with blade corers. The computations were performed on resources provided by UNINETT Sigma2 – the National Infrastructure for High Performance Computing and Data Storage in Norway, account nos. NN9639K and NS9593K. Finally, the publication charges for this article have been funded by a grant from the publication fund of UiT The Arctic University of Norway.

SUPPLEMENTARY MATERIAL

The Supplementary Material for this article can be found online at: https://www.frontiersin.org/articles/10.3389/fmicb.2020.01932/full#supplementary-material

REFERENCES

Abu Laban, N., Tan, B., Dao, A., and Foght, J. (2015). Draft Genome Sequence of Uncultivated Toluene-Degrading Desulfobulbaceae Bacterium Tol-SR, Obtained by Stable Isotope Probing Using [13C6] Toluene. *Genom. Announc.* 3, e1423–e1414. doi: 10.1128/genomeA.01423-1414

Adams, M. M., Hoarfrost, A. L., Bose, A., Joye, S. B., and Girguis, P. R. (2013). Anaerobic oxidation of short-chain alkanes in hydrothermal sediments: potential influences on sulfur cycling and microbial diversity. *Front. Microbiol.* 4:110. doi: 10.3389/fmicb.2013.00110

Åström, E. K. L., Carroll, M. L., Ambrose, W. G., Sen, A., Silyakova, A., and Carroll, J. (2018). Methane cold seeps as biological oases in the high-Arctic deep sea. *Limnol. Oceanogr.* 63, S209–S231. doi: 10.1002/lno.10732

Atkins, M., Hanna, M., Kupetsky, E., Saito, M., Taylor, C., and Wirsen, C. (2002). Tolerance of flagellated protists to high sulfide and metal concentrations potentially encountered at deep-sea hydrothermal vent. *Mar. Ecol. Prog. Ser.* 226, 63–75. doi: 10.3354/meps226063

Beal, E. J., House, C. H., and Orphan, V. J. (2009). Manganese- and iron-dependent marine methane oxidation. *Science* 325, 184–187. doi: 10.1126/science.1169984

Bhattarai, S., Cassarini, C., Rene, E. R., Zhang, Y., Esposito, G., and Lens, P. N. L. (2018). Enrichment of sulfate reducing anaerobic methane oxidizing community dominated by ANME-1 from Ginsburg Mud Volcano (Gulf of Cadiz) sediment in a biotrickling filter. *Bioresour. Technol.* 259, 433–441. doi: 10.1016/j.biortech.2018.03.018

Biddle, J. F., Cardman, Z., Mendlovitz, H., Albert, D. B., Lloyd, K. G., Boetius, A., et al. (2012). Anaerobic oxidation of methane at different temperature regimes in Guaymas Basin hydrothermal sediments. *ISME J.* 6, 1018–1031. doi: 10.1038/ismej.2011.164

Boetius, A., Ravenschlag, K., Schubert, C. J., Rickert, D., Widdel, F., Gieseke, A., et al. (2000). A marine microbial consortium apparently mediating anaerobic oxidation of methane. *Nature* 407, 623–626. doi: 10.1038/35036572

Boetius, A., and Wenzhöfer, F. (2013). Seafloor oxygen consumption fuelled by methane from cold seeps. *Nat. Geosci.* 6, 725–734. doi: 10.1038/ngeo1926

Bomberg, M., Nyyssönen, M., Pitkänen, P., Lehtinen, A., and Itävaara, M. (2015). Active Microbial Communities Inhabit Sulphate-Methane Interphase in Deep Bedrock Fracture Fluids in Olkiluoto. *Finland. Biomed Res. Int.* 2015:979530. doi: 10.1155/2015/979530

Boyce, R. E., Edgar, J. B., and Saunders, N. T. (1973). "Appendix I. Physical Properties - Methods," in *Initial Reports of the Deep Sea Drilling Project*, Edn, 15 (United Kingdom: U.S. Government Printing Office), 1115–1128.

Buck, K. R., and Barry, J. P. (1998). Monterey Bay cold seep infauna: Quantitative comparison of bacterial mat meiofauna with non-seep control sites. *Cah. Biol. Mar.* 39, 333–335.

Buck, K. R., Barry, J. P., and Simpson, A. G. B. (2000). Monterey Bay cold seep biota: Euglenozoa with chemoautotrophic bacterial epibionts. *Eur. J. Protistol.* 36, 117–126. doi: 10.1016/S0932-4739(00)8002980022

Castelle, C. J., Wrighton, K. C., Thomas, B. C., Hug, L. A., Brown, C. T., Wilkins, M. J., et al. (2015). Genomic expansion of domain archaea highlights roles for organisms from new phyla in anaerobic carbon cycling. *Curr. Biol.* 25, 690–701. doi: 10.1016/j.cub.2015.01.014

Cline, J. D. (1969). Spectrophotometric determination of hydrogen sulfide in natural waters. *Limnol. Oceanogr.* 14, 454–458. doi: 10.4319/lo.1969.14.3.0454

Cordes, E. E., Cunha, M. R., Galéron, J., Mora, C., Olu-Le Roy, K., Sibuet, M., et al. (2010). The influence of geological, geochemical, and biogenic habitat heterogeneity on seep biodiversity. *Mar. Ecol.* 31, 51–65. doi: 10.1111/j.1439-0485.2009.00334.x

Corliss, B. H. (1991). Morphology and microhabitat preferences of benthic foraminifera from the northwest Atlantic Ocean. *Mar. Micropaleontol.* 17, 195–236. doi: 10.1016/0377-8398(91)90014-W

Coyne, K. J., Countway, P. D., Pilditch, C. A., Lee, C. K., Caron, D. A., and Cary, S. C. (2013). Diversity and Distributional Patterns of Ciliates in Guaymas Basin Hydrothermal Vent Sediments. *J. Eukaryot. Microbiol.* 60, 433–447. doi: 10.1111/jeu.12051

Dang, H., Li, J., Zhang, X., Li, T., Tian, F., and Jin, W. (2009). Diversity and spatial distribution of amoA -encoding archaea in the deep-sea sediments of the tropical West Pacific Continental Margin. *J. Appl. Microbiol.* 106, 1482–1493. doi: 10.1111/j.1365-2672.2008.04109.x

Daniel, J., Fornari, D. J., and Group, W. T. (2003). A new deep-sea towed digital camera and multi-rock coring system. *Eos Trans. Am. Geophys. Union* 84, 69–73. doi: 10.1029/2003EO080001

Dessandier, P. A., Borrelli, C., Kalenitchenko, D., and Panieri, G. (2019). Benthic Foraminifera in Arctic Methane Hydrate Bearing Sediments. *Front. Mar. Sci.* 2019:6. doi: 10.3389/fmars.2019.00765

Edgar, R. C. (2010). Search and clustering orders of magnitude faster than BLAST. *Bioinformatics* 26, 2460–2461. doi: 10.1093/bioinformatics/btq461

Ettwig, K. F., Butler, M. K., Le Paslier, D., Pelletier, E., Mangenot, S., Kuypers, M. M. M., et al. (2010). Nitrite-driven anaerobic methane oxidation by oxygenic bacteria. *Nature* 464, 543–548. doi: 10.1038/nature08883

Ettwig, K. F., Zhu, B., Speth, D., Keltjens, J. T., Jetten, M. S. M., and Kartal, B. (2016). Archaea catalyze iron-dependent anaerobic oxidation of methane. *Proc. Natl. Acad. Sci.* 113, 12792–12796. doi: 10.1073/PNAS.1609534113

Fenchel, T., and Finlay, B. (2008). Oxygen and the Spatial Structure of Microbial Communities. *Biol. Rev.* 83, 553–569. doi: 10.1111/j.1469-185X.2008.00054.x

Ferré, B., Jansson, P. G., Moser, M., Serov, P., Portnov, A., Graves, C. A., et al. (2020). Reduced methane seepage from Arctic sediments during cold bottom-water conditions. *Nat. Geosci.* 13, 144–148. doi: 10.1038/s41561-019-0515513

Girguis, P. R., Cozen, A. E., and DeLong, E. F. (2005). Growth and population dynamics of anaerobic methane-oxidizing archaea and sulfate-reducing bacteria in a continuous-flow bioreactor. *Appl. Environ. Microbiol.* 71, 3725–3733. doi: 10.1128/AEM.71.7.3725-3733.2005

Gründger, F., Carrier, V., Svenning, M. M., Panieri, G., Vonnahme, T. R., Klasek, S., et al. (2019). Methane-fuelled biofilms predominantly composed of methanotrophic ANME-1 in Arctic gas hydrate-related sediments. *Sci. Rep.* 9:9725. doi: 10.1038/s41598-019-4620946205

Hanson, R. S., and Hanson, T. E. (1996). Methanotrophic Bacteria. *Microbiol. Rev* 60, 439–471. doi: 10.1128/mmbr.60.2.439-471.1996

Hoehler, T. M., Borowski, W. S., Alperin, M. J., Rodriguez, N. M., and Paull, C. K. (2000). "Model, stable isotope, and radiotracer characterization of anaerobic methane oxidation in gas hydrate-bearing sediments of the Blake Ridge," in *Proceedings of the Ocean Drilling Program: Scientific Results*, 79–85 (Texas: College Station). doi: 10.2973/odp.proc.sr.164.242.2000

Hong, W. L., Latour, P., Sauer, S., Sen, A., Gilhooly, W. P., Lepland, A., et al. (2020). Iron cycling in Arctic methane seeps. *Geo Mar. Lett.* 40, 1–11. doi: 10.1007/s00367-020-00649645

Hong, W. L., Torres, M. E., Carroll, J., Crémière, A., Panieri, G., Yao, H., et al. (2017). Seepage from an arctic shallow marine gas hydrate reservoir is insensitive to momentary ocean warming. *Nat. Commun.* 8, 1–14. doi: 10.1038/ncomms15745

Hong, W.-L., Torres, M. E., Portnov, A., Waage, M., Haley, B., and Lepland, A. (2018). Variations in Gas and Water Pulses at an Arctic Seep: Fluid Sources and Methane Transport. *Geophys. Res. Lett.* 45, 4153–4162. doi: 10.1029/2018GL077309

Hovland, M., and Svensen, H. (2006). Submarine pingoes: Indicators of shallow gas hydrates in a pockmark at Nyegga, Norwegian Sea. *Mar. Geol.* 228, 15–23. doi: 10.1016/J.MARGEO.2005.12.005

Hu, B., Shen, L., Lian, X., Zhu, Q., Liu, S., Huang, Q., et al. (2014). Evidence for nitrite-dependent anaerobic methane oxidation as a previously overlooked microbial methane sink in wetlands. *Proc. Natl. Acad. Sci. U. S. A.* 111, 4495–4500. doi: 10.1073/pnas.1318393111

Jacobsen, C. S., Nielsen, T. K., Vester, J. K., Stougaard, P., Nielsen, J. L., Voriskova, J., et al. (2018). Inter-laboratory testing of the effect of DNA blocking reagent G2 on DNA extraction from low-biomass clay samples. *Sci. Rep.* 8:5711. doi: 10.1038/s41598-018-24082-y

James, R. H., Bousquet, P., Bussmann, I., Haeckel, M., Kipfer, R., Leifer, I., et al. (2016). Effects of climate change on methane emissions from seafloor sediments in the Arctic Ocean: A review. *Limnol. Oceanogr.* 61, S283–S299. doi: 10.1002/lno.10307

Jernas, P., Klitgaard-Kristensen, D., Husum, K., Koç, N., Tverberg, V., Loubere, P., et al. (2018). Annual changes in Arctic fjord environment and modern benthic foraminiferal fauna: Evidence from Kongsfjorden, Svalbard. *Glob. Planet. Change* 163, 119–140. doi: 10.1016/j.gloplacha.2017.11.013

Jørgensen, B. B. (1982). Mineralization of organic matter in the sea bed—the role of sulphate reduction. *Nature* 296, 643–645. doi: 10.1038/296643a0

Joye, S. B., Bowles, M. W., Samarkin, V. A., Hunter, K. S., and Niemann, H. (2010). Biogeochemical signatures and microbial activity of different cold-seep habitats

along the Gulf of Mexico deep slope. *Deep Sea Res. Part II Top. Stud. Oceanogr.* 57, 1990–2001. doi: 10.1016/J.DSR2.2010.06.001

Knief, C. (2015). Diversity and habitat preferences of cultivated and uncultivated aerobic methanotrophic bacteria evaluated based on pmoA as molecular marker. *Front. Microbiol.* 6:1346. doi: 10.3389/fmicb.2015.01346

Knittel, K., and Boetius, A. (2009). Anaerobic Oxidation of Methane: Progress with an Unknown Process. *Annu. Rev. Microbiol.* 63, 311–334. doi: 10.1146/annurev.micro.61.080706.093130

Knittel, K., Boetius, A., Lemke, A., Eilers, H., Lochte, K., Pfannkuche, O., et al. (2003). Activity, distribution, and diversity of sulfate reducers and other bacteria in sediments above gas hydrate (Cascadia margin. *Oregon). Geomicrobiol. J.* 20, 269–294. doi: 10.1080/01490450303896

Knittel, K., Lösekann, T., Boetius, A., Kort, R., and Amann, R. (2005). Diversity and distribution of methanotrophic archaea at cold seeps. *Appl. Environ. Microbiol.* 71, 467–479. doi: 10.1128/AEM.71.1.467-479.2005

Koch, S., Berndt, C., Bialas, J., Haeckel, M., Crutchley, G., Papenberg, C., et al. (2015). Gas-controlled seafloor doming. *Geology* 43, 571–574. doi: 10.1130/G36596.1

Könneke, M., Bernhard, A. E., de la Torre, J. R., Walker, C. B., Waterbury, J. B., and Stahl, D. A. (2005). Isolation of an autotrophic ammonia-oxidizing marine archaeon. *Nature* 437, 543–546. doi: 10.1038/nature03911

Krüger, M., Treude, T., Wolters, H., Nauhaus, K., and Boetius, A. (2005). Microbial methane turnover in different marine habitats. *Palaeogeogr. Palaeoclimatol. Palaeoecol.* 227, 6–17. doi: 10.1016/j.palaeo.2005.04.031

Kubo, K., Lloyd, K. G., Biddle, J. F., Amann, R., Teske, A., and Knittel, K. (2012). Archaea of the Miscellaneous Crenarchaeotal Group are abundant, diverse and widespread in marine sediments. *ISME J.* 6, 1949–1965. doi: 10.1038/ismej.2012.37

Lee, D. H., Lee, Y. M., Kim, J. H., Jin, Y. K., Paull, C., Niemann, H., et al. (2019). Discriminative biogeochemical signatures of methanotrophs in different chemosynthetic habitats at an active mud volcano in the Canadian Beaufort Sea. *Sci. Rep.* 9, 1–13. doi: 10.1038/s41598-019-5395053954

Legendre, P., and Legendre, L. (1998). *Numerical Ecology*, 2nd Edn. Netherland: Elsevier Science, 24.

Lenk, S., Arnds, J., Zerjatke, K., Musat, N., Amann, R., and Mußmann, M. (2011). Novel groups of Gammaproteobacteria catalyse sulfur oxidation and carbon fixation in a coastal, intertidal sediment. *Environ. Microbiol.* 13, 758–774. doi: 10.1111/j.1462-2920.2010.02380.x

Liu, X., Li, M., Castelle, C. J., Probst, A. J., Zhou, Z., Pan, J., et al. (2018). Insights into the ecology, evolution, and metabolism of the widespread Woesearchaeotal lineages. *Microbiome* 6:102. doi: 10.1186/s40168-018-0488482

Lloyd, K. G., Schreiber, L., Petersen, D. G., Kjeldsen, K. U., Lever, M. A., Steen, A. D., et al. (2013). Predominant archaea in marine sediments degrade detrital proteins. *Nature* 496, 215–218. doi: 10.1038/nature12033

Lösekann, T., Knittel, K., Nadalig, T., Fuchs, B., Niemann, H., Boetius, A., et al. (2007). Diversity and abundance of aerobic and anaerobic methane oxidizers at the Haakon Mosby Mud Volcano, Barents Sea. *Appl. Environ. Microbiol.* 73, 3348–3362. doi: 10.1128/AEM.0001617

Mackay, J. R. (1998). Pingo growth and collapse, Tuktoyaktuk Peninsula area, western arctic coast, Canada: A long-term field study. *Geogr. Phys. Quat.* 52, 271–323. doi: 10.7202/004847ar

Maignien, L., Parkes, R. J., Cragg, B., Niemann, H., Knittel, K., Coulon, S., et al. (2013). Anaerobic oxidation of methane in hypersaline cold seep sediments. *FEMS Microbiol. Ecol.* 83, 214–231. doi: 10.1111/j.1574-6941.2012.01466.x

Marlow, J. J., Steele, J. A., Case, D. H., Connon, S. A., Levin, L. A., and Orphan, V. J. (2014). Microbial abundance and diversity patterns associated with sediments and carbonates from the methane seep environments of Hydrate Ridge, OR. *Front. Mar. Sci.* 1:1–16. doi: 10.3389/fmars.2014.00044

Martin, R. A., Nesbitt, E. A., and Campbell, K. A. (2010). The effects of anaerobic methane oxidation on benthic foraminiferal assemblages and stable isotopes on the Hikurangi Margin of eastern New Zealand. *Mar. Geol.* 272, 270–284. doi: 10.1016/j.margeo.2009.03.024

Massana, R., Stumm, C. K., and Pedros-Alio, C. (1994). Effects of temperature, sulfide, and food abundance on growth and feeding of anaerobic ciliates. *Appl. Environ. Microbiol.* 60, 1317–1324. doi: 10.1128/aem.60.4.1317-1324.1994

McDonald, I. R., Bodrossy, L., Chen, Y., and Murrell, J. C. (2008). Molecular ecology techniques for the study of aerobic methanotrophs. *Appl. Environ. Microbiol.* 74, 1305–1315. doi: 10.1128/AEM.022332237

Milucka, J., Ferdelman, T. G., Polerecky, L., Franzke, D., Wegener, G., Schmid, M., et al. (2012). Zero-valent sulphur is a key intermediate in marine methane oxidation. *Nature* 491, 541–546. doi: 10.1038/nature11656

Miyazaki, J., Higa, R., Toki, T., Ashi, J., Tsunogai, U., Nunoura, T., et al. (2009). Molecular characterization of potential nitrogen fixation by anaerobic methane-oxidizing archaea in the methane seep sediments at the number 8 Kumano Knoll in the Kumano Basin, offshore of Japan. *Appl. Environ. Microbiol.* 75, 7153–7162. doi: 10.1128/AEM.011841189

Nauhaus, K., Treude, T., Boetius, A., and Kruger, M. (2005). Environmental regulation of the anaerobic oxidation of methane: a comparison of ANME-I and ANME-II communities. *Environ. Microbiol.* 7, 98–106. doi: 10.1111/j.1462-2920.2004.00669.x

Niemann, H., Elvert, M., Hovland, M., Orcutt, B., Judd, A., Suck, I., et al. (2005). *Methane emission and consumption at a North Sea gas seep (Tommeliten area). Biogeosciences Discuss. 2*. Available at: https://hal.archives-ouvertes.fr/hal-00297796 [accessed January 31, 2020].

Niemann, H., Fischer, D., Graffe, D., Knittel, K., Montiel, A., Heilmayer, O., et al. (2009). Biogeochemistry of a low-activity cold seep in the Larsen B area, western Weddell Sea. *Antar. Biogeosci.* 6, 2383–2395. doi: 10.5194/bg-6-23832009

Niemann, H., Linke, P., Knittel, K., Macpherson, E., Boetius, A., Brü Ckmann, W., et al. (2013a). Methane-Carbon Flow into the Benthic Food Web at Cold Seeps-A Case Study from the Costa Rica Subduction Zone. *PLoS One* 8:e74894. doi: 10.1371/journal.pone.0074894

Niemann, H., Lösekann, T., de Beer, D., Elvert, M., Nadalig, T., Knittel, K., et al. (2006). Novel microbial communities of the Haakon Mosby mud volcano and their role as a methane sink. *Nature* 443, 854–858. doi: 10.1038/nature05227

Oksanen, J., Blanchet, F. G., Friendly, M., Kindt, R., Legendre, P., Mcglinn, D., et al. (2019). *Vegan: Community Ecology Package. R Package Version 2.5-5. 2019*. Available at: https://CRAN.R-project.org/package=vegan [accessed December 9, 2019].

Orphan, V. J., House, C. H., Hinrichs, K.-U., McKeegan, K. D., and DeLong, E. F. (2002). Multiple archaeal groups mediate methane oxidation in anoxic cold seep sediments. *Proc. Natl. Acad. Sci. U. S. A.* 99, 7663–7668. doi: 10.1073/pnas.072210299

Panieri, G., Bünz, S., Fornari, D. J., Escartin, J., Serov, P., Jansson, P., et al. (2017). An integrated view of the methane system in the pockmarks at Vestnesa Ridge, 79°N. *Mar. Geol.* 390, 282–300. doi: 10.1016/j.margeo.2017.06.006

Panieri, G., and Sen Gupta, B. K. (2008). Benthic Foraminifera of the Blake Ridge hydrate mound, Western North Atlantic Ocean. *Mar. Micropaleontol.* 66, 91–102. doi: 10.1016/j.marmicro.2007.08.002

Portnov, A., Vadakkepuliyambatta, S., Mienert, J., and Hubbard, A. (2016). Ice-sheet-driven methane storage and release in the Arctic. *Nat. Commun.* 7:10314. doi: 10.1038/ncomms10314

Quast, C., Pruesse, E., Yilmaz, P., Gerken, J., Schweer, T., Yarza, P., et al. (2012). The SILVA ribosomal RNA gene database project: improved data processing and web-based tools. *Nucleic Acids Res.* 41, D590–D596. doi: 10.1093/nar/gks1219

Reeburgh, W. S. (2007). Oceanic Methane Biogeochemistry. *Chem. Rev.* 107, 486–513. doi: 10.1021/CR050362V

Rey, F., and Rune Skjoldal, H. (1987). *Consumption of silicic acid below the euphotic zone by sedimenting diatom blooms in the Barents Sea*. Available at: https://imr.brage.unit.no/imr-xmlui/bitstream/handle/11250/108035/m036p307.pdf?sequence=1 [Accessed July 11, 2019].

Rinke, C., Schmitz-Esser, S., Stoecker, K., Nussbaumer, A. D., Molnár, D. A., Vanura, K., et al. (2006). "Candidatus Thiobios zoothamnicoli," an ectosymbiotic bacterium covering the giant marine ciliate Zoothamnium niveum. *Appl. Environ. Microbiol.* 72, 2014–2021. doi: 10.1128/AEM.72.3.2014-2021.2006

Roalkvam, I., Dahle, H., Chen, Y., Jørgensen, S. L., Haflidason, H., and Steen, I. H. (2012). Fine-Scale Community Structure Analysis of ANME in Nyegga Sediments with High and Low Methane Flux. *Front. Microbiol.* 3:216. doi: 10.3389/fmicb.2012.00216

Roalkvam, I., Jørgensen, S. L., Chen, Y., Stokke, R., Dahle, H., Hocking, W. P., et al. (2011). New insight into stratification of anaerobic methanotrophs in cold seep sediments. *FEMS Microbiol. Ecol.* 78, 233–243. doi: 10.1111/j.1574-6941.2011.01153.x

Robador, A., Müller, A. L., Sawicka, J. E., Berry, D., Hubert, C. R. J., Loy, A., et al. (2016). Activity and community structures of sulfate-reducing microorganisms

in polar, temperate and tropical marine sediments. *ISME J.* 10, 796–809. doi: 10.1038/ismej.2015.157

Rossel, P. E., Elvert, M., Ramette, A., Boetius, A., and Hinrichs, K. U. (2011). Factors controlling the distribution of anaerobic methanotrophic communities in marine environments: Evidence from intact polar membrane lipids. *Geochim. Cosmochim. Acta* 75, 164–184. doi: 10.1016/j.gca.2010.09.031

Ruff, S. E., Biddle, J. F., Teske, A. P., Knittel, K., Boetius, A., and Ramette, A. (2015). Global dispersion and local diversification of the methane seep microbiome. *Proc. Natl. Acad. Sci.* 112, 4015–4020. doi: 10.1073/pnas.1421865112

Schoell, M. (1988). Multiple origins of methane in the Earth. *Chem. Geol.* 71, 1–10. doi: 10.1016/0009-2541(88)9010190105

Schönfeld, J., Alve, E., Geslin, E., Jorissen, F., Korsun, S., Spezzaferri, S., et al. (2012). The FOBIMO (FOraminiferal BIo-MOnitoring) initiative-Towards a standardised protocol for soft-bottom benthic foraminiferal monitoring studies. *Mar. Micropaleontol.* 9, 1–13. doi: 10.1016/j.marmicro.2012.06.001

Seeberg-Elverfeldt, J., Schlüter, M., Feseker, T., and Kölling, M. (2005). Rhizon sampling of porewaters near the sediment-water interface of aquatic systems. *Limnol. Oceanogr. Methods* 3, 361–371. doi: 10.4319/lom.2005.3.361

Sen, A., Aström, E. K. L., Hong, W. L., Portnov, A., Waage, M., Serov, P., et al. (2018). Geophysical and geochemical controls on the megafaunal community of a high Arctic cold seep. *Biogeosciences* 15, 4533–4559. doi: 10.5194/bg-15-45332018

Serov, P., Vadakkepuliyambatta, S., Mienert, J., Patton, H., Portnov, A., Silyakova, A., et al. (2017). Postglacial response of Arctic Ocean gas hydrates to climatic amelioration. *Proc. Natl. Acad. Sci.* 114, 6215–6220. doi: 10.1073/pnas.1619288114

Stahl, D. A., and de la Torre, J. R. (2012). Physiology and Diversity of Ammonia-Oxidizing Archaea. *Annu. Rev. Microbiol* 66, 83–101. doi: 10.1146/annurev-micro-092611150128

Stokke, R., Roalkvam, I., Lanzen, A., Haflidason, H., and Steen, I. H. (2012). Integrated metagenomic and metaproteomic analyses of an ANME-1-dominated community in marine cold seep sediments. *Environ. Microbiol.* 14, 1333–1346. doi: 10.1111/j.1462-2920.2012.02716.x

Takishita, K., Kakizoe, N., Yoshida, T., and Maruyama, T. (2010). Molecular Evidence that Phylogenetically Diverged Ciliates Are Active in Microbial Mats of Deep-Sea Cold-Seep Sediment. *J. Eukaryot. Microbiol.* 57, 76–86. doi: 10.1111/j.1550-7408.2009.00457.x

Takishita, K., Tsuchiya, M., Reimer, J. D., and Maruyama, T. (2006). Molecular evidence demonstrating the basidiomycetous fungus Cryptococcus curvatus is the dominant microbial eukaryote in sediment at the Kuroshima Knoll methane seep. *Extremophiles* 10, 165–169. doi: 10.1007/s00792-005-0495497

Takishita, K., Yubuki, N., Kakizoe, N., Inagaki, Y., and Maruyama, T. (2007). Diversity of microbial eukaryotes in sediment at a deep-sea methane cold seep: surveys of ribosomal DNA libraries from raw sediment samples and two enrichment cultures. *Extremophiles* 11, 563–576. doi: 10.1007/s00792-007-0068-z

Timmers, P. H. A., Widjaja-Greefkes, H. C. A., Ramiro-Garcia, J., Plugge, C. M., and Stams, A. J. M. (2015). Growth and activity of ANME clades with different sulfate and sulfide concentrations in the presence of methane. *Front. Microbiol.* 6:988. doi: 10.3389/fmicb.2015.00988

Vaughn Barrie, J., Cook, S., and Conway, K. W. (2011). Cold seeps and benthic habitat on the Pacific margin of Canada. *Cont. Shelf Res.* 31, S85–S92. doi: 10.1016/J.CSR.2010.02.013

Vigneron, A., Alsop, E. B., Cruaud, P., Philibert, G., King, B., Baksmaty, L., et al. (2019). Contrasting Pathways for Anaerobic Methane Oxidation in Gulf of Mexico Cold Seep Sediments. *mSystems* 4:30834326. doi: 10.1128/msystems.0009118

Vigneron, A., Cruaud, P., Pignet, P., Caprais, J.-C., Cambon-Bonavita, M.-A., Godfroy, A., et al. (2013). Archaeal and anaerobic methane oxidizer communities in the Sonora Margin cold seeps, Guaymas Basin (Gulf of California). *ISME J.* 7, 1595–1608. doi: 10.1038/ismej.2013.18

Vogt, P. R., Crane, K., Sundvor, E., Max, M. D., and Pfirman, S. L. (1994). Methane-generated(?) pockmarks on young, thickly sedimented oceanic crust in the Arctic: Vestnesa Ridge, Fram Strait. *Geology* 22, 255–258. doi: 10.1130/0091-7613(1994)022<0255:mgpoyt>2.3.co;2

Waage, M., Portnov, A., Serov, P., Bünz, S., Waghorn, K. A., Vadakkepuliyambatta, S., et al. (2019). Geological Controls on Fluid Flow and Gas Hydrate Pingo Development on the Barents Sea Margin. *Geochemistry, Geophys. Geosystems* 20, 630–650. doi: 10.1029/2018GC007930

Webster, G., Rinna, J., Roussel, E. G., Fry, J. C., Weightman, A. J., and Parkes, R. J. (2010). Prokaryotic functional diversity in different biogeochemical depth zones in tidal sediments of the Severn Estuary, UK, revealed by stable-isotope probing. *FEMS Microbiol. Ecol.* 72, 179–197. doi: 10.1111/j.1574-6941.2010.00848.x

Wegener, G., Krukenberg, V., Riedel, D., Tegetmeyer, H. E., and Boetius, A. (2015). Intercellular wiring enables electron transfer between methanotrophic archaea and bacteria. *Nature* 526, 587–590. doi: 10.1038/nature15733

Werne, J. P., Baas, M., and Sinninghe Damsté, J. S. (2002). Molecular isotopic tracing of carbon flow and trophic relationships in a methane-supported benthic microbial community. *Limnol. Oceanogr.* 47, 1694–1701. doi: 10.4319/lo.2002.47.6.1694

Wollenburg, J. E., and Mackensen, A. (1998). Living benthic foraminifers from the central Arctic Ocean: Faunal composition, standing stock and diversity. *Mar. Micropaleontol.* 34, 153–185. doi: 10.1016/S0377-8398(98)000073

Yamamoto, M., and Takai, K. (2011). Sulfur Metabolisms in Epsilon- and Gamma-Proteobacteria in Deep-Sea Hydrothermal Fields. *Front. Microbiol*. 2(192):192 doi: 10.3389/fmicb.2011.00192

Yanagawa, K., Sunamura, M., Lever, M. A., Morono, Y., Hiruta, A., Ishizaki, O., et al. (2011). Niche Separation of Methanotrophic Archaea (ANME-1 and-2) in Methane-Seep Sediments of the Eastern Japan Sea Offshore Joetsu. *Tetsuro Urabe Fumio Ina.* 28, 118–129. doi: 10.1080/01490451003709334

Yilmaz, P., Parfrey, L. W., Yarza, P., Gerken, J., Pruesse, E., Quast, C., et al. (2014). The SILVA and "'All-species Living Tree Project (LTP)"' taxonomic frameworks. *Nucleic Acids Res.* 42, D643–D648. doi: 10.1093/nar/gkt1209

Conflict of Interest: The authors declare that the research was conducted in the absence of any commercial or financial relationships that could be construed as a potential conflict of interest.

Paper II

SCIENTIFIC REPORTS

OPEN

Methane-fuelled biofilms predominantly composed of methanotrophic ANME-1 in Arctic gas hydrate-related sediments

Received: 7 February 2019
Accepted: 25 June 2019
Published online: 05 July 2019

Friederike Gründger[1], Vincent Carrier[1], Mette M. Svenning[1,2], Giuliana Panieri[1], Tobias R. Vonnahme[2], Scott Klasek[3] & Helge Niemann[1,4,5]

Sedimentary biofilms comprising microbial communities mediating the anaerobic oxidation of methane are rare. Here, we describe two biofilm communities discovered in sediment cores recovered from Arctic cold seep sites (gas hydrate pingos) in the north-western Barents Sea, characterized by steady methane fluxes. We found macroscopically visible biofilms in pockets in the sediment matrix at the depth of the sulphate-methane-transition zone. 16S rRNA gene surveys revealed that the microbial community in one of the two biofilms comprised exclusively of putative anaerobic methanotrophic archaea of which ANME-1 was the sole archaeal taxon. The bacterial community consisted of relatives of sulphate-reducing bacteria (SRB) belonging to uncultured *Desulfobacteraceae* clustering into SEEP-SRB1 (i.e. the typical SRB associated to ANME-1), and members of the atribacterial JS1 clade. Confocal laser scanning microscopy demonstrates that this biofilm is composed of multicellular strands and patches of ANME-1 that are loosely associated with SRB cells, but not tightly connected in aggregates. Our discovery of methanotrophic biofilms in sediment pockets closely associated with methane seeps constitutes a hitherto overlooked and potentially widespread sink for methane and sulphate in marine sediments.

Microbial biofilms are structured multicellular aggregates of microbes that are enclosed in a matrix of mucoid self-produced extracellular polymeric substances (EPS, or exopolysaccharides)[1–3]. The structural features enhance the ability of microbial interactions within the biofilm, but also increase tolerance to adverse conditions and persistence against hostile environments. In natural marine ecosystems, biofilms are found on different types of surfaces ranging from animal skins and algae, various kinds of particles and aggregates, inert or bio-reactive minerals, and submerged constructions such as pilons or ship hulls[4,5]. Sediments are excellent substrates for microbial colonisation, providing nutrients and different types of electron acceptors and donors[6]. However, knowledge on the formation of biofilms in pockets, cracks or fractures within the sediment matrix is limited, and it is unclear how extensive such subsurface microbial aggregations are[7] along with their potential role as a geological sink for methane and sulphate.

A globally important microbial process in anoxic marine sediments is the anaerobic oxidation of methane (AOM) with sulphate as the terminal electron acceptor[8,9]:

$$CH_4 + SO_4^{2-} \rightarrow HCO_3^- + HS^- + H_2O$$

This process is mediated by anaerobic methanotrophic archaea (ANME-1, -2, -3), typically with partner sulphate-reducing bacteria (SRB) of the *Desulfosarcina/Desulfococcus*-related clade Seep-SRB1 (ANME-1, -2) or *Desulfubulbus* sp. (ANME-3)[10–15]. Because AOM communities depend on the availability of sulphate and

[1]CAGE – Centre for Arctic Gas Hydrate, Environment and Climate, Department of Geosciences, UiT The Arctic University of Norway, Tromsø, Norway. [2]Department of Arctic and Marine Biology, UiT The Arctic University of Norway, Tromsø, Norway. [3]Department of Microbiology, College of Sciences, Oregon State University, Corvallis, OR, USA. [4]Department of Marine Microbiology & Biogeochemistry, and Utrecht University, NIOZ Royal Netherlands Institute for Sea Research, 't Horntje, The Netherlands. [5]Department of Earth Sciences, Faculty of Geosciences, Utrecht University, Utrecht, The Netherlands. Correspondence and requests for materials should be addressed to F.G. (email: friederike.gruendger@bios.au.dk)

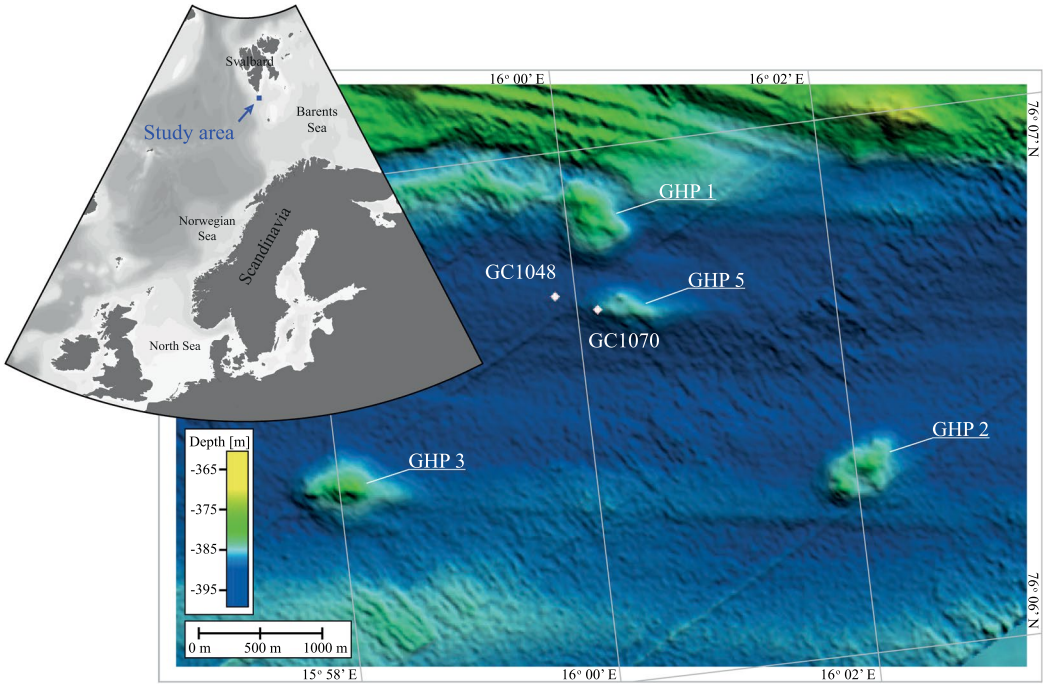

Figure 1. Regional bathymetry and the geographic core positions of GC1048 (76° 06.737N; 15° 59.845E) and GC1070 (76° 06.703N; 16° 00.162E) (white diamonds) at Storfjordrenna south of Svalbard Archipelago. Names to the gas hydrate pingos (GHPs) are given.

methane, they normally occupy (and shape) sulphate-methane transition zones (SMTZ), which are located in reduced sediment layers. These layers can be found several tens to hundred meters below the sediment surface, but at cold seeps (such as Gas Hydrate Pingos - GHPs), elevated methane fluxes lead to a shallower SMTZ in near-surface sediments[16–19]. Indeed, the abundance of AOM communities was generally found to peak at depth of SMTZ[12]. So far, the buildup of biofilms/aggregations primarily comprising ANME/SRB biomass has only been observed in the anoxic waters of the Black Sea where AOM biomass may form reef like structures[20,21]. In addition, at two sites in fractured gas hydrate-bearing sediments of the Pacific and Indian Ocean, Briggs, *et al.*[7] found AOM communities dominating biofilms at depth of the SMTZ. However, our knowledge on AOM community distribution is primarily based on sediment core analyses, which typically does not resolve horizontal variations of microbes clumped in spatially confined biofilms in sediment pockets/cracks[22].

In this study, we report on the finding of macroscopically visible biofilms that we found in pocket-like features in reduced, methane-rich sediments from a GHP area south of the Svalbard archipelago in the Arctic Ocean. Furthermore, we describe the exceptional microbial community composition, which differ strongly from any other environmental biofilm investigated to date.

Material and Methods

Sample collection and processing. Sediments were collected with a gravity corer (GC) during a research expedition (CAGE16-5) with R/V *Helmer Hanssen* in June 2016 to the GHP area at Storfjordrenna, which is south of the Svalbard archipelago in the north-western Barents Sea (Storfjordrenna Trough Mouth Fan, ~390 m water depth). The area is characterized by five GHPs. Four of them show active gas discharge in form of numerous gas flares rising up to 20 m below sea level[23]. At GHPs with active methane seepages, shallow gas hydrate layers were discovered, some of them only 40 cm below sea floor[23]. GHP 5 is proposed to be in a post-active phase of seepage[16], being the one without observed flare activity and gas hydrate recovery. We recovered one sediment core (GC1070; length: 326 cm) from the rim of GHP 5 and a second one (GC1048; length: 335 cm) ~350 m to the west of the edifice (Fig. 1). Immediately after recovery, the cores were cut into 100 cm sections, split longitudinally and sub-sampled in a cold room. In both cores, we found pockets of 4–5 cm length in the sediment matrix filled with a macroscopically visible slimy yellow-greenish biofilm (Fig. 2). Subsamples from these biofilms were taken with a sterile spatula. We obtained a pure biofilm sample from GC1048 (i.e. no sediment particles were visible in the sample), while the sample collected from core GC1070 contained some visible sediment admixture. The samples were transferred into sterile 2-ml Eppendorf tubes. Samples for DNA analyses were stored at −20 °C. Samples for microscopy studies were fixed in 4% (w/v) formaldehyde solution as described by Pernthaler, *et al.*[24] and stored in 1:1 mix of PBS / ethanol at −20 °C. After the cruise, sedimentological descriptions were performed in our home laboratory. For the examination of the core's sediments, smear slides were prepared from the sediments close to the biofilm following the methods described by Marsaglia *et al.*[25] and observed with a petrographic microscope.

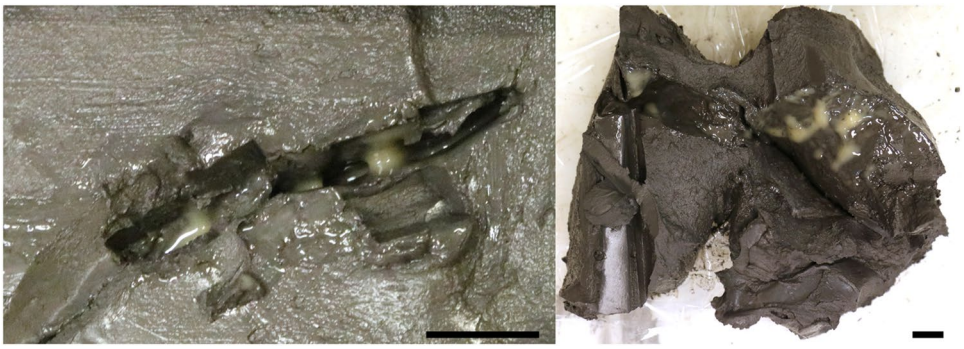

Figure 2. Sediment core GC1048 with biofilm pocket after retrieval, cutting the core into half and sampling. Scale bars = 1 cm.

Fluorescence-*in-situ*-hybridization. For fluorescence-*in-situ*-hybridizations (FISH), 50 µl of fixed biofilm sample was diluted in 1 ml 1 × PBS, filtered on a 25 mm polycarbonate filter (0.2 µm pore size) and embedded in 0.2% w/v Agarose. FISH was done using double-labelling-of-oligonucleotide-probes (DOPE; Stoecker, *et al.*[26]) for *Archaea* (ARCH915; Stahl and Amann[27]) and *Desulfobacteraceae* (DSS658; Mußmann, *et al.*[28]) synthesized by biomers.net GmbH (Ulm/Donau, Germany). The antisense probe NON338[29] was used to test for unspecific staining for the given formamide concentrations. The probes were labelled at the 5′ and 3′ end with Cyanine 3 (ARCH915) and 6-FAM (DSS658, NON338). Hybridizations were done in accordance to published work[30] with 3 h hybridization with DSS658 (50% formamide) followed by ARCH915 (0% formamide). The NON338 probe was incubated for 3 h (0% formamide). After DOPE FISH, the samples were counterstained with DAPI as described by Glöckner *et al.*[31]. Imaging was done with a confocal laser scanning microscope (Axio Observer LSM800, Carl Zeiss Microscopy GmbH, Jena, Germany) using a Plan-Apochromat 63x/1.40 Oil M27 objective. Emission and detection wavelengths were 561 and 535–700 nm for Cy3, 488 and 450–545 nm for 6-FAM, and 405 and 400–600 nm for DAPI.

DNA extraction, 16S rRNA gene amplification and sequencing analysis. DNA from 10 mg of biofilm sample from core GC1048 and 245 mg from core GC1070 was extracted in a clean laminar flow hood using a Qiagen DNeasy PowerSoil kit according to the manufacturer's instructions.

For the amplification of 16S rRNA genes, we used the degenerated primer sets A519F (5′-CAGCMGCCGCGGTAA)[32] and A906R (5′-CAATTCMTTTAAGTTTC)[33] for *Archaea* and Bakt_341F (5′-CCTACGGGNGGCWGCAG) and Bakt_805R (5′-GACTACHVGGGTATCTAATCC) for *Bacteria*[34]. 16S rRNA gene amplification and sequencing were carried out by IMGM Laboratories GmbH (Martinsried, Germany). Cluster generation and bidirectional sequencing by synthesis was performed on Illumina MiSeq next generation sequencing system (Illumina, CA, USA) using reagents kit 500 cycles v2 under the control of MiSeq Control Software v2.5.0.5. Obtained reads were meticulously processed following a modified version of the USEARCH protocol (http://drive5.com/usearch/manual/uparse_pipeline.html; Supplementary Information S1). Taxonomy was assigned using the SILVA database release 132[35]. Non-16S rRNA gene sequences as well as OTUs containing single sequence or best assigned to non-targeted domains were removed. Nucleotide sequences have been deposited at SRA database (https://www.ncbi.nlm.nih.gov/sra) as BioProject with accession number PRJNA506542.

Furthermore, phylogenetic analyses of the abundant OTUs associated with the ANME-1 group and *Desulfobacteracae* were conducted to accurately assess their evolutionary origin from our Illumina MiSeq reads[36]. For this, we selected 19 ANME-1 (min. length: 1300 bp) and 32 *Desulfobacteraceae* sequences (min length: 807 bp) from published phylogenies to form a phylogenetic tree for each taxonomic group. Sequences were aligned using MUSCLE[37] implemented in MEGA 7 and a best-scoring maximum likelihood phylogenetic tree was built in Randomized Axelerated Maximum Likelihood (RAxML; Stamatakis[3]) using the General Time Reversible (GTR) Gamma model. Thereafter, shorter reads of the OTUs collected from biofilm in core GC1048 and GC1070 were aligned to the previously selected sequences and were placed on the built phylogenetic trees using the Evolutionary Placement Algorithm implemented in RAxML[3,36]. Resulting trees were visualized and annotated in Interactive Tree Of Life[38].

Results and Discussion

At GHP 5 and its close vicinity, we recovered two sediment cores (Fig. 1) comprising pockets in the sediment matrix that were filled with a macroscopically visible, slimy, yellow-greenish biofilm (Fig. 2). Pockets/biofilms of 4–5 cm length were found at 305 cmbsf within core GC1048 and at 68 cmbsf within core GC1070 (visualized as yellow symbol in Fig. 3A), which is in both cases less than ten centimetres below the depth of the SMTZ[16]. The cores were composed of glacigenic sediments, with hemipelagic grey mud comprising variable amounts of ice-rafted debris. Ice-rafted debris were deposited during several phases of extensive iceberg production. In both cores, the sediment horizons where the biofilms were found were characterized by laminated hemipelagic grey mud and silts mainly composed of quartz, carbonates, feldspar, and clay minerals. Besides the pockets, we did not observe any other sedimentological feature or sediment colour changes that could indicate a preferential site for biofilm formation.

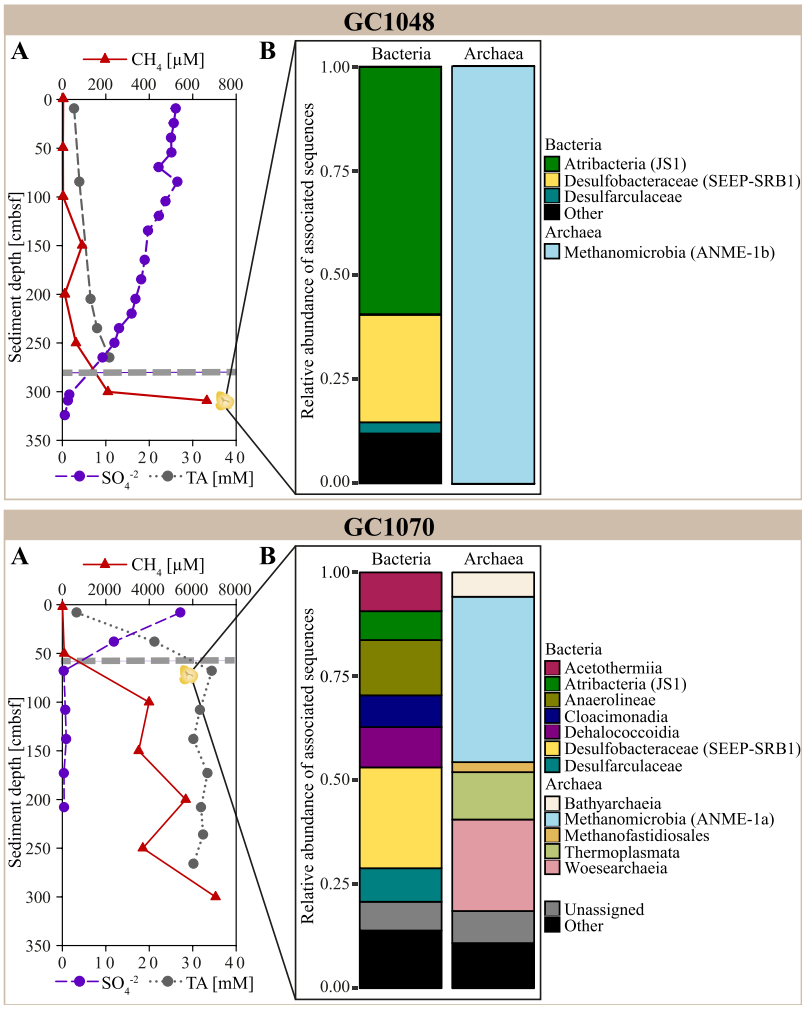

Figure 3. Data from sediment core GC1048 and GC1070. In each box, (**A**) Depth profile of concentrations of alkalinity (TA), sulphate (SO_4^{-2}), and dissolved methane (CH_4)[16]. The dashed grey line indicates the SMT depth of each core. The position of the biofilms is indicated as yellow symbol (GC1048: 305 cmbsf, GC1070: 68 cmbsf). Symbol size do not represent the actual size of biofilm. (**B**) Sequence-based relative abundances of bacterial and archaeal 16S rRNA genes. 'Other' includes taxa with less than 1% relative sequence abundance within the sequence data set. 'Unassigned' includes sequences that could not be assigned to a taxonomic group within their respective domain.

Biofilm microbial composition. For microbial diversity analysis of the two biofilm samples, we processed 82654 archaeal and 74083 bacterial read pairs. In total, reads clustered into 136 archaeal and 238 bacterial OTUs.

The microbial community in the biofilm from GC1048 showed an extremely low diversity (Shannon diversity index of 0.001 and 1.22 for *Archaea* and *Bacteria*, respectively; see Supplementary Table S1). All archaeal sequences clustered exclusively into one OTU (OTU8) that was associated with the anaerobic methanotrophic archaea (ANME) clade ANME-1b (Fig. 4). Among the most abundant bacterial groups, we found members closely related to the typical partner SRB of ANME-1, i.e. *Desulfobacteraceae* clustering into the SEEP-SRB1 clade (26% of all bacterial sequences; Fig. 5). Additional 3% of bacterial sequences were identified as *Desulfatiglans* (*Desulfarculaceae*), which is another common SRB in methane seep environments often associated with ANME[39–41]. Together with the vertical positioning of the biofilm close to the SMTZ, our sequence analyses suggest that the biofilm was predominantly involved in AOM and was mostly comprised of AOM-related biomass.

ANME-1-dominated biofilms in natural environments are very rare. Michaelis, *et al.*[20] reported on microbial mat biomass from microbial reefs in the Black Sea that was comprised of only one archaeal population (belonging to ANME-1) forming consortia with partner SRB of the *Desulfosarcina/Desulfococcus* group. Treude *et al.*[21] described similar mat structures in sediments from the Black Sea. The only other finding of biofilms in 'regular' ocean sediments was made by Briggs, *et al.*[7], who described ANME-dominated biofilms in fractures at depth of the SMTZ at the northern Cascadia Margin and the Indian Ocean. In those biofilms, the ANME-1 clade was identified as the most abundant taxon of a more diverse archaeal community, which included members of *Thermoplasmatales* and *Methanosarcinales*. Thus, our findings of an archaeal community in the biofilm from

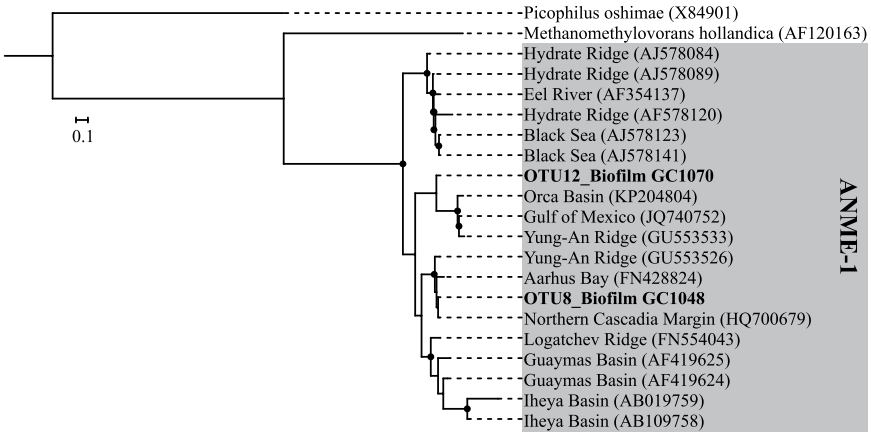

Figure 4. Phylogenetic tree showing evolutionary connections of the dominant OTUs representing biofilm 16S rRNA gene sequences to selected reference sequences of uncultured archaea of ANME-1 clades. Boldface type indicates the sequences obtained in this study. The tree was calculated by using RAxML algorithm. Biofilm sequences (~500 bp) were inserted by using EPA. Black dots at branches represent bootstrap values higher than 50. The bar indicates 10% estimated phylogenetic divergence.

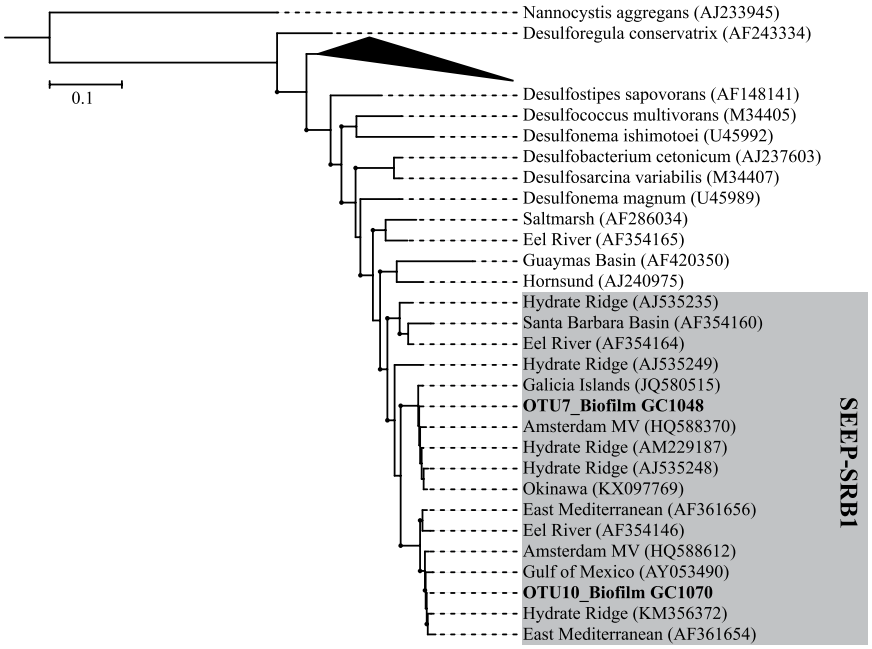

Figure 5. Phylogenetic tree showing evolutionary connections of the dominant OTUs representing biofilm 16S rRNA gene sequences to selected reference sequences of *Desulfobacteraceae* from the environment and isolated strains. Boldface type indicates the sequences obtained in this study. The tree was calculated by using the RAxML algorithm. Biofilm sequences (~500 bp) were inserted by using EPA. Black dots at branches represent bootstrap values greater than 50. The scale bar indicates 10% estimated phylogenetic divergence.

GC1048, which was exclusively comprised of members of the ANME-1b clade is unique and not comparable to any other environmental biofilm found so far.

In addition to AOM-related biomass in core GC1048, we detected members of *Atribacteria* (JS1 clade, 60% of all bacterial sequences). The JS1 clade co-occur especially predominant with organic carbon replete, and methane-rich conditions in anaerobic marine sediments. It has been suggested that this group has an anaerobic heterotrophic lifestyle[42,43] rather than being direct involved in AOM[44,45]. However, the metabolic potential of this uncultured clade and its relation to AOM remains unconstrained, because knowledge on the metabolic potential of JS1 is based on single-cell amplified genome analyses[42]. Other bacterial taxa found in biofilm from core GC1048 were *Bacteroidetes* (4%), *Spirochaetes* and uncultured TA06 clade (3% each; Fig. 3B).

Similar to the biofilm from core GC1048, the archaeal community of the biofilm within core GC1070 was dominated by members of the ANME-1 clade (43%), though, in contrast to GC1048, ANMEs in GC1070 most probably belonged to subgroup a, rather than subgroup b. Furthermore, contrary to GC1048, the microbial diversity within the GC1070 biofilm was higher (Shannon diversity index of 2.28 and 3.29 for *Archaea* and *Bacteria*, respectively). In addition to ANME-1a, we identified members of *Woesearchaeia* (24%), *Thermoplasmata* (MBG-D and DHVEG-1; 14%), *Thermococci* (*Methanofastidiosales;* 3%) and *Bathyarchaeia* (6%). Among members of the domain *Bacteria*, we found the AOM-associated taxa SEEP-SRB1 (24%) and *Desulfatiglans* (8%). Other abundant taxa were *Chloroflexi* (23%, *Anaerolineae/Dehalococcoidia*), *Acetothermia* (9%), *Atribacteria* (JS1 clade, 7%), *Cloacimonetes* (6%), and *Planctomycetes* (2%) (Fig. 3B). We suggest that the higher diversity is caused by the admixture of sediments (and sediment-associated microbes) to the biofilm sample. Indeed, representatives belonging to *Anaerolineae*, *Dehalococcoidia*, *Atribacteria*, *Woesearchaeia*, and MBG-D and DHVEG-1, commonly encountered at methane seeps, can be related to organic matter degradation (e.g. Inagaki, *et al.*[45], Pop Ristova, *et al.*[46], Nunoura, *et al.*[47], Trembath-Reichert, *et al.*[48], Inagaki, *et al.*[49], Cruaud, *et al.*[50]). *Woesearchaeia* are often found in marine environments with high organic matter content[47,51], but are also linked to symbiotic or parasitic lifestyles based on small genome sizes and limited metabolic capabilities[52]. However, at our sampling site, neither siboglinid tubeworms nor any other chemosynthetic macrofauna species were observed[53]. MBG-D and DHVEG-1, *Anaerolineae*, and *Dehalococcoidia* might play a major role in protein, amino acid and fatty acid re-mineralization[50,54]; *Dehalococcoidia* could also mediate reductive dehalogenation and potentially reduce sulphate[55–57]. All those substrates are probably available (at least to some degree) at the sediment horizon where the biofilm within GC1070 was found.

Biogeochemical functioning of biofilm microbes. According to the methane and sulphate concentration profiles (Fig. 3A)[16], the SMTs were likely located at ~300 cmbsf in core GC1048 and ~60 cmbsf in GC1070, i.e. less than ten centimetres above to where we discovered the biofilms. Both cores are characterized by steady-state sulphate-methane dynamics that ensures a consistent supply of both sulphate and methane at the SMTZ[16]. However, the differential depths of the SMTZ in the two cores suggest dissimilar methane fluxes. In GC1048, the SMTZ appeared to be deeper compared to GC1070 implying a lower methane flux in GC1048 than in GC1070.

The co-localisation of the biofilm and the SMTZs together with the prevailing presence of ANME-1 archaea and potential partner SRB in the biofilm samples, thus suggests that these microbes mediate sulphate-dependent AOM[12].

We analysed the cellular structure of the AOM biofilm community from GC1048 by confocal laser scanning microscopy. Images revealed numerous globular tight cell clusters of sulphate-reducing *Desulfobacteraceae* ranging 1–3 µm in diameter (Fig. 6B), but also loose cell formations. Archaeal cells (identified as ANME-1b by sequencing analysis) formed many small tight globular clusters (<1 µm) as well as patches of loose cell formations (Fig. 6A). Similar to previous findings[58,59], we found ANME-1b cells as multicellular strands/chains with length of several tens of micrometres. SRB cells seemed to be loosely associated with some of the multicellular ANME-1b strands and patches (Fig. 6C). In our biofilm sample, we did not observe any direct cell-to-cell contact of SRB and ANME-1b cells as shown for ANME-2/DSS aggregates[10,59,60] or the shell-type consortia of ANME-3 and *Desulfobulbus* spp.[11,61]. Previous studies showed that in sediments, ANME-1 may exist as single cells or as mono-specific chains or clusters without direct, physical association of partner SRB[59–62] raising the question if ANME-1 could also mediate AOM alone[12], as found in some cases for ANME-2[15].

ANME-1a and ANME-1b subgroups only contain uncultivated strains and their phylogenetic distance to each other shows sequence similarity values of <96% based on 16S rRNA genes[60]. In our biofilms, OTU8 clustered confinently into subclade 1b, while OTU12 seems to be closer associated to subclade 1a although that its assignment to one of the two clades is less certain. Still, the phylogenetical assignments of our OTUs to either ANME-1a and 1b is supported by the reference sequences from methane-rich environmental samples shown in Fig. 4. The environmental factors for selecting the two subgroups are still unknown. Both subgroups have been found at methane seeps[12]. The dominance of ANME-1 archaea in or below a SMTZ located some meters below seafloor has also been reported from sediments from a North Sea gas seep (up to 2.5 mM CH_4; Niemann, *et al.*[63]), the Santa Barbara Basin (>3 mM CH_4; Harrison, *et al.*[64]), the Sea of Japan (~1.8 mM CH_4; Yanagawa, *et al.*[65]), all of which are characterized by relatively high methane but rather low sulphate availability. Similarly, ANME-1b archaea were found to dominate highly sulphate-depleted sediments at Haima cold seeps in the South China Sea[66]. Moreover, flow chamber incubation experiment have shown that ANME-1 archaea are more active at high methane flow rates compared to ANME-2, which are only minimally affected by increased flow rates[67]. Only at the Black Sea microbial mat reefs, an ANME-1-dominated AOM community was found in an environment with high methane and high sulphate supply[20]. On the other hand, ANME-1 archaea were also found to dominate highly saline environments with moderate sulphate and rather low methane concentrations at a mud volcano in the Gulf of Cadiz (<0.6 mM CH_4; Maignien, *et al.*[62]) and in hypersaline environments of the Gulf of Mexico (<0.2 mM CH_4; Lloyd, *et al.*[68]). While high methane fluxes, low sulphate concentrations and hypersaline conditions may thus select for ANME-1 clades, the ecological niches of ANME-1a vs. ANME-1b are not well constrained. We can thus only speculate why ANME-1a and ANME-1b clades separately dominate each of the biofilms. Nevertheless, our findings suggest that ANME-1b, when compared to ANME-1a, seems to prevail in deeper, more sulphate-depleted sediments at sites of low methane flux.

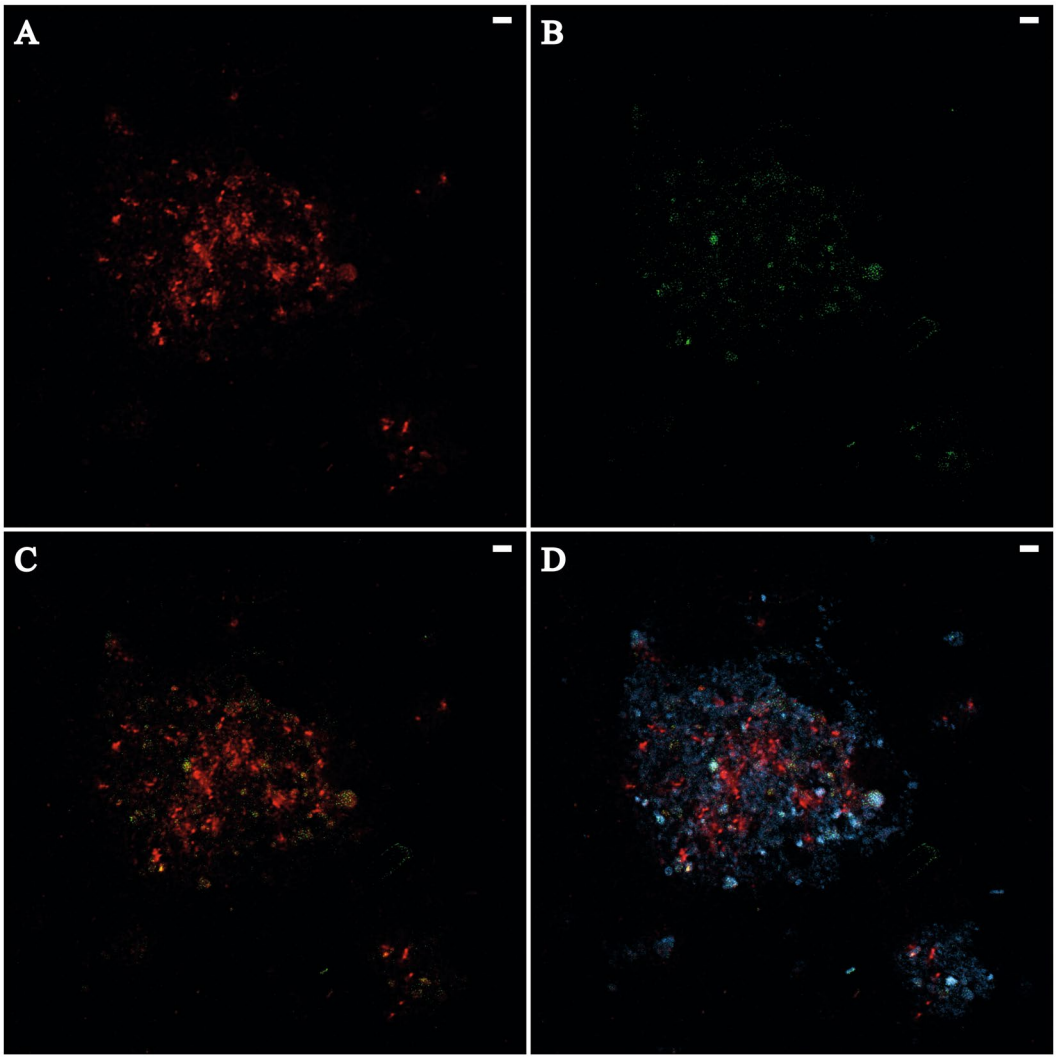

Figure 6. Confocal laser scanning micrographs of *Archaea* and sulphate-reducing bacteria (SRB) in biofilm from GC1048 visualized by FISH. Scale bars = 2 µm. (**A**) Archaeal cells (probe ARCH915 labelled with Cy3 [red]. (**B**) SRB belonging to *Desulfobacteraceae* (probe DSS658 labelled with 6-FAM [green]). (**C**) Overlay of image A and B (probe ARCH915 and DSS658). (**D**) Overlay of image A and B and nucleic acids stained with DAPI [blue].

Summary and Conclusion

In this paper, we report on biofilms that occupy sediment pockets located just below the SMTZ in two cores recovered from a cold seep area characterized by steady-state sulphate-methane dynamics. Both biofilms were dominated by AOM communities comprised of members of ANME-1 and SEEP-SRB1, which have only been reported once previously in the literature[7]. Furthermore, one of the biofilms was exclusively comprised of ANME-1b archaea, which built multicellular strands and patches only loosely associated with SRB cells. This raises the general question if ANME-1 can mediate AOM alone without any partner SRB. The second biofilm was characterized by a higher microbial diversity, possibly caused by admixture of the biofilm sample with surrounding sediments, but with ANME-1a as the dominant archaeal taxa. It remains ambiguous as to which environmental factors control the selection of subgroups ANME-1a or ANME-1b in natural environments. This investigation suggests that ANME-1b, in comparison with ANME-1a, appear to prevail in deeper, more sulphate-depleted sediments with a lower methane flux. Our findings also support the proposition that sub-seafloor sediment pockets and micro-fractures in a methane-related advective system promote AOM biofilm formation by providing pockets and conduits within sediment matrices where methane potentially accumulates or flows through. This constant supply of methane supports the development of AOM communities, which, over time, form biofilms[22]. Sediment pockets and micro-fractures could be more extensive at methane seeps than previously assumed.

Data Availability

Nucleotide sequences have been deposited at SRA database (https://www.ncbi.nlm.nih.gov/sra) as BioProject with accession number PRJNA506542. Detailed information on sequencing read processing workflow are available in the Supplementary Information S1.

References

1. Stoodley, P., Sauer, K., Davies, D. G. & Costerton, J. W. Biofilms as Complex Differentiated Communities. *Annual Review of Microbiology* **56**, 187–209, https://doi.org/10.1146/annurev.micro.56.012302.160705 (2002).
2. Wimpenny, J., Manz, W. & Szewzyk, U. Heterogeneity in biofilms. *FEMS Microbiology Reviews* **24**, 661–671, https://doi.org/10.1111/j.1574-6976.2000.tb00565.x (2000).
3. Stamatakis, A. RAxML version 8: a tool for phylogenetic analysis and post-analysis of large phylogenies. *Bioinformatics* **30**, 1312–1313, https://doi.org/10.1093/bioinformatics/btu033 (2014).
4. Dang, H. & Lovell, C. R. Microbial Surface Colonization and Biofilm Development in Marine Environments. *Microbiology and Molecular Biology Reviews* **80**, 91–138 (2016).
5. Costerton, J. W., Lewandowski, Z., Caldwell, D. E., Korber, D. R. & Lappin-Scott, H. M. Microbial Biofilms. *Annual Review of Microbiology* **49**, 711–745, https://doi.org/10.1146/annurev.mi.49.100195.003431 (1995).
6. Battin, T. J., Besemer, K., Bengtsson, M. M., Romani, A. M. & Packmann, A. I. The ecology and biogeochemistry of stream biofilms. *Nature Reviews Microbiology* **14**, 251 (2016).
7. Briggs, B. R. *et al*. Macroscopic Biofilms in Fracture-Dominated Sediment That Anaerobically Oxidize Methane. *Applied and Environmental Microbiology* **77**, 6780–6787 (2011).
8. Reeburgh, W. S. Oceanic Methane Biogeochemistry. *Chemical Reviews* **107**, 486–513, https://doi.org/10.1021/cr050362v (2007).
9. Barnes, R. O. & Goldberg, E. D. Methane production and consumption in anoxic marine sediments. *Geology* **4**, 297–300 (1976).
10. Boetius, A. *et al*. A marine microbial consortium apparently mediating anaerobic oxidation of methane. *Nature* **407**, 623–626 (2000).
11. Niemann, H. *et al*. Novel microbial communities of the Haakon Mosby mud volcano and their role as a methane sink. *Nature* **443**, 854–858, https://doi.org/10.1038/nature05227 (2006).
12. Knittel, K. & Boetius, A. Anaerobic Oxidation of Methane: Progress with an Unknown Process. *Annual Review of Microbiology* **63**, 311–334, https://doi.org/10.1146/annurev.micro.61.080706.093130 (2009).
13. Hinrichs, K.-U., Hayes, J. M., Sylva, S. P., Brewer, P. G. & DeLong, E. F. Methane-consuming archaebacteria in marine sediments. *Nature* **398**, 802 (1999).
14. Wegener, G., Krukenberg, V., Ruff, S. E., Kellermann, M. Y. & Knittel, K. Metabolic Capabilities of Microorganisms Involved in and Associated with the Anaerobic Oxidation of Methane. *Frontiers in Microbiology* **7**, https://doi.org/10.3389/fmicb.2016.00046 (2016).
15. Milucka, J. *et al*. Zero-valent sulphur is a key intermediate in marine methane oxidation. *Nature* **491**, 541, https://doi.org/10.1038/nature11656 (2012).
16. Hong, W.-L. *et al*. Variations in Gas and Water Pulses at an Arctic Seep: Fluid Sources and Methane Transport. *Geophysical Research Letters* **45**, 4153–4162, https://doi.org/10.1029/2018GL077309 (2018).
17. Iversen, N. & Jørgensen, B. B. Anaerobic methane oxidation rates at the sulfate-methane transition in marine sediments from Kattegat and Skagerrak (Denmark). *Limnol Oceanogr* **30**, 944–955, https://doi.org/10.4319/lo.1985.30.5.0944 (1985).
18. Roussel, E. G. *et al*. Extending the Sub-Sea-Floor Biosphere. *Science* **320**, 1046, https://doi.org/10.1126/science.1154545 (2008).
19. de Beer, D. *et al*. *In situ* fluxes and zonation of microbial activity in surface sediments of the Håkon Mosby Mud Volcano. **51**, 1315–1331 (2006).
20. Michaelis, W. *et al*. Microbial Reefs in the Black Sea Fueled by Anaerobic Oxidation of Methane. *Science* **297**, 1013–1015, https://doi.org/10.1126/science.1072502 (2002).
21. Treude, T., Knittel, K., Blumenberg, M., Seifert, R. & Boetius, A. Subsurface Microbial Methanotrophic Mats in the Black Sea. *Applied and Environmental Microbiology* **71**, 6375–6378, https://doi.org/10.1128/aem.71.10.6375-6378.2005 (2005).
22. Yao, H. *et al*. Fracture-controlled fluid transport supports microbial methane-oxidizing communities at Vestnesa Ridge. *Biogeosciences*, **16**, 2221–2232, https://doi.org/10.5194/bg-16-2221-2019 (2019).
23. Serov, P. *et al*. Postglacial response of Arctic Ocean gas hydrates to climatic amelioration. *Proceedings of the National Academy of Sciences* **114**, 6215–6220, https://doi.org/10.1073/pnas.1619288114 (2017).
24. Pernthaler, J., Glöckner, F.-O., Schönhuber, W. & Amann, R. Fluorescence in situ hybridization (FISH) with rRNA-targeted oligonucleotide probes. *Methods in Microbiology* **30**, 207–226, https://doi.org/10.1016/S0580-9517(01)30046-6 (2001).
25. Marsaglia, K., Milliken, K. & Doran, L. Smear slides of marine mud for IODP core description. *Volume I. Part 1: Methodology and atlas of siliciclastic and volcanogenic components. IODP Technical Note 1*. (2013).
26. Stoecker, K., Dorninger, C., Daims, H. & Wagner, M. Double Labeling of Oligonucleotide Probes for Fluorescence *In Situ* Hybridization (DOPE-FISH) Improves Signal Intensity and Increases rRNA Accessibility. *Applied and Environmental Microbiology* **76**, 922–926, https://doi.org/10.1128/AEM.02456-09 (2010).
27. Stahl, D. A. & Amann, R. Development and Application of Nucleic Acid Probes in Bacterial Systematics. In (Stackebrandt, E. & Goodfellow, M.) Eds, *Nucleic Acid Techniques in Bacterial Systematics* 205–248 (1991).
28. Mußmann, M., Ishii, K., Rabus, R. & Amann, R. Diversity and vertical distribution of cultured and uncultured Deltaproteobacteria in an intertidal mud flat of the Wadden Sea. *Environmental Microbiology* **7**, 405–418, https://doi.org/10.1111/j.1462-2920.2005.00708.x (2005).
29. Wallner, G., Amann, R. & Beisker, W. Optimizing fluorescent *in situ* hybridization with rRNA-targeted oligonucleotide probes for flow cytometric identification of microorganisms. *Cytometry* **14**, 136–143, https://doi.org/10.1002/cyto.990140205 (1993).
30. Snaidr, J., Amann, R., Huber, I., Ludwig, W. & Schleifer, K. H. Phylogenetic analysis and *in situ* identification of bacteria in activated sludge. *Applied and Environmental Microbiology* **63**, 2884–2896 (1997).
31. Glöckner, F. O. *et al*. An *In Situ* Hybridization Protocol for Detection and Identification of Planktonic Bacteria. *Systematic and Applied Microbiology* **19**, 403–406 (1996).
32. Jorgensen, S. L. *et al*. Correlating microbial community profiles with geochemical data in highly stratified sediments from the Arctic Mid-Ocean Ridge. *Proceedings of the National Academy of Sciences* **109**, E2846–E2855, https://doi.org/10.1073/pnas.1207574109 (2012).
33. Baker, G. C., Smith, J. J. & Cowan, D. A. Review and re-analysis of domain-specific 16S primers. *Journal of Microbiological Methods* **55**, 541–555 (2003).
34. Klindworth, A. *et al*. Evaluation of general 16S ribosomal RNA gene PCR primers for classical and next-generation sequencing-based diversity studies. *Nucleic Acids Research* **41**, e1–e1, https://doi.org/10.1093/nar/gks808 (2013).
35. Quast, C. *et al*. The SILVA ribosomal RNA gene database project: improved data processing and web-based tools. *Nucleic Acids Research* **41**, D590–D596, https://doi.org/10.1093/nar/gks1219 (2013).
36. Berger, S. A., Krompass, D. & Stamatakis, A. Performance, Accuracy, and Web Server for Evolutionary Placement of Short Sequence Reads under Maximum Likelihood. *Systematic Biology* **60**, 291–302 (2011).
37. Edgar, R. C. MUSCLE: multiple sequence alignment with high accuracy and high throughput. *Nucleic Acids Research* **32**, 1792–1797 (2004).

38. Letunic, I. & Bork, P. Interactive tree of life (iTOL) v3: an online tool for the display and annotation of phylogenetic and other trees. *Nucleic Acids Research* **44**, W242–W245, https://doi.org/10.1093/nar/gkw290 (2016).
39. Kleindienst, S., Ramette, A., Amann, R. & Knittel, K. Distribution and *in situ* abundance of sulfate-reducing bacteria in diverse marine hydrocarbon seep sediments. *Environmental Microbiology* **14**, 2689–2710, https://doi.org/10.1111/j.1462-2920.2012.02832.x (2012).
40. Cruaud, P. *et al*. Comparative Study of Guaymas Basin Microbiomes: Cold Seeps vs. Hydrothermal Vents Sediments. *Frontiers in Marine Science* **4**, 417, https://doi.org/10.3389/fmars.2017.00417 (2017).
41. Vigneron, A. *et al*. Comparative metagenomics of hydrocarbon and methane seeps of the Gulf of Mexico. *Scientific Reports* **7**, 16015, https://doi.org/10.1038/s41598-017-16375-5 (2017).
42. Nobu, M. K. *et al*. Phylogeny and physiology of candidate phylum 'Atribacteria' (OP9/JS1) inferred from cultivation-independent genomics. *The ISME journal* **10**, 273–286, https://doi.org/10.1038/ismej.2015.97 (2016).
43. Carr, S. A., Orcutt, B. N., Mandernack, K. W. & Spear, J. R. Abundant Atribacteria in deep marine sediment from the Adélie Basin, Antarctica. *Frontiers in Microbiology* **6**, 872–872, https://doi.org/10.3389/fmicb.2015.00872 (2015).
44. Hoshino, T. *et al*. Atribacteria from the Subseafloor Sedimentary Biosphere Disperse to the Hydrosphere through Submarine Mud Volcanoes. *Frontiers in Microbiology* **8**, 1135, https://doi.org/10.3389/fmicb.2017.01135 (2017).
45. Inagaki, F. *et al*. Biogeographical distribution and diversity of microbes in methane hydrate-bearing deep marine sediments on the Pacific Ocean. *Margin. Proceedings of the National Academy of Sciences* **103**, 2815–2820, https://doi.org/10.1073/pnas.0511033103 (2006).
46. Pop Ristova, P., Wenzhöfer, F., Ramette, A., Felden, J. & Boetius, A. Spatial scales of bacterial community diversity at cold seeps (Eastern Mediterranean Sea). *The ISME journal* **9**, 1306, https://doi.org/10.1038/ismej.2014.217 (2014).
47. Nunoura, T. *et al*. Microbial diversity in deep-sea methane seep sediments presented by SSU rRNA gene tag sequencing. *Microbes and Environments* **27**, 382–390, https://doi.org/10.1264/jsme2.ME12032 (2012).
48. Trembath-Reichert, E., Case, D. H. & Orphan, V. J. Characterization of microbial associations with methanotrophic archaea and sulfate-reducing bacteria through statistical comparison of nested Magneto-FISH enrichments. *PeerJ* **4**, e1913, https://doi.org/10.7717/peerj.1913 (2016).
49. Inagaki, F. *et al*. Characterization of C1-Metabolizing Metabolizing Prokaryotic Communities in Methane Seep Habitats at the Kuroshima Knoll, Southern Ryukyu Arc, by Analyzing pmoA, mmoX, mxaF, mcrA, and 16S rRNA Genes. *Applied and Environmental Microbiology* **70**, 7445–7455, https://doi.org/10.1128/aem.70.12.7445-7455.2004 (2004).
50. Cruaud, P. *et al*. Microbial communities associated with benthic faunal assemblages at cold seep sediments of the Sonora Margin, Guaymas Basin. *Frontiers in Marine Science* **2**, 53, https://doi.org/10.3389/fmars.2015.00053 (2015).
51. Fan, X. & Xing, P. The Vertical Distribution of Sediment Archaeal Community in the "Black Bloom" Disturbing Zhushan Bay of Lake Taihu. *Archaea* **2016**, 8, https://doi.org/10.1155/2016/8232135 (2016).
52. Castelle, C. J. *et al*. Genomic Expansion of Domain Archaea Highlights Roles for Organisms from New Phyla in Anaerobic Carbon Cycling. *Current Biology* **25**, 690–701 (2015).
53. Sen, A. *et al*. Geophysical and geochemical controls on the megafaunal community of a high Arctic cold seep. *Biogeosciences* **15**, 4533–4559, https://doi.org/10.5194/bg-15-4533-2018 (2018).
54. Lloyd, K. G. *et al*. Predominant archaea in marine sediments degrade detrital proteins. *Nature* **496**, 215–218, https://doi.org/10.1038/nature12033 (2013).
55. Kaster, A.-K., Mayer-Blackwell, K., Pasarelli, B. & Spormann, A. M. Single cell genomic study of Dehalococcoidetes species from deep-sea sediments of the Peruvian Margin. *The ISME journal* **8**, 1831, https://doi.org/10.1038/ismej.2014.24 (2014).
56. Wasmund, K. *et al*. Genome sequencing of a single cell of the widely distributed marine subsurface Dehalococcoidia, phylum Chloroflexi. *The ISME journal* **8**, 383–397, https://doi.org/10.1038/ismej.2013.143 (2014).
57. Wasmund, K. *et al*. Single-Cell Genome and Group-Specific dsrAB Sequencing Implicate Marine Members of the Class Dehalococcoidia (Phylum Chloroflexi) in Sulfur Cycling. *mBio* **7**, 3, https://doi.org/10.1128/mBio.00266-16 (2016).
58. Roalkvam, I. *et al*. New insight into stratification of anaerobic methanotrophs in cold seep sediments. *FEMS Microbiology Ecology* **78**, 233–243, https://doi.org/10.1111/j.1574-6941.2011.01153.x (2011).
59. Orphan, V. J., House, C. H., Hinrichs, K.-U., McKeegan, K. D. & DeLong, E. F. Multiple archaeal groups mediate methane oxidation in anoxic cold seep sediments. *Proceedings of the National Academy of Sciences* **99**, 7663–7668, https://doi.org/10.1073/pnas.072210299 (2002).
60. Knittel, K., Lösekann, T., Boetius, A., Kort, R. & Amann, R. Diversity and Distribution of Methanotrophic Archaea at Cold Seeps. *Applied and Environmental Microbiology* **71**, 467–479, https://doi.org/10.1128/AEM.71.1.467-479.2005 (2005).
61. Lösekann, T. *et al*. Diversity and Abundance of Aerobic and Anaerobic Methane Oxidizers at the Haakon Mosby Mud Volcano, Barents Sea. *Applied and Environmental Microbiology* **73**, 3348–3362, https://doi.org/10.1128/aem.00016-07 (2007).
62. Maignien, L. *et al*. Anaerobic oxidation of methane in hypersaline cold seep sediments. *FEMS Microbiology Ecology* **83**, 214–231, https://doi.org/10.1111/j.1574-6941.2012.01466.x (2013).
63. Niemann, H. *et al*. Methane emission and consumption at a North Sea gas seep (Tommeliten area). *Biogeosciences* **2**, 335–351, https://doi.org/10.5194/bg-2-335-2005 (2005).
64. Harrison, B. K., Zhang, H., Berelson, W. & Orphan, V. J. Variations in Archaeal and Bacterial Diversity Associated with the Sulfate-Methane Transition Zone in Continental Margin Sediments (Santa Barbara Basin, California). *Applied and Environmental Microbiology* **75**, 1487–1499 (2009).
65. Yanagawa, K. *et al*. Niche Separation of Methanotrophic Archaea (ANME-1 and -2) in Methane-Seep Sediments of the Eastern Japan Sea Offshore Joetsu. *Geomicrobiology Journal* **28**, 118–129, https://doi.org/10.1080/01490451003709334 (2011).
66. Niu, M., Fan, X., Zhuang, G., Liang, Q. & Wang, F. Methane-metabolizing microbial communities in sediments of the Haima cold seep area, northwest slope of the South China Sea. *FEMS Microbiology Ecology* **93**, fix101–fix101, https://doi.org/10.1093/femsec/fix101 (2017).
67. Girguis, P. R., Cozen, A. E. & DeLong, E. F. Growth and Population Dynamics of Anaerobic Methane-Oxidizing Archaea and Sulfate-Reducing Bacteria in a Continuous-Flow Bioreactor. *Applied and Environmental Microbiology* **71**, 3725–3733 (2005).
68. Lloyd, K. G., Lapham, L. & Teske, A. An Anaerobic Methane-Oxidizing Community of ANME-1b Archaea in Hypersaline Gulf of Mexico Sediments. *Applied and Environmental Microbiology* **72**, 7218–7230, https://doi.org/10.1128/aem.00886-06 (2006).

Acknowledgements

We thank the captain, crew, and scientific research party of the R/V *Helmer Hanssen* during CAGE16–5 cruise including the chief scientist Michael Carroll for support and assistance during the cruise. We thank Hallvard L. Olsvik at the Advanced Microscopy Core Facility at the Institute of Medical Biology at UiT for his support at the CLSM. The funding for this study was provided by The Centre for Arctic Gas Hydrate, Environment and Climate (CAGE) and the Research Council of Norway (Grant Number: 223259). The publication charges for this article have been funded by a grant from the publication fund of UiT The Arctic University of Norway.

Author Contributions

F.G. wrote the manuscript with scientific support from H.N. and M.S. All authors discussed the data and contributed to the final manuscript. Biofilm samples were collected by F.G., H.N., S.K. S.K. extracted the DNA. Sequence analysis was performed by V.C. G.P. carried out sedimentological interpretation. T.V. and F.G. performed FISH.

Additional Information

Supplementary information accompanies this paper at https://doi.org/10.1038/s41598-019-46209-5.

Competing Interests: The authors declare no competing interests.

Publisher's note: Springer Nature remains neutral with regard to jurisdictional claims in published maps and institutional affiliations.

Paper III

Niche differentiation of prokaryotic communities and aerobic methanotrophs in surface sediments of an Arctic cold seep

Vincent Carrier[1,2], Mette M. Svenning[1,2], Helge Niemann[2,3,4], Friederike F. Gründger[2,5], Dimitri Kalenitchenko[2]

[1]Department of Arctic and Marine Biology, The Arctic University of Norway, Tromsø, Norway
[2]Centre for Arctic Gas Hydrate, Environment and Climate, The Arctic University of Norway, Tromsø, Norway
[3]Department of Marine Microbiology and Biogeochemistry, Royal Netherlands Institute for Sea Research (NIOZ), and Utrecht University, den Burg, the Netherlands
[4]Department of Earth Sciences, Faculty of Geosciences, Utrecht University, Utrecht, the Netherlands
[5]Department of Bioscience, Arctic Research Centre, Aarhus University, Aarhus, Denmark

Keywords: Arctic, cold seeps, seabed habitats, methanotrophs, bacterial mats, siboglinids, sulphide-oxidation, Methylococcales

Abstract

Arctic gas hydrates bearing mounds south of Svalbard host a chaotic distribution of bacterial mats, fields of tubeworms and methane gas flares. These features typically affect local biogeochemistry, creating different sediment surface ecological niches. However, how these niches shape the microbial communities, particularly the aerobic methanotrophs, remain unknown. In this study, we investigated the surface sediment prokaryotic biodiversity linked to 16S rDNA between those habitats. We compared environmental parameters with community data based on the 16S rDNA and the *pmoA* genes to identify driving environmental factors. Flares and mats were characterized by high concentrations of methane and sulphide at or near sediment surface. Sediment below tubeworms contrasted with low methane and sulphide, but oxygen penetrated deeper. Habitats hosted different microbial communities, where highest diversity was within the tubeworms fields. Methane was oxidized anaerobically near flares by ANME-1. Aerobic methanotrophs were more abundant at flares and inside mats, and both 16S rRNA and *pmoA* genes analyses suggested three key methanotrophs. Two clustered within the uncultivated group Deep Sea Cluster 1, but were together negatively correlated suggesting different niche preferences. Sulphide oxidizing bacteria also shifted in relative abundance and composition, with higher proportions of Campylobacterota at flares and within mats, and higher proportions of *Beggiatoa* at the edges of mats and worm fields. The distance between sulphide and oxygen gradients could be driving distinctions between the sulphide oxidizing communities. Additional shifts in diversity were also observed among suggested organic matter degraders Woesearchaeota, Gammaproteobacteria and Desulfobacterota, which were more diverse near the worms.

Introduction

Up to 23% of the radiative forcing of climate change since pre-industrial time can be explained by the increase of the methane (CH_4) in the atmosphere (Etheridge et al., 1998; Turner et al., 2019). Despite having a lower concentration than CO_2, the significant contribution of CH_4 is explained by its strong radiative efficiency (Etminan et al., 2016). The increase of CH_4 in the atmosphere from anthropogenic and natural sources (Reeburgh, 2007; Saunois et al., 2016), can be attenuated by biological and physical processes. In the marine environment, this attenuation is so efficient that most of the methane released from the seabed does not reach the atmosphere (Myhre et al., 2016). This reduction in the upward flux of CH_4 toward the atmosphere is in a large proportion (up to 80%) driven by microorganisms (Sommer et al., 2006; Boetius and Wenzhöfer, 2013). These pelagic and benthic microorganisms, named methanotrophs, are using CH_4 as a carbon and energy source in anaerobic and aerobic conditions (Hanson and Hanson, 1996; Boetius et al., 2000; Reeburgh, 2007).

In anaerobic conditions, below the sediment surface, CH_4 is oxidized through reverse methanogenesis by different uncultivated groups of anaerobic methanotrophic Archaea (ANME; Boetius et al., 2000). AOM was shown to be possible using nitrite/nitrate (Hu et al., 2014), manganese or iron (Beal et al., 2009; Ettwig et al., 2016), and sulphate (SO_4^{2-}; Nauhaus et al., 2002). AOM results in the production of bicarbonate (HCO_3^-), which precipitate to form authigenic carbonate, and hydrogen sulphide (HS^-) when SO_4^{2-} is used as an electron donor.

In aerobic conditions, found in the water column and the first millimetres of sediment, CH_4 is oxidized by bacteria using oxygen (O_2) as an electron acceptor to form formaldehyde and carbon dioxyde. Methane oxidizing bacteria (MOB) have been described primarily within the Gammaproteobacteria and Alphaproteobacteria, commonly referred as Type I and II methanotrophs, respectively (Hanson and Hanson, 1996; Dunfield et al., 2007; Knief, 2015). Yet, the clustering of a key enzyme of the aerobic methane oxidation (MOx) named methane monooxygenase (*pmoA*) sequences, showed that only half of the formed operational taxonomic units (OTUs) contained cultivated representatives (Knief, 2015), emphasizing the need to reveal their exosystemic role.

In the Arctic, south of Svalbard, CH_4-rich geofluids emitted from gas hydrate mount (GHP) drove changes in the composition of archaeal, bacterial and eukaryotic communities compared to the

reference site (Carrier et al., 2020). The sampling approach, inherited from previous studies in cold-seep areas (de Beer et al., 2006), revealed the biodiversity of CH_4 rich anaerobic sediments. Acknowledging that the anaerobic CH_4 filter is taking up most of the CH_4 (Boetius and Wenzhöfer, 2013), the aerobic filter at the sediment surface is usually overlooked, even it does not benefit from the high buffering capacity of the sediments, witch makes it more sensitive to physical and chemical changes (Physical: temperature, bottom trawling, currents; Chemical: electron acceptor, pH).

Here we used a high-resolution approach to reveal the MOB diversity in HS^- oxidizing bacterial mats, CH_4 flares and chemoautorophic siboglinids worm fields. These three microhabitats, occurring at arctic cold seeps were influenced by the biogeochemistry of the surrounding sediments. However, nothing is known on how these habitats influence, if they do, the diversity of the MOB.

We aimed to (i) test if the communities were significantly different between habitat, (ii) identify key taxonomic groups driving the dissimilarities and (iii) combined 16S rRNA and pmoA genes to characterize the MOB communities between the different habitats. We used amplicon sequencing combined with electrochemical measurement to describe the microbial community and their habitat. Through this study, we revealed that the different habitats are associated with contrasting physicochemical characteristics that shape the prokaryotic diversity. ANME-1 were almost solely detected at gas flares, which also hosted with bacterial mats highest relative abundances of MOB. The combination of 16S rRNA and *pmoA* genes analyses demonstrated that the MOB community was composed of three main bacteria: two of them were assigned to the same uncultivated environmental group of Deep Sea Clusters, but presented opposite habitat preferences. Furthermore, we revealed shifts in the composition of sulphide oxidizing bacteria, another key group of local primary producers. The Campylobacterota and Beggiatoales contrasted in niches inclination, potentially driven by the proximity of oxygen and sulphide availability.

Materials and methods

Sampling site

Storfjordrenna is located south of Svalbard, at the entrance of Storfjorden. At 380m deep, five gas hydrate bearing pingos (GHPs) were discovered (Serov et al., 2017). The GHPs have a diameter ranging from 280m to 450m and a height from 8m to 10m. CH_4 seeping from the GHPs was

predominantly of thermogenic origin (Serov et al., 2017). Cores taken from the GHPs revealed gas hydrate-bearing sediments within few meters below sediment surface. The sampling campaign was carried out between 22nd October and 02nd November 2018 onboard RV *Kronprins Haakon*. The seafloor of 2 GHPs, GHPs 1 and 3, were visually scanned using a ROV (AEGIR6000, Norway) to locate areas where bacterial mats, siboglinid worm fields and gas flare activity could be observed. A seafloor area of GHP 3 comprising a mixture of the features mentioned above was selected for sampling (Fig. 1).

Sampling procedure

Using the ROV, push cores were used to sample sediments in each four habitat types (Fig.1): within a bacterial mat (BM) and a siboglinid worms field (SF), plus the edge of each habitat, defined as bacterial edge (BE) and siboglinid worms edge (SE).

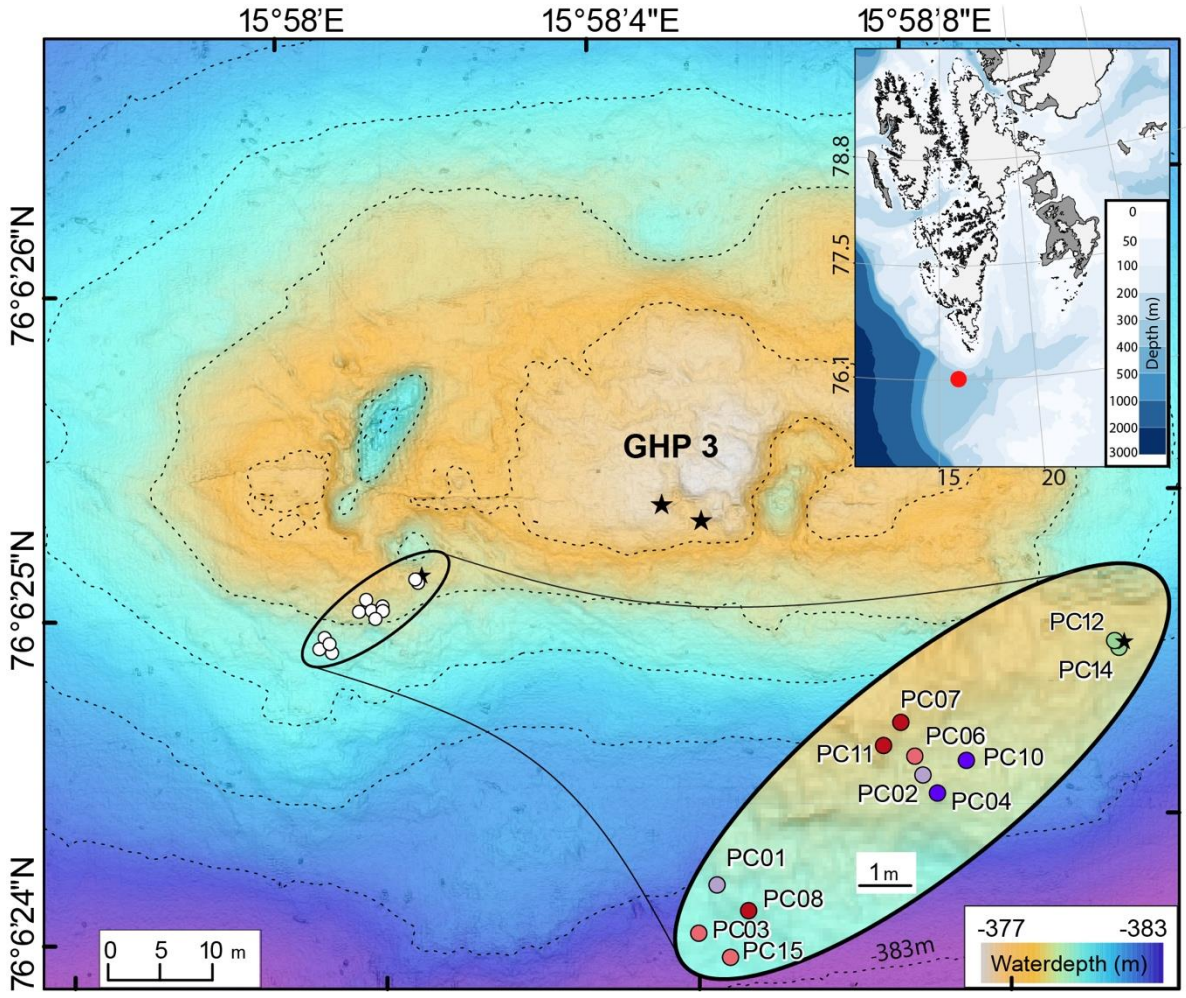

Figure 1: Gelogical dome structure referred to as Gas Hydrate Pingo 3 (GHP 3), located at the mouth of Storfjordrenna, 50 km south of Svalbard. Dots represent locations of the different push cores (PC) and the stars indicate CH_4 gas flares observed using the ROV camera. Sediment cores were taken near a gas flare (green dots), within bacterial mats (dark blue dots), siboglinid fields (dark red dots) and at edges of bacterial mats and siboglinid fields (light blue and light red dots, respectively).

Two cores from SF ($PC07_{SF}$ and $PC11_{SF}$), one core from SE ($PC06_{SE}$), one core from BE ($PC02_{BE}$) and two core from BM ($PC04_{BM}$ and $PC10_{BM}$) were successfully retrieved in the first area (Fig 1B). On a second dive in a nearby area on GHPs we took additional core, one from SF ($PC08_{SF}$), two from SE ($PC03_{SE}$ and $PC15_{SE}$) and one from BE ($PC01_{BE}$; Fig S1B, Fig 1C). Finally, two push cores were also retrieved directly on gas flares ($PC12_{FL}$ and PC 14_{FL}). During ROV operations, push cores retrieved from the ROV were stored on the seafloor in a metallic basket. Once the basket was brought back onboard, cores were immediately moved to a cold room (4°C) for further processing.

Porewater Geochemistry

Porewater geochemistry (CH_4, HS^-, O_2) was measured on a subset of cores. In a cold room, HS^- and O_2 were immediately measured *in situ* using probes from Unisense (Aarhus, DE). The microsensor profiling of the O_2 in the upper sediments was performed using a miniaturized 100 µm width Clarks type electrode (OX-100,Unisense, Aarhus, Denmark) and a microsensor multimeter (Unisense, Aarhus, Denmark). Oxygen concentrations were profiled vertically, perpendicular to the surface of the sediment, with a resolution of 100 to 250 µm using a motorized micromanipulator. Sulfur was measured using a micro sensor that convert H_2S into HS^- ions in an alkaline electrolyte contained in the electrode tip. It is then immediately oxidized by ferricyanide, producing sulfur and ferrocyanide. The sensor signal is generated by the re-oxidation of ferrocyanide at the anode within the tip of the sensor (P. Jeroschewski et al., 1996).

Afterwards, cores were cut and CH_4 concentrations and porosity were measured from 3 mL of bulk sediments per approx. 4-5 cm intervals in all cores, following the same protocol used in Carrier et al., (2020). Four cores ($PC04_{BM}$, $PC02_{BE}$, $PC06_{SE}$ and $PC07_{SF}$) formed a section line of few meters long and a 2D representation of the porewater geochemistry along this section was created using approximated surface calculated with the MBA package on R (Finley et al., 2017).

TNA extraction, DNA Sequencing and Sequences Analyses

The first 2 cm below the sediment surface (cmbsf) were transferred a Whirl-Pak® sterile sampling bag (Nasco, United States) and directly frozen at -80°C. Exceptionally, because of the angle of the sediment surface in PC12FLFlare, two surface samples were taken from $PC14_{FL}$ of the GF habitat ($PC14s_{FL}$ for surface and $PC14b_{FL}$ for below surface). The samples were stored at -80°C on RV Kronprins Haakon and transferred frozen to the laboratory at UiT The Arctic University of Norway at the end of the cruise.

For DNA/RNA isolation, the samples were transferred in grinding jar sets (Qiagen, Germany), priory cooled down in liquid nitrogen, and grinded using a TissueLyser II (Qiagen, Germany) at 30 Hz for 30 seconds. From the grinded sediments, approximately 0.25g were transferred in G2 DNA/RNA enhancer bead tubes (Ampliqon, Denmark) for physical lysis. Nucleic acids were extracted following a phenol/chloroform extraction protocol (Griffiths et al., 2000) modified by Urich et al. (2008). Once the TNA samples were quality checked using electrophoresis gels, the

DNA concentrations were measured using a Qubit 2.0 Fluorometer (Thermo Fisher Scientific, United States) and normalized before being sent to the IMGM Laboratories GmbH (Planegg, Germany) for library preparation and amplicon sequencing. For each sample, Bacteria and Archaea were amplified using same 16S rDNA degenerate primers to target the V3-V4 regions used for samples collected in the same area (Carrier et al., 2020).

To identify the CH_4 oxidising bacteria (or methanotrophs) in the different habitats, the particulate methane monooxygenase gene *pmoA* was amplified from each sample using the degenerated primer pair wcpmoA189f and wcpmoA661r (Tavormina et al., 2008), a primer pair optimized for targeting marine aerobic methanotrophs. Library generation was conducted in accordance with the company's protocols before being sequenced using a MiSeq System (Illumina inc., United States).

Paired-end reads were processed using derived workflow (Carrier et al., 2020) from the USEACH suggested protocol[1] (Edgar, 2010). The Silva database release 138 (Quast et al., 2012) was used for taxonomy assignment of the 16S libraries and the taxonomy of the OTUs from the *pmoA* libraries were assigned using the *pmoA* gene reference database produced by Yang et al., 2016. For the 16S libraries, sequences that were not classified to their domain were discarded prior to further analyses and singletons were removed for all libraries. For the 16S libraries, OTUs were constructed at 97% pairwise sequence identity. For the *pmoA* libraries, OTUs were constructed at 86% pairwise sequence identity, a cut-off corresponding to the 97% similarity of the 16S rRNA gene (Wen et al., 2016). Paired-end nucleotide reads will be deposited at Sequence Read Archive[2] Genebank as BioProject prior to publication.

Statistical Analyses

Archaeal libraries were rarefied at 14 800 sequences while the libraries for Bacteria and *pmoA* were rarefied at 15 000 sequences, corresponding to the lowest number of sequences in one sample. Alpha diversity indices (OTUs observed, Shannon, Simpson and chao1) and rarefaction curves were calculated for each library on the abundance of OTUs using USEARCH (Edgar, 2010). Prior to further analyses, OTU tables were imported and centered log-ratio transformed (CLR) on R using package Phyloseq v1.34.0 (Aitchison, 1982; McMurdie and Holmes, 2013). Beta diversity,

[1] http://drive5.com/usearch/manual/uparse_pipeline.html
[2] http://www.ncbi.nlm.nih.gov/sra

measuring divergence in the composition of communities between the different sediment samples, was calculated on the relative abundance of the OTUs using the Bray-Curtis dissimilarity index. Hierarchical clusters were calculated using the package Vegan v2.5-5 package on R (Oksanen et al., 2019) using the average method and were plotted along barplots illustrating the relative abundances of most abundant taxonomic groups using ggplot2 package on R (Wickham, 2016).

To statically test if the difference in the community composition of the different habitats is significant or not for each library types (Archaea, Bacteria and *pmoA*), a permutational multivariate analysis of variance (PERMANOVA) was performed on the CLR transformed OTU matrices (Anderson, 2017). Using the Vegan v2.5-5 package in R (Oksanen et al., 2019), the Bray Curtis dissimilarity index was selected and PERMANOVA analyses were performed at 999 permutations. The PERMANOVA was repeated twice, first with all samples segregated by their habitat types (SF, SE, BM, BE, FL), and then within each habitat (SF, BM, FL), subtracting the samples from the edges. Because the interpretation of the PERMANOVA analyses depend on an homogenous variance within the different habitats (Anderson, 2017), the multivariate dispersions was calculated using betadisper and the null hypothesis of the absence of difference in dispersion between habitats was tested using a permutation test, both functions implemented in Vegan v2.5-5 package on R (Oksanen et al., 2019). Dissimilarity between the different groups was visualized using principal component analyses (PCA) on the CLR transformed OTU matrices using the package Phyloseq v1.34.0 implemented in R (McMurdie and Holmes, 2013). To identify archaeal and bacterial biomarkers of the different habitats linear discriminant analyses effect size (LEfSe) were performed and visualized in cladograms (Segata et al., 2011), i.e. taxonomic groups that explain the differences in the microbial community structure of the different habitats. These analyses were conducted using the package microbiomeMarker v0.0.1.9 on R (Cao, 2020).

Phylogenetic Analyses

Phylogenetic analyses of the abundant 16S and *pmoA* OTUs associated to bacterial methanotrophs were conducted to accurately assess their evolutionary origin and positive correlations between the dominant OTUs of the 16S and the *pmoA* libraries. In total, 71 gammaproteobacterial methanotrophs 16S sequences (min length: 1300 bp) and 65 *pmoA* sequences (min length: 460 bp) were selected from published phylogenies in addition to reference sequences in the pmoA and 16S Silva release 138 databases (Quast et al., 2012; Knief, 2015; Yang et al., 2016) for the 16S

and pmoA tree, respectively. For both trees, *pmoA* and 16S sequences of the alphaproteobacterial *Methylosinus sporium* were used as the outgroup. Sequences were aligned using MUSCLE (Edgar, 2004) implemented in MEGA 7 (Kumar et al., 2016) and best-scoring maximum likelihood phylogenetic trees, used as reference trees, were built using Randomized Axelerated Maximum Likelihood (RAxML), calculated based on the General Time Reversible (GTR) Gamma model (Stamatakis, 2014). Selected OTUs from the this study were aligned to the sequences selected to built their respective reference tree and were placed on these using the Evolutionary Placement Algorithm implement in RAxML. Resulting trees were visualized and annotated using the packages treeio and ggtree on R (Yu et al., 2017; Wang et al., 2020). Spearman correlations between the abundant OTUs of the 16S and *pmoA* libraries were calculated using the package rstatix on R (Kassambara, 2020) with a significance level at 0.95.

Results

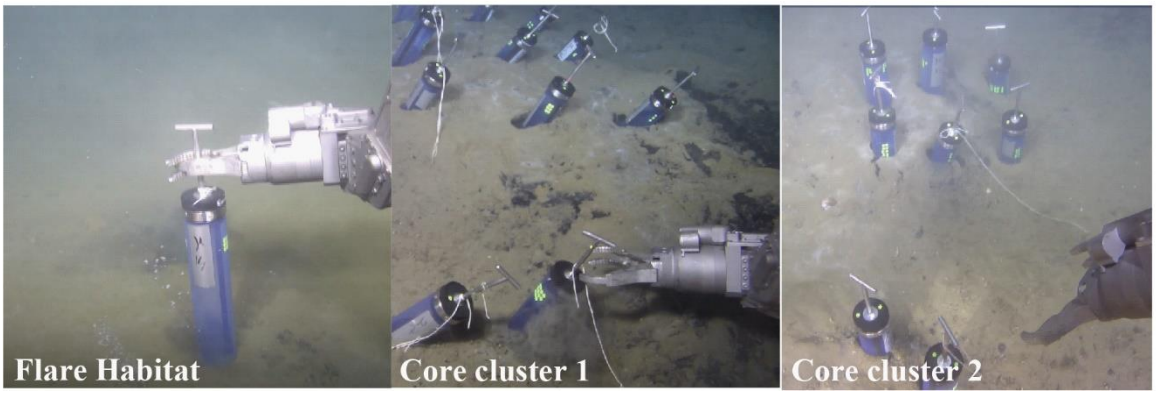

Figure 2: Images taken by the ROV of the three clusters of sediment cores retrieved from the GHP 3 illustrated in Figure 1. $PC12_{FL}$ and $PC14_{FL}$ were taken on an active gas flare (left picture) and the remaining cores were taken in two grids covering bacterial mats and siboglinid fields.

Environmental Characterization and Geochemistry

Three sediment samples ($PC12_{FL}$), including two extruded from the same PC ($PC14s_{FL}$ and $PC14b_{FL}$), were taken directly on an active CH_4 gas flare (Figures 1 & 2). Near the gas flare, the seafloor was generally soft, although authigenic carbonates were visible. Other sources of CH_4 gas bubbles were also visible in the surrounding. Below the seafloor surface, at core $PC14_{FL}$, CH_4 concentrations reached a maximum of 5775 µM at 8 cmbsf (Figure 3). At same depth co-occurred the maximum HS^- concentration at 105.54 mV. O_2 was depleted throughout the core.

At SF and BM, the sediment was soft and there was an absence of antigenic carbonates. These could be found widespread on the GHP, but areas of thicker mats or denser SF were commonly less than a meter radius. We could not observe a combination of both thick bacterial mats and dense siboglinid fields. When both habitats were overlapping, mats would be thinner and fields less dense. Cores $PC04_{BM}$ and $PC10_{BM}$ were taken from sediments where bacterial mats were thicker, while cores $PC01_{BE}$ and $PC02_{BE}$ at their edges where the bacterial mats were thinner (Figure 2). Within the BM, the O_2 at sediment surface is anoxic but its penetration depth increases to below 1 cmbsf toward the BE (Figure 3). Along the section, highest concentrations of CH_4 and HS^- were retrieved under BM. In BM, CH_4 and HS^- concentrations reached a peak of 6268 µM at 22 cmbsf and of 197.19 mV at 28 cmbsf, respectively. CH_4 and HS^- concentrations below BME were lower, reaching 4660 µM at 16 cmbsf and 88.73 mV at 28 cmbsf, but remained higher than under siboglinid fields. Within the SF, the O_2 could penetrate below 1 cmbsf and no apparent differences in O_2 concentrations between cores taken below SF and SE (Figure 3). Below the SE, traces of CH_4 could be measured, reaching an average (avg) of 1700 µM between 10 and 20 cmbsf. HS^- concentrations were also detected, attaining 122.16 mV at 11 cmbsf and a maximum of 173.58 mV at 23 cmsbf. Toward sediments below SF, concentrations of CH_4 and HS^- were reduced and could generally not be detected. Geochemical profiles (O_2, CH_4 and HS^-) of each core are available as Supplementary Information (Supplementary Figures 1-3).

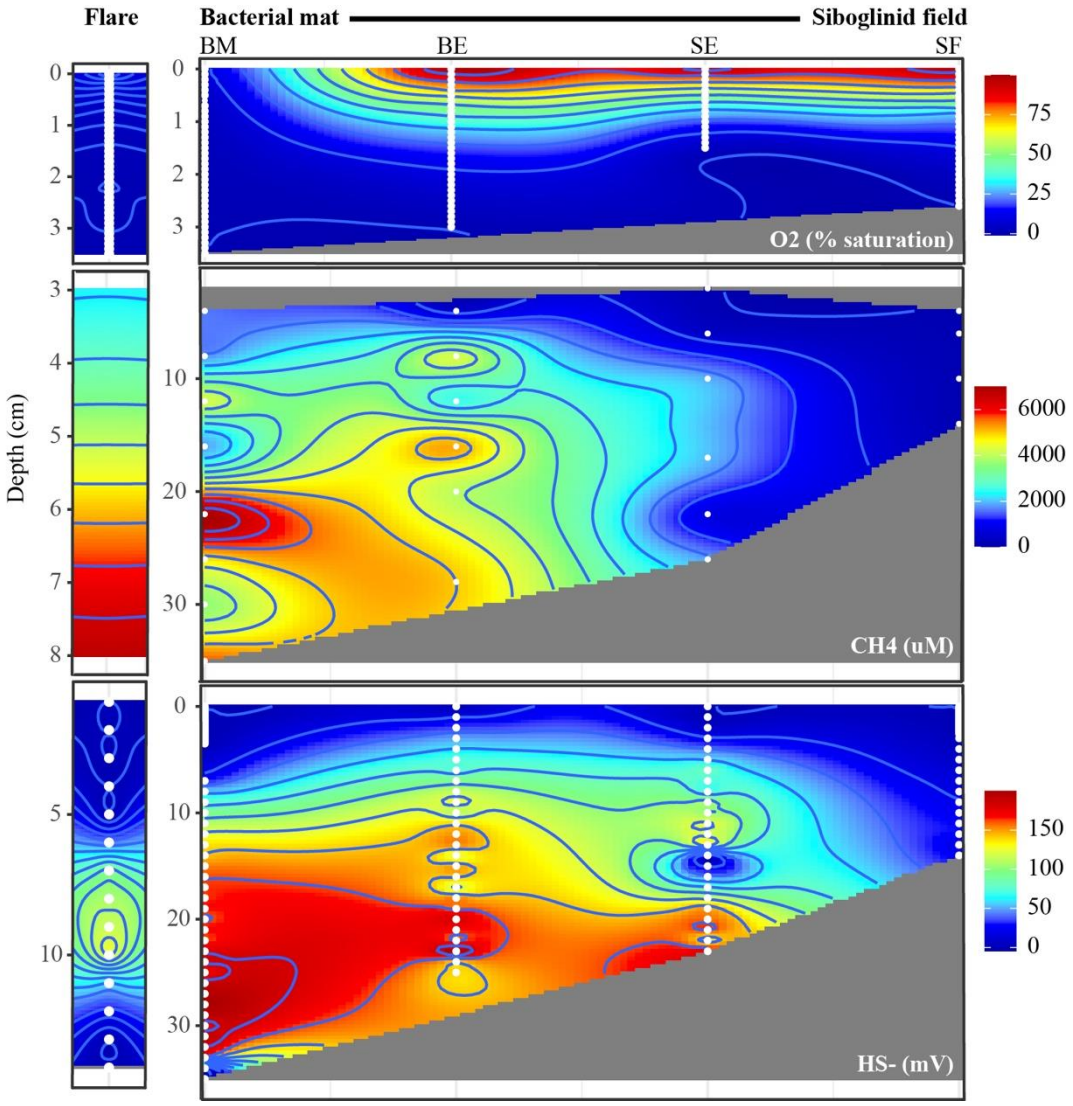

Figure 3: Physicochemical profile (O_2, CH_4 and HS^-) in 2D across an approximately 2 m long line section from the cores $PC04_{BM}$, $PC02_{BE}$, $PC06_{SE}$ and $PC07_{SF}$, from the bacterial mat (BM), the edge of the bacterial mat (BE), the edge of a siboglinid field (SE) and within (SF). White dots represent data points and profiles for each cores and are available as Supplementary Information (SI Figures 1, 2 and 3).

Sequence Analyses

Once pair-ends reads were quality filtered, 2680, 2122 and 34 OTUs were successfully assigned to the archaeal, bacterial and *pmoA* libraries, respectively. After rarefaction 2314, 2101 and 34 OTUs remained. For the bacterial and archaeal libraries, the coverage of biodiversity in a sample after rarefaction was assessed visually using rarefaction curves of the richness (number of OTUs) per sample and these are available as Supplementary Information (Supplementary Figure 4). Throughout the text, OTUs retrieved from the Archaeal and Bacterial 16S rRNA gene in addition

to from the *pmoA* gene libraries will be referred as OTU aX, OTU bX and OTU pX, respectively (where X is the OTU ID).

Similarities between habitats

Table 1: Permutational Multivariate Analysis of Variance (PERMANOVA; R^2) and (testing for homogeneity of group dispersions; F) in addition to their significance (p). Analyses were run on their habitat types (FL, BM, BE, SE, SF) or their nature (flare, bacterial mats or siboglinid worms). A significant PERMOVA result support the hypothesis that the microbial community composition between the different groups differ and the R^2 illustrate the effect size. A significant betadisper result support that the variance within each habitat or nature types is significant.

	Habitat				Nature			
Library	R^2	*p*	F	*p*	R^2	*p*	F	*p*
Archaea	**0.45063**	0.001	**4.6787**	0.019	**0.24286**	0.004	**5.2308**	0.041
Bacteria	**0.53698**	0.001	2.1235	0.181	**0.28437**	0.004	**12.905**	0.001
pmoA	0.40047	0.108	2.0618	0.18	0.16959	0.435	**4.59089**	0.048

PERMANOVA analyses were used to test the hypothesis that the OTUs composition between the five habitats differ. Beforehand, the assumption of homogeneity of variance within groups was tested using betadisper, which a significant result would reject the null hypothesis of no different in dispersion between habitats. While the betadisper test was non-significant for the Bacteria, it was significant for Archaea (Table 1). Results from PERMANOVA analyses revealed that the OTUs composition between the five habitats significantly differed, at an effect size of 45.06% and 53.70% for the Archaea and Bacteria, respectively. Dissimilarities between the different habitats were visualised using PCA (Figure 4A) where 34.5% and 43.6% of the variance are explained by the first two axis for Archaea and Bacteria, respectively. LDA analyses, revealing significant key microbial markers of the different habitats, were subsequently performed exclusively on samples taken from FL, BM and SF (Figure 4B). Within the Archaea, Methanosarcina was a taxonomic marker for the flair habitat (F), while the Woesearchaeales were composed of OTUs particularly abundant at bacterial mat habitat (BM). Within the Bacteria, campylobacterial groups were markers the communities at FL, while the proteobacteria Desulfosarcinaceae and Halieaceae were more predominant at SF habitat and Bacterioidia at BM habitat.

Microbial biodiversity between habitats

Within the Archaea, betadiversity analyses demonstrated that communities at BM, BE and SE showed higher similarity than with communities at SF or FL (Figure 5). At the flare, the methanotrophic Methanosarcina, particularly an OTU assigned to the ANME-1, composed a large fraction of all sequences retrieved in a sample, reaching between 17% in core $PC12_{FL}$ to 48% in core $PC14b_{FL}$. Woesearchales was a second important taxonomic group at FL, identified by avg 43% of the sequences. Within the SF, the Woesearchales was the predominant taxonomic group, composing between 49% of the sequences in $PC07_{SF}$ and 70% in $PC08_{SF}$. The communities were also characterized by a higher proportion of Nitrosophaeira (avg of 22%), primarily assigned to the genus *Nitrosopumilus*, Asgardarchaeota (avg of 7%) and Bathyarchaeia (avg of 3%). The higher abundance of Nitrososphaeria at SF is primarily dominated by the emergence of OTU a2, reaching 22% in SF in contrast to 10% in BM, while the second abundant OTU a9, assigned to Nitrososhaeria, remained at similar relative abundance (Supplementary Figure 5A). Two cores, $PC07_{SF}$ and $PC11_{SF}$, also showed 8 to 5% of the sequences assigned to ANME-1, respectively. Sediment archaeal communities retrieved at BM, BE and SE demonstrated together a similar composition, largely dominated by Woeasarchales (avg of 79%). FL and SF habitats hosted a large diversity of low abundant OTUs assigned to Woesearchales, while in contrast, abundant Woesearchales OTUs at BM, BME and SF represented a large fraction of the sequences. Within the BM, BE and SE habitats, 4 OTUs composed 14 to 36% of all sequences, while they represented 4% to 10% of the sequences in the FL and SFE habitats (Supplementary Figure 5B).

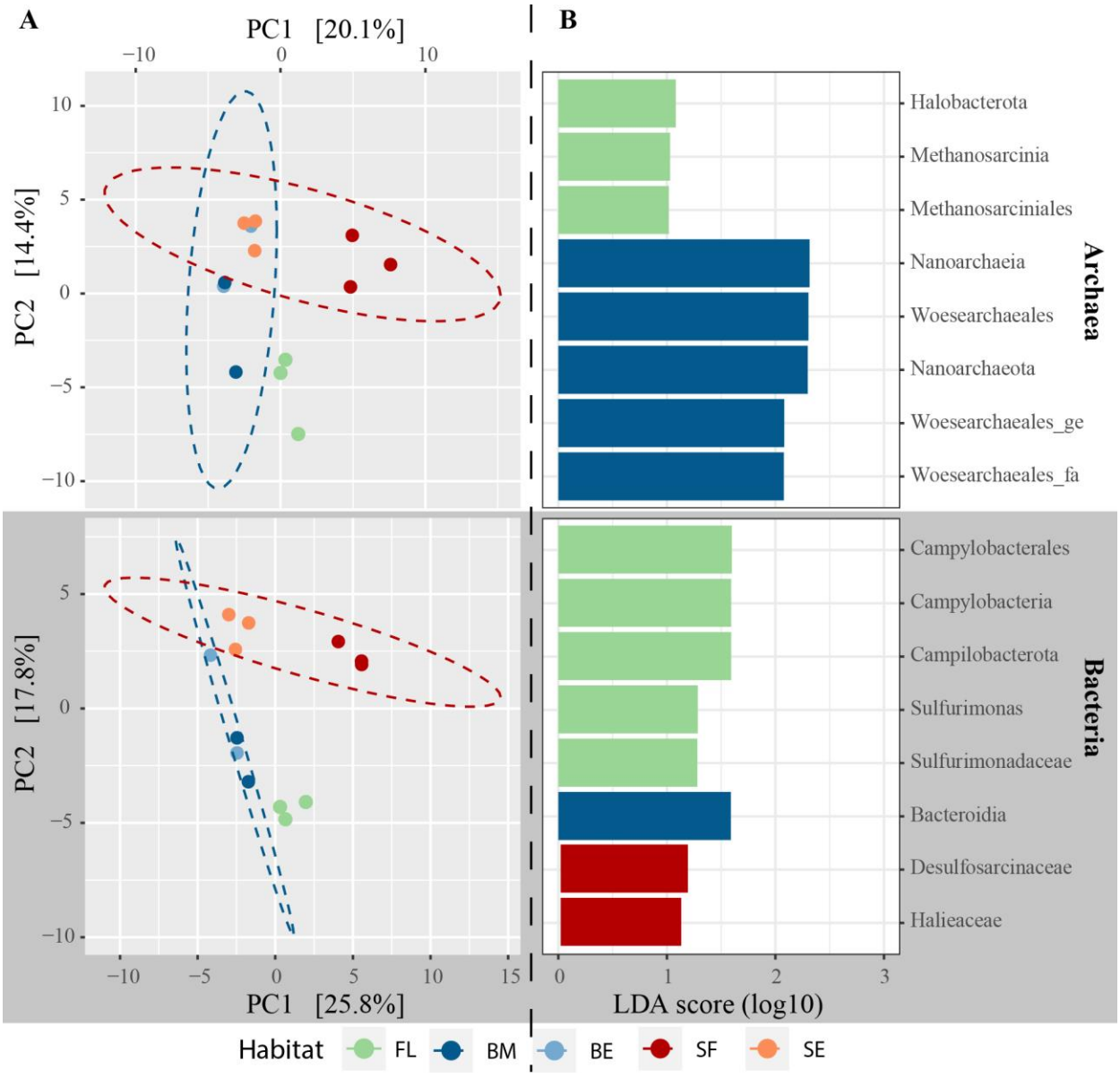

Figure 4: (A) Principal component analyses calculated based on the centered log ratio (CLR) transformed OTUs composition of the different sediment cores to illustrate the similarities between the different habitat types. PC1 and PC2 explains 34.5% and 43.5% of the variance within the archaeal and bacterial communities, respectively. Ellipses were built around communities taken either from bacterial mats (BM & BE) or from siboglinid fields (SF and SE). (B) Significant microbial markers of the different communities retrieved either at the flare (F), within the BM or the SF, identified using linear discriminant analyses based on the CLR transformed OTUs composition.

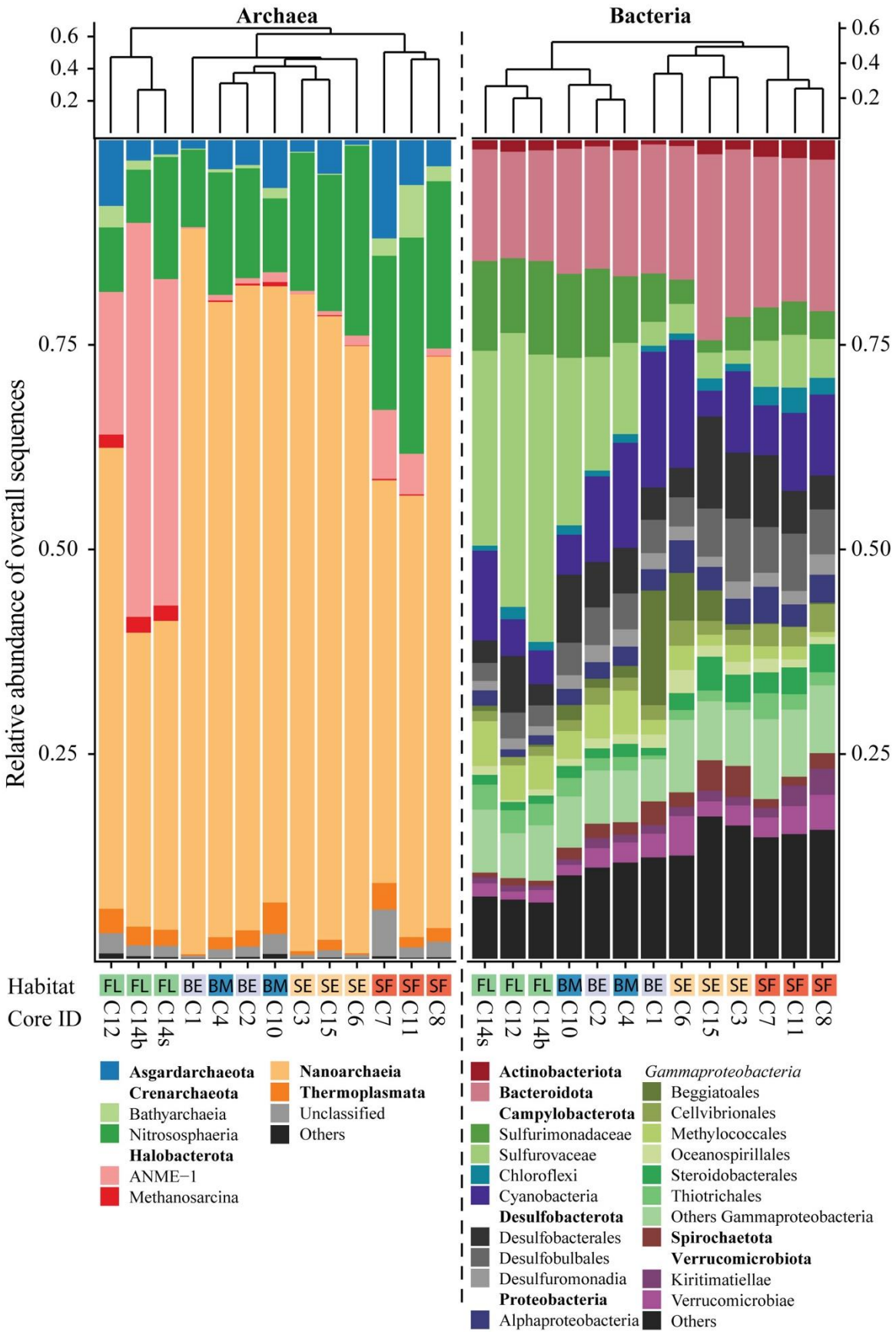
Archaea
Bacteria
0.6
0.4
0.2
0.75
0.50
0.25
Relative abundance of overall sequences
Habitat
Core ID
FL FL FL BE BM BE BM SE SE SE SF SF SF
C12 C14b C14s C1 C4 C2 C10 C3 C15 C6 C7 C11 C8
FL FL FL BM BE BM BE SE SE SE SF SF SF
C14s C12 C14b C10 C2 C4 C1 C6 C15 C3 C7 C11 C8
Asgardarchaeota
Crenarchaeota
Bathyarchaeia
Nitrososphaeria
Halobacterota
ANME−1
Methanosarcina
Nanoarchaeia
Thermoplasmata
Unclassified
Others
Actinobacteriota
Bacteroidota
Campylobacterota
Sulfurimonadaceae
Sulfurovaceae
Chloroflexi
Cyanobacteria
Desulfobacterota
Desulfobacterales
Desulfobulbales
Desulfuromonadia
Proteobacteria
Alphaproteobacteria
Gammaproteobacteria
Beggiatoales
Cellvibrionales
Methylococcales
Oceanospirillales
Steroidobacterales
Thiotrichales
Others Gammaproteobacteria
Spirochaetota
Verrucomicrobiota
Kiritimatiellae
Verrucomicrobiae
Others

Figure 5: Relative abundance of the most abundant taxonomic groups belonging to Archaea or Bacteria. The sediment communities were clustered using calculation based on the Bray-Curtis dissimilatory index from the composition of archaeal (left chart) and bacterial (right chart) OTUs. Communities from the same habitat type, i.e. from sediments taken either near a gas flare (FL), within (BM) or at the edge of a bacterial mat (BM & BE) or from within or at the edge of a siboglinid field (SF & SE).

Within the Bacteria, beta diversity analyses demonstrated that communities differed mainly along two clusters, one grouping libraries representing FL, BM and BE, while libraries from SF and SE were in a separate cluster (Figure 5). The first cluster were dominated by Campylobacterota Sulfurimonadaceae and Sulfurovaceae. While the relative abundance of sequences assigned to Sulfurimonadaceae varied little across the different habitat, at an average of 6% ± 3%, the proportion of Sulfurovaceae increased in surface communities of FL and BM, reaching a maximum of 35% and 20%, respectively. Another taxonomic group more abundant in this cluster included Methylococcales. Higher relative abundances of sequences assigned to Methylococcales were found in communities at FL (avg of 5%) and BM (avg of 4%) habitats, while lowest was found in SF (avg. of 1%).

Among communities within SF and SE, a larger fraction of the sequences was assigned to diverse predominant taxonomic groups composing a larger proportion of the communities than in FL, BM and BE. These groups included the gammaproteobacteria Beggiatoales, Cellvibrionales and Steroidobacterales, in addition to Chloroflexi, Spirochaetota and Verrucomicrobiota. Desulfubacterota was another dominating taxonomic group within habitats SF and SE, primarily composed of Desulfobacterales and Desulfobulbales. Representatives from clades of sulphate-reducing bacteria (SRB) groups found at cold seeps were nearly absent. Throughout all habitats, Bacteroidota remained a predominant taxonomic group throughout all habitats.

Diversity and distributions of aerobic methanotrophs

Among the bacterial libraries, the relative abundance of aerobic methanotrophs was primarily assigned to the gammaproteobacteria Methylococcales (Figure 5). Within the Methylococcales, four OTUs predominated (Supplementary Figure 6A). Phylogeny of Methylococcales showed that OTUs b23 and b50 clustered closely together with a cultivated representative of *Methyloprofundus sedimenti* (Figure 7). Both OTUs shared approximately 98% sequence similarity with a strain of *Methyloprofundus* sp. (sequence KF484906.1). Their relative abundances of sequences assigned to this strain were particularly higher below FL, with an average of 3.4% of all sequences. OTU b14 clustered in a separate subclade and number of sequences assigned to OTU b14 were higher

below BM, BE and SE, reaching up to 1.6% in those habitats (Figure 7; Supplementary Figure 5A). The OTU b14 shared 97% sequence similarity with uncultured sequences retrieved from sediments of Haakon Mosby Mud Volcano (sequence KX581184.1) and from the intestine extract of a crab (sequence AB981863). However, it shared only 94% sequence similarity with the above-mentioned strain of *Methyloprofundus* sp. Finally, OTU b66 had higher relative abundances in FL and BM, but the variability among the different habitats was smaller.

Within the *pmoA* libraries, sequences were primarily associated to the groups Deep-Sea Cluster (DSC) 1 and *Methylomonas* sp., especially in communities at the FL, BM and BE habitats. Communities retrieved from SF and SE included a higher proportion of other groups such as DSC 3, PS-80 and unclassified Methylococacceae. Most of the sequences within the *pmoA* libraries were assigned to three OTUs (Figure 7; Supplementary Figure 5B).

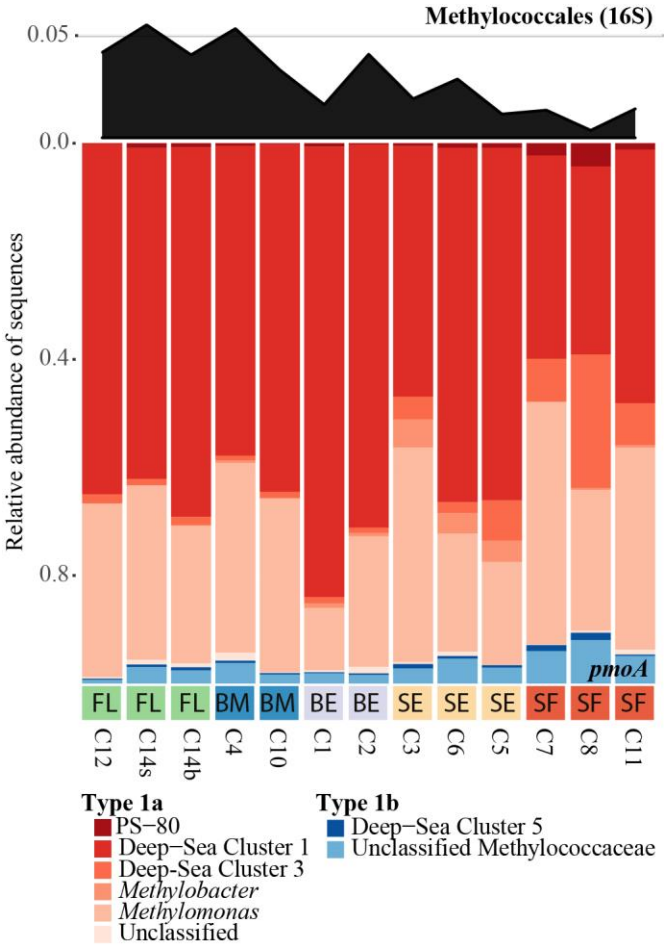

Figure 6: Relative abundance of the taxonomic groups that contain sequences associated to bacterial methanotrophs based on the 16S (upper chart) and pmoA libraries (lower chart).

Two OTUs (p1 and p1002) belonged to the group of uncultivated sequences DSC 1, in two separate subclades. OTU p1002 shared 97% sequence similarity with an uncultivated bacterium retrieved from a cold seep (sequence: KC751387.1), and 92% to a strain of *Methyloprofundus* sp. (sequence: AP023240.1). OTU p1 shared only 90% sequence similarity with an uncultivated bacterium detected at the Haakon Mosby Mud Volcano (sequence: KX581208.1). OTU p1 was more predominant in the BM, BE and SE habitats, with on average 44% of the sequences in a sample assigned to this OTU compared to 5% in the other. In contrast, an average of 48% of the sequences from *pmoA* libraries from habitats FL and SF were assigned to OTU p1002, compared to 20% in the other habitats. The third abundant *pmoA* OTU (OTU p100), showed less variation across the different habitats (avg of 29 ± 8%). Correlation analyses demonstrated significant positive correlation between abundant OTUs from 16S and *pmoA* libraries. The OTU b14 correlated with

OTU p1, while OTUs b23 and b50 correlated with OTU p1002. OTU b66 and OTU p100 showed positive correlation, but was non-significant (Figure 7).

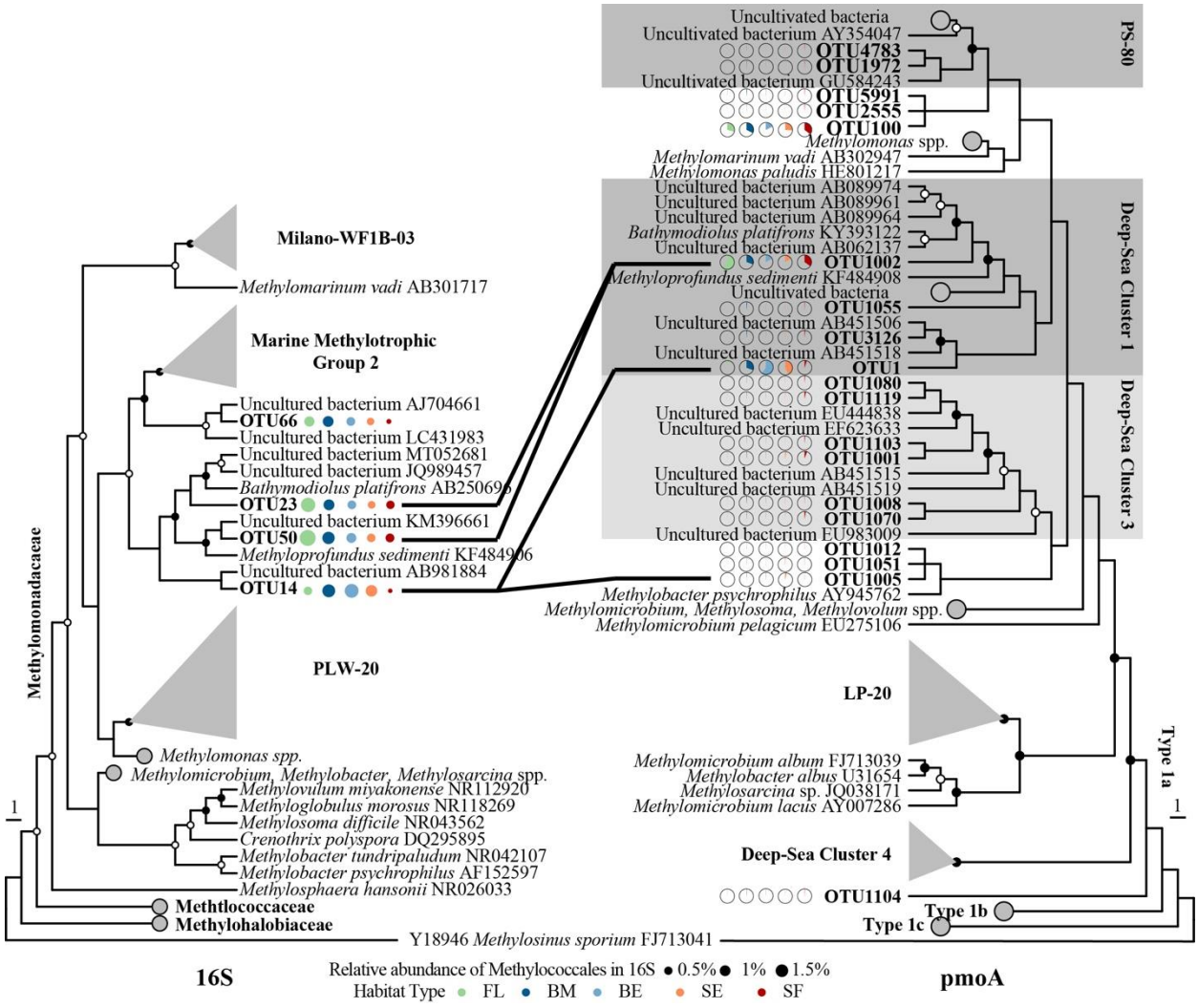

Figure 7: Phylogenetic trees showing evolutionary connections of the dominant OTUs (relative abundance >1%) representing 16S rRNA gene sequences (left) and pmoA rRNA gene sequences (right) to selected reference sequences from the environment and isolated strains. Boldface type indicates the short sequences obtained in this study. The trees were calculated by using the RAxML algorithm and *Methylosimus sporium* was used as an outgroup for both trees. The approx. 464 bp long 16S OTUs were placed on a reference tree containing sequences of a minimum length of 1320 bp. The approx. 467 bp long pmoA OTUs were aligned on a reference tree contain sequences of similar lengths. White and bacterial internal nodes indicate bootstraps values of >50 and >80, respectively. Lines connecting OTUs between the trees illustrate significant positive spearman correlation values. The averaged relative abundance of each 16S OTUs at the different habitats is presented by the colored point size while the averaged relative abundance of each pmoA OTUs is presented as relative pie charts.

Discussion

In this study, we revealed that arctic CH_4 seepages are locally transforming the seabed through the formation of a chemical gradient that promote the development of a specific microbial and macrofaunal community.

It was demonstrated previously that gas hydrates pingos are not structured as mud volcano and does not show a concentric chemical gradient (Carrier et al., 2020). This typical arctic structure, formed after the last deglaciation (Serov et al., 2017) are full of authigenic carbonate (Yao et al., 2021). In addition of mirroring past and actual microbial AOM, carbonates can funnel the reduce fluid formed around the gas hydrate to promote the formation of a patchy environment (Crémière et al., 2016). At the Storfjordrenna GHPs, the surface microbial community was structured according to the amount of geofluids that percolate through the sediments and by the subsequent anaerobic oxidation of this gas by ANME groups which is forming HS^-.

Aerobic methanotrophs takes advantage of the sediment surface methane gradient formed by the local bypass of the anaerobic methane filter

At cold seeps, CH_4 is consumed deep in the sediment by AOM and the remaining CH_4 escapes the biological filter through advective flux of gaseous CH_4 toward the sediment surface (Orphan et al., 2001). Because of this local increase of CH_4 potentially induced by the presence of carbonate, the relative abundance of Methylococcales retrieved in the 16S rRNA gene libraries was 3-4 fold higher at FL and BM compared to SF. Both 16S and *pmoA* based libraries were dominated by only 3 and 4 abundant OTUs, respectively, and highlighted different MOB community structure between these different habitats (Figure 7). Within the *pmoA* libraries, which give a functional overview of the diversity, sequences were assigned primarily to three OTUs: two were placed within the Deep-Sea Cluster 1 (DSC 1), and one was closely related to *Methylomonas* spp. Compared to *Methylomonas* spp, which is detected at similar proportions in all samples, the DSC 1 OTUs were mostly detected at gas flares and in bacterial mats surface sediments. Deep-Sea Cluster 1 enclose uncultivated sequences of the *pmoA* gene that have almost exclusively been retrieved from marine habitats (Lüke and Frenzel, 2011; Knief, 2015). However, further assigning environmental preferences to each groups have remained unresolved yet.

Assigning habitat preferences is complex as representatives both from DSC 1 have been detected at equal frequency in the sediments and water column (Knief, 2015), highlighting the wide range of habitat that these microorganisms can colonise. This suggests that niche differentiation among marine uncultured MOB could not be resolved by the current classification of Deep-Sea Clusters. The heterogeneity of ecotypes within these groups is further strengthened in our results by the alternated dominance of OTUs phylogenetically affiliated to DSC 1.

Within the DSC 1, significant positive correlations were found between the *pmoA* OTU p1002 and 16S OTUs b23/b50, and between *pmoA* OTU p1 and 16S OTU b14 (Figure 7). These combinations suggests the existence of two distinct aerobic methanotrophs. Here, we will refer to the former combination as MOB1 and the latter MOB2. MOB1 shared high sequence similarity with several uncultured sequences (100 sequences with above 96% similarity). In contrast, MOB2 had sequence similarity with less sequences (13 sequences with above 86% similarity), the highest being with uncultured bacterial sequences from Haakon Mosby Mud Volcano (97.41% similarity, sequence: KX581194.1).

Changes in O_2, CH_4 and HS^- concentrations are known to impact the structure of the methanotrophic community (Hernandez et al., 2015; Mayr et al., 2020; Delgado Vela et al., 2021). In our case, MOB1 that is predominant near the flare is detected in habitats characterised by a high concentration of CH_4 and HS^- and suboxic conditions. MOB2 dominates the MOB DSC 1 community at the edges of the bacterial mats siboglinid fields, where CH_4 and HS^- were depleted and O_2 available.

Therefore, the concentrations of CH_4 that is much higher at gas flares and within sediments below bacterial mats, in comparison to the other habitats is a good parameter to explain the MOB1/MOB2 repartition. One hypothesis could be that MOB1, which is globally found in marine settings, colonized high CH_4-rich sediments in the Barents Sea, whereas MOB2 thrive in CH_4 depleted sediments at cold seeps. However, other factors unconsidered in this study that were previously shown to select particular groups of Methylococcaceae, such as availability of ammonium/nitrite (Nyerges et al., 2010) or pH (Danilova et al., 2013), could be driving the niche differentiation between MOB1 and MOB2.

Anaerobic methane oxidation forms hydrogen sulphide that promote anoxic conditions in surface sediment.

Methane consumed by AOM described previously at the GHPs (Carrier et al., 2020) promote the release of HS^-, which was detected in our sampling grid. This dissolved gas supports the development of bacterial mats made by microorganisms using HS^- oxidation as energy source. Sulphide oxidizers is a major functional group in cold seeps ecosystems, being, in addition to methanotrophs, an alternative source of primary production of biomass for higher trophic levels (Taylor et al., 2001; Lichtschlag et al., 2010; Niemann et al., 2013). These chemoautotrophs can either be observed as chemosynthetic ecto- and endosymbionts for some meiofauna (Nakagawa and Takai, 2008) and microfauna (Dubilier et al., 2008), or as free-living microbes able to form bacterial mats.

In the gas flare, sulphide-oxidizing bacteria (SOB) were primarily represented by the Campylobacterota, previously known as Epsilonproteobacteria, where representatives mostly belonged to the Sulfurovaceae (up to 35% of all sequences in a sample) but also to the sulfurimonadaceae. These families also remained predominant in cores taken within bacterial mats, but their relative abundance, particularly for sulfurovaceae, was reduced within the siboglinid fields. In contrast, the Beggiatoales are nearly absent at the gas flares and represent a small fraction (less than 2%) of the sequences in the bacterial mats whereas, their relative abundance increases at the edges of the bacterial mats and of the siboglinids field, concomitant with the deepening of the HS^- maximum (from approximately 15 to 20 cmbsf). These observations are in line with the ecology of these organisms. Campylobacterota are known to dominate environments where HS^- and electron acceptors are both present (Madrid et al., 2001; Macalady et al., 2008; Grünke et al., 2011). In contrast, the beggiatoales dominates sediments where HS^- and O_2 do not overlap (McHatton et al., 1996; Preisler et al., 2007).

The SOB community composition could also result from a temporal succession, where mats of *Sulfurovum* spp. would be early colonizers and Beggiatoales would establish in more mature mats (Patwardhan et al., 2018). In the early stages, *Sulfurovum* spp., able to tolerate high concentrations of HS^-, would detoxify the sediments from HS^- leading to the colonization of more HS^- sensible SOB such as Beggiatoales. However as shown by our O_2 profile the use of O_2 as electron acceptor by SOB is creating anoxic conditions at the sediment surface. This has a direct effect on the

settlement of the fixed macrofauna larvae that cannot settle in such anoxic environment because larvae needs O_2 to develop as observed on hydrothermal vent (Marsh et al., 2001). Consequently, the siboglinids are kept at the edge of the seeping point therefore explains the gradient observed in our study.

Siboglinids fields has the potential to be an oasis of life fuelled by chemoautotrophic energy that can host organisms not adapted to cold seeps conditions.

Siboglinids are frenulates known to host SOB as endosymbionts and recent investigations at cold seeps in northern Barents Sea confirmed the presence of primarily Gammaproteobacteria SOB in *Oligobrachia* sp. (Sen et al., 2018). The absence of SOB in sigoblinid fields is explained by the location of sulphide-oxidizing endosymbionts that are located within the trophosome below the sediment surface. The symbiosis between siboglinid worms and SOB endosymbionts allows the supply of O_2 from the seawater and HS^- from deep sediment layers. Therefore, O_2 is present at the sediment surface and are not consumed by CH_4 or sulfur oxidisers that would lack they reductant. The LDA analyses demonstrated that microbes involved in organic compounds degradation are influenced by the habitats (Fig 4). Within the siboglinid fields, the Chloroflexi, Desulfobacterota and Verrucomicrobiota showed higher relative abundances. These bacterial groups are commonly found in marine sediments (Miyatake et al., 2009; Leri et al., 2010; Hedlund, 2015; Dyksma et al., 2018). Interestingly, none of the Desulfobacterota, were assigned to known seeps related sulfate reducing bacteria, such as the clades SEEP-SRB1 to 4 (Knittel et al., 2003). The structure of the prokaryotic communities at siboglinid fields was diverse and similar to the community structure of the reference site in Carrier et al. (2020). We hypothesised that the siboglinids mucus and faeces could be enriching the sediment in labile carbon and therefore promote the development of organic matter degradation associated microbes.

Conclusion

Our study demonstrated that the composition of the prokaryotic community varied between different habitats over few meters square areas. Key ecological functions at cold seeps, such CH_4 and HS^- oxidation in addition to organic compounds degradation, were likely performed by various taxa, although more exhaustive genomic and cultivation studies would be required to confirm their role. We particularly identified three potential active MOBs, two of them thriving in contrasting niches. One of the MOBs showed little similarity to other available MOB sequences, highlighting

one of the uniqueness of this ecosystem. The focus on aerobic methanotrophs in our study presents its novelty in extending our knowledge on CH_4 fate at the sediments-water interface in the Arctic Ocean. Furthermore, sediment cores taken from different habitats also demonstrated a strong variability in SOBs. These presented changing biodiversity between the different habitats, features covering large proportions of the seafloor around Arctic cold seeps. In parallel of performing complementary genomic and cultivation studies to reveal the local microbial metabolisms and activity, investigations at additional Arctic cold seeps will also be needed to assess the representability of the GHPs.

Conflict of Interest

The authors declare that the research was conducted in the absence of any commercial or financial relationships that could be construed as a potential conflict of interest.

Author Contributions

VC, MS, HN, FG and DK initially designed the project and VC, MS and DK contributed to the sampling. Laboratory manipulations, sequence analyses and statistics were performed by VC and DK with advices from MS, FG and HN. The manuscript was written by VC with the inputs from FG, HN, MS and DK.

Funding

The study was funded by the Research Council of Norway through the Centre of Excellence for Arctic Gas Hydrate, Environment and Climate (grant number: 223259).

Acknowledgements

The authors are grateful for the help from the crew of *FF Kronprins Haakon* and would like to acknowledge the contribution of the chief scientist Dr. Stefan Buenz during the CAGE 18-5 campaign. The authors would also like to acknowledge the technical assistance of Pavel Serov in the analyses of the physico-chemical parameters. Finally, the authors would like to recognize members of the Centre for Arctic Gas Hydrate and Environment (The Arctic University of Norway, Tromsø) for their expertise.

Data availability Statement

The amplicon libraries datasets for this study will be found at the Sequence Read Archive Genebank[3] as BioProject once the publication will be ready to be submitted. Environmental parameters are available in the supplementary material.

Bibliography

Aitchison, J. (1982). The Statistical Analysis of Compositional Data.

Anderson, M. J. (2017). "Permutational Multivariate Analysis of Variance (PERMANOVA)," in *Wiley StatsRef: Statistics Reference Online* (Chichester, UK: John Wiley & Sons, Ltd), 1–15. doi:10.1002/9781118445112.stat07841.

Beal, E. J., House, C. H., and Orphan, V. J. (2009). Manganese- and iron-dependent marine methane oxidation. *Science* 325, 184–7. doi:10.1126/science.1169984.

Boetius, A., Ravenschlag, K., Schubert, C. J., Rickert, D., Widdel, F., Gieseke, A., et al. (2000). A marine microbial consortium apparently mediating anaerobic oxidation of methane. *Nature* 407, 623–626. doi:10.1038/35036572.

Boetius, A., and Wenzhöfer, F. (2013). Seafloor oxygen consumption fuelled by methane from cold seeps. *Nat. Geosci.* 6, 725–734. doi:10.1038/ngeo1926.

Cao, Y. (2020). microbiomeMarker: microbiome biomarker analysis. Available at: https://github.com/yiluheihei/microbiomeMarker.

Carrier, V., Svenning, M. M., Gründger, F., Niemann, H., Dessandier, P. A., Panieri, G., et al. (2020). The Impact of Methane on Microbial Communities at Marine Arctic Gas Hydrate Bearing Sediment. *Front. Microbiol.* 11, 1932. doi:10.3389/fmicb.2020.01932.

Crémière, A., Lepland, A., Chand, S., Sahy, D., Kirsimäe, K., Bau, M., et al. (2016). Fluid source and methane-related diagenetic processes recorded in cold seep carbonates from the Alvheim channel, central North Sea. *Chem. Geol.* 432, 16–33. doi:10.1016/J.CHEMGEO.2016.03.019.

Danilova, O. V., Kulichevskaya, I. S., Rozova, O. N., Detkova, E. N., Bodelier, P. L. E., Trotsenko, Y. A., et al. (2013). Methylomonas paludis sp. nov., the first acidtolerant member of the genus Methylomonas, from an acidic wetland. *Int. J. Syst. Evol. Microbiol.* 63, 2282–2289. doi:10.1099/ijs.0.045658-0.

de Beer, D., Sauter, E., Niemann, H., Kaul, N., Foucher, J.-P., Witte, U., et al. (2006). In situ fluxes and zonation of microbial activity in surface sediments of the Håkon Mosby Mud Volcano. *Limnol. Oceanogr.* 51, 1315–1331. doi:10.4319/lo.2006.51.3.1315.

Delgado Vela, J., Bristow, L. A., Marchant, H. K., Love, N. G., and Dick, G. J. (2021). Sulfide alters microbial functional potential in a methane and nitrogen cycling biofilm reactor. *Environ. Microbiol.* 23, 1481–1495. doi:10.1111/1462-2920.15352.

Dubilier, N., Bergin, C., and Lott, C. (2008). Symbiotic diversity in marine animals: the art of

[3] http://www.ncbi.nlm.nih.gov/sra

harnessing chemosynthesis. *Nat. Rev. Microbiol. 2008 610* 6, 725–740. doi:10.1038/nrmicro1992.

Dunfield, P. F., Yuryev, A., Senin, P., Smirnova, A. V., Stott, M. B., Hou, S., et al. (2007). Methane oxidation by an extremely acidophilic bacterium of the phylum Verrucomicrobia. *Nat. 2007 4507171* 450, 879–882. doi:10.1038/nature06411.

Dyksma, S., Lenk, S., Sawicka, J. E., and Mußmann, M. (2018). Uncultured Gammaproteobacteria and Desulfobacteraceae Account for Major Acetate Assimilation in a Coastal Marine Sediment. *Front. Microbiol.* 9, 3124. doi:10.3389/fmicb.2018.03124.

Edgar, R. C. (2004). MUSCLE: Multiple sequence alignment with high accuracy and high throughput. *Nucleic Acids Res.* 32, 1792–1797. doi:10.1093/nar/gkh340.

Edgar, R. C. (2010). Search and clustering orders of magnitude faster than BLAST. *Bioinformatics* 26, 2460–2461. doi:10.1093/bioinformatics/btq461.

Etheridge, D. M., Steele, L. P., Francey, R. J., and Langenfelds, R. L. (1998). Atmospheric methane between 1000 A.D. and present: Evidence of anthropogenic emissions and climatic variability. *J. Geophys. Res. Atmos.* 103, 15979–15993. doi:10.1029/98JD00923.

Etminan, M., Myhre, G., Highwood, E. J., and Shine, K. P. (2016). Radiative forcing of carbon dioxide, methane, and nitrous oxide: A significant revision of the methane radiative forcing. *Geophys. Res. Lett.* 43, 12,614-12,623. doi:10.1002/2016GL071930.

Ettwig, K. F., Zhu, B., Speth, D., Keltjens, J. T., Jetten, M. S. M., and Kartal, B. (2016). Archaea catalyze iron-dependent anaerobic oxidation of methane. *Proc. Natl. Acad. Sci.* 113, 12792–12796. doi:10.1073/PNAS.1609534113.

Finley, A., Banerjee, S., and Hjelle, Ø. (2017). MBA: Multilevel B-Spline Approximation. Available at: https://cran.r-project.org/package=MBA.

Griffiths, R. I., Whiteley, A. S., O'Donnell, A. G., and Bailey, M. J. (2000). Rapid method for coextraction of DNA and RNA from natural environments for analysis of ribosomal DNA- and rRNA-based microbial community composition. *Appl. Environ. Microbiol.* 66, 5488–5491. doi:10.1128/AEM.66.12.5488-5491.2000.

Gründger, F., Carrier, V., Svenning, M. M., Panieri, G., Vonnahme, T. R., Klasek, S., et al. (2019). Methane-fuelled biofilms predominantly composed of methanotrophic ANME-1 in Arctic gas hydrate-related sediments. *Sci. Rep.* 9, 9725. doi:10.1038/s41598-019-46209-5.

Grünke, S., Felden, J., Lichtschlag, A., Girnth, A. C., De Beer, D., Wenzhöfer, F., et al. (2011). Niche differentiation among mat-forming, sulfide-oxidizing bacteria at cold seeps of the Nile Deep Sea Fan (Eastern Mediterranean Sea). *Geobiology* 9, 330–348. doi:10.1111/j.1472-4669.2011.00281.x.

Hanson, R. S., and Hanson, T. E. (1996). Methanotrophic Bacteria. *Microbiol. Rev.* 60, 439–471. Available at: http://mmbr.asm.org/ [Accessed February 14, 2020].

Hedlund, B. P. (2015). " Verrucomicrobiae ," in *Bergey's Manual of Systematics of Archaea and Bacteria* (Wiley), 1–5. doi:10.1002/9781118960608.cbm00054.

Hernandez, M. E., Beck, D. A. C., Lidstrom, M. E., and Chistoserdova, L. (2015). Oxygen availability is a major factor in determining the composition of microbial communities involved in methane oxidation. *PeerJ* 2015, e801. doi:10.7717/peerj.801.

Kassambara, A. (2020). rstatix: Pipe-Friendly Framework for Basic Statistical Tests. Available at: https://cran.r-project.org/package=rstatix.

Knief, C. (2015). Diversity and habitat preferences of cultivated and uncultivated aerobic methanotrophic bacteria evaluated based on pmoA as molecular marker. *Front. Microbiol.* 6. doi:10.3389/fmicb.2015.01346.

Knittel, K., Boetius, A., Lemke, A., Eilers, H., Lochte, K., Pfannkuche, O., et al. (2003). Activity, distribution, and diversity of sulfate reducers and other bacteria in sediments above gas hydrate (Cascadia margin, Oregon). *Geomicrobiol. J.* 20, 269–294. doi:10.1080/01490450303896.

Kumar, S., Stecher, G., and Tamura, K. (2016). MEGA7: Molecular Evolutionary Genetics Analysis Version 7.0 for Bigger Datasets. *Mol. Biol. Evol.* 33, 1870–1874. doi:10.1093/MOLBEV/MSW054.

Leri, A. C., Hakala, J. A., Marcus, M. A., Lanzirotti, A., Reddy, C. M., and Myneni, S. C. B. (2010). Natural organobromine in marine sediments: New evidence of biogeochemical Br cycling. *Global Biogeochem. Cycles* 24, 4017. doi:10.1029/2010GB003794.

Lichtschlag, A., Felden, J., Brüchert, V., Boetius, A., and de Beer, D. (2010). Geochemical processes and chemosynthetic primary production in different thiotrophic mats of the Håkon Mosby Mud Volcano (Barents Sea). *Limnol. Oceanogr.* 55, 931–949. doi:10.4319/lo.2010.55.2.0931.

Lüke, C., and Frenzel, P. (2011). Potential of pmoA amplicon pyrosequencing for methanotroph diversity studies. *Appl. Environ. Microbiol.* 77, 6305–9. doi:10.1128/AEM.05355-11.

Macalady, J. L., Dattagupta, S., Schaperdoth, I., Jones, D. S., Druschel, G. K., and Eastman, D. (2008). Niche differentiation among sulfur-oxidizing bacterial populations in cave waters. *ISME J. 2008 26* 2, 590–601. doi:10.1038/ismej.2008.25.

Madrid, V. M., Taylor, G. T., Scranton, M. I., and Chistoserdov, A. Y. (2001). Phylogenetic Diversity of Bacterial and Archaeal Communities in the Anoxic Zone of the Cariaco Basin. *Appl. Environ. Microbiol.* 67, 1663–1674. doi:10.1128/AEM.67.4.1663-1674.2001.

Marsh, A. G., Mullineaux, L. S., Young, C. M., and Manahan, D. T. (2001). Larval dispersal potential of the tubeworm Riftia pachyptila at deep-sea hydrothermal vents. *Nat. 2001 4116833* 411, 77–80. doi:10.1038/35075063.

Mayr, M. J., Zimmermann, M., Guggenheim, C., Brand, A., and Bürgmann, H. (2020). Niche partitioning of methane-oxidizing bacteria along the oxygen–methane counter gradient of stratified lakes. *ISME J.* 14, 274–287. doi:10.1038/s41396-019-0515-8.

McHatton, S. C., Barry, J. P., Jannasch, H. W., and Nelson, D. C. (1996). High Nitrate Concentrations in Vacuolate, Autotrophic Marine Beggiatoa spp. *Appl. Environ. Microbiol.* 62.

McMurdie, P. J., and Holmes, S. (2013). phyloseq: An R Package for Reproducible Interactive Analysis and Graphics of Microbiome Census Data. *PLoS One* 8, e61217. doi:10.1371/journal.pone.0061217.

Miyatake, T., MacGregor, B. J., and Boschker, H. T. S. (2009). Linking microbial community function to phylogeny of sulfate-reducing Deltaproteobacteria in marine sediments by combining stable isotope probing with magnetic-bead capture hybridization of 16S rRNA. *Appl. Environ. Microbiol.* 75, 4927–4935. doi:10.1128/AEM.00652-09.

Myhre, C. L., Ferré, B., Platt, S. M., Silyakova, A., Hermansen, O., Allen, G., et al. (2016). Extensive release of methane from Arctic seabed west of Svalbard during summer 2014 does not influence the atmosphere. *Geophys. Res. Lett.* 43, 4624–4631. doi:10.1002/2016GL068999.

Nakagawa, S., and Takai, K. (2008). Deep-sea vent chemoautotrophs: Diversity, biochemistry and ecological significance. *FEMS Microbiol. Ecol.* 65, 1–14. doi:10.1111/j.1574-6941.2008.00502.x.

Nauhaus, K., Boetius, A., Kruger, M., and Widdel, F. (2002). In vitro demonstration of anaerobic oxidation of methane coupled to sulphate reduction in sediment from a marine gas hydrate area. *Environ. Microbiol.* 4, 296–305. doi:10.1046/j.1462-2920.2002.00299.x.

Niemann, H., Linke, P., Knittel, K., Macpherson, E., Boetius, A., Brü Ckmann, W., et al. (2013). Methane-Carbon Flow into the Benthic Food Web at Cold Seeps-A Case Study from the Costa Rica Subduction Zone. *PLoS One* 8. doi:10.1371/journal.pone.0074894.

Nyerges, G., Han, S. K., and Stein, L. Y. (2010). Effects of ammonium and nitrite on growth and competitive fitness of cultivated methanotrophic bacteria. *Appl. Environ. Microbiol.* 76, 5648–5651. doi:10.1128/AEM.00747-10.

Oksanen, J., Blanchet, F. G., Friendly, M., Kindt, R., Legendre, P., Mcglinn, D., et al. (2019). Package "vegan" Title Community Ecology Package. Available at: https://cran.r-project.org/web/packages/vegan/vegan.pdf [Accessed August 31, 2019].

Orphan, V. J., Hinrichs, K. U., Ussler, W., Paull, C. K., Taylor, L. T., Sylva, S. P., et al. (2001). Comparative Analysis of Methane-Oxidizing Archaea and Sulfate-Reducing Bacteria in Anoxic Marine Sediments. *Appl. Environ. Microbiol.* 67, 1922–1934. doi:10.1128/AEM.67.4.1922-1934.2001.

P. Jeroschewski, *,†, C. Steuckart, † and, and Kühl‡, M. (1996). An Amperometric Microsensor for the Determination of H2S in Aquatic Environments. *Anal. Chem.* 68, 4351–4357. doi:10.1021/AC960091B.

Patwardhan, S., Foustoukos, D. I., Giovannelli, D., Yücel, M., and Vetriani, C. (2018). Ecological succession of sulfur-oxidizing epsilon- And gammaproteobacteria during colonization of a shallow-water gas vent. *Front. Microbiol.* 9, 2970. doi:10.3389/fmicb.2018.02970.

Preisler, A., De Beer, D., Lichtschlag, A., Lavik, G., Boetius, A., and Joørgensen, B. B. (2007). Biological and chemical sulfide oxidation in a Beggiatoa inhabited marine sediment. *ISME J.* 1, 341–353. doi:10.1038/ismej.2007.50.

686 Quast, C., Pruesse, E., Yilmaz, P., Gerken, J., Schweer, T., Yarza, P., et al. (2012). The SILVA
687 ribosomal RNA gene database project: improved data processing and web-based tools.
688 *Nucleic Acids Res.* 41, D590–D596. doi:10.1093/nar/gks1219.

689 Reeburgh, W. S. (2007). Oceanic methane biogeochemistry. *Chem. Rev.* 107, 486–513.
690 doi:10.1021/cr050362v.

691 Saunois, M., Bousquet, P., Poulter, B., Peregon, A., Ciais, P., Canadell, J. G., et al. (2016). The
692 global methane budget 2000-2012. *Earth Syst. Sci. Data* 8, 697–751. doi:10.5194/essd-8-
693 697-2016.

694 Segata, N., Izard, J., Waldron, L., Gevers, D., Miropolsky, L., Garrett, W. S., et al. (2011).
695 Metagenomic biomarker discovery and explanation. *Genome Biol.* 12, R60. doi:10.1186/gb-
696 2011-12-6-r60.

697 Sen, A., Duperron, S., Hourdez, S., Piquet, B., Léger, N., Gebruk, A., et al. (2018). Cryptic
698 frenulates are the dominant chemosymbiotrophic fauna at Arctic and high latitude Atlantic
699 cold seeps. *PLoS One* 13, e0209273. doi:10.1371/journal.pone.0209273.

700 Serov, P., Vadakkepuliyambatta, S., Mienert, J., Patton, H., Portnov, A., Silyakova, A., et al.
701 (2017). Postglacial response of Arctic Ocean gas hydrates to climatic amelioration. *Proc.*
702 *Natl. Acad. Sci.* 114, 6215–6220. doi:10.1073/pnas.1619288114.

703 Sommer, S., Pfannkuche, O., Linke, P., Luff, R., Greinert, J., Drews, M., et al. (2006). Efficiency
704 of the benthic filter: Biological control of the emission of dissolved methane from
705 sediments containing shallow gas hydrates at Hydrate Ridge. *Global Biogeochem. Cycles*
706 20, n/a-n/a. doi:10.1029/2004GB002389.

707 Stamatakis, A. (2014). RAxML version 8: a tool for phylogenetic analysis and post-analysis of
708 large phylogenies. *Bioinformatics* 30, 1312–1313. doi:10.1093/bioinformatics/btu033.

709 Tavormina, P. L., Ussier, W., and Orphan, V. J. (2008). Planktonic and sediment-associated
710 aerobic methanotrophs in two seep systems along the North American margin. *Appl.*
711 *Environ. Microbiol.* 74, 3985–3995. doi:10.1128/AEM.00069-08.

712 Taylor, G. T., Iabichella, M., Ho, T. Y., Scranton, M. I., Thunell, R. C., Muller-Karger, F., et al.
713 (2001). Chemoautotrophy in the redox transition zone of the Cariaco Basin: A significant
714 midwater source of organic carbon production. *Limnol. Oceanogr.* 46, 148–163.
715 doi:10.4319/lo.2001.46.1.0148.

716 Turner, A. J., Frankenberg, C., and Kort, E. A. (2019). Interpreting contemporary trends in
717 atmospheric methane. doi:10.1073/pnas.1814297116.

718 Urich, T., Lanzén, A., Qi, J., Huson, D. H., Schleper, C., and Schuster, S. C. (2008).
719 Simultaneous Assessment of Soil Microbial Community Structure and Function through
720 Analysis of the Meta-Transcriptome. *PLoS One* 3, e2527.
721 doi:10.1371/journal.pone.0002527.

722 Wang, L.-G., Lam, T. T.-Y., Xu, S., Dai, Z., Zhou, L., Feng, T., et al. (2020). Treeio: An R
723 Package for Phylogenetic Tree Input and Output with Richly Annotated and Associated
724 Data. *Mol. Biol. Evol.* 37, 599–603. doi:10.1093/molbev/msz240.

Wen, X., Yang, S., and Liebner, S. (2016). Evaluation and update of cutoff values for methanotrophic pmoA gene sequences. *Arch. Microbiol.* 198, 629–636. doi:10.1007/s00203-016-1222-8.

Wickham, H. (2016). *ggplot2: Elegant Graphics for Data Analysis*. Springer-Verlag New York Available at: https://ggplot2.tidyverse.org.

Yang, S., Wen, X., and Liebner, S. (2016). pmoA gene reference database (fasta-formatted sequences and taxonomy). Available at: https://doi.org/10.5880/GFZ.5.3.2016.001.

Yao, H., Panieri, G., Lehmann, M. F., Himmler, T., and Niemann, H. (2021). Biomarker and Isotopic Composition of Seep Carbonates Record Environmental Conditions in Two Arctic Methane Seeps. *Front. Earth Sci.* 0, 755. doi:10.3389/FEART.2020.570742.

Yu, G., Smith, D. K., Zhu, H., Guan, Y., and Lam, T. T. (2017). <scp>ggtree</scp> : an <scp>r</scp> package for visualization and annotation of phylogenetic trees with their covariates and other associated data. *Methods Ecol. Evol.* 8, 28–36. doi:10.1111/2041-210X.12628.

740 **Supplementary Information**

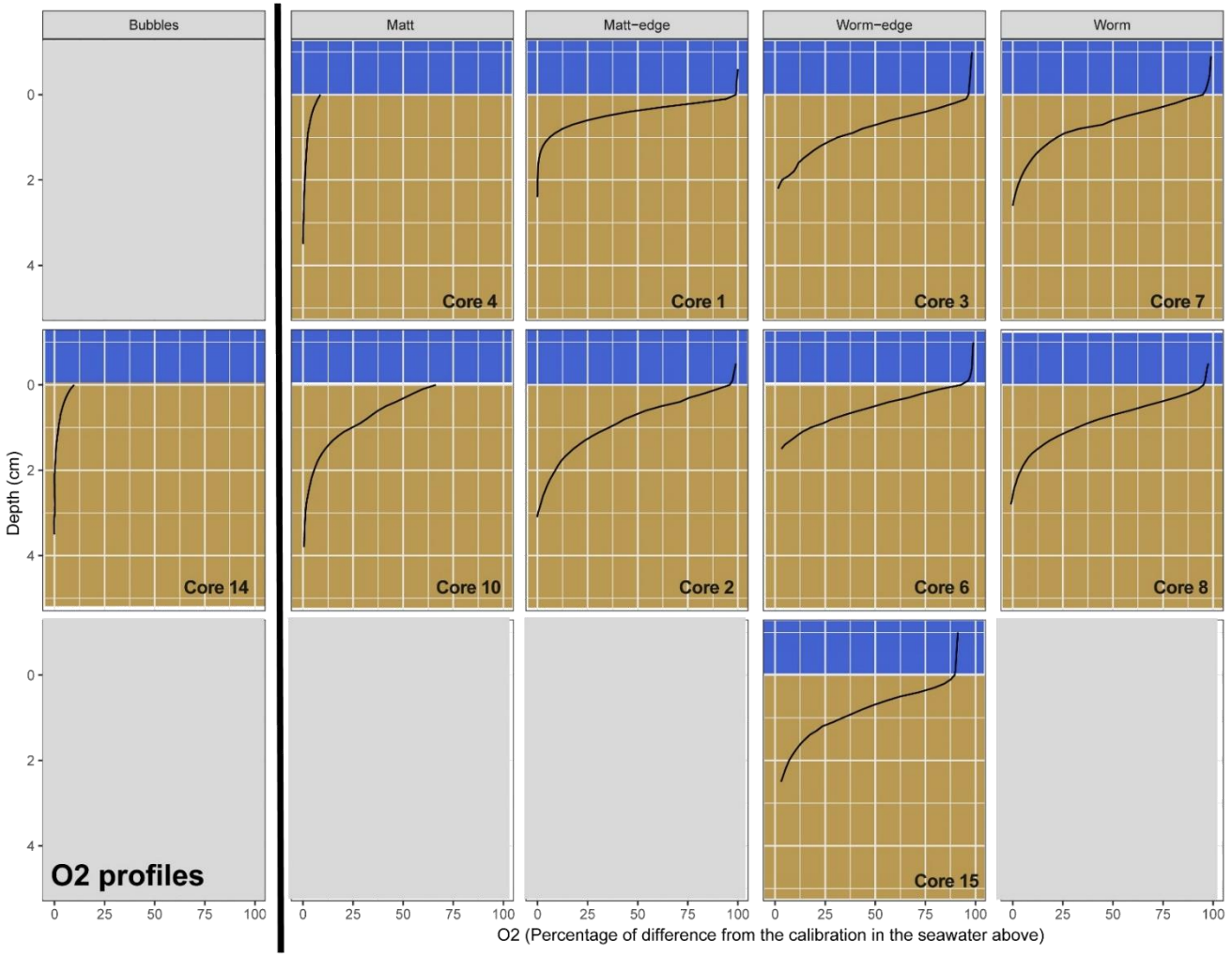

741

742 Figure SI 1: Vertical profile of oxygen (O_2) in percentage of difference from the calibration in the seawater above along depth, for each sediment
743 cores taken at different habitats. O_2 for $PC12_{FL}$ and $PC11_{SF}$ could not be measured.

744

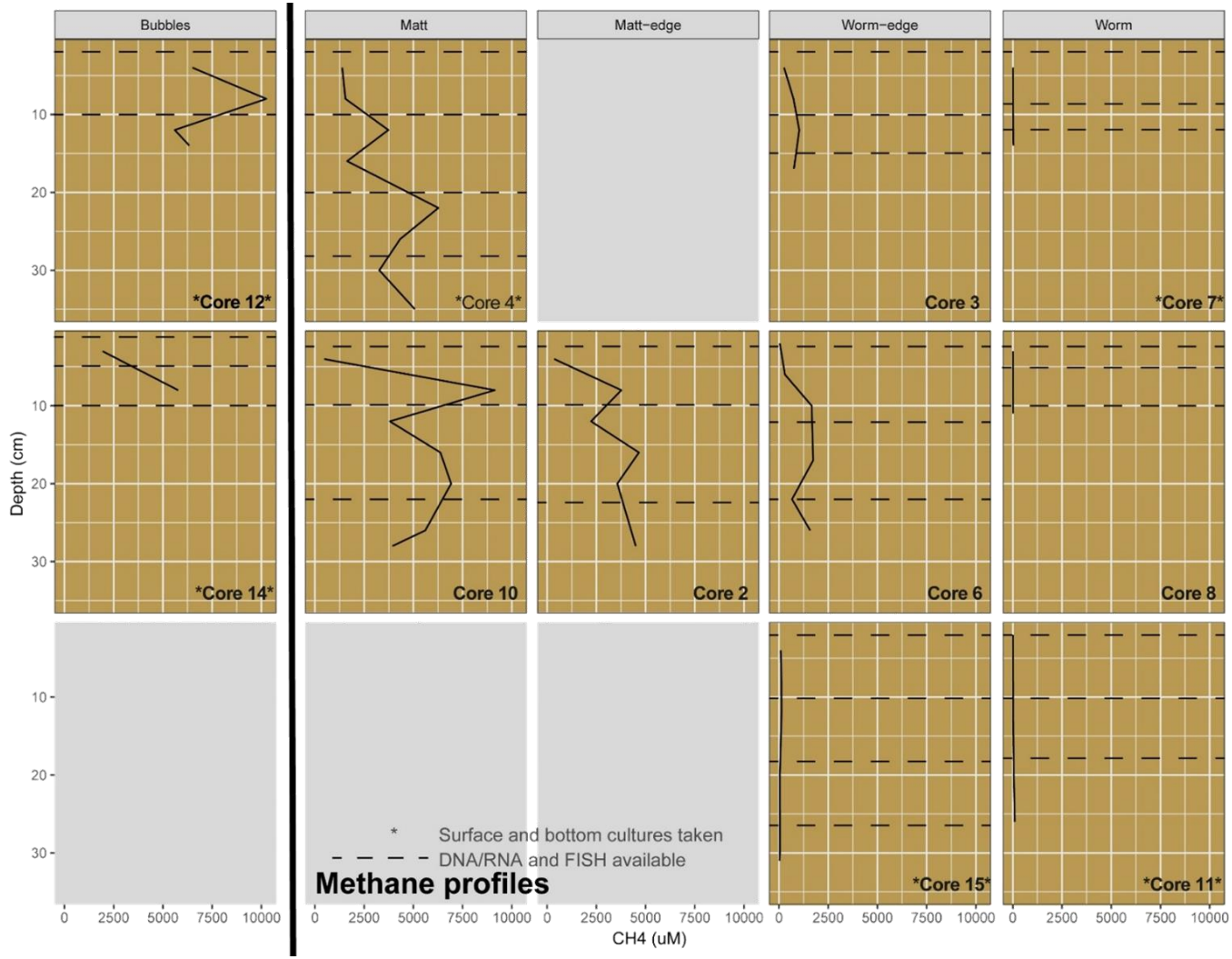

Figure SI 2: Vertical profile of methane (CH_4) for each sediment cores taken at different habitats. CH_4 for $PC01_{BE}$ could not be measured.

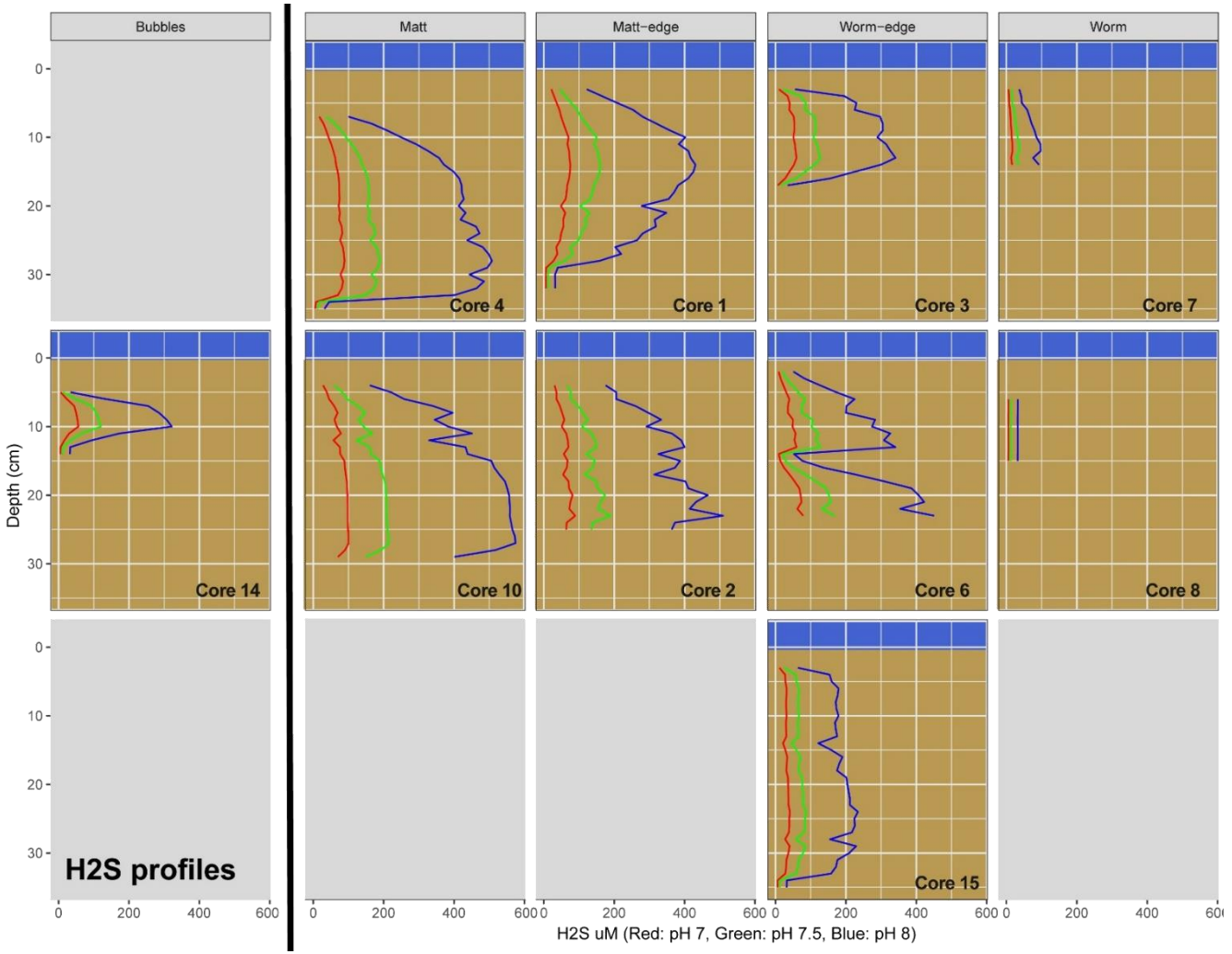

Figure SI 3: Vertical profile of hydrogen sulfide (HS^-) in mV, for each sediment cores taken at different habitats. HS^- for $PC12_{FL}$ and $PC11_{SF}$ could not be measured.

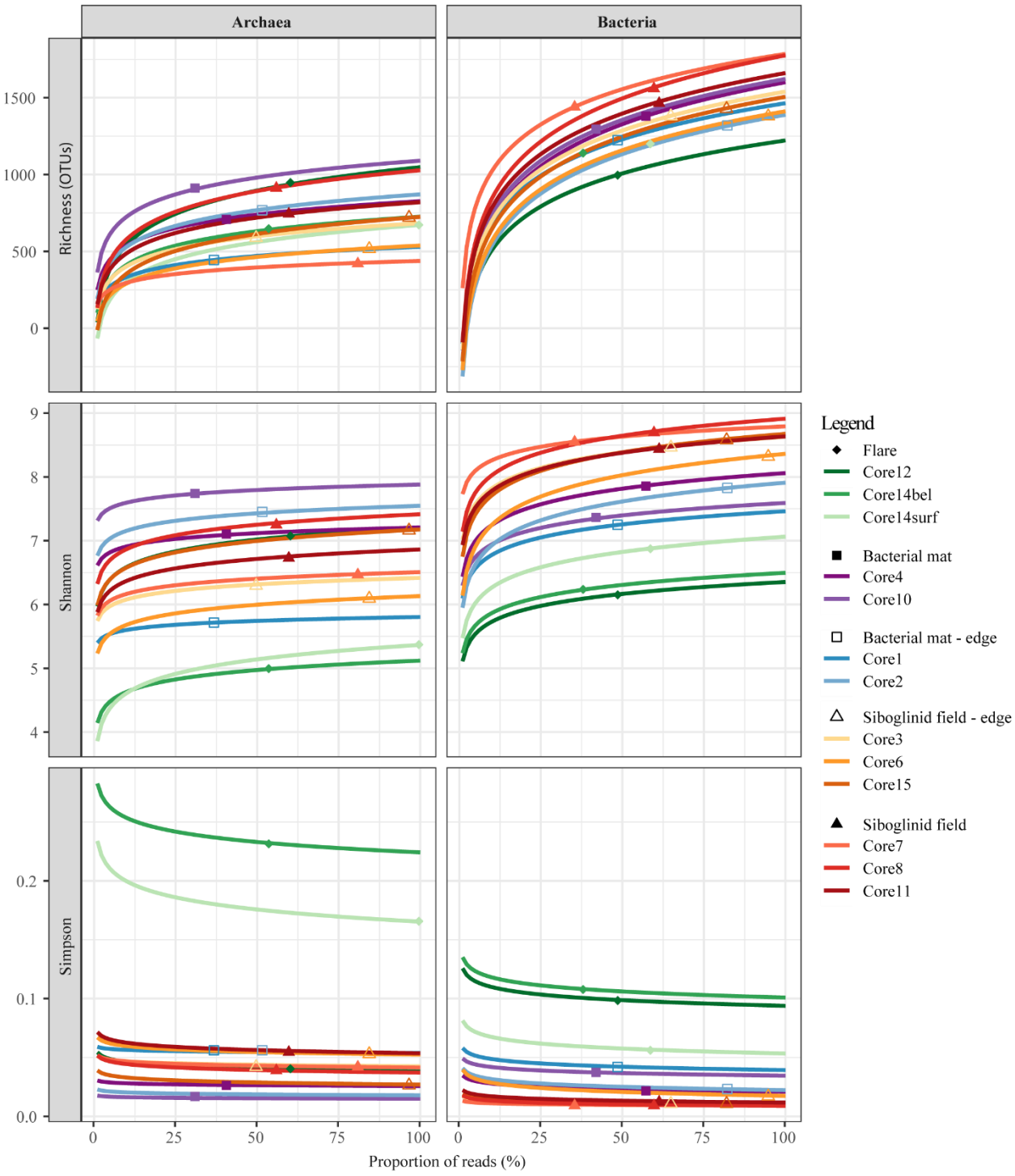

753

754 Figure SI 4: Alphadiversity anaylses showing variability of richness (number of OTUs), Shannon and
755 Simpson indices for the archaeal and bacterial libraries along the proportion of reads sampled in a library.
756 Dots represent the proportion at which libraries were rarerfied (14 900 sequences for Archaea, 15 000 for
757 Bacteria). Shapes of the dots represent the habitat type of the library and colors indicate the core ID.

758

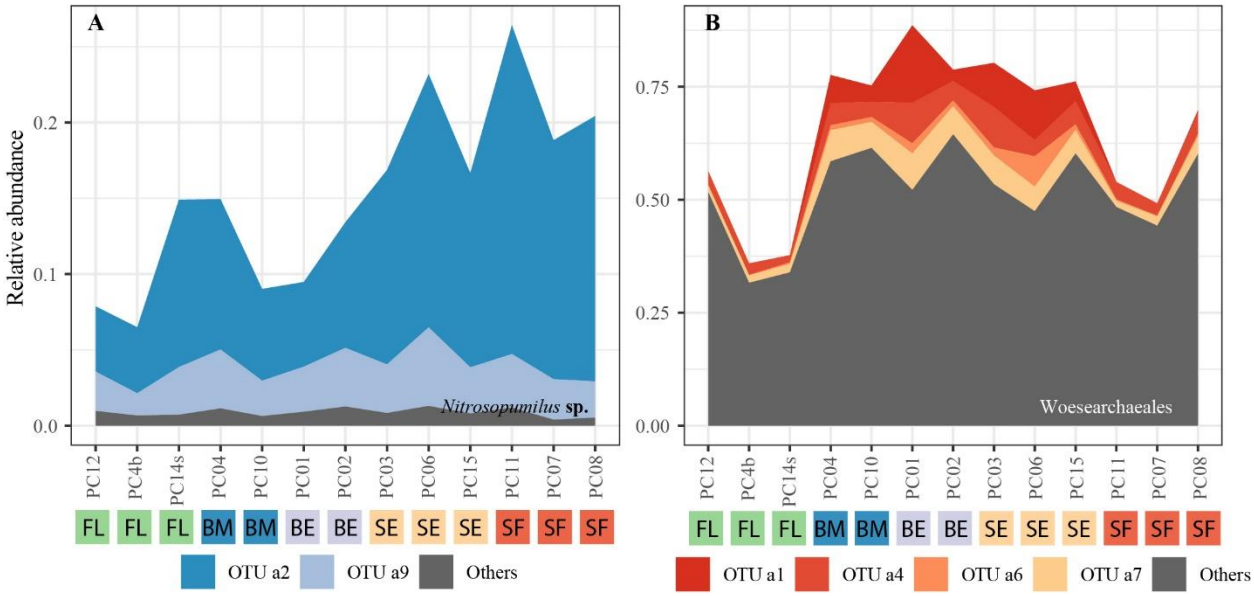

759
760 Figure SI 5: Relative abundance of key abundant archaeal OTUs from the genus Nitrosopumilus (A) and
761 from the uncultivated group Woesearchales (B).

762

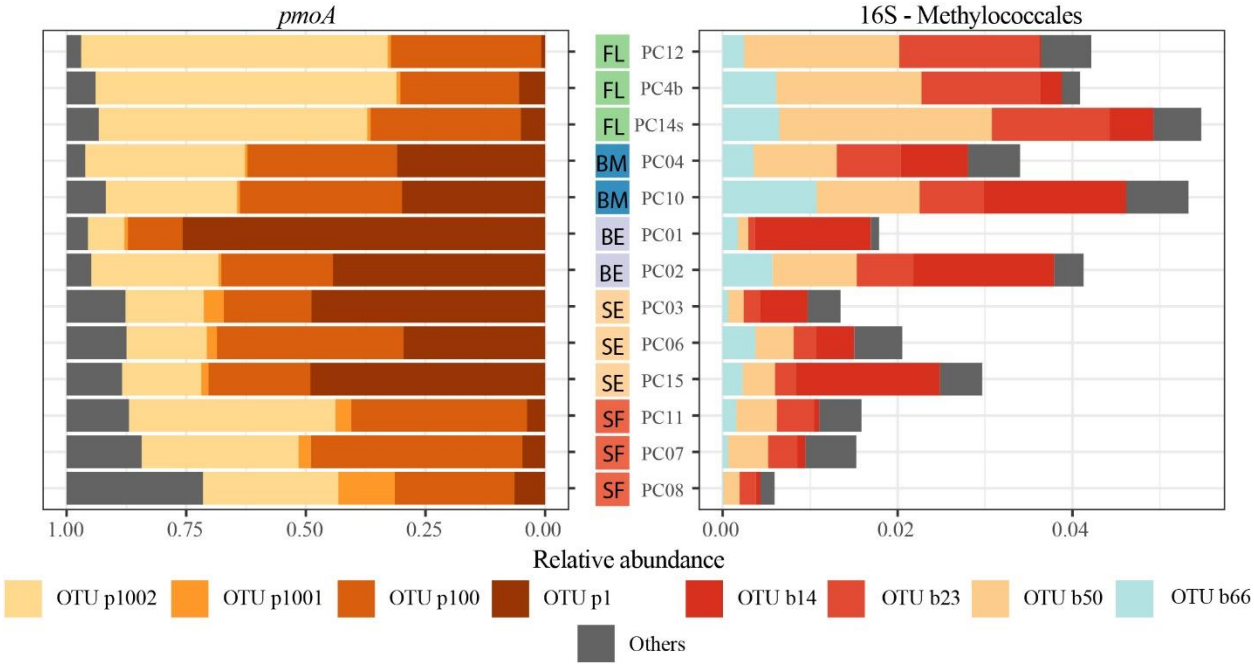

763

764 Figure SI 6: Relative abundance the most abundant OTUs from *pmoA* libraries (A) and the
765 Gammaproteobacteria Methylococcales (B).

766

Paper IV

LIMNOLOGY and OCEANOGRAPHY

ASLO

Limnol. Oceanogr. 66, 2021, 1896–1914

doi: 10.1002/lno.11731

Seasonal shifts of microbial methane oxidation in Arctic shelf waters above gas seeps

Friederike Gründger,[1,2*] **David Probandt**,[3] **Katrin Knittel**,[3] **Vincent Carrier**,[1,4] **Dimitri Kalenitchenko**,[1] **Anna Silyakova**,[1] **Pavel Serov**,[1] **Bénédicte Ferré**,[1] **Mette M. Svenning**,[1,4] **Helge Niemann**[5,6,1]

[1]CAGE—Centre for Arctic Gas Hydrate, Environment and Climate, Department of Geosciences, UiT The Arctic University of Norway, Tromsø, Norway
[2]Arctic Research Centre, Department of Biology, Aarhus University, Aarhus, Denmark
[3]Department of Molecular Ecology, Max Planck Institute for Marine Microbiology, Bremen, Germany
[4]Department of Arctic and Marine Biology, UiT The Arctic University of Norway, Tromsø, Norway
[5]Department of Marine Microbiology & Biogeochemistry, NIOZ Royal Netherlands Institute for Sea Research, Texel, The Netherlands
[6]Department of Earth Sciences, Faculty of Geosciences, Utrecht University, Utrecht, The Netherlands

Abstract

The Arctic Ocean subseabed holds vast reservoirs of the potent greenhouse gas methane (CH_4), often seeping into the ocean water column. In a continuously warming ocean as a result of climate change an increase of CH_4 seepage from the seabed is hypothesized. Today, CH_4 is largely retained in the water column due to the activity of methane-oxidizing bacteria (MOB) that thrive there. Predicted future oceanographic changes, bottom water warming and increasing CH_4 release may alter efficacy of this microbially mediated CH_4 sink. Here we investigate the composition and principle controls on abundance and activity of the MOB communities at the shallow continental shelf west of Svalbard, which is subject to strong seasonal changes in oceanographic conditions. Covering a large area (364 km^2), we measured vertical distribution of microbial methane oxidation (MOx) rates, MOB community composition, dissolved CH_4 concentrations, temperature and salinity four times throughout spring and summer during three consecutive years. Sequencing analyses of the *pmoA* gene revealed a small, relatively uniform community mainly composed of type-Ia methanotrophs (deep-sea 3 clade). We found highest MOx rates (7 nM d^{-1}) in summer in bathymetric depressions filled with stagnant Atlantic Water containing moderate concentrations of dissolved CH_4 (< 100 nM). MOx rates in these depressions during spring were much lower (< 0.5 nM d^{-1}) due to lower temperatures and mixing of Transformed Atlantic Water flushing MOB with the Atlantic Water out of the depressions. Our results show that MOB and MOx in CH_4-rich bottom waters are highly affected by geomorphology and seasonal conditions.

Temperature rise in the Arctic and its impact on the environment is more severe than for any other region on Earth (Masson-Delmotte et al. 2006; Hansen et al. 2013). The Arctic Ocean holds vast reservoirs of CH_4, which has a 32-fold higher greenhouse warming potential than carbon dioxide and may be released into the ocean and the atmosphere (Etminan et al. 2016). The majority of the CH_4 reservoirs across the Arctic shelves are temperature-sensitive, e.g., subsea permafrost (Shakhova et al. 2010) and gas hydrates in shallow sediments (Westbrook et al. 2009; Berndt et al. 2014). Gaseous CH_4 released from the seafloor becomes dissolved and can then be utilized by aerobic methane-oxidizing bacteria (MOB), which use CH_4 as an energy source and carbon substrate for growth (e.g., Hanson and Hanson 1996; Murrell 2010). In the ocean, aerobic microbial methane oxidation (MOx) is the final sink for

*Correspondence: friederike.gruendger@bio.au.dk

Additional Supporting Information may be found in the online version of this article.

Author Contribution Statement: F.G. and H.N. designed the project. F.G., H.N., V.C. collected the samples, carried out the main experiments. A.S. provided and analyzed hydrographic data. D.P., D.K., V.C., and K.K. carried out bioinformatic and quantification analyses. P.S. analyzed CH_4 concentrations. M.S. and H.N. supervised the research and contributed with scientific discussions. F.G. carried out interpretation of the experiments and wrote the manuscript with contribution from all co-authors.

CH_4 before it is liberated to the atmosphere (Reeburgh 2007), but little is known about the diversity, abundance, distribution, and activity of MOB (Tavormina et al. 2008; Mau et al. 2013; Steinle et al. 2015). For example, high amounts of CH_4 were rapidly consumed by MOB following the deep-water horizon accident (Crespo-Medina et al. 2014) and MOB were found to effectively consume CH_4 from the water column if hydrographic conditions provide continuity for MOB (Steinle et al. 2015, 2017). However, MOx can also be very low despite high CH_4 concentrations in marine waters for reasons that are still unclear (Bussmann 2013).

Aerobic MOB are phylogenetically divided into Gammaproteobacteria (type I MOB), Alphaproteobacteria (type II MOB) (e.g., Hanson and Hanson 1996; Knief 2015), and Verrucomicrobia (type III MOB) (Dunfield et al. 2007; Op den Camp et al. 2009; van Teeseling et al. 2014). Common to almost all MOB is the presence of the membrane-bound particulate methane monooxygenase, the enzyme responsible for the initial step of methane oxidation. The highly conserved *pmoA* gene, encoding a subunit of the particulate methane monooxygenase, is most frequently used as a molecular marker both for detection and phylogeny of MOB via cultivation-independent methods (Tavormina et al. 2008; Knief 2015). Potential methane-oxidizing uncultivated clades like the deep-sea clades 1–5 (Lüke and Frenzel 2011) have been identified by this approach. Especially in marine environments, great uncertainties exist about the factors that determine MOB activity and community structure. From the Arctic marine environment, a number of studies report on MOx activity and MOB community composition in relation to environmental factors such as CH_4 concentrations and hydrography (e.g., Mau et al. 2013; Steinle et al. 2015; Osudar et al. 2016). However, all those studies are single snap-shots of the prevailing situation at the place and time of sampling. For example, studies focusing

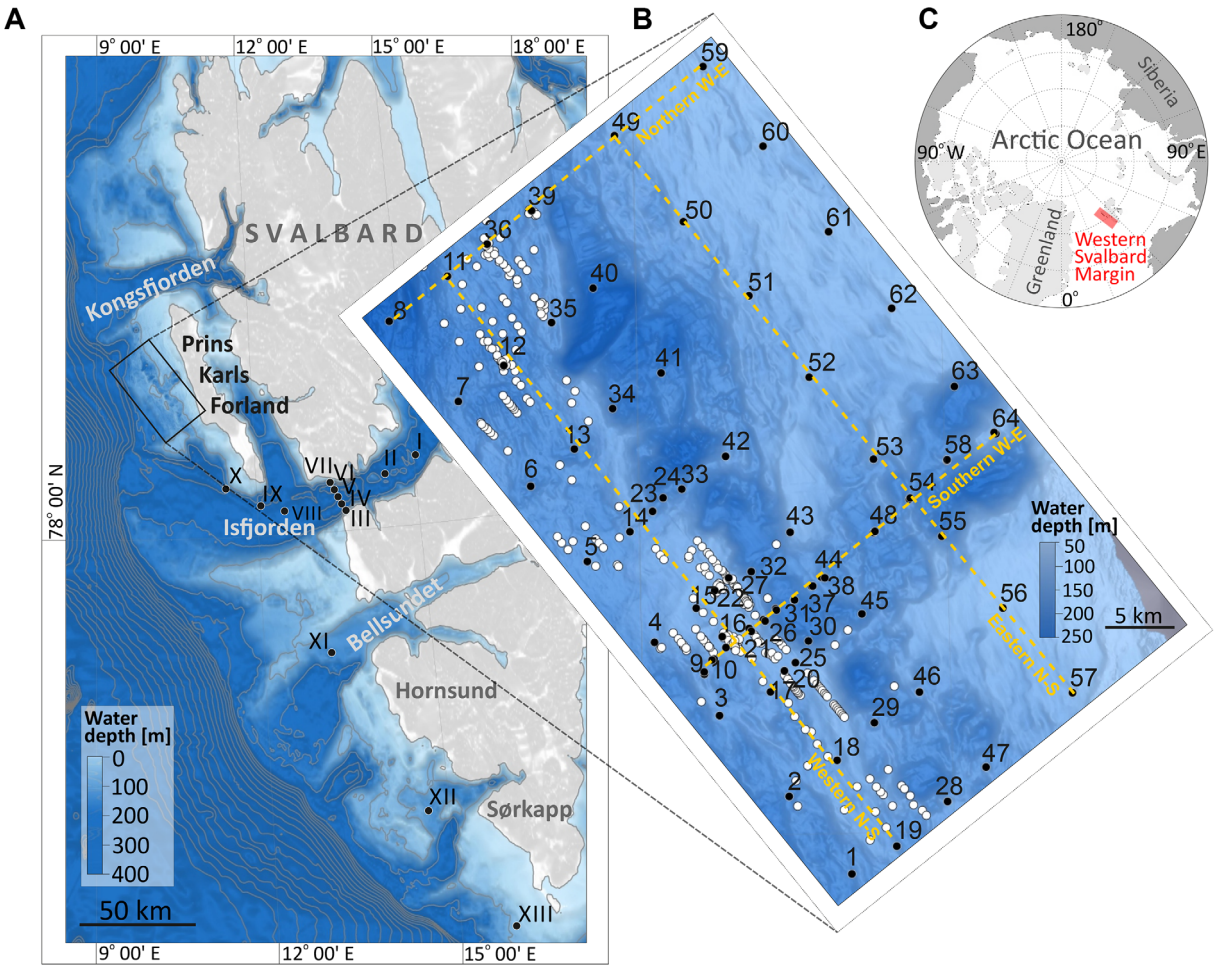

Fig 1. Bathymetric map of the study areas west off Svalbard archipelago showing hydrographic sampling stations indicated by black dots at Isfjorden (Stas. I–X), Outer Bellsundet (Sta. XI), Outer Hornsund (Sta. XII), and Sørkappøya (Sta. XIII) (**A**). Detailed map of the shallow shelf west of Prins Karls Forland including gas flare locations (white dots) and 64 sampling stations arranged in a grid. At stations along the four transects (conducted from North to South and West to East, yellow dashed lines), sampling for methane oxidation rates and microbial molecular analyses were conducted in addition to hydrographic profiles and CH_4 concentrations, which were usually conducted at all stations (**B**). Global view of our sampling area at the western Svalbard margin (**C**).

on areas around the Svalbard archipelago, i.e., the continental slope west of Prins Karls Forland (Gentz et al. 2014), Storfjorden in the south-east (Mau et al. 2013), and the Svalbard margin between Bjørnøya and Kongsfjordrenna (south to west Svalbard) (Mau et al. 2017), were only conducted without temporal repetition in August/September. Only Steinle et al. (2015) compared spatiotemporal replicates collected during several surveys at the Svalbard continental margin in late August. Time series studies covering seasonal changes of CH_4 input and microbial CH_4 turnover in the water column in the Arctic have so far not been published, and little knowledge exists on the community composition of Arctic Ocean MOB (James et al. 2016; Ferré et al. 2020).

In this study, we investigate the fate of CH_4 in the water column at the continental margin west of Svalbard, specifically the shallow shelf west off Prins Karls Forland. This area is characterized by CH_4 seepage (Portnov et al. 2016; Silyakova et al. 2020). Despite extensive release of CH_4 from the sediment in this area, almost no CH_4 was found to reach the atmosphere (Myhre et al. 2016). Our main objectives were (1) to study the composition and activity of the methanotrophic communities, (2) to investigate seasonal shifts and, related to these, (3) the differential hydrographical settings and their influence on MOB activity and distribution within the study area. To meet these aims, we conducted sampling surveys in the spring, late spring and summer.

We found that community changes of MOB are marginal, but that MOx capacity is influenced by seasonal shifts and varies according to site-specific geographical features and changing hydrographical conditions.

Methods

Study area

Our study area stretches along the continental margin off western Svalbard from the shallow shelf west of Prins Karls Forland towards the southern tip of Svalbard including Isfjorden, Isfjorden Trough, Outer Bellsundet, Outer Hornsund, and Sørkappøya (Fig. 1). Water depth in these areas ranges from 50 to 160 m. The shallow shelf west of Prins Karls Forland is characterized by an irregular bathymetry showing numerous large depressions encompassed by a series of moraine ridges termed the Forlandet moraine complex (Landvik et al. 2005; Fig. 1B). Here, along the Forlandet moraine complex in 80–90 m water depth, a vast number of gas flares (~200 flares, identified by acoustic signatures of gas bubbles in the water) were previously mapped (Sahling et al. 2014; Silyakova et al. 2020). The $\delta^{13}C$ values of the emitted CH_4 and the absence of higher hydrocarbons in the seeping gas indicates a microbial CH_4 origin (Graves et al. 2017; Mau et al. 2017). The seepage region west of Prins Karls Forland lies > 200 m shallower than the upper limit of the methane hydrate stability zone and unlikely results from CH_4 hydrates dissociating in situ. However, lateral migration of CH_4 from a hypothesized gas hydrate dissociation front at deeper shelf settings may at least partly fuel the seeps on the shallow shelf (Sarkar et al. 2012).

The hydrodynamics in our study area are complex (see also Silyakova et al. 2020). The East Spitsbergen Current flows along the Svalbard islands southwards on the east side, following the coast around the island's southern tip and then turns northwards on the west side of the island (Nilsen et al. 2008). Here, it flows as a coastal current on the shelf and is composed of less saline and cold Arctic Water (34.30–34.80, −1.5 to 1.0°C) into our study area. To the west of the shelf, the northernmost extension of the North Atlantic Current, the West Spitsbergen Current (Aagaard et al. 1987) is composed of relatively saline and warm Atlantic Water (> 34.65, > 3.0°C) and also flows northward. Although the East Spitsbergen Current and West Spitsbergen Current are separated by a front, frequent mixing occurs and the West Spitsbergen Current may also flood the shelf (Steinle et al. 2015). Seasonality defines the different portions of mixed water masses. Atlantic Water transforms into Transformed Atlantic Water (> 34.65, 1.0–3.0°C) by losing heat to the atmosphere and adjacent waters and freshening due to meltwater from glaciers, snow and sea ice. Whereas Intermediate Water (34.00–34.65, > 1.0°C) is formed by entrainment and mixing mechanisms at the boundary of Surface Water with underlying Atlantic Water or Transformed Atlantic Water. Surface Waters are freshened by melt water and warmed by solar heat in summer (< 34.00, < 1.0°C). Waters that overwinter in fjords become colder and fresher, and are then classified as Local Water mass (34.30–34.85, −0.5 to 1.0°C). Water masses are classified according to Cottier et al. (2005).

Sampling strategy

Samples were taken within three successive years (2015–2017) during four expeditions with R/V *Helmer Hansen*,

Table 1. Sampling strategy and definitions of water samples/horizon taken from the water column.

Water depth	CH_4	MOx	16S rRNA	Water level	Water layer
5 m below sea surface	x	x	x	8	Surface
15 m below sea surface	x	x		7	
25 m below sea surface	x	x		6	
Intermediate 2	x	x	x	5	Intermediate
Intermediate 1	x	x		4	
25 m above seafloor	x	x	x	3	Bottom
15 m above seafloor	x	x		2	
5 m above seafloor	x	x	x	1	

CAGE16-4 (spring: 2–4 May 2016), CAGE17-1 (spring: 16–20 May 2017), CAGE16-5 (late spring: 17–22 June 2016), and CAGE15-3 (summer: 1–3 July 2015). At the shallow shelf west of Prins Karls Forland, we collected samples at 64 hydrographic stations arranged in a grid pattern covering an area of approximately 14 × 26 km. All stations were sampled successively (total sampling time of the entire grid < 72 h). The positions of transects and stations were selected according to their coverage of specific features found at the seafloor such as gas flares or bathymetric depressions (Fig. 1B). For example, the western N-S transect follows the main ridge of the Forlandet moraine complex and covers numerous CH_4 flares. The southern W-E transect features a flare cluster in the west and covers bathymetric depressions towards the east. During the June survey in 2016, time constrains allowed us to only sample 12 of the 64 stations. Those 12 stations were located along the western N-S, eastern N-S, and southern W-E transects (Fig. 1B, Table S1).

At all stations, hydrographic parameters (salinity, temperature, pressure) were recorded at 24 Hz with a Conductivity-temperature-depth profiler (SBE 911 plus CTD; Sea-Bird Electronics, Inc., USA) equipped with twelve 5-liter Teflon-lined Niskin bottles. Only downcasts were used for hydrographic profiling. With the CTD-mounted Niskin bottles, we collected discrete water samples from eight water levels (1–8): 5, 15, 25 m above seafloor, 5, 15, 25 m below sea level, and two additional intermediate sampling levels evenly spaced between 25 m below sea level and 25 m above seafloor (actual sampling depth depending on water depth; Table 1). Water from the Niskin bottles was subsampled immediately upon recovery. Dissolved CH_4 concentrations were measured in all eight water levels of the entire sampling grid. MOx rates were measured in all eight water levels along four transects, which run from north to south (eastern N-S and western N-S) and west to east (northern W-E and southern W-E) (comprising 31 stations, Fig. 1B). Samples for phylogenetic analyses were recovered during sampling campaigns in July 2015 as well as May and June 2016 (but not in May 2017) from water levels 1, 2, 3, 5, and 8 from all stations where MOx rates were measured. During the May 2016 campaign, six stations (Stas. 9, 16, 31, 44, 54, and 64) along the southern W-E transect were repeatedly investigated 2 days after the first sampling to monitor rapid variations of hydrographic conditions and their effects on MOx activity and bacterial community changes.

In addition to the shallow shelf west of Prins Karls Forland, in May and June 2016 we investigated the water column at Isfjorden (Stas. I and II), Isfjorden Trough (III–X), Outer Bellsundet (XI), Outer Hornsund (XII), and Sørkappøya (XIII) (Fig. 1A, Table S1) in the same manner as described above. CTD and dissolved CH_4 concentration data from the surveys in July 2015 and June 2016 of the area west of Prins Karls Forland were published by Silyakova et al. (2020).

Methane concentration measurements

Methane concentrations were determined using a headspace method as described by Silyakova et al. (2020). In order to calculate the content of dissolved CH_4 of the entire sampling area at the shallow shelf of Prins Karls Forland, we defined three water layers with consideration of the uneven bathymetry (Silyakova et al. 2020). Water layers were defined as the "Bottom Water Layer" from seafloor to 25 m above seafloor (comprising levels 1, 2, and 3), the "Surface Water Layer" from the ocean surface down to 25 m depth (comprising levels 8, 7, and 6), and the "Intermediate Layer" between 25 m below the ocean surface and 25 m above seafloor (comprising levels 5 and 4) (Table 1).

Methane oxidation rate measurements

Methane oxidation rates were determined according to previous publications (Niemann et al. 2015; Steinle et al. 2015) with modifications as described in Ferré et al. (2020). For the water column at the sampling area west of Prins Karls Forland, the mean areal turnover of CH_4 was calculated by integrating distinct MOx rates over depth yielding results in m^{-2} d^{-1} for each water layer and the entire water column (Steinle et al. 2017). We then calculated weighted MOx means for each layer, considering uneven horizontal spacing of the hydro cast stations (for a more detailed description of the computation of the weighted means see Silyakova et al. (2020)). Upscaled to the size of the sampling grid (423 km^2), these weighted means translate to a total CH_4 turnover per day for each water layer and the entire water body of the sampling grid. To compare the capacity of MOx to retain CH_4, we then calculated the fraction of CH_4 consumed per day:

$$CH_4\ \text{turnover per day}\ (\%) = MOx/CH_4 \times 100 \quad (1)$$

Bacterial community analyses

Seawater samples for molecular analysis were collected in sterile, high-density polyethylene bottles and usually processed immediately after subsampling. However, time constraints sometimes required storage of samples at 4°C in the dark before further processing, but storage time never exceed 4 h. We filtered a volume of 1 liter of sample on membrane filters (Whatman Nuclepore Track-Etched PC, 0.22 μm, Merck Millipore, MA) by applying a gentle vacuum of ~ 0.5 bar and stored filters at −20°C until further analyses. Total DNA from membrane filters was extracted following the method of Pilloni et al. (2012) and DNA content in each sample was quantified using a spectrophotometer (Nanodrop, ND-1000, Thermo Scientific, MA).

For the amplification of the bacterial 16S rRNA gene, we selected samples retrieved in July 2015, May 2016 and June 2016 from distinct water levels from Prins Karls Forland (Stas. 9, 10, 19, 49, 54, 58; levels 1, 3, 5, and 8), from Isfjorden (Sta.

I; levels 1 and 3) and Outer Bellsundet (Sta. XI; levels 2 and 4) (Table S1). We used the degenerated primer pair Bakt_341F and Bakt_805R resulting in about 450 bp amplicons covering the V3-4 region of the 16S rRNA gene (Herlemann et al. 2011). For the amplification of the particulate methane monooxygenase gene (*pmoA*), we selected samples from the abovementioned sampling campaigns from the water level 1 from Prins Karls Forland stations 9, 10, 49, 54, 58, and Isfjorden (Sta. I), and from water level 2 from Outer Bellsundet (Sta. XI). Water levels 1 and 2 were selected, because of elevated MOx rates, which were measured at these particular water levels at the chosen stations. The primer pair wcpmoA189f and wcpmoA661r for marine water column MOB (Tavormina et al. 2008) was used for amplification. Gene analyses of 16S rRNA and *pmoA* amplicons were performed by IMGM Laboratories GmbH (Martinsried, Germany). Cluster generation and bidirectional sequencing (2×300 nt) by synthesis was accomplished on the Illumina MiSeq next generation sequencing platform (Illumina, CA) using reagents kit 500 cycles v2 under the control of MiSeq Control Software v2.5.1.3. Sequence data have been submitted to the GenBank Sequence Read Archives (https://www.ncbi.nlm.nih.gov/sra) under BioProject ID: PRJNA642858 (16S rRNA) and PRJNA641979 (*pmoA*).

Processing of 16S rRNA gene sequences was achieved as outlined in the following. Using BBMerge software version 37.02 (BBTools package, Brian Bushnell, Walnut Creek, CA), we performed the initial data processing of the raw sequences (primer trimming, quality filtering at a minimum of 99.1% base call accuracy, and read assembly of forward and reverse read with an overlap of 20 bp by default strictness setting). The resulting reads were processed according to the MiSeq standard operating procedure (Kozich et al. 2013) with MOTHUR version 1.39.5 (Schloss et al. 2009) including pre-clustering at 99% sequence similarity and de novo-based chimera removal using UCHIME (Edgar et al. 2011) to remove artificial diversity. Sequences were aligned and classified using the SILVA reference database (Release 132; Quast et al. 2013). Sequences classified as "no relative," chloroplast, archaeal and eukaryotic 16S rRNA were removed. Afterwards, bacterial sequences were clustered into operational taxonomic units (OTUs) at 97% sequence similarity, using the OptiClust algorithm. To reduce artificial diversity, rare $OTU_{0.97}$ that were represented by only ≤ 2 sequences in the whole dataset were removed as suggested for short fragment 16S rRNA gene data (Allen et al. 2016). Prior to diversity analysis, OTUs retrieved for the blank DNA extraction and the no template negative control from the library preparation were also removed from the entire data set.

After MOTHUR sequence processing and prior to statistical and diversity analysis, the community dataset was randomly rarified to the lowest number of sequences found per sample (1083). We conducted alpha and beta diversity analyses using the program R with the vegan package (v. 2.5-6; https://CRAN.R-project.org/package=vegan). Displaced alpha diversity values are the means of 25 iterations. Hierarchical clustering and Non-Metric Multidimensional Scaling (NMDS) analyses are based on the Bray–Curtis dissimilarity index. Spearman's rank correlation of bacterial phyla at the family level and selected environmental variables was conducted with R package Hmisc (v.4.4-0; https://CRAN.R-project.org/package=Hmisc). Only those family level clades (SILVA taxonomy v.132) that contributed $\geq 0.5\%$ to total sequences in at least one sample were considered.

We processed *pmoA* amplicons as follows: The raw sequences were treated following our open-access pipeline (https://github.com/dimikalen/MS_UIT_CAGE/blob/master/CAGE_MiSeq_SOP.sh). Briefly, forward and reverse reads were merged using BBmerge (v37.36; Bushnell et al. 2017) and quality filtered with a maxEE parameter of 1 in VSEARCH (v2.9.0; Rognes et al. (2016)). To reduce the computational need in the following steps, unique sequences were extracted. Operational phylogenetic units (OPUs) were defined by using USEARCH (v11; Edgar (2010)) applying a similarity threshold of 97%. The most abundant reads of each OPU were then selected to find the closest known sequences in the *pmoA* gene reference database (on nucleotide level, Wen et al. (2016)) using the Wang method in MOTHUR (v1.39; Schloss et al. 2009). All raw *pmoA* reads were then mapped back to the reference reads of the *pmoA* $OPU_{0.97}$, as recommended in the USEARCH documentation, in order to construct the final OPU table. The OPU table was subsequently rarefied at 1600 sequences. Hierarchical clustering based on the weighted Unifrac distance metric (Lozupone et al. 2011) was computed by using Qiime (Caporaso et al. 2010) and visualizations were made in R (stats package v3.6.1). For phylogenetic analysis of the two most abundant OPUs, we selected 52 *pmoA* sequences from cultured and uncultured MOB published by Lüke and Frenzel (2011), Knief (2015) and in the NCBI GenBank (https://www.ncbi.nlm.nih.gov/). Sequences were aligned using MUSCLE implemented in MEGA 7 (Edgar 2004) and trimmed to retain only shared base pair positions. We built a best-scoring maximum likelihood phylogenetic tree (based on nucleotides) in Randomized Axelerated Maximum Likelihood (RAxML, version 8.2) using the General Time Reversible (GTR) Gamma model (Stamatakis 2014). Thereafter, OPU1 and 2 were aligned to the previously selected sequences and placed into the built phylogenetic tree using the Evolutionary Placement Algorithm implemented in RAxML. The resulting tree was visualized and annotated in Interactive Tree Of Life (Letunic and Bork 2016).

Results

Our data were collected during sampling surveys in the Arctic spring (May 2016, 2017, the month with the coldest bottom water temperatures; Berndt et al. (2014)), late spring (June 2016) and summer (July 2015). We mainly investigated a large seep area at the shallow shelf west of Prins Karls Forland and six additional regions, which are hydrographically connected to the Prins Karls Forland shelf area: Isfjorden (I–VII), Isfjorden Trough (VIII–X), and three stations towards the southern tip

of Svalbard: Outer Bellsundet (XI), Outer Hornsund (XII), and Sørkappøya (XIII). We collected discrete water samples for geochemical and microbiological analyses from eight defined water levels, whereas CTD measurements were made continuously throughout the water column. To simplify the following discussion about comparing processes at the ocean surface or close to the seafloor, we use the three main water layers, "Bottom Water Layer," "Surface Water Layer" and "Intermediate Layer" (as defined previously) in order to account for the differential water depth at the various stations.

Hydrographic setting

In May 2016, the entire water column was dominated by Transformed Atlantic Water with high salinity of 34.9–35.0 and temperatures between 1.6 and 2.3°C (Fig. 2A–D). In contrast, the water column in May 2017 was dominated by relatively warm (2–4.8°C) and saline (34.6–34.8) Atlantic Water. Water in the bathymetric depressions was slightly colder (2.3–2.8°C) and therefore classified as Transformed Atlantic Water (Fig. 2E–H). In June 2016, the bottom water was composed of Transformed Atlantic Water (lowest temperature 2.3°C) at the gas flare area (southern part of the western N-S transect) and within the bathymetric depressions, while we found warmer Atlantic Water (3–5°C) in the upper water column. Both water masses were characterized by salinities of 34.6–34.9 (Fig. 2I–K). A strong stratification was observed in July 2015 (Fig. 2L–O). At the bottom of the water column, specifically in bathymetric depressions, water was saline and relatively warm Atlantic Water (34.9, ~3.5°C) with fractions of Transformed Atlantic Water admixture. At the main gas flare

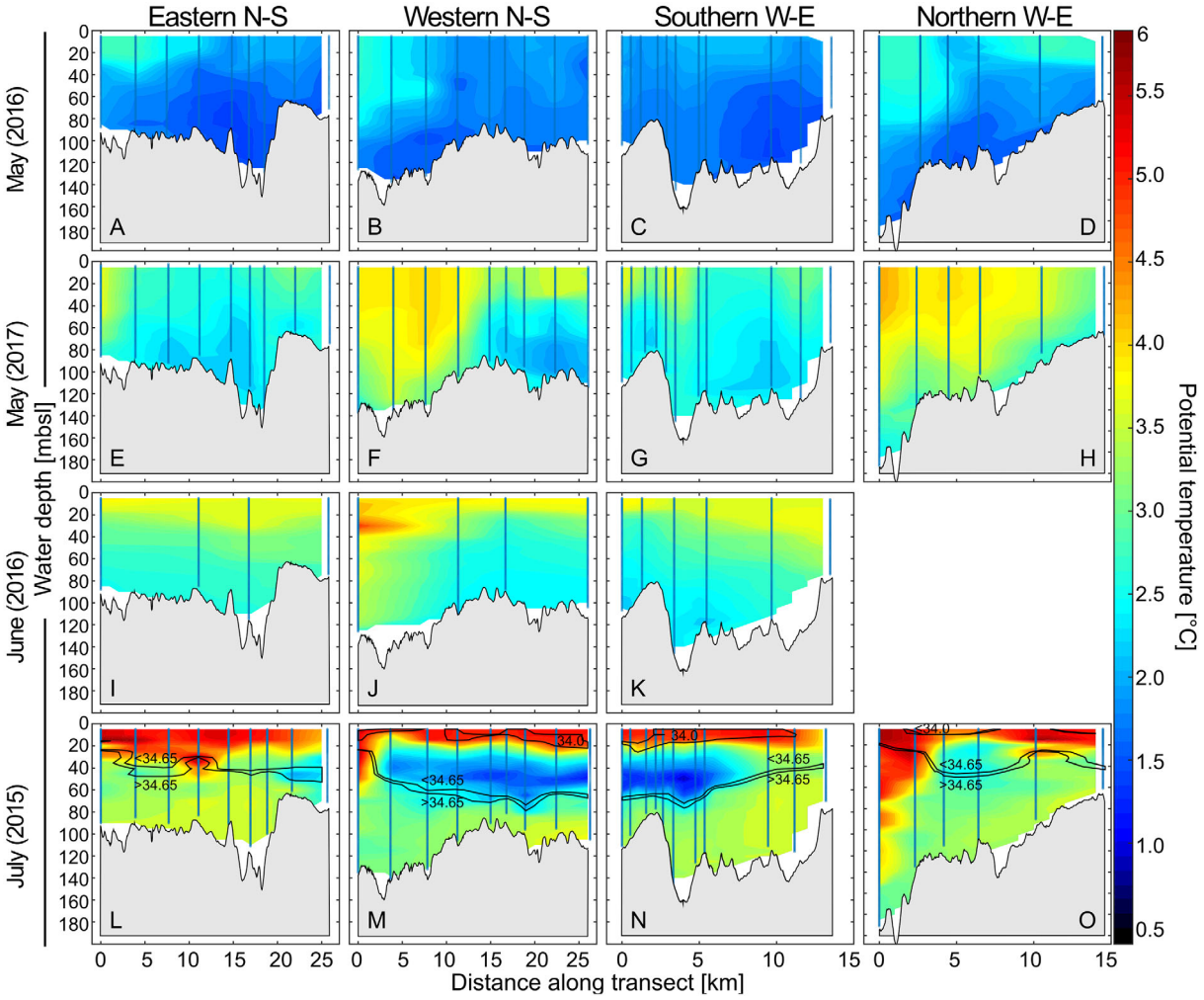

Fig 2. Profiles of potential temperature in the water column along transects at the shallow shelf west of Prins Karls Forland (**A–O**) from four sampling surveys in May, June, and July within three successive years (2015–2017). For each sampling survey, water depth on the *y*-axis is given in meters below sea level (mbsl). Vertical lines represent stations for continuous CTD measurements. The color code shows measured and linearly interpolated temperature values (°C). Selected salinity horizons (values in psu) are indicated by black lines in **L–O**. In May and June (**A–K**), no salinity horizons were observed due to a well-mixed water column with constant high salinity levels (34.6–35.0). Each plot contains the bathymetrical baseline (black line above gray area) characteristic for each transect. In June 2016, only three transects were conducted.

area, cold Intermediate Water (34–34.3, 1.3–2°C) lay above warmer Atlantic Water. Surface Water with temperatures of 4.5–5.5°C and low salinity (28.5–34.0) dominated the surface water down to ~20 m (Fig. 2L–M). The detailed hydrographic setting in May 2016 and July 2015 at the shelf west of Prins Karls Forland has been described by Silyakova et al. (2020).

At Isfjorden and Isfjorden Trough in May 2016, surface water temperatures were colder compared to the Prins Karls Forland shelf, i.e., between −0.2 and 1.2°C and with average salinities around 34.6, indicating Local Water and Intermediate Water formed due to local cooling and freshening over winter. Below the surface water layer, water salinity and temperature increased (> 34.86, 2.2–2.7°C) indicating that the Atlantic Water transformed into Transformed Atlantic Water in the fjord (Fig. S1A). The water column at the central stations of the Isfjorden Trough crossing transect (Stas. IV and V), was characterized by relatively warm Atlantic Water (35, 3.3°C) at the surface, which decreased in salinity and temperature to 34.8 and 1.6°C at 300 m water depth turning into Transformed Atlantic Water, indicating that at deeper depths, water masses were strongly influenced by mixing with West Spitsbergen Current waters. The lateral stations at the trough, i.e., those in proximity to the fjords sites, showed cold Surface Water (southern Sta. III: $T = -0.2$°C, $S = 34.6$; northern Stas. VI and VII: $T = 0.7$°C, $S = 34.8$), which turned into slightly warmer (2.2°C) and more saline water (34.9) at 35 m water depth, indicating that Surface Water lost more heat to the atmosphere than deeper waters, and that water was still mixing with the West Spitsbergen Current waters; Transformed Atlantic Water was dominating the deep-water column down to 365 m water depth (> 34.86, 1.6–2.7°C). Further inside Isfjorden (Stas. I and II), close to Longyearbyen, the entire water column was comprised of Local Water with salinity of 34.8 and temperatures of 0.8–1.2°C (Fig. S1A).

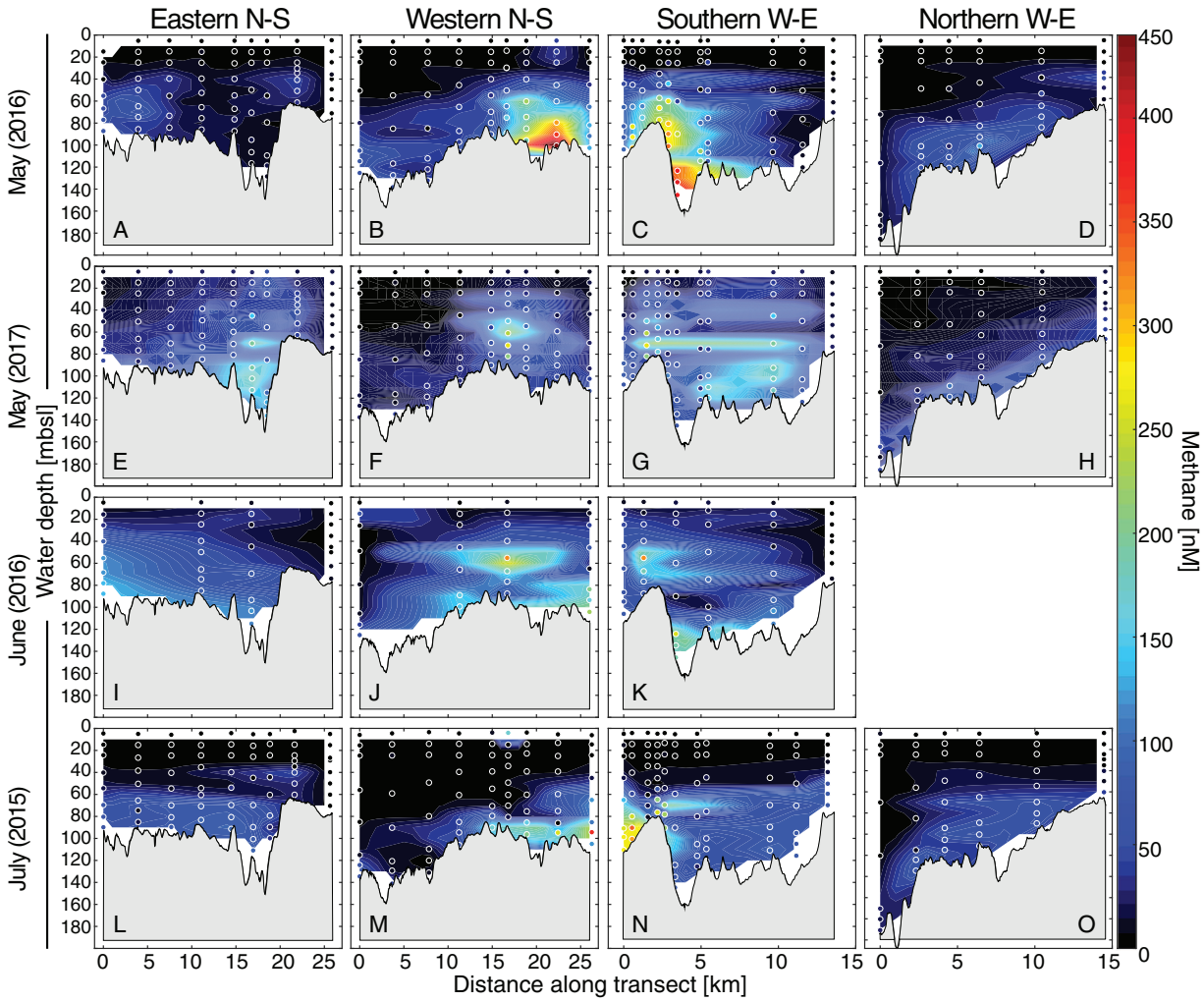

Fig 3. Profiles of dissolved CH_4 in the water column along transects at the shallow shelf west of Prins Karls Forland (**A–O**) from four sampling surveys in May, June, and July within three successive years (2015–2017). For each sampling survey, water depth on the *y*-axis is given in meters below sea level (mbsl). White circles represent single water samples. The color code shows measured and linearly interpolated CH_4 concentrations (nM). Each plot contains the bathymetrical baseline (black line above gray area) characteristic for each transect. In June 2016, only three transects were conducted.

In June 2016, Isfjorden surface waters down to 40 m were considerably fresher and warmer (34.2, 4.7°C) than in May 2016, most likely due to freshening through melting of glaciers, snow and sea ice and heating from the atmosphere (Fig. S1B).

Compared to Isfjorden in June 2016, a similar structuring of the water column was observed outside Bellsundet. In late June, surface temperatures were ~4°C, heated up by the atmosphere and surface salinities of 34.3–34.65 indicate the influence of Arctic Water, carried by the East Spitsbergen Current. Similarly, at Outer Hornsund, southwards from Bellsundet, surface salinity was not higher than 34.6, indicating the presence of Arctic Water transported by the East Spitsbergen Current (Fig. S1B).

Water column methane content

The entire water column was CH_4 oversaturated with respect to the atmospheric equilibrium concentration, which is ~ 3 nM at the ambient salinity and temperature conditions (Wiesenburg and Guinasso (1979) (Table S2). In the area west of Prins Karls Forland, we observed CH_4 plumes with concentrations of up to 437 nM. High concentrations were mainly encountered in bottom waters within the flare cluster, most dominantly in the southwest of the sampling grid, but the extent of the plumes differed greatly between the surveys (Figs. 3, S2). For example, we found elevated CH_4 concentrations extending widely from west to east in May 2017 (Fig. 3E–H) and June 2016 (Fig. 3I–K). In contrast, the eastward extension was less pronounced in May 2016 (Fig. 3A–D) and a clearly defined CH_4 plume was located at the intersection of the southern W-E and the western N-S transect (Fig. 3B,C). Nevertheless, the mean content of dissolved CH_4 in the water column was similar when comparing the different surveys (3483, 3547, and 3745 μmol m^{-2} in May 2016, May 2017, and July 2015, respectively) (Table 2, Fig. S2). In June 2016, the mean content of dissolved CH_4 reached 5644 μmol m^{-2} due to the reduced number of stations (12 out of 64 stations) that were sampled during this survey, and that many of the sampled stations were located above active flares (see sampling strategy), which in turn translated to higher mean values (see the calculated mean content of dissolved CH_4 for the reduced number of stations for all surveys in Table S2). Therefore, dissolved CH_4 values from June 2016 are not directly comparable to values from the other surveys.

In general, CH_4 concentrations were highest in bottom waters, translating to inventories that were also highest at the Bottom Water Layer (2127–2867 μmol m^{-2}) compared to the Intermediate (795–1008 μmol m^{-2}) and Surface Water Layer (83–412 μmol m^{-2}) (Table 2).

At Isfjorden (Stas. I and II) we observed elevated concentrations of 26 and 57 nM (May and June 2016, respectively) in the Bottom Water Layer, whereas at the Isfjorden Trough CH_4 was generally low, with average values of 9 nM in the Bottom and 3 nM in the Surface Water Layer (May 2016). At Outer Bellsundet, Outer Hornsund and Sørkappøya, CH_4 concentrations in the Bottom Water Layers were 18, 12, and 24 nM, respectively, and 11, 4, and 17 nM in surface waters (Table S2).

Methane oxidation activity

Highest MOx activity was generally found in bottom waters, although the magnitude of activity greatly varied

Table 2. Inventory of dissolved CH_4 and microbial methane oxidation activity calculated for the sampling area at the shallow shelf of Prins Karls Forland. Surface, Intermediate, and Bottom refers to the defined water layers (Table 1) of the water column. Total values are the sum of all three water layer values per sampling campaign. The order of sampling campaigns in this table follows the cycle of the seasons where May corresponds to Arctic spring and July to summer.

	Dissolved methane				Methane oxidation activity					
	Surface	Interm.	Bottom	Total	Surface	Interm.	Bottom	Total	CH_4 oxid. per day*	100% turnover**
	Mean content (μmol m^{-2})				Mean turnover (μmol m^{-2} d^{-1})				(%)	(d)
May (2016)	100	928	2456	3483	0.006	0.18	0.33	0.51	0.015	6777
May (2017)	412	1008	2127	3547	0.104	0.48	1.46	2.02	0.057	1754
July (2015)	83	795	2867	3745	0.089	1.73	25.72	27.54	0.735	136

	Dissolved methane				Methane oxidation activity			
	Surface	Interm.	Bottom	Total	Surface	Interm.	Bottom	Total
	Total content in the area ($\times 10^5$ mol)				Total turnover in the area (mol d^{-1})			
May (2016)	0.37	3.38	8.94	12.68	2	65	120	187
May (2017)	1.50	3.67	7.74	12.91	38	173	532	736
July (2015)	0.30	2.89	10.44	13.63	32	630	9362	10,024

*Percentage of CH_4 that is oxidized per day.
**Time in days that it would take to totally oxidize the available CH_4.

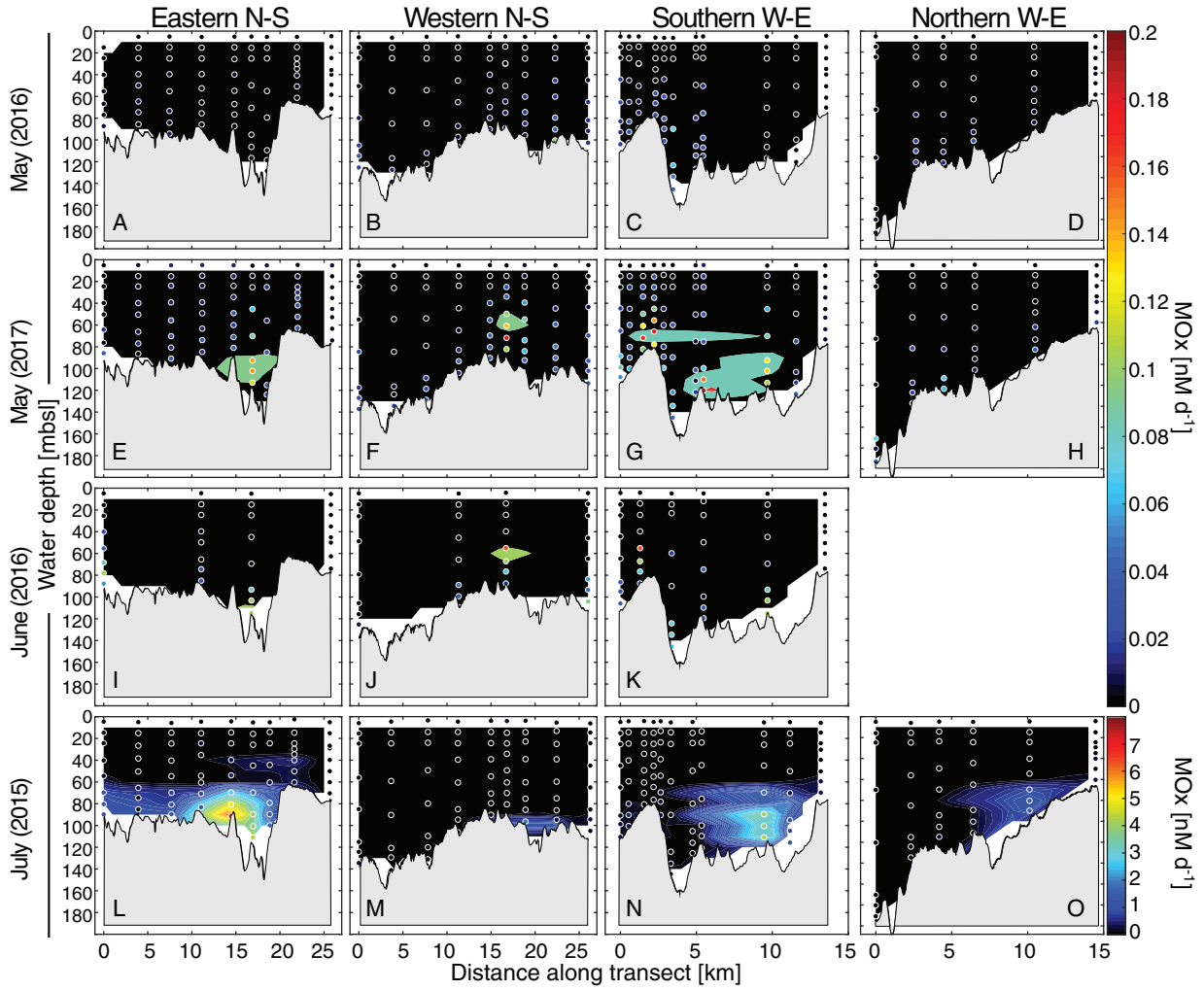

Fig 4. Profiles of microbial CH_4 oxidation (MOx) rates in the water column along transects at the shallow shelf west of Prins Karls Forland (**A–O**) from four sampling surveys in May, June, and July within three successive years (2015–2017). For each sampling survey, water depth on the *y*-axis is given in meters below sea level (mbsl). White circles represent single water samples. The color code shows measured and linearly interpolated MOx rates (nM d^{-1}). Each plot contains the bathymetrical baseline (black line above gray area) characteristic for each transect. In June 2016, only three transects were conducted. Note that we have used the same interpolation settings for all transects (with a resolution of 0.1 nM d^{-1}), but have chosen two color scales for the July vs. May and June expeditions.

between surveys (Figs. 4, S3). We found a MOx maximum value of 7.1 nM d^{-1} in the south-east part of the sampling area at the Prins Karls Forland shelf in July 2015 (Sta. 53; Fig. S4). In contrast, MOx maxima in May 2016, May 2017 and June 2016, were more than an order of magnitude lower with values of 0.09, 0.16, and 0.23 nM d^{-1}, respectively (Fig. S4). Similarly to maximum rates, depth integrated MOx activity in the Bottom Water Layer was also highest in July 2015 (25.72 nmol m^{-2} d^{-1}) and substantially lower in May 2016 (0.33 nmol m^{-2} d^{-1}), May 2017 (1.46 nmol m^{-2} d^{-1}) and June 2016 (1.67 nmol m^{-2} d^{-1}). In the Surface Water Layer, average MOx activity was generally below 0.1 nmol m^{-2} d^{-1} (Table 2, Fig. S3).

Among the stations along the transect inside Isfjorden, highest MOx activity was in the bottom waters at Sta. I (0.04 nM d^{-1} in May and 0.5 nM d^{-1} in June 2016 (Fig. S4); no samples were taken in Isfjorden in 2015). MOx rates at Outer Bellsundet, Outer Hornsund and Sørkappøya were < 0.04 nM d^{-1} (Table S2).

Methanotrophic community

The particulate methane monooxygenase gene (*pmoA*) was sequenced from selected bottom water samples with elevated MOx rates. The selected samples originated from the flare area (Sta. 9 May 2016 and 10 July 2015), the bathymetric depression zone (Stas. 54 May, June 2016, July 2015 and 58 May 2016, July 2015), Sta. 49 located at the north-east corner of the sampling grid (May 2016 and July 2015), Sta. I at Isfjorden (May and June 2016), and from Outer Bellsundet (Sta. XI June 2016) (Fig. 1, Table S1). The number of generated *pmoA* sequences ranged

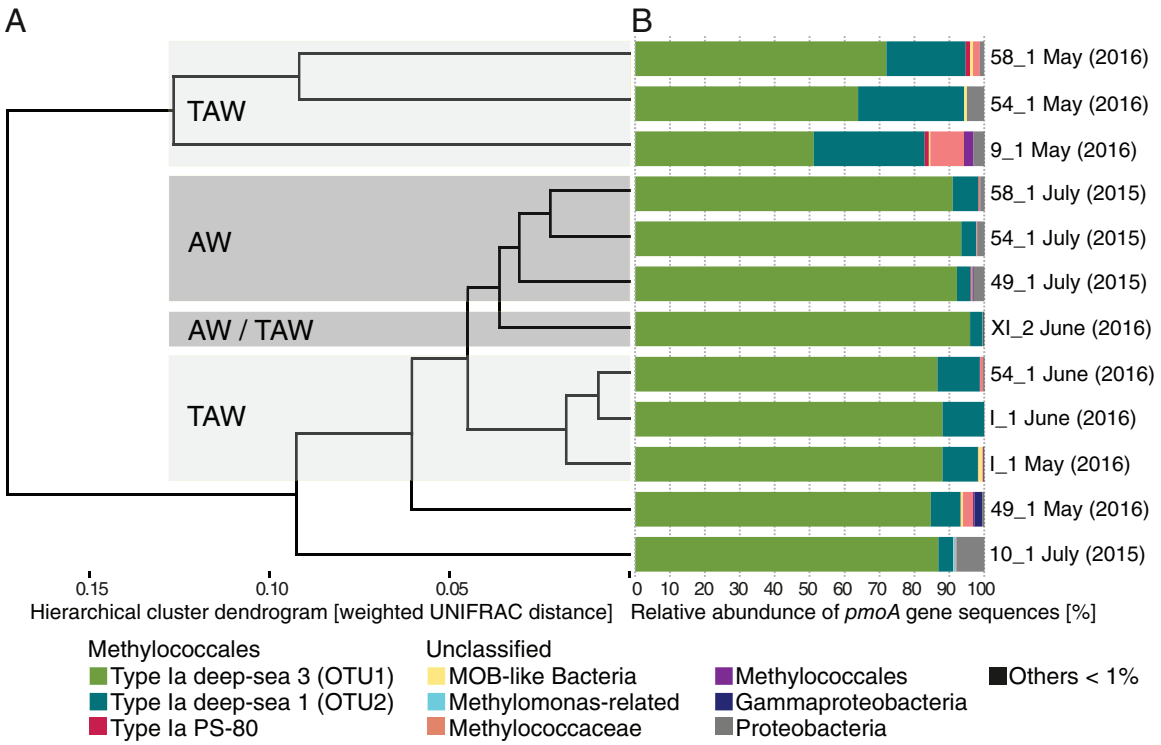

Fig 5. Hierarchical clustering of OPUs derived from *pmoA* gene sequences (**A**) and relative abundance (**B**) of the methanotrophic community from selected stations from the shallow shelf of Prins Karls Forland, Isfjorden (I) and Outer Belsundet (XI) investigated over three sampling surveys in May 2016, June 2016, and July 2015. Sample IDs derive from the station number (see sampling grid in Fig.1B) and water levels (1: 5 m above seafloor, 2: 15 m above seafloor). Gray squares show predominant water masses found at the bottom water level at the stations (AW: Atlantic Water, TAW: Transformed Atlantic Water).

from 20,132 to 44,469 per sample. After processing, quality reads clustered into 70 OPUs with absolute abundance of maximum 34,299 and minimum 424 reads across samples. The most abundant OPUs were related to the gammaproteobacterial deep-sea 3 and deep-sea 1 clades, both of which are subgroups of gammaproteobacterial Methylococcaceae Type Ia MOB according to Lüke and Frenzel (2011) (Figs. 5, S6). In bottom water samples from May 2016, the relative abundance of Type Ia deep-sea 1 MOB was higher compared to the other months. In addition, OPUs belonging to unclassified Proteobacteria or Methylococcaceae-related genera only showed low sequence abundance.

Bacterial diversity

Our 16S rRNA gene analyses of water column bacterial community compositions revealed a great phylogenetic diversity and spatial variability. After sequence processing of > 1.2 million raw sequences from 57 samples, 11,705 OTUs were generated.

The majority of the 16S rRNA gene sequences clustered into OTUs which are taxonomically affiliated with Alphaproteobacteria (34%), Gammaproteobacteria (30%), Bacteroidetes (25%), and Verrucomicrobia (4%) (Fig. 6B). Among the Alphaproteobacteria, the most abundant families were SAR11 clade I, SAR11 clade II and Rhodobacteraceae (*Planktomarina* and *Sulfitobacter*). Relatives of Gammaproteobacteria were mainly affiliated with Nitrincolaceae, Thioglobaceae, SAR86 clade, Porticoccaceae, and Methylophagaceae. The majority of the Bacteroidetes sequences were classified as Flavobacteriaceae with the dominant genera *Polaribacter* 1, *Polaribacter*, NS5 marine group, and *Aurantivirga*. Other abundant Bacteroidetes were NS9 marine group, Cryomorphaceae and Bacteroidaceae. Among the Verrucomicrobia, Rubritaleaceae was the most abundant family. Sequences affiliated with *Luteolibacter* and *Roseibacillus* were present in low amounts in almost all samples, but slightly more abundant in bottom waters sampled in July 2015.

Only few 16S rRNA gene sequences were associated with known methanotrophic or methylotrophic bacteria OTUs (related to either Alpha- or Gammaproteobacteria; Fig. 6D). Known MOB found in the data set were related to clade Milano-WF1B-03 (6 OTUs; Heijs et al. (2005)), found in samples from bottom waters at Stas. 54 and 58 in July 2015 and at station IF in May and June, and to the *Methyloprofundus* clade (4 OTUs) found at Stas. 9 and 19 sampled in May 2016. Furthermore, OTUs affiliated to *Methylobacterium*, *Methyloceanibacter*, and unclassified Methylomonaceae (one OTU each) were identified.

Methylotrophs were represented by members related to uncultured Methylophagaceae (110 OTUs in total) present in samples from the shelf west off Prins Karls Forland taken in June 2016 and July 2015; one OTU was identified as *Methylophaga* and found at Sta. I, Isfjorden. *Methylotenera* (two OTUs) was encountered in the whole water column in July 2015 and other genera of the family Methylophilaceae (OM43 clade, 72 OTUs) were present at all seasons. Known MOB accounted for 0.05% of all sequences, and known methylotrophs accounted for 1.08% of all sequences (Fig. 6D).

Community beta diversity analysis revealed the time of sampling (sampling campaign) as one dominant factor shaping the bacterial community composition (envfit, $p \leq 0.05$). The dissimilarity of the bacterial community was particular apparent in samples retrieved in May 2016 (spring) compared to samples from June 2016 and July 2015 (late spring/summer; Fig. 7A). In addition to the sampling campaign, water depth was a second variable that significantly correlated with community dissimilarity ($p \leq 0.05$). To reduce the masking of seasonal effects on the beta diversity analysis, we subsequently focused on samples retrieved from single sampling campaigns. Here, water temperature and depth, both independent environmental variables, influenced the communities ($p \leq 0.05$). Since these factors/variables (together with salinity) also define the classification of water masses (see section Hydrographic setting), water masses are indicated in Fig. 7B–D. In June 2016 and July 2015, communities revealed similarities according to water masses (Fig. 7C,D). Analogously, medium or high active MOB communities were more similar to one another. At Isfjorden and Outer Bellsundet, where water mass properties were highly affected by local features, communities were distinctively different to most of the other communities found at the shelf west off Prins Karls Forland, especially in June 2016 (Fig. 7C).

Supplementing NMDS-based analysis, we conducted canonical correspondence analysis (CCA). Similar to NMDS, CCA also indicated that water temperature, depth, and salinity significantly influenced the community composition (Table 3). For the bacterial communities in May and June 2016, these environmental variables adequately described the variation of the community composition, as supported by a significant level for the CCA Model (ANOVA; $p \leq 0.009$ and $p \leq 0.002$, respectively). In contrast, the composition of samples retrieved in July 2015 showed a much higher variation than could adequately be explained by the investigated environmental variables included in the model ($p \leq 0.129$), suggesting that additional unidentified factors played a major role. When taking community-dependent variables into account, such as amount of extracted DNA and CH_4 oxidation, both correlated with the identified communities (Table 3).

To identify a possible correlation of bacterial phyla with methane oxidation rates, we conducted a Spearman's rank correlation analysis on family level. Following clades depicted the greatest positive correlations: unclassified members of the OCS116 clade, Nitrosomonadaceae, Cellvibrionaceae, clade OM182, clade ZD0405, Thiothrichaceae, Rubritaleaceae, and Verrucomicrobiaceae (Fig. S7). Many of these families also depicted a positive correlation with CH_4 concentration and water level. Methane concentration, water depth and methane oxidation rates were also strongly correlated with another.

Repeated sampling

Hydrographical parameters (salinity, temperature, pressure), concentration of dissolved CH_4 and MOx activity were repeatedly measured at Stas. 9, 16, 31, 44, 54, and 64 over a 2-day time period (Table S1). Water mass properties only showed marginal differences (Fig. S8A,D). Stations located above or close to the flare area (Stas. 9, 19, 31, and 44) showed stronger variations in CH_4 concentrations in samples from greater water depths. MOx activity rates from all six stations (Fig. S8C,F) in addition to the 16S rRNA gene sequencing results from Sta. 9, showed high similarities when comparing the two time points (Fig. 6B).

Discussion

The shallow shelf west off Prins Karls Forland is characterized by numerous gas flares at the ridge of the Forlandet moraine complex as well as the many bathymetric depressions extending eastwards from the moraine. The water column at the shallow shelf is a hydrographically complex and dynamic system with seasonal variations in water mass properties. Individual gas flares transport differential amounts of CH_4 into the water column, and total CH_4 flux on the shelf also varies over time (Silyakova et al. 2020). However, a seasonal connection with high CH_4 fluxes during the warm season and ~ 80% lower fluxes during cold bottom water conditions, as found at the shelf break below 360 m water depth (Ferré et al. 2020), is not evident on the shallow shelf, where active flare clusters occur at 90 m. Such a depth is far above the uppermost limit of the shifting gas hydrate stability zone, which was found to be in between 380 and 400 m water depth (Berndt et al. 2014). We repeatedly investigated the shallow shelf over a time period of 3 years covering the Arctic spring (May 2016, 2017), late spring (June 2016) and summer (July 2015) and their specific hydrographic conditions. Our study reveals the activity, distribution and structure of methane-oxidizing communities in the water column on the shallow shelf west of Svalbard.

Spatiotemporal variations of methane content in the entire water body

Similar to previous studies on CH_4 dynamics in coastal waters of Svalbard (e.g., Damm et al. 2005; Graves et al. 2015; Mau et al. 2017), we generally observed highest CH_4 concentrations in bottom waters. In our sampling grid west of Prins Karls Forland (Fig. 1B), CH_4 concentrations frequently exceeded 100 nM in particular at gas flares locations (Fig. 3). Methane concentrations in surface waters were supersaturated compared to atmospheric concentrations across all surveys

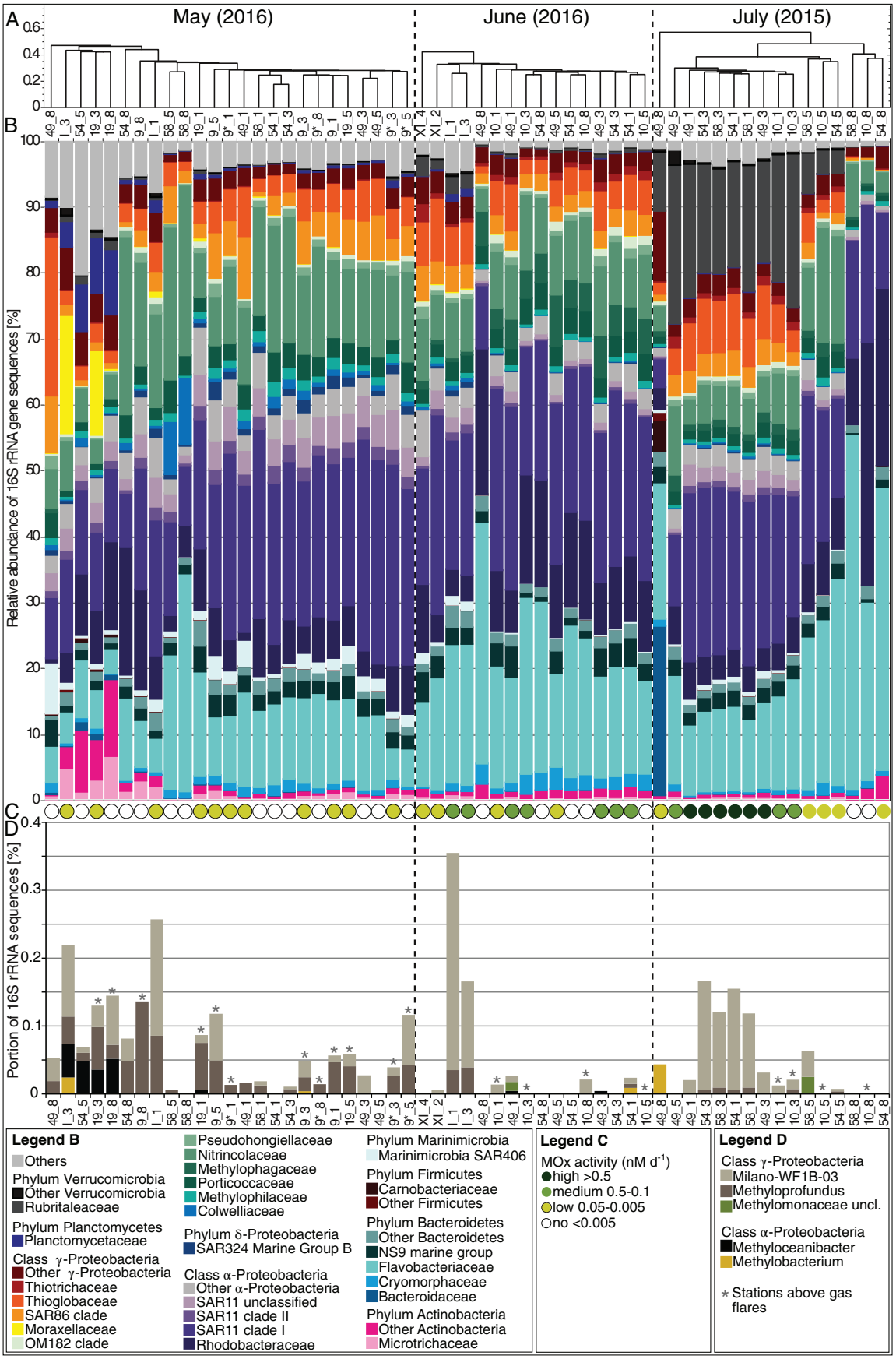

Fig 6. Legend on next page.

(1–5 fold on average). However, substantial impacts on atmospheric CH_4 concentrations in the region of the western Svalbard continental margin could not be confirmed (Myhre et al. 2016).

Furthermore, the integrated CH_4 inventory of the three water layers of the sampling grid during the surveys in spring (May 2016 and 2017), late spring (June 2016) and summer (July 2015), shows up to three times higher CH_4 values at the Bottom Water Layer compared to the Intermediate and Surface Water Layers, as a result of the CH_4 seepage from the seafloor (Table 2, Fig. S2). Moreover, the total content of dissolved CH_4 in the area (423 km^2) is consistent with values of ~ 13×10^5 mol $area^{-1}$ in spring (May 2016/17) and summer (July 2015). The seemingly high total CH_4 content in late spring (June 2016) is caused by an under-sampling of the survey area (see section Water column methane content and Study area and Sampling strategy).

Our values from May 2016/17 and July 2015, together with previously published flux data (Silyakova et al. 2020), indicate comparably steady CH_4 inputs in our study area during the investigated seasons. In contrast, seep activity in deeper water levels at the shelf break are strongly reduced during times with low bottom water temperatures (Ferré et al. 2020), because the uprising CH_4 "freezes out" as gas hydrate in surface sediments, building up a seasonal gas hydrate capacitor that is reduced in summer.

Moreover, our repeated sampling over the short time period of 2 days in May 2016 showed negligible variations in CH_4 concentration and water mass properties (Fig. S8A,D), and neither the bacterial MOx activity (Fig. S8C,F) nor the community composition (Fig. 6B) revealed any remarkable differences between the two time points. These findings indicate that hydrographic and biogeochemical variations during one sampling of the entire grid were most probably low (Steinle et al. 2015).

Spatiotemporal variations of methane oxidation activity

Methane oxidation in the ocean is the final sink for dissolved CH_4 before its release into the atmosphere (e.g., Reeburgh 2007; Steinle et al. 2015). Previous studies report that elevated MOx activity in marine environments is related to high CH_4 concentrations (Valentine et al. 2001; Mau et al. 2013; Crespo-Medina et al. 2014; Steinle et al. 2015). In our study, we also found elevated MOx rates in methane-rich bottom waters. But in the CH_4 plumes, MOx was not substantially elevated (Figs. S2, S3). This has been found elsewhere, too (Crespo-Medina et al. 2014; Steinle et al. 2015, 2017), and a literature review only revealed a correlation of MOx and CH_4 contents on logarithmic scales (James et al. 2016). The rather loose dependency of MOx and CH_4 concentrations indicates that microbial community abundance, and possibly other factors such as the availability of micronutrients, seems at least equally important in determining the efficacy of the microbial CH_4 filter in the water column (Steinle et al. 2015).

Our study area is characterized by steady CH_4 contents between seasons, but similarly to the spatial variation of MOx within one sampling campaign, we found large seasonal differences in MOx activity. In the Arctic spring (May) and late spring (June), MOx rates were generally low (weighted mean: < 2.02 μmol m^{-2} d^{-1}; total MOx: < 736 mol d^{-1}; Table 2). In contrast, in summer (July), MOx in the entire area was about one order of magnitude higher (weighted mean: 27.54 μmol m^{-2} d^{-1}; total MOx: 10,024 mol d^{-1}). It is also noteworthy that the maximum MOx value measured in summer (July; 7.2 nM d^{-1}) was much higher compared to previous measurements conducted in the area around Svalbard. Steinle et al. (2015) measured MOx rates of up to 3.2 nM d^{-1} at the continental slope west of our study area in Arctic summer (August). Mau et al. (2017) published rates of up to 2.2 nM d^{-1} in a CH_4 plume located more southerly between Hornsundbanken and Isfjordbanken west of Spitsbergen from the same season (August/September).

We discovered that the capacity of MOx shows a high spatiotemporal variation. The high MOx rate in summer translates to a turnover time of the CH_4 inventory of the entire sampling grid (13.63×10^5 mol) of about 136 d. In contrast, the turnover time was substantially longer in spring (1754–6777 d). While MOx plays a substantial role in retaining CH_4 in the Arctic summer, it seems of rather lower importance in winter. Similar seasonal differences were also found at the shelf break west of our study area (Steinle et al. 2015; Ferré et al. 2020). In general, the turnover times at the Prins Karls Forland shelf are within the intermediately high to low range when compared to previously reported turnover times of weeks to a few years from methane-rich, Arctic waters (Mau et al. 2013; Steinle et al. 2015; James et al. 2016). Turnover times of several decades are rare and typically restricted to oceanic deep waters with very low CH_4 contents (< 10 nM) (Rehder et al. 1999; Heeschen et al. 2003; James et al. 2016).

Fig. 6. Differential bacterial community structure based on 16S rRNA genes investigated over three sampling surveys of the shelf west of Prins Karls Forland, Isfjorden and Outer Belsundet. (**A**) Hierarchical clustering of bacterial communities of each sampling survey is based on subsampled Bray–Curtis dissimilarity matrix (OTU) and the complete linkage method. Stability of clusters was tested by bootstrapping 1000 times. (**B**) Relative abundance of bacteria based on 16S rRNA gene sequences are sorted according the hierarchical clustering within each sampling survey. Only taxa with abundances of >1% of total sequences are shown. (**C**) Simplified ranking of measured methane oxidation (MOx) activities per sample. (**D**) Proportion of 16S rRNA sequences, which were assigned to methanotrophic bacteria. Sample IDs are derived from the station number (see sampling grid in Fig. 1B) and water levels (1: 5 m above seafloor, 3: 25 m above seafloor, 5: Intermediate water level, 8: 5 m below sea surface, I: Isfjorden, XI: Outer Belsundet). Sta. 9 was repeatedly sampled during the sampling campaign; repeated samples are therefore marked with asterisks (9*_1 to 8).

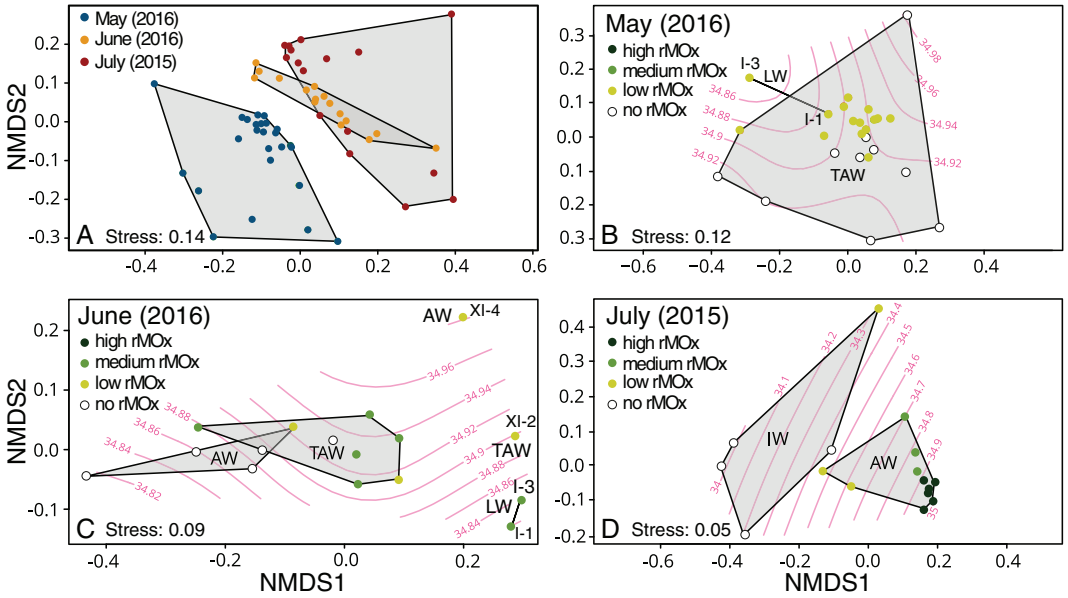

Fig 7. Seasonal correlation of microbial communities from all samples retrieved from all sampling surveys (**A**) and between microbial communities and salinity (red lines and values) according to single sampling campaigns (**B–D**). Non-metric multidimensional scaling (NMDS) derive from the Bray–Curtis dissimilarity index. AW: Atlantic Water; TAW: Transformed Atlantic Water; LW: Local Water; IW: Intermediate Water; I: Isfjorden (water levels 1 and 3); XI: Outer Bellsundet (water levels 2 and 4). Methane oxidation rates (rMOx) are defined as high: >0.5, medium: 0.5–0.1, low: 0.05–0.005, no: <0.005 nM d^{-1}.

Table 3. Canonical correspondence analysis (CCA) significance values of independent and dependent variables. Values marked with * indicate values of significance. Temp: temperature; Fluor: fluorescence; CH_4: dissolved methane concentrations; DNA: 16S rRNA gene sequencing analysis; MOx: methane oxidation rates. The order of sampling campaigns in this table follows the cycle of the Arctic seasons where May corresponds to spring, June to late spring, and July to summer.

		Independent variables					Dependent variables	
	ANOVA, CCA model	Temp.	Depth	Salinity	Fluor.	CH_4	DNA	MOx
May (2016)	0.009*	0.005*	0.050	0.315	0.155	0.275	0.560	0.030*
June (2016)	0.002*	0.005*	0.005*	0.150	0.015*	0.580	0.025*	0.005*
July (2015)	0.129	0.025*	0.005*	0.005*	0.465	0.165	0.005*	0.035*

Hydrographical dynamics on the shelf

The spatiotemporal variations of CH_4 content and MOx activity indicate two contrasting mixing regimes at the shelf, both of which have profound effects on MOx activity as well as the bacterial community composition.

The first scenario is characterized by a water column dominated by Atlantic Water as it was typically the case in summer (July; Fig. 2L–O). Atlantic Water episodically floods the shallow shelf in the form of numerous eddies caused by the West Spitsbergen Current that meanders eastwards onto the shelf (Nilsen et al. 2008; Steinle et al. 2015). The dense Atlantic Water replaces the shelf water, less saline (though colder) Arctic Water brought by the East Spitsbergen Current, and fills up the bathymetric depressions (Silyakova et al. 2020). This phenomenon was particularly apparent at the eastern end of the southern W-E transect, where the depressions are 40 m deeper than the surrounding seafloor. There, we found hot spots of MOx activity with 2–3 times higher rates than those reported previously from the continental shelf around Svalbard (Mau et al. 2013; Gentz et al. 2014; Steinle et al. 2015, 2017) although CH_4 concentrations were only moderately high in the depressions compared to gas flare locations in the western part of the sampling grid (Figs. S2, S3). Prior to flooding the shelf, Atlantic Water has an offshore history where CH_4 concentrations are low (Steinle et al. 2015). When swept over the CH_4 seeps at the shelf break (i.e., west of the study area), Atlantic Water becomes charged with CH_4, but MOx rates in the water column are initially low because of the initially low MOB content in this water mass (Steinle et al. 2015). When reaching the depressions, methane-enriched Atlantic Water becomes trapped as these depressions provide a sheltered environment with long residence times. This supports MOB

community growth and leads to an elevated MOx capacity (James et al. 2016). Due to the hydrographic complexity of the area, the frequency at which these depressions are filled with dense Atlantic Water and how frequently they are flushed with water of different origins, remains unknown.

The second scenario is characterized by frequent water mass shifts as a result of intense mixing in the study area. Mixing is furthermore responsible for the dispersion of dissolved CH_4. Meandering of the West Spitsbergen Current, flooding and flushing of the shallow shelf occur more often in winter and spring (von Appen et al. 2016; Silyakova et al. 2020). Moreover, the upwelling of Atlantic Water onto the shelf and into fjords in winter enhances the mixing of Transformed Atlantic Water and Local Water that reside there (Cottier et al. 2007). Arctic Water, often together with sea ice floes, both transported with the East Spitsbergen Current from the Northern Barents Sea (Nilsen et al. 2016) additionally contribute to the residing water mass replacement. The frequent mixing does not provide stable conditions for microbial community development. In other words, the short residence times and the frequent exchange of water masses in the bathymetric depressions with water masses containing only low amounts of MOB leads to an overall low abundance of water column MOB and thus MOx activity, which is less effective in retaining CH_4. In contrast, the CH_4 charged water masses are transported away from the CH_4 point sources and disperse in the lee of the seep (Graves et al. 2015). Consequently, we only observed low MOx activity in spring (Fig. 4A–H).

Composition of the methane-oxidizing bacterial community

We evaluated the methanotrophic and other methylotrophic communities in bottom water level from stations located at the shelf west off Prins Karls Forland (Stas. 9, 10, 49, 54, and 58), Isfjorden (I) and Outer Bellsundet (XI), which were collected in the Arctic spring and late spring (May and June), and summer (July). These samples were selected for *pmoA* gene amplicon sequencing because of their elevated MOx rates, which suggested the presence of active MOB.

The prevalent members of the MOB community in all samples, and irrespective of the water mass, were dominated by Type Ia deep-sea 3 MOB (OPU1) with variable but minor shares of Type Ia deep-sea 1 MOB (OPU2; Fig. 5B). OPU1 shares 98% sequence similarity with an uncultured MOB from the water column above the Oregon seep system at Hydrate Ridge (sequence FJ858282, GenBank; Hansman et al. (2017); Fig. S6). OPU2 shares 92% sequence similarity with *Methyloprofundus sedimenti* (sequence KF484908; Tavormina et al. (2015); relating to the family level, Yarza et al. (2014)), which is a known obligate MOB of the family Methylomonaceae, isolated from marine surface sediment from Monterey Canyon off the coast of California (USA) (Fig. S6). Both, the deep-sea 1 and 3 subgroups, mainly constitute mesophilic uncultured MOB from marine and freshwater environments (Lüke and Frenzel 2011; Knief 2015; Hansman et al. 2017). Our data show that a higher percentage of Type Ia deep-sea 3 MOB (OPU1) was found in Atlantic Water and Atlantic Water/Transformed Atlantic Water, i.e., the water mass prevailing in the bathymetric depressions where we also found high MOx activities. This suggests that Type Ia deep-sea 3 MOB is the main driver for active MOx in our study area.

The majority of the identified OTUs from the 16S rRNA gene sequences are related to heterotrophic bacteria that are often found to be the predominant representatives of bacterioplankton communities worldwide, seemingly having a major ecological role in marine food webs (Giovannoni and Stingl 2005). Where instead the relative abundance of MOB in the total bacterial community is low (0.05% of the total 16S rRNA gene sequences) and therefore comparisons among MOB should be considered with care. The presence of OTUs related to *Methyloprofundus* sp. and Milano-WF1B-03, the two most abundant MOB in the 16S rRNA data set, coincide with the locations of MOx hot spots—in the depression in summer (July) and above CH_4 flares in spring (May) (Fig. 6C,D). OTUs related to the known methylotrophs (Methylophagaceae: *Methylophaga* and Methylophilaceae: *Methylotenera* and OM43 clade), which are present in all of our samples, were frequently found in marine and freshwater ecosystems where they profit from C1-compounds, such as methanol and methylamine, released as a product of methane monooxygenase activity of MOB (Neufeld et al. 2007, 2008; Moussard et al. 2009). However, it also has been suggested that Methylophilaceae species might be able to incorporate CH_4 directly (Redmond et al. 2010).

We also identified high abundances of sequences affiliated with Verrucomicrobia (Fig. 6B). Members of this phylum have been found globally in a variety of aerobic and anaerobic marine environments (Freitas et al. 2012), but only a few species were isolated and characterized so far, and relatively little knowledge exists on the metabolic capabilities of Verrucomicrobia. We found members of the family Rubritaleaceae genus *Luteolibacter*, which are highly abundant in samples associated with high MOx activity (July 2015, primarily in the bottom water level; Fig. 6B). *Luteolibacter* comprises six known species that are described as chemoheterotrophs utilizing a variety of carbon sources (Zhang et al. 2017). None of them has been tested for MOx activity and to the best of our knowledge, no genome data from this genus are available. Yet, some other members of the Verrucomicrobia ("Ca. *Methylacidimicrobium*," "Ca. *Methylacidiphilum kamchatkense*" strain Kam1, V4 and SolV) were found to mediate MOx (Dunfield et al. 2007; Pol et al. 2007; Kruse et al. 2019). Methanotrophic Verrucomicrobia have multiple operons encoding the particulate methane monooxygenase with identical *pmoCAB* operon structure when compared to proteobacterial MOB (Op den Camp et al. 2009). However, despite the similar operon structure, no standard *pmoA* primer set can amplify verrucomicrobial *pmoA* genes, which seems to be only detectable by shot-gun genome

sequencing (Dunfield et al. 2007; Pol et al. 2007). As a result, the abundance, distribution and diversity of Verrucomicrobia MOB has been overlooked in most ecological studies (Bergmann et al. 2011). We did not detect any Verrucomicrobia-related species with our *pmoA* sequencing approach and although the obvious co-occurrence of *Luteolibacter sp.* (class Verrucomicrobia) with high MOx rates shown here is remarkable, we can only speculate if the *Luteolibacter* at the Prins Karls Forland shelf are involved in MOx (directly or indirectly) or if their abundance maximum is related to factors that are independent of CH_4-dynamics.

Origin of methane-oxidizing bacteria

The meandering of the West Spitsbergen Current causes occasional flooding events of the shallow shelf at Prins Karls Forland with Atlantic Water (Steinle et al. 2015; Silyakova et al. 2020). Because of the general south–north direction of the West Spitsbergen Current, it thus seems likely that the residual Atlantic Water that we found in the bathymetric depressions in summer had, before being trapped in the bathymetric depressions, passed our southern stations, i.e., Outer Bellsundet, Outer Hornsund, and Sørkappøya. At these stations, we found elevated CH_4 concentrations around seeps, which were discovered along the Svalbard margin (Mau et al. 2017). Furthermore, we found high similarities between the MOB communities found at the shallow shelf offshore Prins Karls Forland and at the southern stations (Fig. 5A). For example, the MOB communities at Stas. 49, 54 and 58 (all offshore Prins Karls Forland) in summer (July 2015) comprise more than 90% of Type Ia deep-sea 3 MOB, just like the MOB community at Outer Bellsundet in late spring (June 2016; Fig. 5B). The bottom water layers of all southern stations were characterized by the influence of warm and saline Atlantic Water (similar to the bathymetric depressions offshore Prins Karls Forland in the summer).

Wilkins et al. (2013) suggested that the advection of microorganisms originating from upstream-locations, which then colonize sites downstream, shape the microbial community at the downstream locations. It also appears that increasing opportunities for colonization (and subsequent growth) are more relevant than the numbers of transported organisms. Translated to our study, this converts into the following: the microbes from Outer Bellsundet (upstream site) colonize the shelf west of Prins Karls Forland (downstream site). The specific hydrographic setting at the downstream site, i.e., sheltered conditions comprising CH_4 and nutrient-rich water that is trapped in the depressions due to flooding events and strong stratification of the water column in summer allows MOB communities to develop. These factors are then also more important than the sheer number of MOB cells being transported from the southern stations to the Prins Karls Forland shelf. Moreover, the inoculation theory leads to the assumption that the blooming MOB community from the Prins Karls Forland shelf could be in turn an inoculum for other "MOx systems" further north, and that seeding and inoculation via water mass transport is an important vector connecting spatially separated habitats (Wilkins et al. 2013).

Conclusion

Spatiotemporal changes in MOx activity and MOB community structure in the water column above CH_4 seeps at the shallow shelf west of Svalbard are primarily a consequence of the seasonal variations of the hydrographical regimes. The two different scenarios presented in this study clearly show that seasonality strongly affects the MOB community structures and MOx capacity. Moreover, the distribution of MOB communities along the shallow shelf is most likely caused by physical transport, while site-specific geomorphological characteristics such as the shallow Forlandet moraine complex featuring numerous bathymetric depressions, enhance this effect. We suggest that the origin of the initial MOB "inoculum" in the bathymetric depressions offshore Prins Karls Forland might originate from seep regions further south. Once the MOB are trapped in bathymetric depressions, they are more sheltered from rapidly changing and dynamic conditions of the upper water column. Such sheltered conditions promote community growth, which in turn results in elevated MOx in summertime. Seasonality (especially in winter and spring, when the water column is subjected to deep mixing) is profoundly under-represented in studies on microbial habitat structure in Arctic water column habitats. Systematic time-series measurements covering the different, including harsh/bad weather seasons, would allow for a more comprehensive understanding of biogeochemical processes influenced by seasonal change-related microbial community variations. This would further improve our qualitative and quantitative understanding of important microbial processes in a warming Arctic Ocean.

References

Aagaard, K., A. Foldvik, and S. R. Hillman. 1987. The West Spitsbergen current: Disposition and water mass transformation. J. Geophys. Res. Oceans **92**: 3778–3784.

Allen, H. K., et al. 2016. Pipeline for amplifying and analyzing amplicons of the V1–V3 region of the 16S rRNA gene. BMC. Res. Notes **9**: 380.

Bergmann, G. T., and others. 2011. The under-recognized dominance of Verrucomicrobia in soil bacterial communities. Soil Biol. Biochem. **43**: 1450–1455.

Berndt, C., and others. 2014. Temporal constraints on hydrate-controlled methane seepage off Svalbard. Science **343**: 284–287.

Bushnell, B., J. Rood, and E. Singer. 2017. BBMerge – Accurate paired shotgun read merging via overlap. PLOS ONE **12**: e0185056. https://doi.org/10.1371/journal.pone.0185056

Bussmann, I. 2013. Distribution of methane in the Lena Delta and Buor-Khaya Bay, Russia. Biogeosciences **10**: 4641–4652.

Caporaso, J. G., and others. 2010. QIIME allows analysis of high-throughput community sequencing data. Nat. Methods **7**: 335–336.

Cottier, F., V. Tverberg, M. Inall, H. Svendsen, F. Nilsen, and C. Griffiths. 2005. Water mass modification in an Arctic fjord through cross-shelf exchange: The seasonal hydrography of Kongsfjorden, Svalbard. J. Geophys. Res. **110**: (C12005). doi:10.1029/2004JC002757

Cottier F. R., Nilsen F., Inall M. E., Gerland S., Tverberg V., Svendsen H. 2007. Wintertime warming of an Arctic shelf in response to large-scale atmospheric circulation. Geophysical Research Letters **34**: 1–5. doi:10.1029/2007GL029948

Crespo-Medina, M., and others. 2014. The rise and fall of methanotrophy following a deepwater oil-well blowout. Nat. Geosci. **7**: 423–427.

Damm, E., A. Mackensen, G. Budéus, E. Faber, and C. Hanfland. 2005. Pathways of methane in seawater: Plume spreading in an Arctic shelf environment (SW-Spitsbergen). Cont. Shelf Res. **25**: 1453–1472.

Dunfield, P. F., and others. 2007. Methane oxidation by an extremely acidophilic bacterium of the phylum Verrucomicrobia. Nature **450**: 879–882.

Edgar, R. C. 2004. MUSCLE: Multiple sequence alignment with high accuracy and high throughput. Nucleic Acids Res. **32**: 1792–1797.

Edgar, R. C. 2010. Search and clustering orders of magnitude faster than BLAST. Bioinformatics **26**: 2460–2461.

Edgar, R. C., B. J. Haas, J. C. Clemente, C. Quince, and R. Knight. 2011. UCHIME improves sensitivity and speed of chimera detection. Bioinformatics **27**: 2194–2200.

Etminan, M., G. Myhre, E. J. Highwood, and K. P. Shine. 2016. Radiative forcing of carbon dioxide, methane, and nitrous oxide: A significant revision of the methane radiative forcing. Geophys. Res. Lett. **43**: 12,614–612,623.

Ferré, B., and others. 2020. Reduced methane seepage from Arctic sediments during cold bottom-water conditions. Nat. Geosci. **13**: 144–148.

Freitas, S., and others. 2012. Global distribution and diversity of marine Verrucomicrobia. ISME J. **6**: 1499–1505.

Gentz, T., E. Damm, J. Schneider von Deimling, S. Mau, D. F. McGinnis, and M. Schlüter. 2014. A water column study of methane around gas flares located at the West Spitsbergen continental margin. Cont. Shelf Res. **72**: 107–118.

Giovannoni, S. J., and U. Stingl. 2005. Molecular diversity and ecology of microbial plankton. Nature **437**: 343–348.

Graves, C. A., and others. 2015. Fluxes and fate of dissolved methane released at the seafloor at the landward limit of the gas hydrate stability zone offshore western Svalbard. J. Geophys. Res. Oceans **120**: 6185–6201.

Graves, C. A., and others. 2017. Methane in shallow subsurface sediments at the landward limit of the gas hydrate stability zone offshore western Svalbard. Geochim. Cosmochim. Acta **198**: 419–438.

Hansen, J., M. Sato, G. Russell, and P. Kharecha. 2013. Climate sensitivity, sea level and atmospheric carbon dioxide. Philos. Trans. R. Soc. A: Math. Phys. Eng. Sci. **371**: 20120294. http://dx.doi.org/10.1098/rsta.2012.0294

Hansman, R. L., A. R. Thurber, L. A. Levin, and L. I. Aluwihare. 2017. Methane fates in the benthos and water column at cold seep sites along the continental margin of Central and North America. Deep-Sea Res. I Oceanogr. Res. Pap. **120**: 122–131.

Hanson, R. S., and T. E. Hanson. 1996. Methanotrophic bacteria. Microbiol. Rev. **60**: 439–471.

Heeschen, K. U., A. M. Tréhu, R. W. Collier, E. Suess, and G. Rehder. 2003. Distribution and height of methane bubble plumes on the Cascadia Margin characterized by acoustic imaging. Geol. Res. Lett. **30**: 1463.

Heijs, S. K., J. S. Sinninghe Damsté, and L. J. Forney. 2005. Characterization of a deep-sea microbial mat from an active cold seep at the Milano mud volcano in the Eastern Mediterranean Sea. FEMS Microbiol. Ecol. **54**: 47–56.

Herlemann, D. P. R., M. Labrenz, K. Jürgens, S. Bertilsson, J. J. Waniek, and A. F. Andersson. 2011. Transitions in bacterial communities along the 2000 km salinity gradient of the Baltic Sea. ISME J. **5**: 1571–1579.

James, R. H., and others. 2016. Effects of climate change on methane emissions from seafloor sediments in the Arctic Ocean: A review. Limnol. Oceanogr. **61**: S283–S299.

Knief, C. 2015. Diversity and habitat preferences of cultivated and uncultivated aerobic methanotrophic bacteria evaluated based on pmoA as molecular marker. Front. Microbiol. **6**: 1346.

Kozich, J. J., S. L. Westcott, N. T. Baxter, S. K. Highlander, and P. D. Schloss. 2013. Development of a dual-index sequencing strategy and curation pipeline for analyzing amplicon sequence data on the MiSeq illumina sequencing platform. Appl. Environ. Microbiol. **79**: 5112–5120.

Kruse, T., C. M. Ratnadevi, H.-A. Erikstad, and N.-K. Birkeland. 2019. Complete genome sequence analysis of the thermoacidophilic verrucomicrobial methanotroph "*Candidatus Methylacidiphilum kamchatkense*" strain Kam1 and comparison with its closest relatives. BMC Genomics **20**: 642.

Landvik, J. Y., and others. 2005. Rethinking late Weichselian ice-sheet dynamics in coastal NW Svalbard. Boreas **34**: 7–24.

Letunic, I., and P. Bork. 2016. Interactive tree of life (iTOL) v3: An online tool for the display and annotation of phylogenetic and other trees. Nucleic Acids Res. **44**: W242–W245.

Lozupone, C., M. E. Lladser, D. Knights, J. Stombaugh, and R. Knight. 2011. UniFrac: An effective distance metric for microbial community comparison. ISME J. **5**: 169–172.

Lüke, C., and P. Frenzel. 2011. Potential of pmoA amplicon pyrosequencing for methanotroph diversity studies. Appl. Environ. Microbiol. **77**: 6305–6309.

Masson-Delmotte, V., and others. 2006. Past and future polar amplification of climate change: Climate model

intercomparisons and ice-core constraints. Climate Dynam. **26**: 513–529.

Mau, S., and others. 2017. Widespread methane seepage along the continental margin off Svalbard - From Bjørnøya to Kongsfjorden. Sci. Rep. **7**: 42997.

Mau, S., J. Blees, E. Helmke, H. Niemann, and E. Damm. 2013. Vertical distribution of methane oxidation and methanotrophic response to elevated methane concentrations in stratified waters of the Arctic fjord Storfjorden (Svalbard, Norway). Biogeosciences **10**: 6267–6278.

Moussard, H., N. Stralis-Pavese, L. Bodrossy, J. D. Neufeld, and J. C. Murrell. 2009. Identification of active methylotrophic bacteria inhabiting surface sediment of a marine estuary. Environ. Microbiol. Rep. **1**: 424–433.

Murrell, J. C. 2010. The aerobic methane oxidizing bacteria (Methanotrophs). *In* K. N. Timmis [ed.], Handbook of hydrocarbon and lipid microbiology. Berlin Heidelberg: Springer-Verlag.

Myhre, C. L., and others. 2016. Extensive release of methane from Arctic seabed west of Svalbard during summer 2014 does not influence the atmosphere. Geophys. Res. Lett. **43**: 4624–4631.

Neufeld, J. D., H. Schäfer, M. J. Cox, R. Boden, I. R. McDonald, and J. C. Murrell. 2007. Stable-isotope probing implicates Methylophaga spp and novel Gammaproteobacteria in marine methanol and methylamine metabolism. ISME J. **1**: 480–491.

Neufeld, J. D., R. Boden, H. Moussard, H. Schäfer, and J. C. Murrell. 2008. Substrate-specific clades of active marine methylotrophs associated with a phytoplankton bloom in a temperate coastal environment. Appl. Environ. Microbiol. **74**: 7321–7328.

Niemann, H., and others. 2015. Toxic effects of lab-grade butyl rubber stoppers on aerobic methane oxidation. Limnol. Oceanogr.: Methods **13**: 40–52.

Nilsen, F., F. Cottier, R. Skogseth, and S. Mattsson. 2008. Fjord–shelf exchanges controlled by ice and brine production: The interannual variation of Atlantic Water in Isfjorden, Svalbard. Cont. Shelf Res. **28**: 1838–1853.

Nilsen, F., R. Skogseth, J. Vaardal-Lunde, and M. Inall. 2016. A simple shelf circulation model: Intrusion of Atlantic Water on the West Spitsbergen Shelf. J. Phys. Oceanogr. **46**: 1209–1230.

Op den Camp, H. J. M., and others. 2009. Environmental, genomic and taxonomic perspectives on methanotrophic Verrucomicrobia. Environ. Microbiol. Rep. **1**: 293–306.

Osudar, R., S. Liebner, M. Alawi, S. Yang, I. Bussmann, and D. Wagner. 2016. Methane turnover and methanotrophic communities in arctic aquatic ecosystems of the Lena Delta, Northeast Siberia. FEMS Microbiol. Ecol. **92**: fiw116. https://doi.org/10.1093/femsec/fiw116

Pilloni, G., M. S. Granitsiotis, M. Engel, and T. Lueders. 2012. Testing the limits of 454 pyrotag sequencing: Reproducibility, quantitative assessment and comparison to T-RFLP fingerprinting of aquifer microbes. PLoS One **7**: e40467.

Pol, A., K. Heijmans, H. R. Harhangi, D. Tedesco, M. S. M. Jetten, and H. J. M. Op den Camp. 2007. Methanotrophy below pH 1 by a new Verrucomicrobia species. Nature **450**: 874–878.

Portnov, A., S. Vadakkepuliyambatta, J. Mienert, and A. Hubbard. 2016. Ice-sheet-driven methane storage and release in the Arctic. Nat. Commun. **7**: 10314.

Quast, C., and others. 2013. The SILVA ribosomal RNA gene database project: Improved data processing and web-based tools. Nucleic Acids Res. **41**: D590–D596.

Redmond, M. C., D. L. Valentine, and A. L. Sessions. 2010. Identification of novel methane-, ethane-, and propane-oxidizing bacteria at marine hydrocarbon seeps by stable isotope probing. Appl. Environ. Microbiol. **76**: 6412–6422.

Reeburgh, W. S. 2007. Oceanic methane biogeochemistry. Am. Chem. Soc. **107**: 486–513.

Rehder, G., R. S. Keir, E. Suess, and M. Rhein. 1999. Methane in the northern Atlantic controlled by microbial oxidation and atmospheric history. Geophys. Res. Lett. **26**: 587–590.

Rognes, T., T. Flouri, B. Nichols, C. Quince, and F. Mahé. 2016. VSEARCH: A versatile open source tool for metagenomics. PeerJ **4**: e2584.

Sahling, H., and others. 2014. Gas emissions at the continental margin west off Svalbard: Mapping, sampling, and quantification. Biogeosci. Discuss. **11**: 7189–7234.

Sarkar, S., and others. 2012. Seismic evidence for shallow gas-escape features associated with a retreating gas hydrate zone offshore West Svalbard. J. Geophys. Res.-Solid Earth **117**: 1–18. doi:10.1029/2011JB009126

Schloss, P. D., and others. 2009. Introducing mothur: Open-source, platform-independent, community-supported software for describing and comparing microbial communities. Appl. Environ. Microbiol. **75**: 7537–7541.

Shakhova, N., I. Semiletov, A. Salyuk, V. Yusupov, D. Kosmach, and Ö. Gustafsson. 2010. Extensive methane venting to the atmosphere from sediments of the east Siberian Arctic shelf. Science **327**: 1246–1250.

Silyakova, A., and others. 2020. Physical controls of dynamics of methane venting from a shallow seep area west of Svalbard. Cont. Shelf Res. **194**: 104030.

Stamatakis, A. 2014. RAxML version 8: A tool for phylogenetic analysis and post-analysis of large phylogenies. Bioinformatics **30**: 1312–1313.

Steinle, L., and others. 2015. Water column methanotrophy controlled by a rapid oceanographic switch. Nat. Geosci. **8**: 378–382.

Steinle, L., and others. 2017. Effects of low oxygen concentrations on aerobic methane oxidation in seasonally hypoxic coastal waters. Biogeosciences **14**: 1631–1645.

Tavormina, P. L., and others. 2015. *Methyloprofundus sedimenti* gen. nov., sp. nov., an obligate methanotroph from ocean sediment belonging to the 'deep sea-1' clade of marine methanotrophs. Int. J. Syst. Evol. Microbiol. **65**: 251–259.

Tavormina, P. L., W. Ussler, and V. J. Orphan. 2008. Planktonic and sediment-associated aerobic methanotrophs in

two seep systems along the North American margin. Appl. Environ. Microbiol. **74**: 3985–3995.

Valentine, D. L., D. C. Blanton, W. S. Reeburgh, and M. Kastner. 2001. Water column methane oxidation adjacent to an area of active hydrate dissociation, Eel River Basin. Geochim. Cosmochim. Acta **65**: 2633–2640.

van Teeseling, M. C. F., and others. 2014. Expanding the verrucomicrobial methanotrophic world: Description of three novel species of Methylacidimicrobium gen. nov. Appl. Environ. Microbiol. **80**: 6782–6791.

von Appen, W. J., U. Schauer, T. Hattermann, and A. Beszczynska-Möller. 2016. Seasonal cycle of mesoscale instability of the West Spitsbergen current. J. Phys. Oceanogr. **46**: 1231–1254.

Wen, X., S. Yang, and S. Liebner. 2016. Evaluation and update of cutoff values for methanotrophic pmoA gene sequences. Arch. Microbiol. **198**: 629–636.

Westbrook, G. K., and others. 2009. Escape of methane gas from the seabed along the West Spitsbergen continental margin. Geophys. Res. Lett. **36**: 1–5.

Wiesenburg, D. A., and N. L. Guinasso. 1979. Equilibrium solubilities of methane, carbon monoxide, and hydrogen in water and sea water. J. Chem. Eng. Data **24**: 356–360.

Wilkins, D., E. van Sebille, S. R. Rintoul, F. M. Lauro, and R. Cavicchioli. 2013. Advection shapes Southern Ocean microbial assemblages independent of distance and environment effects. Nat. Commun. **4**: 2457.

Yarza, P., and others. 2014. Uniting the classification of cultured and uncultured bacteria and archaea using 16S rRNA gene sequences. Nat. Rev. Microbiol. **12**: 635–645.

Zhang, C., and others. 2017. Luteolibacter flavescens sp. nov., isolated from deep seawater. Int. J. Syst. Evol. Microbiol. **67**: 729–735.

Acknowledgments

We would like to thank the captain, crew, and scientific research party of the R/V *Helmer Hanssen* as well as the chief scientists of the cruises: CAGE15-3, CAGE16-4, CAGE16-5, and CAGE17-1. We are particularly grateful to the participants at BareLab, the Russian Scientific Center on Spitsbergen, and Anna Nikulina from the Arctic and Antarctic Research Institute (AARI) for their unelaborated and kind provision of laboratory facilities at Barentsburg. Matteus Lindgren is thanked for measuring methane concentrations in CAGE17-1 samples, JoLynn Carroll for her assistance in initiating the project, and Greta Reintjes for support in statistical analysis. Computations were performed using resources provided by UNINETT Sigma2—the National Infrastructure for High Performance Computing and Data Storage in Norway, account numbers NN9639K and NS9593K. This study is funded by CAGE (Centre for Arctic Gas Hydrate, Environment and Climate), Norwegian Research Council grant no. 223259.

Conflict of Interest

None declared.

Submitted 14 July 2020
Revised 29 November 2020
Accepted 01 March 2021

Associate editor: Lauren Juranek